Evidence-Based Complementary and Alternative Medicine

Discovery of Novel Animal-Based Medicinal Products with Therapeutic Potential in Evidence-Based Traditional Medicine

Lead Guest Editor: Gunhyuk Park
Guest Editors: Yong-ung Kim and Irawan W. Kusuma

Discovery of Novel Animal-Based Medicinal Products with Therapeutic Potential in Evidence-Based Traditional Medicine

Evidence-Based Complementary and Alternative Medicine

Discovery of Novel Animal-Based Medicinal Products with Therapeutic Potential in Evidence-Based Traditional Medicine

Lead Guest Editor: Gunhyuk Park
Guest Editors: Yong-ung Kim and Irawan W. Kusuma

Editorial Board

Contents

Hindawi
Evidence-Based Complementary and Alternative Medicine
Volume 2019, Article ID 1626543, 3 pages
https://doi.org/10.1155/2019/1626543

Editorial

Discovery of Novel Animal-Based Medicinal Products with Therapeutic Potential in Evidence-Based Traditional Medicine

Gunhyuk Park,[1] **Yong-ung Kim**,[2] **and Irawan W. Kusuma**[3]

[1]*Herbal Medicine Reseources Research Center, Korea Institute of Oriental Medicine, 111 Geonjae-ro, Naju-si, Jeollanam-do 58245, Republic of Korea*
[2]*Department of Pharmaceutical Engineering, College of Biomedical Science, Daegu Haany University, Gyeongsan, Republic of Korea*
[3]*Forest Products Chemistry Laboratory, Faculty of Forestry, Mulawarman University, Samarinda, Indonesia*

Correspondence should be addressed to Gunhyuk Park; gpark@kiom.re.kr

Received 5 December 2019; Accepted 5 December 2019; Published 19 December 2019

Animals have been used as traditional medicinal resources for the treatment and relieve of a myriad of illnesses and diseases in practically every human culture. The traditional use of animals and their products for medicinal purposes has been documented since ancient times in civilizations from East Asia and Africa. In China, more than 1500 animals are used as medicine; in India, 15–20% of Ayurvedic medicine is based on animal-derived substances, whereas in Latin America, 584 medicinal animal species have been recorded. Ho Jun, a Korean court physician (1610 AD), wrote "Dongui-Bogam," which contains references to nearly 95 insects only and its substances. Recently, as such, there is an active study of the animal-based medicine. Animal-based medicines have been elaborated from parts of the animal body, from products of its metabolism (corporal secretions and excrements), or from nonanimal materials (nests and cocoons). Also, recently insects have proven to be very important as sources of drugs for modern medicine since they have immunological, analgesic, antibacterial, diuretic, anesthetic, and antirheumatic properties. Animals have been methodically tested by pharmaceutical companies as sources of drugs to the modern medical science. Regarding fish, several compounds have been extracted and these are employed as remedies in the official medicine. Toxins in snake, spider, centipede, and other species' venom have shown promise for treating chronic pain, heart conditions, blood clots, and type 2 diabetes. However, many animal medicines have not yet been tested for efficacy. To scale up production of such medicines at an industrial level, it is important to lay the scientific foundation to recognize them as potential therapeutics and to provide insights into their pharmacological activity and other relevant aspects; these studies may pave the way to develop new drugs that would potentially alleviate human suffering. Thus, new pharmacological therapeutic strategies, involving the use of animal-based medicinal products or compositions of multiple extracts, are being designed to specially act on biochemical targets.

In this special issue, investigators contribute original research articles and review articles that would facilitate the understanding of the basic mechanisms as well as the development of new and promising complementary and alternative strategies for the potential of animal-based medicinal products.

Y. Zhu et al. reported the seizures of chronic epilepsy rats injected by pentylenetetrazol-kindled through inhibiting the abnormal discharge of hippocampal neurons in epileptic rats. They suggested that treatment of epilepsy pill can effectively improve the spatial learning and memory ability of the epilepsy model. Also, the dingxian pills might interfere with epilepsy as well as cognitive dysfunction through the Egr3-GABRA4 signal, NRG1-ErbB4 signal, and ERK-Arc pathway. Thus, this may be a candidate for the treatment of convulsant.

H.-S. Lim et al. reported potential subacute toxicity of Mantidis Ootheca water extract during a 2-week repeated oral administration of doses of 0, 50, 150, or 450 mg/kg/day to C57BL/6 male mice by gavage. They suggested a 14-day

repeated oral dosing of Mantidis Ootheca extract to mice firstly resulted in a significant alteration in clinical signs, body weight, and hematological, biochemical, and histopathological parameters at doses of ≤450 mg/kg/day. The authors have judged that the Mantidis Ootheca is safe up to 450 mg/kg and is helpful in further development.

Then, T. Wang et al. confirmed the validation and stability of concentration analysis method of the Mecasin (Gamijakyakgamchobuja-Tang) preparations using high-performance liquid chromatography. They suggested that preparations at concentrations of 50 mg/ml and 200 mg/ml in sterilized distilled water were homogeneous and stable for 4 hours at room temperature and for 7 days in refrigerated conditions. This method for analyzing Mecasin preparations was deemed suitable. Additionally, this study promotes the development of reliable manufactured medicines and conduct of good research through definitive quality controls for Mecasin as a complex herbal medicine, with the aim of treating amyotrophic lateral sclerosis.

J. Tan et al. investigated the methanolic extract of *Aspongopus chinensis* can inhibit the proliferation of MDA-MB-453 and HCC-1937 cells by inducing cell cycle arrest; the oleic acid and palmitic acid were found to be the main compounds in *Aspongopus chinensis*. Their results suggested that *Aspongopus chinensis* can be a potential natural alternative or can provide a complementary therapy for breast cancer.

D. A. Putri et al. reported bioactive compounds in *Chromolaena odorata* with reactive oxygen species scavenging activity. Among the tested five extracts, the ethyl acetate extract exhibited the highest inhibitory effect against ABTS radical and α-glucosidase rat intestinal enzyme. Further investigations focus on the identification of the other active flavanone compounds responsible for the antioxidant as well as α-glucosidase inhibitory activity of *Chromolaena odorata* ethyl acetate extract. So, these beneficial active ingredients are thought to be able to be developed as a growth factor for insect breeding farms in the future.

D. Lee et al. reported that musk of muskrat protects neurons against focal cerebral ischemia in rats with functional restoration. In relation to the immunohistochemical studies, the effects of musk of muskrat may be due to their anti-inflammatory properties by inhibiting Cox-2 expression. Based on these findings, it is tempting to suppose that musk of muskrat could be considered as a substitute for musk of musk deer in view of the traditional use of stroke treatment. The authors concluded musk of muskrat a candidate for the treatment of focal cerebral ischemia.

T. Jiang et al. reported that *Scolopendra subspinipes mutilans* treatment improved mean arterial pressure, heart rate, central venous pressure, fatigue, palpitation, and shortness breath in the coronary heart disease patients. Meanwhile, *Scolopendra subspinipes mutilans* intervention reduced the levels of blood lactate, creatine kinase isoenzyme, serum troponin T, CRP, IL-1β, IL-6, and TNF-α, and malondialdehyde and increased superoxide dismutase level. Also, *Scolopendra subspinipes mutilans* treatment reduced the levels of IL-1β and IL-6 and increased the levels of IL-10 and TGF-β. *Scolopendra subspinipes mutilans* had better anti-inflammatory effects. *Scolopendra subspinipes mutilans* treatment increased the percentage of CD4 + CD25 + FoxP3 Treg cells and reduced the percentage of CD4 + IL-17 T cells. *Scolopendra subspinipes mutilans* ameliorated rheumatic heart disease by affecting the percentage of CD4 + CD25 + FoxP3 Treg and CD4 + IL17 T cells. Thus, this study may provide a new molecular mechanism for rheumatic heart disease treatment.

B. Gong et al. investigated the safety and efficacy of the Herbal Medicine C-117 formula in the treatment of carotid atherosclerosis-vulnerable plaques. After 180 days of medication, the plaque Crouse scores of the two groups were lower than before, and the total cholesterol and blood lipids decreased compared with those before treatment. The change of the C-117 formula group was statistically significant, but no significant differences were found when comparing groups after treatment. Although adverse events occurred during the 6-month treatment, there was no liver or kidney dysfunction, and all adverse events were associated with a weak correlation with the C-117 formula. Thus, they believe that the C-117 formula provided better results.

At present, the prevention and treatment of cardiovascular disease in the world are facing severe challenges. So, Xinmailong Injection, which is derived from the animal medicine Periplaneta Americana, has certain advantages in the clinical treatment of cardiovascular disease. S.-S. Lin et al. reported that Xinmailong Injection can protect cardiomyocytes and maintain the normal function of the heart in various ways, thus effectively preventing the development of cardiovascular disease. Therefore, Xinmailong Injection has great potential for clinical application, and more basic researches need to be carried out to explore the medicinal value of Xinmailong Injection.

In addition, L. Han et al. in a research article investigated that the zebrafish model provides a huge balance between scale and applicability. Based on this model, new gelatin has the protective effect on hematopoietic injury induced by chemotherapy, which is shown by its reversal effect on thrombocytopenia and erythrocyte reduction induced by chemotherapeutic drugs. Its mechanism may be related to the promotion of the expression of key hematopoietic factors.

J.-B. Zou et al. indicated that the combination of Kangfuxin liquid and proton pump inhibitors for treatment of patients with gastric ulcers could improve the total efficacy rate and that the efficacy rate and gastroscopy rate reduce adverse events and the recurrence rate. That study's importance stems from its inclusion of an extended meta-analysis and updated information, which have raised confidence in the effectiveness of Kangfuxin liquid.

We hope that the readers will be interested in animal-based medicinal products and that this special issue will attract the interest of the scientific community, thereby supporting further investigations that lead to the discovery of novel strategies and therapeutic medicinal products for use in the field of evidence-based traditional medicine.

Conflicts of Interest

The editors declare that they have no conflicts of interest regarding the publication of the special issue.

Acknowledgments

The guest editorial team would like to express gratitude to all the authors for their interest in selecting this special issue as a venue for disseminating their scholarly work. The editors also wish to thank the anonymous reviewers for their careful reading of the manuscripts submitted to this special issue and their many insightful comments and suggestions. The English proofreading of this article was supported by a grant on the Establishment of Application Base for Chung-bu Medicinal Materials Described in the Dong Ui Bo Gam (KSN1812410) from the Korea Institute of Oriental Medicine, Republic of Korea.

Gunhyuk Park
Yong-ung Kim
Irawan W. Kusuma

Hindawi
Evidence-Based Complementary and Alternative Medicine
Volume 2019, Article ID 1324969, 13 pages
https://doi.org/10.1155/2019/1324969

Review Article

Therapeutic Efficacy of Kangfuxin Liquid Combined with PPIs in Gastric Ulcer

Jun-Bo Zou,[1] **Xiao-Fei Zhang**,[1] **Ya-Jun Shi**,[1] **Jia Tai**,[1] **Yu Wang**,[1] **Yu-Lin Liang**,[1] **Fang Wang**,[2] **Jiang-Xue Cheng**,[1] **Jing Wang**,[1] **and Dong-Yan Guo**[1]

[1]*Shaanxi Province Key Laboratory of New Drugs and Chinese Medicine Foundation Research; Pharmacy College, Shaanxi University of Chinese Medicine, Xianyang, China*
[2]*Key Laboratory of Modern Prepararation of Traditional Chinese Medicine, Ministry of Education, Jiangxi University of Traditional Chinese Medicine, Nanchang, China*

Correspondence should be addressed to Ya-Jun Shi; 2051004@sntcm.edu.cn

Received 17 March 2019; Revised 20 June 2019; Accepted 9 July 2019; Published 30 September 2019

Guest Editor: Gunhyuk Park

Objective. To evaluate the clinical efficacy and safety of Kangfuxin liquid (KFX) combined with proton pump inhibitors (PPIs) in the treatment of gastric ulcer (GU). *Materials and Methods*. Electronic databases including PubMed, Wanfang, CNKI, VIP, Embase, Cochrane Library, and CBM were examined for appropriate articles without language limitations on key words before March 10, 2019. RevMan 5.3 software was applied to execute outcome assessment and finish the meta-analysis. *Results*. 22 articles involving 2,024 patients with a gastric ulcer were selected. Total efficacy rate and efficacy rate of gastroscopy were significantly enhanced for the combination of KFX with PPIs compared to those of PPI treatment alone (OR = 6.95, 95% CI: 4.87, 9.91, $P < 0.00001$; OR = 2.96, 95% CI: 1.98, 4.42, $P < 0.00001$, respectively). Same results were found for different PPIs in combination on total efficacy rate, respectively. The combination also significantly reduced the adverse events (OR = 0.39, 95% CI: 0.22, 0.70, $P = 0.002$). In addition, KFX combined with PPI could suppress the inflammation (MD = −6.11, 95% CI: −7.45, −4.77, $P < 0.00001$), reduce the recurrence rate (OR = 0.31, 95% CI: 0.14, 0.70, $P = 0.005$), and enhance the clearance rate of *Helicobacter pylori* (HP, OR = 3.76, 95% CI: 1.80, 7.87, $P = 0.0004$). It seemed like the combination would influence immune function by increasing levels of T-lymphocyte subsets CD4 and CD8 but not CD3 (MD = 2.40, 95% CI: 1.25, 3.55, $P < 0.0001$); MD = 25.72, 95% CI: 14.55, 36.90, $P < 0.00001$; MD = 0.72, 95% CI: −0.66, 2.09, $P = 0.31$, respectively). *Conclusion*. KFX combined with PPIs in treatment of patients with GU could improve the total efficacy rate and efficacy rate of gastroscopy and reduce adverse events and the recurrence rate. However, the results of this study should be handled with care due to the limitations. Several rigorous RCTs are in need to confirm these findings.

1. Introduction

Peptic ulcer (PU) is a common and prevalent disease worldwide. Infection of *Helicobacter pylori* (HP), nonsteroidal anti-inflammatory drugs (NSAIDs), and aspirin drug usage are considered to be the major causative factors of PU. Taking other medications including glucocorticoids, some antitumor drugs, and anticoagulant drugs is also inducements for PU, which cannot be neglected [1]. Prevalence rates of PU reach up to 5%–10% in 2009 [2] and continue to rise due to unhealthy lifestyle, drug usage, and diet custom. Gastric ulcer (GU) is one of the common types appearing mostly in middle-aged and elderly people [3].

Suppressing gastric acid production is the most important measure to relieve clinical symptoms and promote healing. Proton pump inhibitors (PPIs) are the initial therapy for GU [4]. The first generation PPIs includes omeprazole, pantoprazole, and lansoprazole. The second generation PPIs including esomeprazole, ilaprazole, and rabeprazole have faster onset time, longer action time, and fewer side effects. PPIs are the best drugs for treating acid-related diseases in the last dozen years. The medication

amount of PPIs in domestic hospitals of 16 key cities in China reached 4.5 billion yuan in 2016 with an increase of 6% over the previous year, and it still presents a rising trend [5]. But long-term use of PPIs can cause a series of new safety issues, such as adverse renal effects [6], hypomagnesaemia [7], increased risk of dementia [8], increased risk of infection and osteoporosis [9], fracture risk [10], vitamin B12 deficiency, occurrence or development of atrophic gastritis, interstitial nephritis, microscopic colitis, increased risk of serious skin allergy, and so on [11, 12]. Combination with traditional Chinese medicine provides an alternative to improve the current situation of PPI usage.

Kangfuxin liquid (KFX) is a Chinese patent medicine extracted from *Periplaneta americana*. China Food and Drug Administration (CFDA) approved it in 1998. As an animal medicine, amino acids are considered as the main ingredients which are used as quality control for preparation. Efficacy of KFX is described as promoting blood circulation, nourishing yin, and promoting granulation. For oral administration, it is used for gore block, stomach bleeding, gastric and duodenal ulcers, phthisis with yin deficiency, and aiding in the treatment of tuberculosis. For external application, it is used for treating incised wound, trauma, ulcers, fistula, burns, and bedsore. Amounts of clinical trials have demonstrated that KFX is beneficial to cure GU [13–15], which is also supported by animal experiments [16]. Previous meta-analysis confirmed that KFX combined with PPIs was superior to PPIs alone in the treatment of GU [17, 18]. We provide an updated and extended meta-analysis with detailed information for efficacy (Figure 1).

2. Methods and Program

2.1. Literature Retrieval Strategy. Keywords "kangfuxin (KFX)" [Title/Abstract] OR "*Periplaneta americana*" [Title/Abstract] AND "Gastric ulcer" [Title/Abstract] OR "peptic ulcer" [Title/Abstract] OR "digestive ulcer" [Title/Abstract] OR "PPI" (including Esomeprazole, Omeprazole, Lansoprazole, Rabeprazole, Pantoprazole) [Title/Abstract] were used as search items in electronic databases including PubMed, Wanfang, CNKI, VIP, Embase, Cochrane Library, and CBM. Articles published before March 10, 2019, was examined without language limitations in order to obtain a comprehensive retrieval. All relevant articles were downloaded into EndNote software (version X7, Thomson Reuters, Inc., New York, USA) for further exploration. Duplicate records were integrated. Full-text review was performed while the title/abstract was thought to be thematic. The job above was executed by two investigators independently. Conflicts were resolved by consensus and discussion.

2.2. Inclusion and Exclusion Criteria. Based on the suggestions of a gastroenterologist, we designed the inclusion criteria as follows: (1) Patients in RCTs diagnosed as having gastric ulcers by meeting the criteria of Diagnosis and Treatment of Digestive Ulcer Disease (DTDUD) version 2016, 2013, 2008, or Practical Clinical Diagnosis and Treatment of Digestive Disease (PCDTDD, part 1) version 2005, or the Guiding Principle of Clinical Research of new TCM on the Treatment of Peptic Ulcer (GPCRTPU), or Diagnostics of Digestive Diseases (DDD) version 2006 [19], or carrying out gastroscopy. (2) All trials mentioned were confined as RCTs. (3) Patients in treatment groups received KFX solution combined with PPI while control groups received PPI alone. (4) The total efficacy rate was the least outcome measurement to be reported.

We also designed the exclusion criteria as follows: (1) References such as reviews, case reports, animal experiments, comments, and so on that are thought to be athematic. (2) The diagnostic standard in the statement was ambiguous. (3) Trials emphasized on other peptic ulcers but not gastric ulcer. (4) Trials mentioned other interventions of essential treatment to GU but not only PPI alone.

2.3. Characteristics of Study Assessment. Information including methods, participants, interventions, and outcomes was extracted and arranged (Tables 1 and 2). Characteristics of included studies were assessed by two searchers independently according to the Cochrane Handbook for Systematic Reviews of Interventions [41]. Disagreement was resolved by the consensus. Risk of bias was evaluated as follows: random sequence generation (A, selection bias), allocation concealment (B, selection bias), blinding of participants and personnel (C, performance bias), blinding of outcome assessment (D, detection bias), incomplete outcome data (E, attrition bias), selective reporting (F, reporting bias), and other biases (G). Three levels were applied to judge the quality of each item. "Low risk" indicates description of methods or procedures was adequate while "high risk" means not adequate or incorrect and "unclear risk" means missing description.

2.4. Data Analysis. Data analysis was performed using Review Manager 5.3 (Cochrane Collaboration). Outcome indices such as total efficacy rate and efficacy rate of gastroscopy were regarded as dichotomous variables and presented as the odds ratio (OR) with 95% confidence intervals (95% CI). Levels of inflammatory cytokines such as IL-6, TNF-α, and TGF-β1 and T-lymphocyte subsets including CD3, CD4, and CD8 were continuous variables which were presented as the mean difference (MD) with 95% CI. Q statistic and I^2 tests were applied to assess the heterogeneity among studies. A fixed-effects model was used to analyze data with low heterogeneity ($P > 0.1$ and $I^2 \leq 50\%$), while a random-effects model was used to analyze data with high heterogeneity ($P < 0.1$ or $I^2 > 50\%$). Potential publication bias was revealed by funnel plots.

3. Results

3.1. Characteristics of the Eligible Studies. Six hundred eighty-eight articles were identified through database searching, in which 386 articles were removed as duplicates.

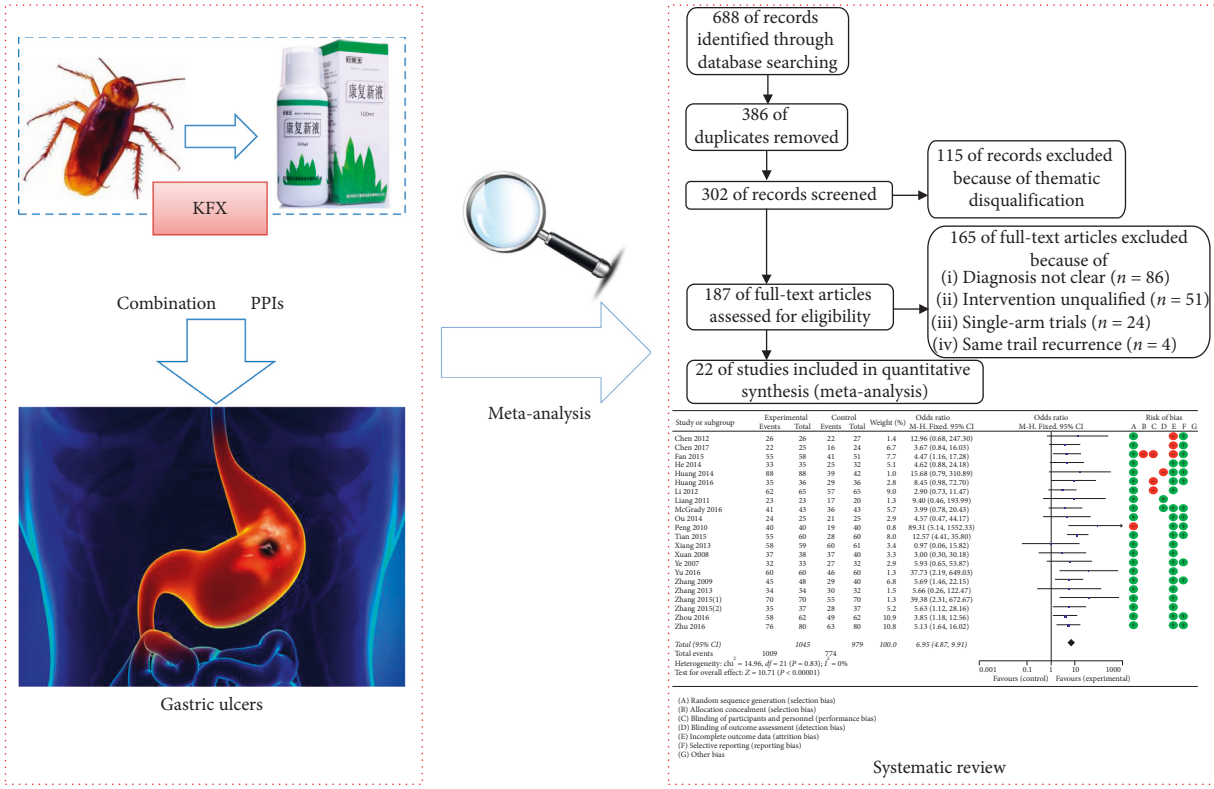

Figure 1: Work flow of the present study.

115 articles in 302 remaining were excluded on thematic disqualification. Then, 187 articles remained for further full-text review. 165 studies were excluded in this procedure for the following reasons: diagnosis in 86 articles was vague, 51 studies mentioned unfit interventions, 24 studies were single-arm designs, and 4 articles were the recurrence of the same trial. 22 studies [20–40, 42] were included in quantitative synthesis finally (Figure 2).

Two thousand twenty-four patients with a gastric ulcer (1045 cases in the experimental group and 979 cases in the control group) were taken in this meta-analysis. The age of the patients ranged from 17 to 75 years, and there was no obvious difference in terms of age and sex between the two groups (Table 1). Trials were conducted between 2007 and 2017, and all were RCTs with a comparison between a combination of KFX solution and PPI and PPI treatment alone. 4 studies [20, 21, 22, 23] reported the combination with esomeprazole, 5 with omeprazole [24–27, 39], 3 with lansoprazole [28–30], 3 with rabeprazole [31–33], and 7 with pantoprazole [34–38, 40, 42]. The treatment duration ranged from 1 to 4 weeks, and 2 articles [24, 40] reported a follow-up which ranged from half a year to 1 year. 10 trials [22, 26, 27, 29, 34, 36, 38–40, 42] reported adverse events and side effects. All trials reported a total efficacy rate in outcome measures, 15 studies [20–24, 27–32, 34, 35, 37, 38] reported the efficacy rate of gastroscopy, 3 studies [25, 34, 39] reported the clearance of HP, 2 studies [24, 39] reported the recurrence rate, and 2 trials [29, 34] reported the levels of inflammatory cytokines and T-lymphocyte subsets (Table 2).

3.2. Quality of Included Trials Assessment. According to the Cochrane risk of bias estimation, all trials mentioned a randomized allocation of participants while 1 trial used a wrong method, so the selection bias (A) on random sequence generation was considered to be "low risk." Detailed information on allocation concealment, blinding of participants and personnel, and blinding of outcome assessment of all studies was ambiguous even wrong, from which the selection bias (B) on allocation concealment, performance bias (C), and detection bias (D) were identified as "unclear risk." All experimental data included in articles were complete, so the attrition bias (E) and reporting bias (F) were considered to be low for 22 trials. There was insufficient information to assess the existence of other significant risk of bias, so other bias (G) of included trials were determined as "unclear risk."

3.3. Outcome Measures with Subgroup Analysis

3.3.1. Total Efficacy Rate of KFX Combined with PPI versus PPI Alone. Total efficacy rate generally consists of grade of 6 clinical symptoms as follows: epigastric pain, belching, acid regurgitation, heartburn, satiety, nausea, and vomiting. Mark was given by assessing the severity and frequency of each item. For severity assessment, 0 points means asymptomatic, 1 point means symptoms were mild, 2 points between 1 and 3, and 3 points means symptoms were unbearable. For judgment of frequency, 0 points means asymptomatic, 1 point means the symptom have onset every

Table 1: Characteristics of eligible studies.

Author and published year (references)	Cases T/C	Diagnostic standard	Age (years), range, mean	Sex (male/female)
Li, 2012 [20]	65/65	DTDUD (2008)	T: 24–69, 43.2 C: 22–70, 41.3	T: 45/20 C: 47/18
Xiang, 2013 [21]	59/61	GPCRTPU	T: 39.4 C: 40.7	NR
Zhang, 2009 [22]	25/24	DDD (2006)	T: 27–52, 38 C: 29–58, 39	T: 16/9 C: 13/11
Zhang, 2013 [23]	34/32	Gastroscopy	T: 24–68, 34 C: 20–65, 32	T: 20/14 C: 19/13
Huang, 2014 [24]	88/42	Gastroscopy	T: 18–60, NR C: 18–60, NR	NR
Huang, 2016 [25]	36/36	DTDUD (2013)	T: 29–76, 35.6 C: 28–74, 35.5	T: 21/15 C: 20/16
McGrady, 2016 [26]	43/43	DTDUD (2013)	T: 20–65, 35.6 C: 20–66, 36.1	T: 28/15 C: 25/18
Xuan, 2008 [27]	38/40	Gastroscopy	T: 20–65, NR C: 20–65, NR	NR
Zhu, 2016 [28]	80/80	Gastroscopy	T: 23–67, 38.9 C: 19–65, 39.4	T: 52/28 C: 49/31
Zhou, 2016 [29]	62/62	Gastroscopy	T: 47.2 C: 46.4	T: 37//25 C: 36/26
He, 2014 [30]	35/32	Gastroscopy	T: 18–72, 43 C: 20–75, 45	T: 23/12 C: 22/10
Chen, 2012 [31]	26/27	Gastroscopy	24–78, 61.5	28/25
Ou, 2014 [32]	25/25	Gastroscopy	25–60, 45	26/24
Yu, 2016 [33]	60/60	DTDUD (2013)	18–70, NR	T: 40/20 C: 42/18
Chen, 2017 [15]	25/24	DTDUD (2016)	T: 27–67, 44.5 C: 26–68, 45.2	T: 14/11 C: 15/9
Fan, 2015 [34]	58/51	Gastroscopy	T: 43.8 C: 42.6	T: 29/29 C: 30/21
Liang, 2011 [35]	23/20	Gastroscopy	T: 31–77, 49.1 C: 27–72, 46.6	T: 15/8 C: 11/9
Peng, 2010 [36]	40/40	Gastroscopy	T: 19–43, 33.5 C: 19–42, 32.4	T: 26/14 C: 28/12
Tian, 2015 [37]	60/60	PCDTDD (2005)	T: 17–67, 34.5 C: 19–71, 33.5	T: 42/18 C: 40/20
Ye, 2007 [38]	33/32	Gastroscopy	T: 20–63, 38.5 C: 20–65, 39.8	NR
Zhang, 2015 [39]	70/70	NR	T: 23–72, 45.2 C: 25–70, 43.3	T: 42/28 C: 43/27
Zhang, 2015 [40]	37/37	Gastroscopy	T: 29–72, 34.7 C: 28–75, 35.8	T: 26/11 C: 24/13

T, trial group; C, control group; NR, no report.

3~4 days while 2 points means every 2 days, and 3 points means each day. The aggregate score was further divided into three levels: excellent, efficacious, and inefficient. All studies reported the total efficacy rate. A meta-analysis of these trials using a fixed-effect model demonstrated that KFX combined with PPI treatment significantly improved the total efficacy rate in the treatment of gastric ulcers (OR = 6.95, 95% CI: 4.87, 9.91; $P < 0.00001$). There was no statistically significant heterogeneity among individual trials ($P = 0.83$, $I^2 = 0\%$). Risk of bias of each study is also listed (Figure 3). Further investigation was taken to explore the effectiveness of KFX combined with different PPIs for treating gastric ulcers. The total efficacy rate of KFX combined with omeprazole was significantly improved compared to omeprazole treatment alone (OR = 5.63, 95% CI: 2.35, 13.50; $P = 0.0001$). No statistically significant heterogeneity was found among individual studies ($P = 0.90$, $I^2 = 0\%$). Same results were found for the other PPIs as follows: KFX combined with esomeprazole (OR = 3.70, 95% CI: 1.57, 8.72; $P = 0.003$), heterogeneity ($P = 0.69$, $I^2 = 0\%$). KFX combined with lansoprazole (OR = 4.51, 95% CI: 2.16, 9.04; $P < 0.0001$), heterogeneity ($P = 0.94$, $I^2 = 0\%$). KFX combined with rabeprazole (OR = 14.43, 95% CI: 3.35, 62.14; $P = 0.0003$), heterogeneity ($P = 0.49$, $I^2 = 0\%$). KFX combined with pantoprazole (OR = 10.93, 95% CI: 5.96, 20.07; $P < 0.00001$), heterogeneity ($P = 0.32$, $I^2 = 15\%$). All meta-analyses above were analyzed using a fixed-effect model (Figure 4).

Table 2: Intervention characteristics of included studies.

Study ID (name, year)	Intervention		Duration/ follow-up	Adverse events	Outcome measures
	Trial group	Control group (essential treatment)			
Li, 2012 [20]	KFX, 10 mL, TID + essential treatment	Esomeprazole, 40 mg, QD, Po	4 weeks/NR	NR	Total efficacy rate, efficacy rate of gastroscopy
Xiang, 2013 [21]	KFX, 10 mL, TID + essential treatment	Esomeprazole, 40 mg, QD, Po	4 weeks/NR	NR	Total efficacy rate, efficacy rate of gastroscopy
Zhang, 2009 [22]	KFX, 10 mL, TID + essential treatment	Esomeprazole, 40 mg, QD, Po	4 weeks/NR	T: 2 cases nausea, 1 case diarrhea; C: 2 cases nausea	Total efficacy rate, efficacy rate of gastroscopy
Zhang, 2013 [23]	KFX, 10 mL, TID + essential treatment	Esomeprazole, 20 mg, QD, Po	4 weeks/NR	NR	Total efficacy rate, efficacy rate of gastroscopy
Huang, 2014 [24]	KFX, 10 mL, TID + essential treatment	Omeprazole, 20 mg, BID, Po	4 weeks/1 year	NR	Total efficacy rate, efficacy rate of gastroscopy, recurrence rate
Huang, 2016 [25]	KFX, 10 mL, TID + omeprazole, 20 mg, QD, Po	Omeprazole, 20 mg, BID, Po	T: 28 days/NR C: 14 days/NR	NR	Total efficacy rate, clearance rate of HP
McGrady, 2016 [26]	KFX, 10 mL, TID + essential treatment	Omeprazole, 20 mg, BID, Po	4 weeks/NR	T: 1 case headache, 1 case nausea; C: 3 cases headache, 2 cases nausea, 2 cases constipation	Total efficacy rate
Xuan, 2008 [27]	KFX, 10 mL, TID + omeprazole, 20 mg, QD, Po	Omeprazole, 20 mg, BID, Po	4 weeks/NR	T: 1 case rash over axillae; C: 1 case insomnia	Total efficacy rate, efficacy rate of gastroscopy
Zhu, 2016 [28]	KFX, 10 mL, TID + essential treatment	Lansoprazole, 30 mg, QD, Po	2 weeks/NR	NO	Total efficacy rate, efficacy rate of gastroscopy
Zhou, 2016 [29]	KFX, 10 mL, TID + essential treatment	Lansoprazole, 30 mg, QD, Po	4 weeks/NR	T: 2 cases dizziness and diarrhea; C: 11 cases nausea and diarrhea	Total efficacy rate, efficacy rate of gastroscopy, inflammatory cytokines, T-lymphocyte subsets
He, 2014 [30]	KFX, 10 mL, TID + essential treatment	Lansoprazole, 30 mg, QD, Po	4 weeks/NR	NO	Total efficacy rate, efficacy rate of gastroscopy
Chen, 2012 [31]	KFX, 10 mL, TID + essential treatment	Rabeprazole, 10 mg, QD, Po	4 weeks/NR	NR	Total efficacy rate, efficacy rate of gastroscopy
Ou, 2014 [32]	KFX, 10 mL, TID + essential treatment	Rabeprazole, 10 mg, QD, Po	5 weeks/NR	NR	Total efficacy rate, efficacy rate of gastroscopy
Yu, 2016 [33]	KFX, 10 mL, TID + essential treatment	Rabeprazole, 20 mg, QD, Po	3 weeks/NR	NR	Total efficacy rate
Chen, 2017 [15]	KFX, 10 mL, TID + essential treatment	Pantoprazole, 40 mg, BID, Po	2 weeks/NR	T: 1 case rash; C: 2 cases nausea, 1 case rash	Total efficacy rate
Fan, 2015 [34]	KFX, 10 mL, TID + essential treatment	Pantoprazole, 40 mg, QD, Po	4 weeks/NR	T: NO; C: 5 cases diarrhea	Total efficacy rate, efficacy rate of gastroscopy, inflammatory cytokines, T-lymphocyte subsets, clearance rate of HP
Liang, 2011 [35]	KFX, 10 mL, TID + essential treatment	Pantoprazole, 40 mg, BID, intravenous drip	2 weeks/NR	NR	Total efficacy rate, efficacy rate of gastroscopy
Peng, 2010 [36]	KFX, 10 mL, TID + essential treatment	Pantoprazole, 40 mg, BID, Po	10 days/NR	T: 1 case diarrhea; C: 2 cases diarrheoa, 1 case bellyache	Total efficacy rate

Table 2: Continued.

Study ID (name, year)	Intervention		Duration/ follow-up	Adverse events	Outcome measures
	Trial group	Control group (essential treatment)			
Tian, 2015 [37]	KFX, 10 mL, QD + essential treatment	Pantoprazole, 40 mg, QD, Po	1 month/NR	NR	Total efficacy rate, efficacy rate of gastroscopy
Ye, 2007 [38]	KFX, 10 mL, TID + essential treatment	Pantoprazole, 40 mg, QD, Po	4 weeks/NR	T: 4 cases digestive symptoms; C: 3 cases digestive symptoms	Total efficacy rate, efficacy rate of gastroscopy
Zhang, 2015 [39]	KFX, 10 mL, TID + essential treatment	Pantoprazole, 40 mg, BID, intravenous drip	1 week/half a year	T: 1 case diarrhea; C: 2 cases diarrhea, 1 case headache, 1 case rash	Total efficacy rate, recurrence rate
Zhang, 2015 [40]	KFX, 10 mL, TID + omeprazole, 20 mg, QD, Po	Omeprazole, 20 mg, BID, Po	T: 4 weeks/NR C: 2 weeks/NR	T: 2 case diarrhea; C: NO	Total efficacy rate, clearance rate of HP

QD, once a day; BID, twice a day; TID, three times a day; KFX, Kangfuxin Solution; Po, oral administration; HP, *Helicobacter pylori*; NR, no report.

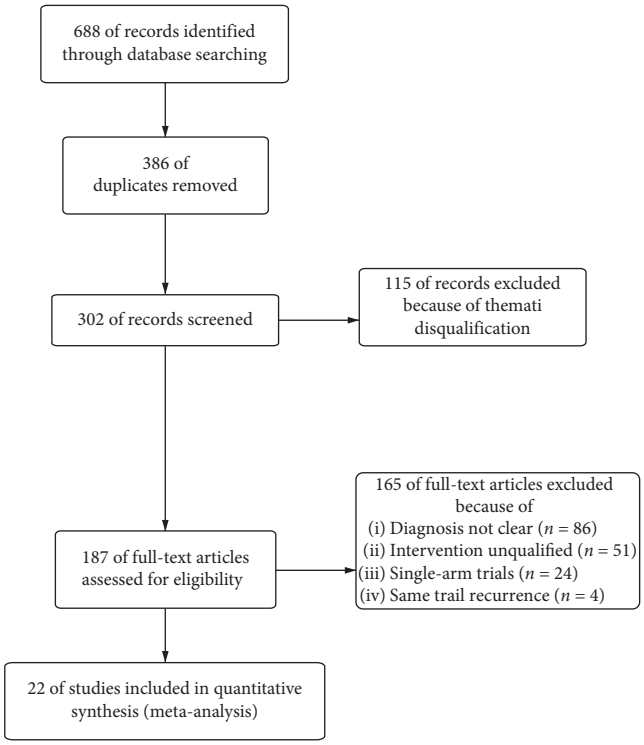

Figure 2: Process of the study extracted for the meta-analysis.

3.3.2. KFX Combined Different PPIs on Efficacy Rate of Gastroscopy versus PPI Alone. Criteria for judging the efficacy rate of gastroscopy were set as follows: clinical recovery was defined as that inflammation surrounding ulcer disappeared or the ulcer was scar over; the excellent effectiveness was identified as that ulcer disappeared but inflammation still existed; the efficacious effectiveness was defined as that the area of ulcer narrowed more than 50% or only a small amount of moss film attached to ulcer; and inefficient effect was that the area of ulcer narrowed less than 50% or no obvious change observed compared to prior treatment. 12 of 15 articles [22–24, 27, 28, 30–32, 34, 35, 37, 38] provided the efficacy rate of gastroscopy properly. A fixed-effect model demonstrated that KFX combined with PPI therapy significantly improved the efficacy rate of gastroscopy (OR = 2.96, 95% CI: 1.98, 4.42; $P < 0.00001$). No statistically significant heterogeneity was found among individual studies ($P = 0.77$, $I^2 = 0\%$). 2 trials [24, 27] provided the combination of KFX and omeprazole treatment versus omeprazole alone; a fixed-effect model meta-analysis demonstrated that the combination significantly improved the efficacy rate of gastroscopy (OR = 6.28, 95% CI: 1.32, 28.89; $P = 0.02$) with heterogeneity ($P = 0.40$, $I^2 = 0\%$). 2 studies [22, 23] reported the combination of KFX and esomeprazole treatment (OR = 5.11, 95% CI: 1.38, 18.96; $P = 0.01$) with heterogeneity ($P = 0.69$, $I^2 = 0\%$). 2 studies [28, 30] reported the combination of KFX and lansoprazole treatment (OR = 3.85, 95% CI: 1.58, 9.39; $P = 0.003$) with heterogeneity ($P = 0.73$, $I^2 = 0\%$). 2 studies [31, 32] reported the combination of KFX and rabeprazole treatment (OR = 7.26, 95% CI: 1.25, 42.24; $P = 0.03$) with heterogeneity ($P = 0.54$, $I^2 = 0\%$). 4 studies [34, 35, 37, 38] reported the combination of KFX and pantoprazole treatment (OR = 1.87, 95% CI: 1.08, 3.24; $P = 0.02$) with heterogeneity ($P = 0.87$, $I^2 = 0\%$). A fixed-effect model was applied to finish the above-mentioned meta-analysis (Figure 5).

3.3.3. Adverse Events. Ten trials provided descriptions on adverse events generally including nausea, diarrhea, headache, constipation, rash, insomnia, dizziness, and bellyache (Table 2). A fixed-effect model analysis certified that the combination of KFX and PPI treatment reduced clinical adverse events significantly (OR = 0.39, 95% CI: 0.22, 0.70; $P = 0.002$). No statistically significant heterogeneity was found among individual studies ($P = 0.41$, $I^2 = 3\%$; Figure 6).

3.3.4. Inflammatory Cytokines. Two trials [29, 34] reported the anti-inflammatory effects of KFX combined with PPI therapy versus PPI treatment alone. The serum contents of TNF-α, IL-6, and TGF-β1 were the common indices provided by the 2 studies. The pooled analysis (using a random-effect model) demonstrated that KFX combined with PPI treatment significantly relieved the inflammation of patients compared to PPI therapy alone (MD = −6.11, 95% CI: −7.45,

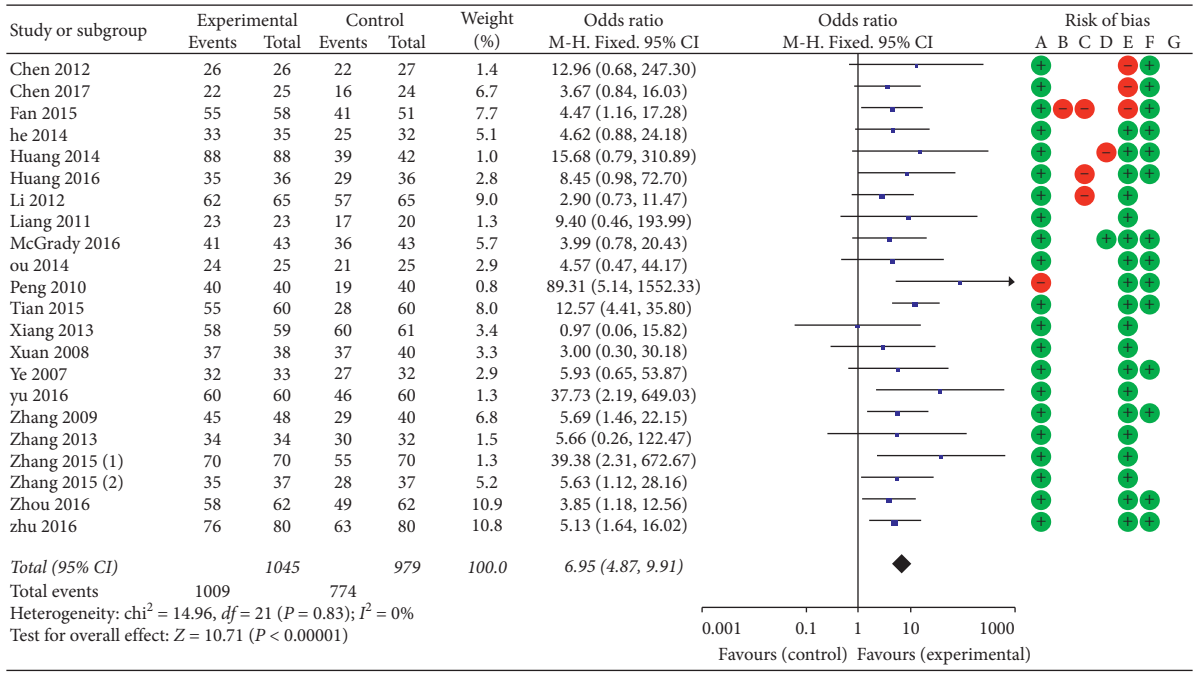

FIGURE 3: Forest plot of the total efficacy rate in patients treated with KFX + PPI and PPI alone and risk of bias. I^2 and P are the criteria for the heterogeneity test; ◆, pooled odds ratio; —■—, odds ratio; and 95% CI. Quality assessment was conducted by Review Manager 5.3 according to Cochrane Handbook for Systematic Reviews of Interventions version 5.1.0. Red circle, high risk of bias; green circle, low risk of bias; and blank, unclear risk of bias.

−4.77; $P < 0.00001$). Statistically significant heterogeneity was observed among individual studies ($P = 0.0002$, $I^2 = 80\%$). The further investigation was taken in subgroups. Combination treatment significantly reduced the serum content of TNF-α (MD = −6.10, 95% CI: −7.83, −4.37; $P < 0.00001$). No statistically significant heterogeneity was observed among individual studies ($P = 0.21$, $I^2 = 35\%$). Influence of combination on IL-6 was reported as (MD = −4.91, 95% CI: −6.55, −3.27; $P < 0.00001$). Statistically significant heterogeneity ($P = 0.05$, $I^2 = 75\%$) was observed among individual studies. Influence of combination on TGF-β1 was provided as (MD = −8.84, 95% CI: −15.30, −2.38; $P < 0.007$) with heterogeneity ($P = 0.0002$, $I^2 = 93\%$; Figure 7). In consideration of the 2 trials reported KFX combined with lansoprazole and pantoprazole separately, the significant heterogeneity may be mainly generated by the different clinical treatments.

3.3.5. T-Lymphocyte Subsets. T-lymphocyte subset, which is the crucial index of immune function, was provided in 2 studies [29, 34]. There was heterogeneity in the index of CD8. Therefore, a random-effect model was used. There was no heterogeneity in the indices of CD3 and CD4; the fixed-effect model was thus used. The MD with 95% CI of serum CD3, CD4, and CD8 levels were (MD = 0.72, 95% CI: −0.66, 2.09; $P = 0.31$), (MD = 2.40, 95% CI: 1.25, 3.55; $P < 0.0001$), and (MD = 25.72, 95% CI: 14.55, 36.90; $P < 0.00001$), respectively. There was no difference between the experimental group and control group ($P = 0.12$; Figure 8).

3.3.6. Recurrence Rate. Two trials [24, 39] reported the recurrence rate in treatment. A meta-analysis (using a fixed-effect model) demonstrated that KFX combined with PPI significantly reduced the recurrence rate compared to PPI therapy alone (OR = 0.31, 95% CI: 0.14, 0.70; $P = 0.005$). No statistically significant heterogeneity was found among individual studies ($P = 0.77$, $I^2 = 0\%$; Figure 9(a)).

3.3.7. Clearance Rate of HP. Helicobacter Pylori (HP) was thought to be the mainly inducing factor of GU. 3 studies [25, 34, 39] provided the clearance rate of HP in clinical treatment. A fixed-effect model analysis proved that the combination of KFX and PPI treatment enhanced the clearance of HP significantly (OR = 3.76, 95% CI: 1.80, 7.87; $P = 0.0004$). No statistically significant heterogeneity was found among individual studies ($P = 0.62$, $I^2 = 0\%$; Figure 9(b)).

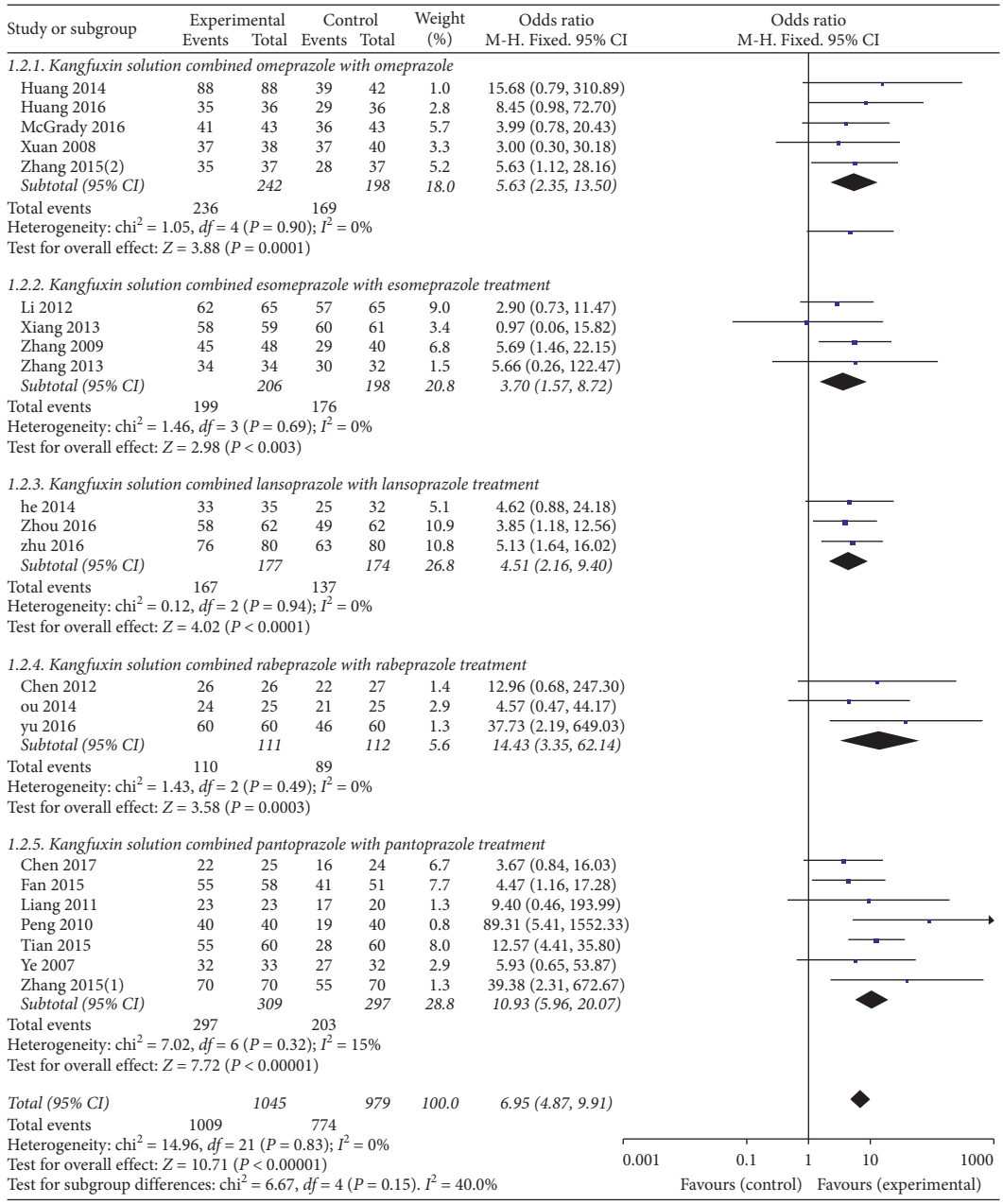

Figure 4: Forest plot of the total efficacy rate in patients treated with KFX + different PPI and PPI alone. I^2 and P are the criteria for the heterogeneity test; ◆, pooled odds ratio; —■—, odds ratio; and 95% CI.

3.3.8. Publication Bias. A funnel plot was used to express publication bias. When the indices were provided by more than 9 cases, the publication was explored. In the present study, the funnel plot of combination of KFX and PPIs versus PPIs therapy alone on total efficacy rate and adverse events was applied. The plots were generally symmetric, suggesting that there was no obvious publication bias (Figures 10(a) and 10(b)).

4. Discussion

"No acid, no ulcer" said by Schwartz indicated that excessive gastric acid secretion and GU are highly related. PPIs are the very class of medicines that are invited to decrease gastric acid secretion via inhibiting the H^+/K^+-ATP pump of the parietal cell. United States Food and Drug Administration (FDA) approved the first PPI omeprazole in 1980s. Today, 5 other PPIs are also employed to treat a variety of acid-related conditions such as duodenal ulcers, gastric ulcers, and *Helicobacter pylori* eradication. PPIs are widely accepted to be the most effective treatment for symptom relief of gastro-oesophageal reflux [43–45]. Due to its good effect and the growing number of PPIs available over-the-counter, market of PPIs booms rapidly. However, accompanied by continuous appearance of adverse effects we discussed earlier, some scholars expressed concern about unnecessary use of PPIs which is so high in their latest review [46]. The huge market sales in China suggest that the consumption of PPIs

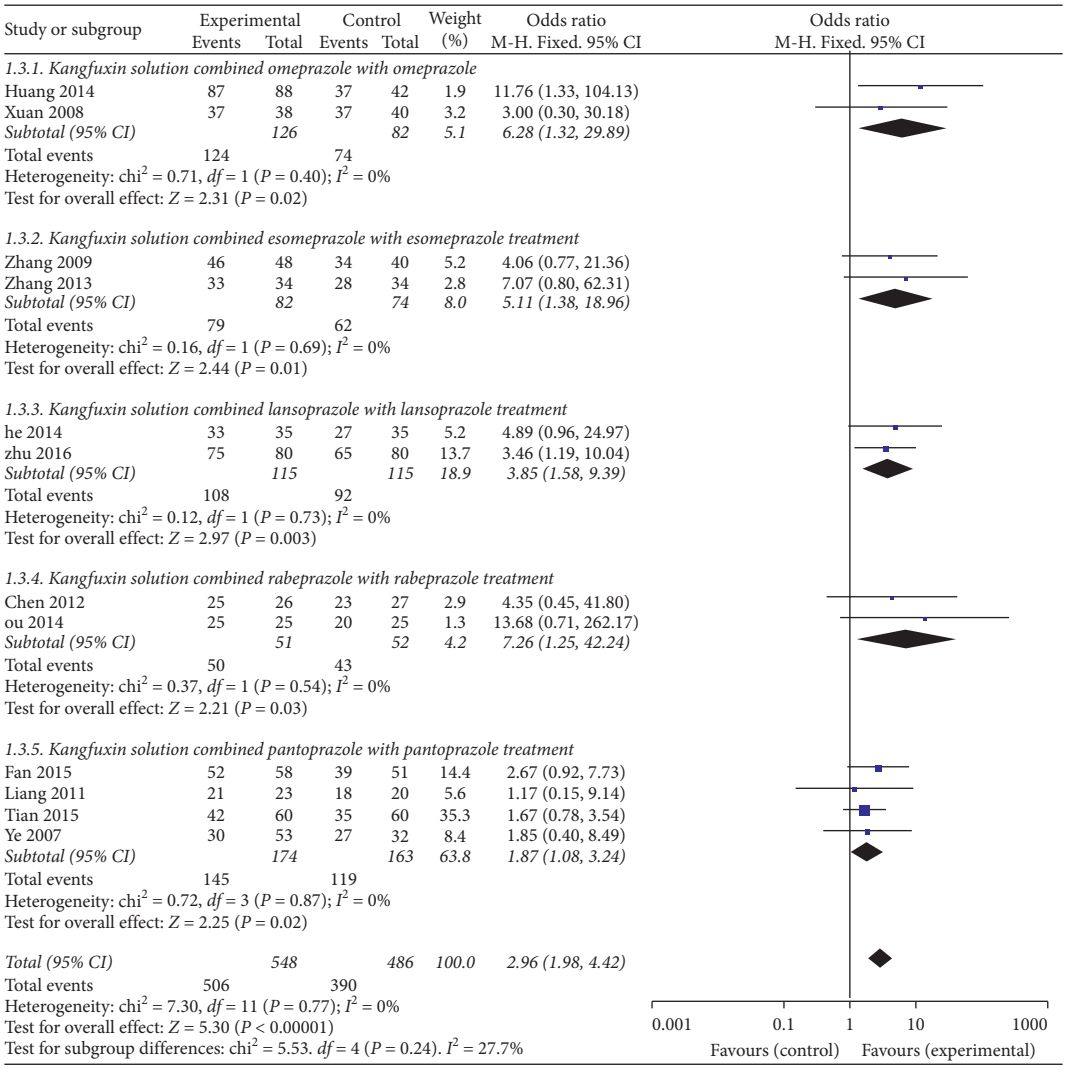

Figure 5: Forest plot of the efficacy rate of gastroscopy in patients treated with KFX + different PPI and PPI alone. I^2 and P are the criteria for the heterogeneity test; ◆, pooled odds ratio; —■—, odds ratio; and 95% CI.

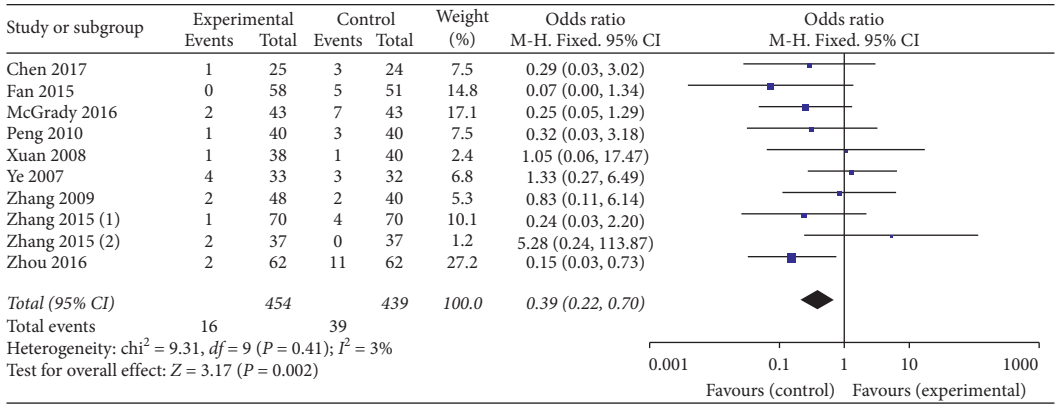

Figure 6: Forest plot of adverse events in patients treated with KFX + PPI and PPI alone. I^2 and P are the criteria for the heterogeneity test; ◆, pooled odds ratio; —■—, odds ratio; and 95% CI.

is very enormous [5]. Scholars in China also put an immense concern on overmedication of PPIs [11]. Actions should be taken to pull back PPIs to the road of rational drug use.

Periplaneta americana also known as cockroach is an insect of *Blattodea* recorded most early in "Sheng Nong's herbal classic." It was classified as middle grade. CFDA has

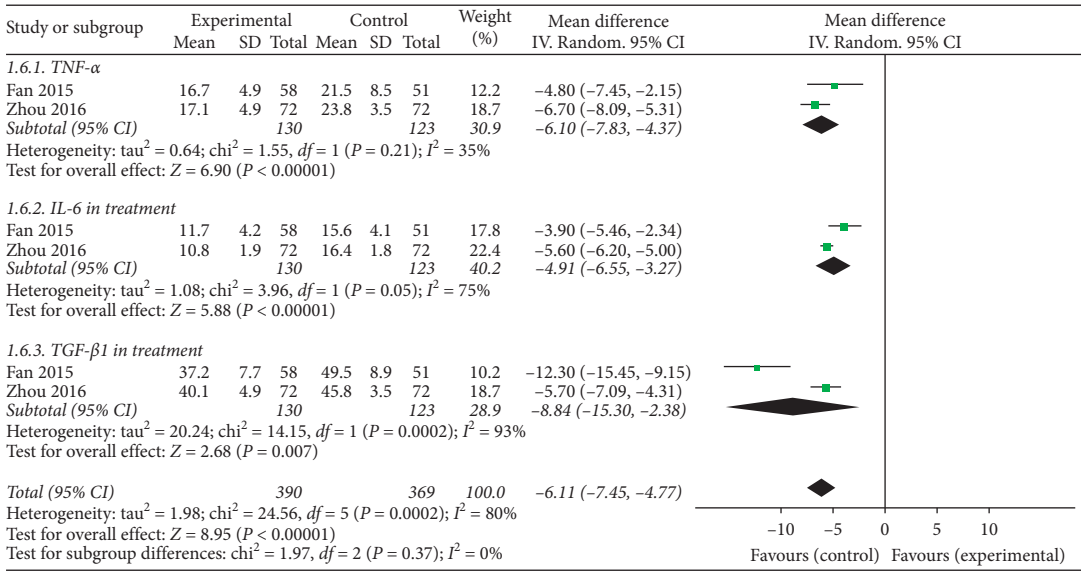

Figure 7: Forest plot of inflammation cytokines in patients treated with KFX + PPI and PPI alone. I^2 and P are the criteria for the heterogeneity test; ◆, pooled mean difference; —■—, mean difference; and 95% CI.

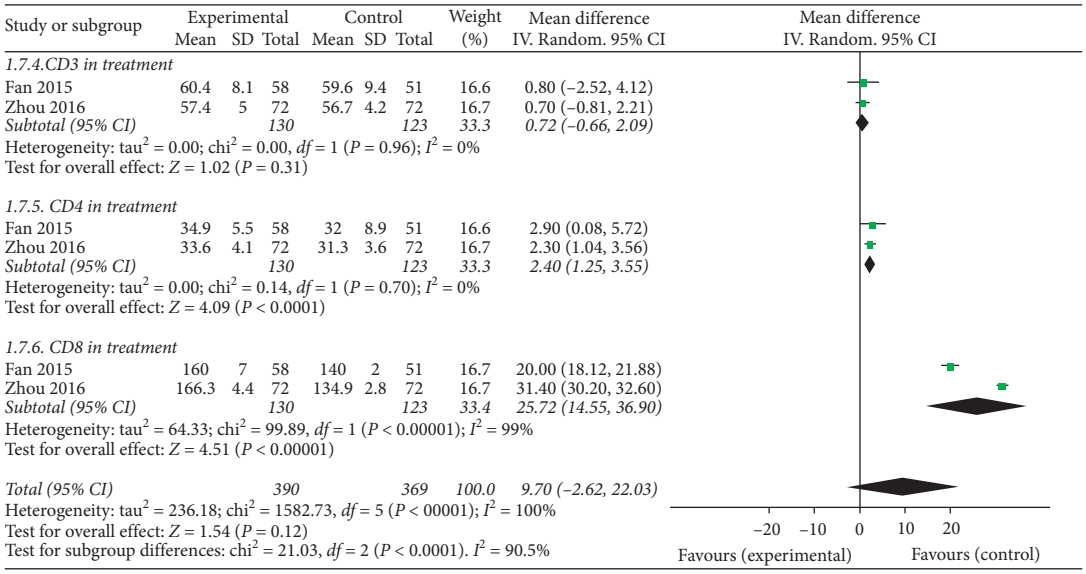

Figure 8: Forest plot of T-lymphocyte subsets in patients treated with KFX + PPI and PPI alone. I^2 and P are the criterion for the heterogeneity test; ◆, pooled mean difference; —■—, mean difference; and 95% CI.

approved 4 patent drugs including Kangfuxin liquid, Ganlong capsule, Xiaozheng Yigan tablets, and Xinmailong injection all extracted from *Periplaneta americana* but aimed at different diseases. Our previous study has demonstrated that extract of *Periplaneta americana* had good protective effects on GU in animal models [47, 48]. Recent meta-analysis conformed that KFX combined with PPIs was superior to PPIs alone in the treatment of GU in total efficacy rate [17, 18]. Here, in this paper, we further affirmed these findings and report an extended result. Compared to PPIs therapy alone, combination with KFX exerted significant improvement in total efficacy rate and efficacy rate of gastroscopy ($P < 0.00001$, $P < 0.00001$, respectively). The combination also reduced the adverse events and the recurrence rate ($P = 0.002$, $P = 0.005$, respectively). It was also associated with a significant enhancement of HP clearance ($P = 0.0004$). The efficacy may be associated with relieving the inflammation of patients ($P < 0.00001$) but not boosting immunity ($P = 0.12$). Conclusions on recurrence rate, clearance of HP, inflammatory cytokines, and T-lymphocyte subsets are based on only two or three small-sample studies which should be treated with caution.

We also performed a subgroup analysis on KFX combined with different PPIs on total efficacy rate. No obvious difference was found between PPIs though the second generation PPIs including esomeprazole and rabeprazole was claimed for having better affects. Firstly, we apologized

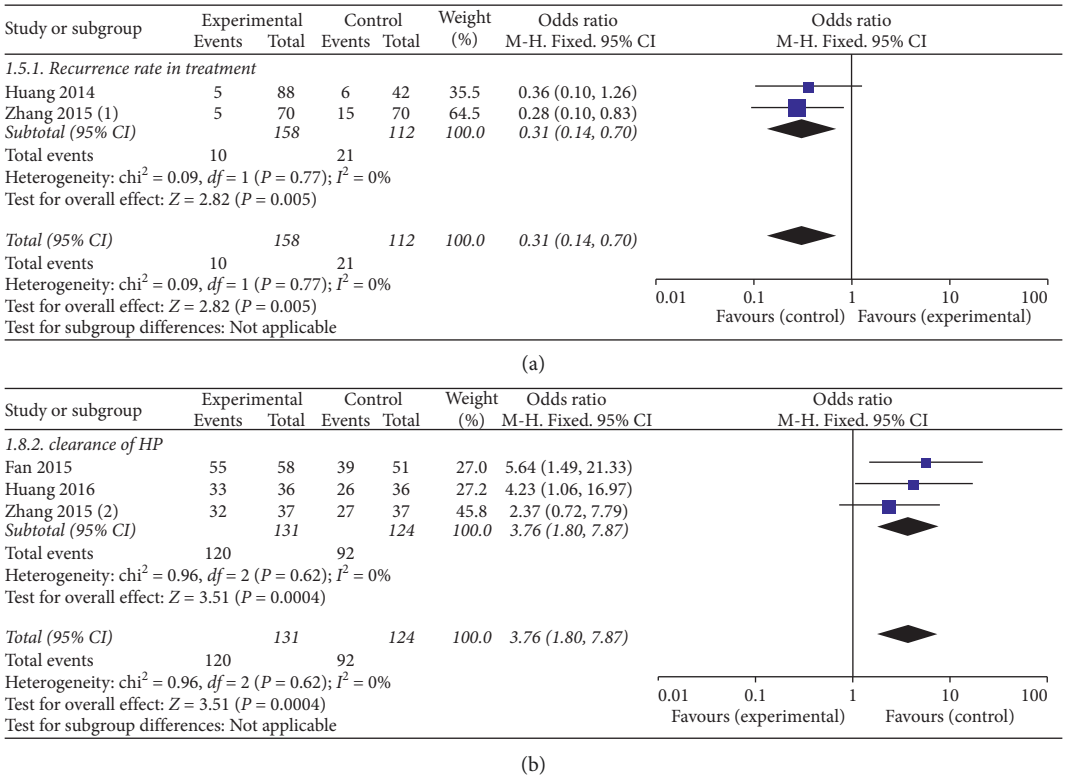

Figure 9: Forest plot of (a) the recurrence rate and (b) the clearance of HP in patients treated with KFX + PPI and PPI alone. I^2 and P are the criteria for the heterogeneity test; ◆, pooled odds ratio; —■—, odds ratio; and 95% CI.

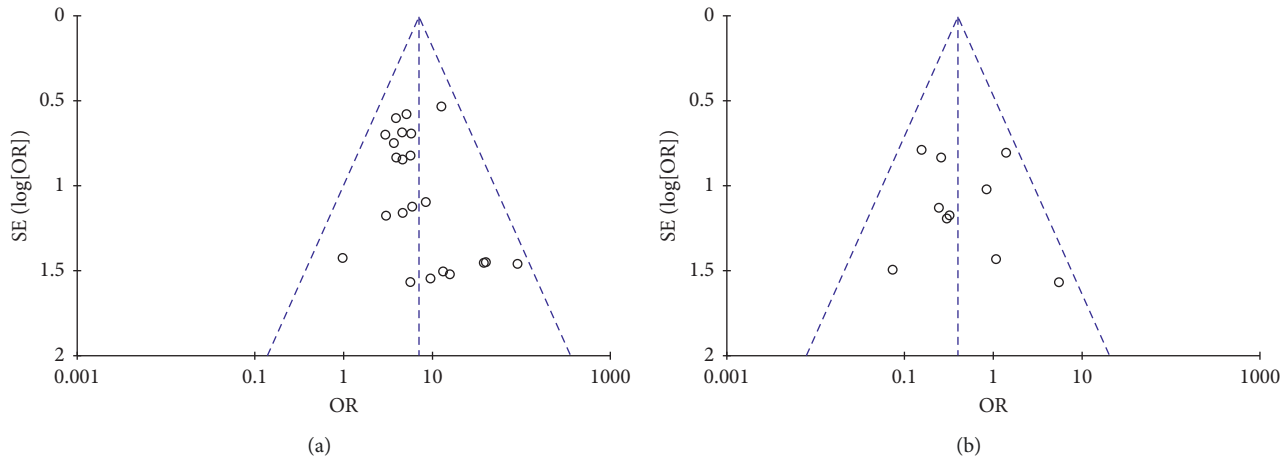

Figure 10: Funnel plot for the publication bias: (a) total efficacy rate; (b) adverse events.

for the limitations of our work, but we also found an explanation in the methodologies of trials included. Most of the trials put a final assessment on improvement of total efficacy rate instead of interval evaluation that may lead to a different conclusion.

Three articles [27, 40, 42] reported anaphylaxis, such as rash of PPIs, which reminds us that we should also pay attention to adverse reactions in short-term medication. The US FDA issued a warning on all PPIs in 2010 stating that patients should use the lowest dose and shortest duration of PPI therapy due to the increased risks [46]. Combination with TCM should be taken into consideration for effect-enhancing and/or side effect-mitigating.

The current research is not registered, and there may be a small offset, but the meta-analysis was produced strictly in accordance with the process of systematic review. However, due to the low quality of clinic trials cited, the accuracy of the results in this paper will be affected to some extent and should be handled cautiously.

5. Conclusion

These findings indicate that the combination of KFX and PPIs may significantly improve the total efficacy rate and efficacy rate of gastroscopy and reduce clinical adverse events. Due to the small sample size and limitations of this study, we sound a cautious note that KFX combined with PPIs may relieve the inflammation of patients, boost immunity, reduce recurrence rate, and enhance the clearance of HP. However, our findings must be handled with care because of the low quality of clinic trials cited. Other rigorous and large-scale RCTs are in need to confirm these results.

Disclosure

Junbo Zou and Xiaofei Zhang are co-first authors.

Conflicts of Interest

The authors declare that they have no conflicts of interest.

Authors' Contributions

J-BZ, X-FZ, and JT searched articles in electronic databases and wrote the manuscript. YW, Y-LL, and FW analyzed the data. J-BZ, J-XC, and JW performed data extraction. Y-JS designed the study and amended the paper. Junbo Zou and Xiaofei Zhang contributed equally to this work.

Acknowledgments

This work was supported by Chinese Medicine Pharmaceutical Key Discipline of Shaanxi province (grant number 303061107); Key Research and Development plan of Shaanxi province (grant number 2018SF-314); Natural Science Foundation of China (grant number 81703720); Project of Education Department of Shaanxi province (grant number 18JK0208); and Discipline Innovation Team Project of Shaanxi University of Chinese Medicine (2019-YL11).

Supplementary Materials

Preferred Reporting Items for Systematic Reviews and Meta-Analyses (PRISMA) guidelines containing 27 checklist items of the PRISMA statement pertain to the content of a systematic review and meta-analysis, which include the title, abstract, methods, results, discussion, and funding. (*Supplementary Materials*)

References

[1] X. L. Zhang, J. B. Guo, F. Han, W. W. Niu, and Y. X. Luo, "Clinical advances on digetive diseases in 2016," *Clinical Focus*, vol. 32, pp. 121–131, 2017.

[2] Z. J. Yang, "Research progress in peptic ulcer," *Inernal Medicine of China*, vol. 4, pp. 925–928, 2009.

[3] W. Y. Bai, C. Zhou, and D. M. Guo, "Epidemiolgy of peptic ulcer. Medicine and philosophy," *Clinical Decision Making Forum Edition*, vol. 31, pp. 11–13, 2010.

[4] Diseases EcoCJoD, "Standard of diagnosis and treatment of digestive ulcer disease," *Chinese Journal of Digestive Diseases*, vol. 36, pp. 508–513, 2016.

[5] D. S. Cai, *Golden Age of PPI under the Erosion of "Acid Rain", See "Prazole" Family! MENET*, Guangzhou Biaodian Medical Information Co. Ltd, Guangzhou, Guangdong Province, China, 2017, http://www.menet.com.cn.

[6] P. Malavade and S. Hiremath, "Proton pump inhibitors: more indigestion than relief?," *Indian Journal of Nephrology*, vol. 27, no. 4, pp. 249–257, 2017.

[7] L. Pasina, D. Zanotta, S. Puricelli, D. C. Djignefa, and G. Bonoldi, "Proton pump inhibitors and risk of hypomagnesemia," *European Journal of Internal Medicine*, vol. 26, no. 7, pp. e25-e26, 2015.

[8] S. N. Lin and Y. M. Li, "Current situation of progress in long-term use of proton pump inhibitors may increase the risk of dementia," *The Chinese Journal of Clinical Pharmacology*, vol. 33, pp. 849–852, 2017.

[9] P. Chen, X. J. Tang, and D. H. Wu, "The risks of long-term proton pump inhibitoers on gastric ulcer patients," *Chinese Journal of Integrated Traditional and Western Medicine*, vol. 23, pp. 615–618, 2015.

[10] L.-A. Fraser, W. D. Leslie, L. E. Targownik, A. Papaioannou, J. D. Adachi, and CaMos Research Group, "The effect of proton pump inhibitors on fracture risk: report from the Canadian multicenter osteoporosis study," *Osteoporosis International*, vol. 24, no. 4, pp. 1161–1168, 2013.

[11] Z. B. Lei, "Adverse reactions and rational use of proton pump inhibitors," *World Chinese Journal Of Digestology*, vol. 24, pp. 3468–3475, 2016.

[12] A. J. Schoenfeld and D. Grady, "Adverse effects associated with proton pump inhibitors," *JAMA Internal Medicine*, vol. 176, no. 2, pp. 172–174, 2016.

[13] J. Li, "Review on Kangfuxin liquid in treating peptic ulcer," *Contemporary Medicine Forum*, vol. 12, pp. 166-167, 2014.

[14] X. L. Ye, G. R. Zheng, and J. J. Zhang, "Research progress on Kangfuxin liquid in treating peptic ulcers," *Chinese Journal of Integrated Traditional and Western Medicine*, vol. 22, pp. 343–345, 2014.

[15] Y. C. Chen, "Research progess on Kangfuxin liquid in treating peotic ulcer," *Chinese Medicine Modern Distance of China*, vol. 15, pp. 141–143, 2017.

[16] H. C. Zhang, F. N. Geng, Y. M. Shen, H. Liu, Y. Zhao, and C. G. Zhang, "Research progress of Kangfuxin Ye in pharmacological action and clinical application," *Chinese Journal of Ethnomedicine and Ethnopharmacy*, vol. 26, pp. 57–60, 2017.

[17] L. Liu and S. J. Fei, "A meta-analysis on Kangfuxin liquid combined with PPI in treatment of peptic ulcer," *Chinese Journal of Integrated Traditional and Western Medicine*, vol. 23, pp. 891–893, 2015.

[18] L. Liu, D. X. Yang, D. Jiang, and J. Fan, "A systematic review of effectiveness and safety of Kangfuxin combined with Pantoprazole for peptic ulcer," *Chinese Traditional Patent Medicine*, vol. 36, pp. 491–497, 2014.

[19] Q. K. Chen, X. X. He, and Z. H. Zhu, *Diagnostics of Digestive Disease*, People's Medical Publishing House, Beijing, China, 2006.

[20] H. Li, "Analysis on the efficacy of Kangfuxin liquid combined with esomeprazole for the treatment of peptic ulcer," *Journal of Clinical Research*, vol. 10, pp. 1879-1880, 2012.

[21] Z. G. Xiang, Y. Zheng, X. F. Chen, K. J. Li, S. L. Yang, and X. L. Tang, "Efficacy analysis of peptic ulcer treated with

Kangfuxin and esomeprazole," *World Journal of Integrated Traditional and Western Medicine*, vol. 8, pp. 156–158, 2013.
[22] G. Q. Zhang and J. Z. Guo, "Treatment of Kangfuxin liquid with eisomeoprazole on 48 cases peptic ulcers," *Chinese Journal of Integrated Traditional and Western Medicine*, vol. 17, pp. 54-55, 2009.
[23] M. R. Zhang and Z. L. Wan, "Efficacy analysis of peptic ulcer treated with Kangfuxin liquid and esomeprazole," *Journal of North Pharmacy*, vol. 10, pp. 6-7, 2013.
[24] J. R. Huang and G. M. Mao, "Efficacy analysis of peptic ulcer treated with Kangfuxin and omeprazole on 88 cases," *West China Journal of Pharmaceutical Sciences*, vol. 29, pp. 227-228, 2014.
[25] B. Huang and C. H. Liu, "Efficacy analysis of gatric ulcer treated with Kangfuxin and omeprazloe," *Chinese Journal of Modern Drug Application*, vol. 10, pp. 219-220, 2016.
[26] W. McGrady, "Analysis of therapeutic effect of Kangfuxin liquid combined with omeprazole on gastric ulcer," *Systems Medicine*, vol. 1, pp. 34–36, 2016.
[27] Z. H. Xuan, "Kanfuxin fluid combined with little omeprazole treat gastric ulcer in active stage," *Journal of Zhejiang Chinese Medical University*, vol. 32, pp. 789-790, 2008.
[28] Q. Zhu and S. F. Li, "Systematic evaluation of peptic ulcer treated with Kangfuxin liquid and lansoprazole," *Chinese Rural Health Service Administration*, vol. 36, pp. 1075–1077, 2016.
[29] L. Zhou, Y. J. Fan, and F. Y. Chen, "Regulatory effect of combination of Kangfuxin and PPI on inflammation cytokine and immunity of refractory peptic ulcer," *Chinese Journal of Gerontology*, vol. 36, pp. 4262–4264, 2016.
[30] X. M. He, "Efficacy of peptic ulcer treated with Kangfuxin and lansoprazole," *Sichuan Medical Journal*, vol. 35, pp. 1041-1042, 2014.
[31] J. Chen, "The therapeutic effect of Kangfuxin liquid in combination with rabeprazole on digestive ulcers," *Chinese Journal of Clinical Rational Drug Use*, vol. 5, p. 43, 2012.
[32] J. Ou, "The therapeutic effect of Kangfuxin liquid in combination with rabeprazole on peptic ulcers," *Modern Diagnosis and Treatment*, vol. 25, pp. 2011-2012, 2014.
[33] W. Yu, "Clinical observation of Kangfuxin in treatment of peptic ulcer," *Chinese Community Doctors*, vol. 32, pp. 127-128, 2016.
[34] X. Q. Fan, "Efficacy of gastric ulcer treated with Kangfuxin and PPI," *Journal of Chinese Medicinal Materials*, vol. 38, pp. 869–871, 2015.
[35] L. Liang, G. M. Huang, and D. P. Yang, "Efficacy of peptic ulcer treated with Kangfuxin and PPI on 23 cases," *West China Journal of Pharmaceutical Sciences*, vol. 26, pp. 92-93, 2011.
[36] Y. L. Peng, "Effcicacy of peptic ulcer treated with Kangfuxin and pantoprazole on 40 cases," *Guangxi Medical Journal*, vol. 32, pp. 192-193, 2010.
[37] P. Tian and J. He, "Kanfuxin fluid combined with pantomeprazole treat gastric ulcer in active stage," *Chinese Journal of Modern Drug Application*, vol. 9, pp. 129-130, 2015.
[38] H. J. Ye, H. Y. Wang, and Y. Q. Qiu, "Efficacy of Kangfuxin liquid in combination with pantoprazole on peptic ulcer," *Chinese Journal of Gastroenterology and Hepatology*, vol. 16, pp. 274–276, 2007.
[39] J. Zhang and M. Ren, "Obseravation of efficacy of gastric ulcer treated with Kangfuxin and omeprazole on 74 cases," *Journal of Taishan Medical College*, vol. 36, pp. 1179-1180, 2015.
[40] J. M. Zhang, "Clinical efficacy of peptic ulcer treated with Kangfuxin liquid and pantoprazole," *Journal of North Pharmacy*, vol. 12, pp. 57-58, 2015.
[41] J. J. Deeks, J. P. T. Higgins, D. G. Altman, and S. Green, *Cochrane Handbook for Systematic Reviews of Interventions Version 5.1.0*, Cochrane, London, UK, 2011.
[42] G. M. Chen, "Efficacy obeservation of peptic ulcer treated with Kangfuxin and pantoprazole," *Shenzhen Journal of Integrated Traditional Chinese and Western Medicine*, vol. 27, pp. 90-91, 2017.
[43] P. O. Katz, L. B. Gerson, and M. F. Vela, "Guidelines for the diagnosis and management of gastroesophageal reflux disease," *American Journal of Gastroenterology*, vol. 108, no. 3, pp. 308–328, 2013, quiz 29.
[44] G. Holtmann, M.-A. Bigard, P. Malfertheiner, and R. Pounder, "Guidance on the use of over-the-counter proton pump inhibitors for the treatment of GERD," *International Journal of Clinical Pharmacy*, vol. 33, no. 3, pp. 493–500, 2011.
[45] S. Haag, J. M. Andrews, P. H. Katelaris et al., "Management of reflux symptoms with over-the-counter proton pump inhibitors: issues and proposed guidelines," *Digestion*, vol. 80, no. 4, pp. 226–234, 2009.
[46] M. L. Maes, D. R. Fixen, and S. A. Linnebur, "Adverse effects of proton-pump inhibitor use in older adults: a review of the evidence," *Therapeutic Advances in Drug Safety*, vol. 8, no. 9, pp. 273–297, 2017.
[47] J. B. Zou, *Investigation of Effective Parts in Periplaneta Americana and Prelininary Estalisment of a Quality Control Method Based on Chemical-Enzyme Biological Effects*, Chengdu University of TCM, Chengdu, China, 2016.
[48] J. B. Zou, W. T. Sang, F. Wang, S. Q. Yang, T. Zhang, and N. Zeng, "Protective effects of *Periplaneta Americana* extract on mice with ethanol-induced acute gastric uler," *Chinese Traditional Patent Medicine*, vol. 38, pp. 2325–2331, 2016.

Hindawi
Evidence-Based Complementary and Alternative Medicine
Volume 2019, Article ID 8918943, 11 pages
https://doi.org/10.1155/2019/8918943

Research Article

Protective Effect and Mechanisms of New Gelatin on Chemotherapy-Induced Hematopoietic Injury Zebrafish Model

Liwen Han,[1] **Haotian Kong**,[1] **Fasheng Liu**,[1,2] **Xiaobin Li**,[1] **Shanshan Zhang**,[1] **Xuanming Zhang**,[1] **Yong Wu**,[3] **Hua Yang**,[3] **Aiping Zhang**,[2] **and Kechun Liu**[1]

[1]*Biology Institute, Qilu University of Technology (Shandong Academy of Sciences), Engineering Research Center of Zebrafish Models for Human Diseases and Drug Screening of Shandong Province, Jinan, Shandong 250103, China*
[2]*School of Pharmaceutical Science of Shanxi Medical University, Taiyuan, Shanxi 030001, China*
[3]*Shandong Fupai Ejiao Co., Ltd., Jinan 250103, China*

Correspondence should be addressed to Aiping Zhang; zhangap1@163.com and Kechun Liu; liukechun2000@163.com

Received 18 April 2019; Revised 20 July 2019; Accepted 1 August 2019; Published 21 August 2019

Guest Editor: Gunhyuk Park

The aim of the study is to explore the protective effect of new gelatin (NG, Xin'ejiao in China) on hematopoietic injury caused by chemotherapy. Zebrafish, at 48 hours post fertilization (hpf), was treated with different chemotherapeutic drugs to establish the zebrafish hematopoietic damage model with reduced thrombocytes and erythrocytes. The protecting effects of NG on the thrombocytes and erythrocytes were observed, respectively, on zebrafish models. Then, the RT-PCR method was used to detect the change of mRNA level of the hematopoiesis-related cytokines *scl1*, *c-myb*, *pu.1*, *GATA1*, and *runx1* genes. The results showed that 50 $\mu g \cdot mL^{-1}$ and 100 $\mu g \cdot mL^{-1}$ NG rescued and increased the thrombocytes numbers induced by vinorelbine (NVB) and chloramphenicol (CHL) and the erythrocytes numbers induced by methotrexate (MTX), doxorubicin (ADM), and mechlorethamine hydrochloride (MH) in zebrafish models. Meanwhile, the mRNA expression of *scl1*, *c-myb*, and *GATA1* genes in the NG treatment group was raised compared with the MTX treatment group. Also, the mRNA expression of *pu.1* and *Runx1* in the NG treatment group was reduced compared with the MTX treatment group. In consequence, traditional Chinese medicine NG showed a certain degree protective effect on hematopoiesis injury induced by chemotherapy in this study, which may depend on the promotion of erythrocytes proliferation and the regulation of the hematopoietic genes level.

1. Introduction

As a traditional Chinese medicine (TCM), Colla corii asini (CCA, Ejiao) is a gelatin-like preparation derived from donkey hide. It has been widely used for sedation, anticoagulation, vasodilatation, and hematopoiesis, as well as the improvement in cellular immunity and radioprotection in Asia [1]. However, with the rapid increase in the use of donkey-derived gelatin, the shortage of donkey skin has become the main obstacle. Therefore, the development and research of gelatin derived from other animal skins is of great significance for the wide market application of Ejiao.

New gelatin (NG, Xin'ejiao in China) is a solid gelatin made from the skin of pig (*Sus scrofa domestica Brisson*). It is produced in only one company in China. According to TCM theory, the NG has the effect of nourishing yin deficiency, nourishing blood, and stopping bleeding. It can be used to treat weak anemia, menstrual disorders, vomiting blood, and blood stasis. So far, there is no adequate modern pharmacological research of NG, which restricts its clinical applications.

Chemotherapy is widely used for clinical treatment of tumors. Most antitumor drugs often cause injury of healthy tissues and cells while killing tumor cells. The hematopoietic system is one of common targets of chemotherapy [2]. Recently, the role of TCM in relieving chemotherapy side effects and improving the quality of life of cancer patients has attracted widespread attention of experts at home and

from abroad [3]. It has been reported that cancer patients who took Ejiao after chemotherapy exhibited improvement in bone marrow transplantation and leukopenia [4]. However, little is known whether NG has similar effect of improving hematopoietic function of chemotherapy patients.

Zebrafish is a common small tropical fish with an adult body length of about 3–5 cm. Previous studies have shown that the genome of zebrafish is 87% homologous to humans. It has the advantages of small size, rapid propagation with a large amount of production, early embryo transparent in vitro, and a similar hematopoietic system as humans. It is another important vertebrate model after mice, which has been widely used in the field of life science research. Small molecules and drugs can easily penetrate embryos of zebrafish, and large-scale drug screening can be performed by simply soaking with zebrafish [5, 6]. Therefore, zebrafish has become a reliable animal model for studying the human hematopoietic system and related diseases. These models can be employed for examination of etiology of the diseases at the molecular and cellular levels and testing the effectiveness of screened drugs [7]. In this paper, the zebrafish model was used to study the pharmacological effects of NG in the treatment of hematopoietic injury caused by chemotherapy drugs, which may identify the scientific evidence for clinical application of NG.

2. Materials and Methods

2.1. Reagents. The following reagents were used: NG (Shandong Fujiao Group, Donga Town Ejiao Co., Ltd, lot: 15060022); vinorelbine (Beijing Century Aoke Biotechnology Co., Ltd., lot: 170410); chloramphenicol (Genvien, USA, lot: 6428010150); methotrexate (China Food and Drug Control Institute, lot: 100138–201606); mechlorethamine hydrochloride (Shanghai Aladdin Biochemical Technology Co. Ltd., lot: G1414051); doxorubicin (China Food and Drug Control Institute, lot: 130509–201302); Trizol (Coolaber, lot: SL2075); HiScript II Q RT SuperMix for qPCR (+gDNA wiper) (Vazyme, Nanjing, China, lot: R123-01); and AceQ qPCR SYBR Green Master Mix (Vazyme, Nanjing, China, lot: Q111-01/02/03).

2.2. Zebrafish Maintenance. Adult zebrafish were raised in the Key Laboratory of Drug Screening Technology of Shandong Academy of Sciences. The maintenance of zebrafish was done in accordance with Economic Cooperation and Development (OECD). The adult zebrafish AB strain and the Tg (CD41 : EGFP) transgenic zebrafish lines were used in this study. The light and dark alternate culture was adopted, and it was kept in the light for 14 h after 10 h, and the cycle temperature was controlled at $28 \pm 0.5^{\circ}C$ by the air-conditioner system to ensure normal spawning. Before the experiment, the female and male zebrafish were placed in the oviposition tank in proportion to 1 : 1 or 1 : 2 and were separated by the partition board. After drawing off the partition before the illumination the next day, the female and male zebrafish chased each other after contact and spawned. The embryos were collected within 1 h after the partition board was removed and were incubated in light incubator at 28°C.

2.3. Effect of NG on the Number of Thrombocytes Induced by Chemotherapeutic Drugs in Zebrafish. The Tg (CD41 : EGFP) zebrafish embryos developed to 48 hpf after fertilization were treated with 1 $mg{\cdot}mL^{-1}$ chain protease to remove the egg membrane. Then, the zebrafish embryos were randomly placed into 24-well plates at a density of 10 per well and were treated with vinorelbine (NVB) and chloramphenicol (CHL), respectively, as hematopoietic injury model. At the same time, each pore was added different doses of NG and nutrient solution to 2 mL; then, the final concentration of NVB and CHL was 100 and 150 $\mu g{\cdot}mL^{-1}$ and the NG was 25, 50, and 100 $\mu g{\cdot}mL^{-1}$. A 0.5% DMSO solvent group was used as the control group, while all the experimental groups were set up in three parallel groups and placed in a light incubator with the lid covering and incubated under the temperature and light control. After 24 hours, the images of each embryo was observed and collected by fluorescence microscope, and thrombocytes in the cloaca to tail region of zebrafish were counted by Image-Pro Plus software.

2.4. Effect of NG on the Number of Erythrocytes Induced by Chemotherapy Drugs in Zebrafish. The AB strain zebrafish at 24 hpf were treated with 1 $mg{\cdot}mL^{-1}$ chain protease to remove the egg membrane and were randomly placed into 24-well plates at a density of 30 per well. They were randomly divided into the solvent control group and the model group (methotrexate with 600 $\mu g{\cdot}mL^{-1}$, doxorubicin with 150 $\mu g{\cdot}mL^{-1}$, and mechlorethamine hydrochloride with 150 $\mu g{\cdot}mL^{-1}$), and the model module (methotrexate 600 $\mu g{\cdot}mL^{-1}$, doxorubicin with 150 $\mu g{\cdot}mL^{-1}$, and mechlorethamine hydrochloride with 150 $\mu g{\cdot}mL^{-1}$) different concentrations of NG group (25, 50, and 100 $\mu g{\cdot}mL^{-1}$) were processed together. At 24 h after exposure, the erythrocytes of zebrafish were stained by o-Dianisidine in dark. After 15 min, the embryos were washed three times, and the specimens were photographed by a microscope. The number of erythrocytes of the yolk sac of zebrafish larvae was observed and quantified according to the staining intensity of erythrocytes in the yolk sac (SI) and analyzed by Image-Pro Plus 5.1 [8]. The staining intensity can be measured by integral optical density (IOD). In order to reduce the interference of melanin in yolk sac in zebrafish, it is necessary to add thiourea when the zebrafish develops to 12 hpf to inhibit melanin production.

2.5. Quantitative Real-Time Reverse Transcription PCR (qRT-PCR). Total RNA was extracted from 40 zebrafish larvae using Trizol reagent (Invitrogen, USA), and cDNA was synthesized by reverse transcription using HiScript II Q RT SuperMix. cDNA was amplified by LightCycler® 96 fluorescence quantitative PCR. The amplification program of RT-PCR was as follows: denaturation at 95°C for 5 min, and then at 95°C for 10 s and 55°C for 30 s, with a total of 45 cycles. PCR instrument automatically collected the

fluorescence signals after each cycle annealing. In the calculation of gene expression, β-actin was used as an internal reference gene, and the fold-change of the genes tested was assessed using the 2-ΔΔCt method [9]. The primer sequence is shown in Table 1.

2.6. Data Analysis. The data were analyzed by the SPSS 18 software, and all data were expressed in $\overline{x} \pm s$. The Kolmogorov–Smirnov test is used to test the experimental data to investigate whether the data conform to the normal distribution, and when the data do not show the normal distribution, the data are converted to the normal distribution by logarithmic transformation. One-way ANOVA was used to analyze and compare data of different treatment groups. The LSD method was used to compare the two groups, and test standard $\alpha = 0.05$ (bilateral).

3. Result

3.1. Effect of NG on Thrombocytes Formation in Zebrafish after Treatment with Chemotherapeutic Drugs. Tg (CD41 : EGFP) transgenic zebrafish was marked by green fluorescent protein (GFP) in CD41, which showed a green fluorescence under the fluorescence microscope. The CD41-GFP$^+$ cells were corresponding to the number of thrombocytes in zebrafish.

The thrombocytes of zebrafish in vinorelbine module are shown in Figure 1, which showed that compared with the control group, the number and fluorescence intensity of the CD41-GFP$^+$ cells in the caudal hematopoietic tissue of the zebrafish in the vinorelbine model group were significantly decreased, indicating that the vinorelbine affected the formation of thrombocytes in zebrafish and damaged the hematopoietic system of zebrafish in a certain range. With the addition of different doses of NG, the number of CD41-GFP$^+$ cells increased gradually, and the number of CD41-GFP$^+$ cells increased with the increase of the concentration of NG, showing a significant dose-dependent effect, indicating NG has a strong repair effect on the decrease of thrombocytes caused by vinorelbine.

Similarly, after chloramphenicol treatment, the formation of CD41-GFP$^+$ cells in zebrafish was also inhibited, and the number of CD41-GFP$^+$ cells decreased significantly (Figure 2). After the treatment of different concentrations of NG, the number of CD41-GFP$^+$ cells increased. Compared with the model group, the 25 μg·mL^{-1} NG had statistical difference, and there was a significant dose-dependent effect in the concentration range of 25–100 μg·mL^{-1}.

3.2. Effect of NG on the Erythrocyte Production of Zebrafish after Treatment with Chemotherapeutic Drugs. Methotrexate is an antifolic acid antitumor drug. Figure 3 shows that the number of erythrocytes in juvenile zebrafish decreased significantly after treatment with 600 μg·mL^{-1} methotrexate for 24 h and decreased to 46.2% compared with the control group, which has a significant statistical difference. After the treatment of NG, it was found that the content of erythrocytes in zebrafish increased significantly with the increase of the dose of NG. When the dose of NG was 50 μg·mL^{-1}, the erythrocytes content reached 75.6% compared with the methotrexate model, which increased by 54.6%, indicating that the NG has a good therapeutic effect on the reduction of the number of erythrocytes caused by methotrexate.

Table 1: Primers used in real-time PCR.

Gene	Primer orientation	Sequence of primer (5′-3′)
β-Actin	Forward	GAACCGCTGCCTCTTCTTCCTCC
	Reverse	CCCTGTTAGACAACTACCTCCCTTT
runx1	Forward	ACATATCAGAGAGCCATAAAG
	Reverse	CAGATATGGATACGACTGC
scl	Forward	TCCCAGAGACCCGCTGAGCG
	Reverse	CAGGAGGGTGTGTTGGGATG
pu.1	Forward	AGAGAGGGTAACCTGGACTG
	Reverse	AAGTCCACTGGATGAATGTG
c-myb	Forward	TTTCTACCGAATCGAACAGATG
	Reverse	CAATCACCCGTTGGTCTTCT
GATA1	Forward	AAGATGGGACAGGCCACTAC
	Reverse	TGCTGACAATCAGCCTCTTTT

The amount of erythrocytes in zebrafish after treatment with doxorubicin is shown in Figure 4. The doxorubicin of 150 μg·mL^{-1} significantly inhibited the formation of erythrocytes in zebrafish, and the number of erythrocytes in zebrafish increased with the increase of the concentration of the NG.

The effect of mechlorethamine hydrochloride hydrochloride on erythrocytes of zebrafish is shown in Figure 5. The erythrocytes content of zebrafish decreased significantly after treatment with 150 μg·mL^{-1} mechlorethamine hydrochloride, which indicated that mechlorethamine hydrochloride interfered the formation of erythrocytes in zebrafish. After the treatment of different concentrations of NG, the staining intensity of erythrocytes in the yolk sac was increased, indicating the increasing number of erythrocytes.

3.3. Effect of NG on the Expression of Hematopoietic-Related Factors in Zebrafish. As shown in Figure 6, after 600 μg·mL^{-1} methotrexate treatment, compared with the control group, the mRNA expression of hematopoietic stem cell generation related genes such as *scl1* and *GATA1* affecting hematopoietic stem cells differentiating between erythrocytes and transcription factor *c-myb* gene decreased, while the expression of *pu.1* gene that affected the differentiation of hematopoietic stem cells to the myeloid cells and the transcription factor *Runx1* gene increased significantly in the process of hematopoiesis. After the treatment of NG, the expression of *scl1*, *GATA1*, and *c-myb* increased in a dose-dependent manner, while the expression of *pu.1* and *Runx1* genes decreased.

4. Discussion

Bone marrow is the most important hematopoietic organ in the hematopoietic system. It is composed of hematopoietic cells at different mature stages such as erythrocytes,

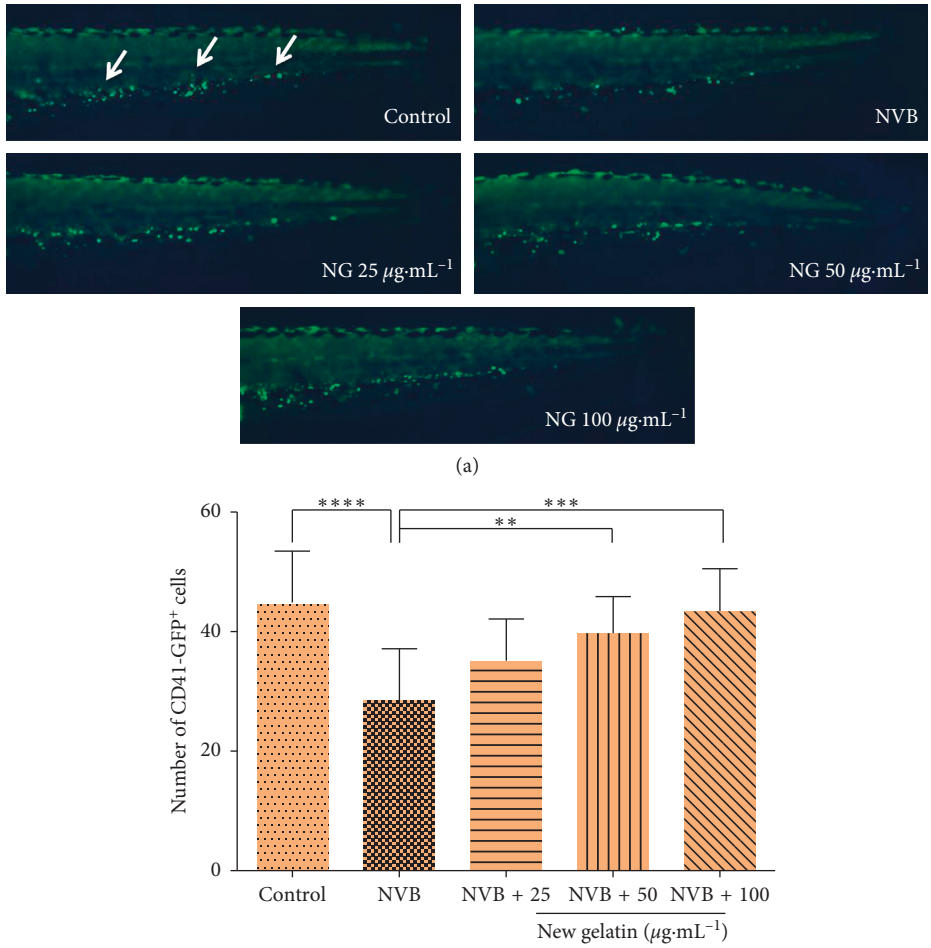

Figure 1: Effect of NG on the number of thrombocytes in zebrafish induced by vinorelbine (NVB). The number of CD41-GFP$^+$ cells was counted in the caudal hematopoietic tissue area of zebrafish. (a) Phenotypes of larvae of Tg (CD41 : EGFP) lines. (b) Number of CD41-GFP$^+$ cells at 72 hpf. The values are expressed as mean ± SEM ($n = 10$). $^{****}P < 0.001$ versus Ctl, $^{**}P < 0.01$, $^{***}P < 0.001$ versus NVB.

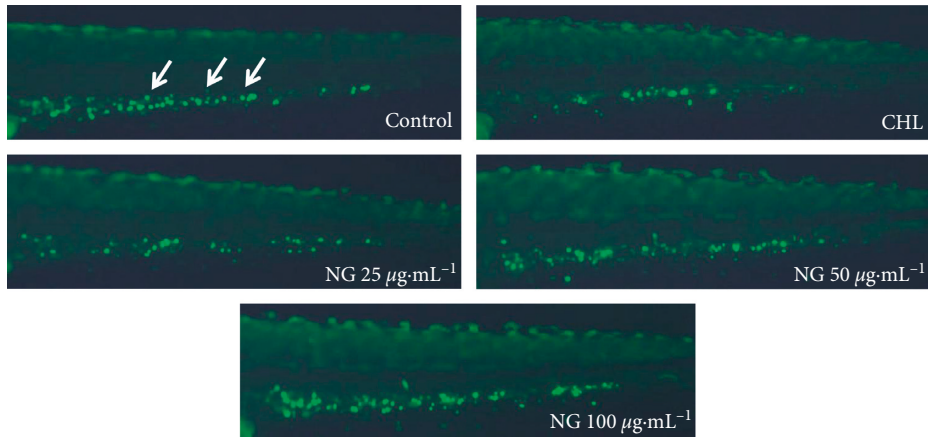

Figure 2: Continued.

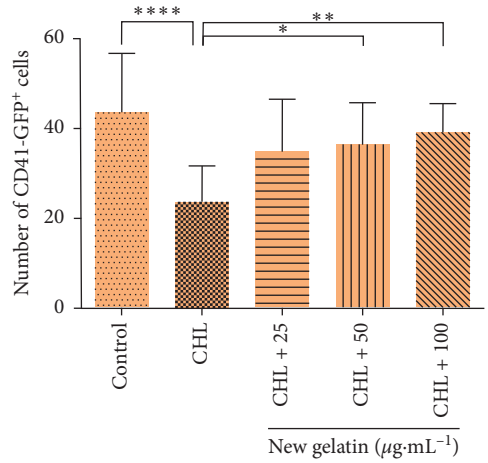

(b)

Figure 2: Effect of NG on the number of thrombocytes in zebrafish induced by chloramphenicol (CHL). The number of CD41-GFP$^+$ cells was counted in the caudal hematopoietic tissue area of zebrafish. (a) Phenotypes of larvae of Tg (CD41 : EGFP) lines. (b) Number of CD41-GFP$^+$ cells at 72 hpf. The values are expressed as mean ± SEM ($n = 10$). $^{****}P < 0.001$ versus Ctl, $^{**}P < 0.01$, $^{***}P < 0.001$ versus CHL.

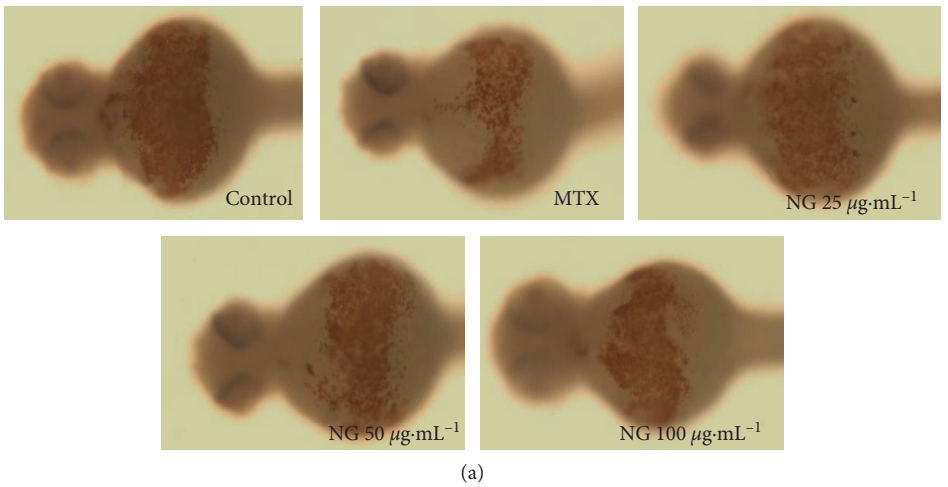

(a)

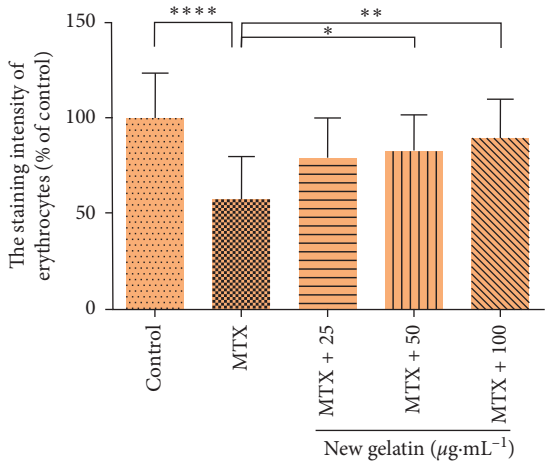

(b)

Figure 3: Effect of NG on the number of erythrocytes in zebrafish induced by methotrexate (MTX). (a) Phenotypes of larvae of wild-type AB lines. (b) The staining intensity of erythrocytes at 48 hpf. The values are expressed as mean ± SEM ($n = 30$). $^{****}P < 0.001$ versus Ctl, $^{*}P < 0.05$, $^{**}P < 0.01$ versus MTX.

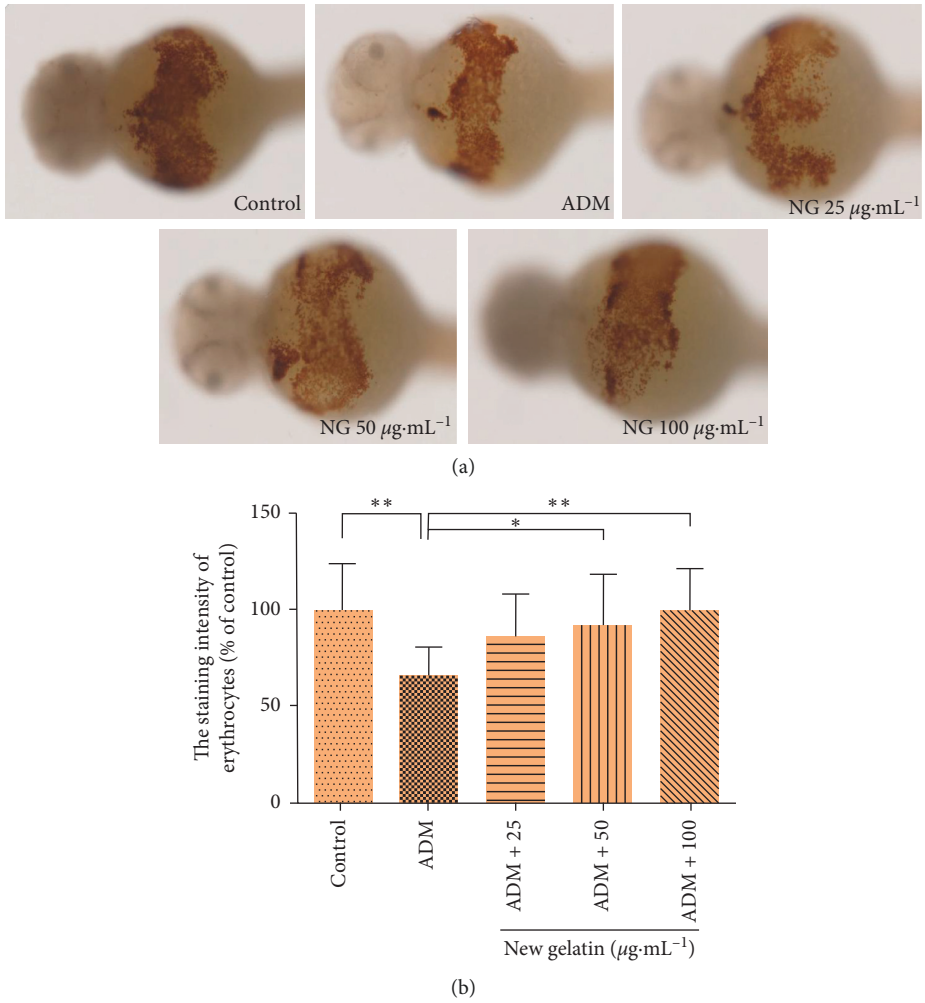

Figure 4: Effect of NG on the number of erythrocytes in zebrafish induced by doxorubicin (ADM). (a) Phenotypes of larvae of wild-type AB lines. (b) The staining intensity of erythrocytes at 48 hpf. The values are expressed as mean ± SEM ($n = 30$). $^{**}P < 0.01$ versus Ctl, $^{*}P < 0.05$, $^{**}P < 0.01$ versus ADM.

leukocytes, and platelets. Bone marrow hemopoietic tissue is so active in cell division that it is very sensitive to radiation and chemotherapeutic agents. Myelosuppression induced by radio therapy and chemotherapy is a big problem restricting the therapeutic effect of tumor. Thus, in order to enhance the therapeutic effect and improve the prognosis with no low side effects, seeking the drugs which can alleviate the myelosuppression caused by chemoradiotherapy is very crucial and challenging [10].

As a representative bulk Chinese medicine product, the price for Ejiao has been rising in recent years. It has become a very expensive Chinese medicine product. NG, the introduction of Ejiao alternatives, which is made from animal skin, has stirred up a strong public interest. It is of great significance to study the pharmacological effects of gelatin products from different skin sources by scientific methods for the correct clinical application of different types of gelatin. Based on the TCM theory, NG and Ejiao are expected to show similar efficacy and can be used interchangeably in most cases. There are many reports about Ejiao in the literature, but reports about NG are very few. From the point of view of hematopoietic injury induced by chemotherapy, the protective effect of NG on hematopoietic injury was explored in this paper. Studies have shown that there is no significant difference in free amino acids and total amino acids and trace elements between Ejiao and NG. This seems to simply confirm that NG and Ejiao have similar effects [11]. In a study of regulation of Ejiao and NG on hematopoietic injury induced by ^{60}Co irradiation in mice, Xia found that the treatment effect of NG on hematopoietic injury was better than Ejiao [12]. The results of this study are consistent with the results of NG in reversing hematopoietic injury, which further confirm the blood-replenishing effect of NG. Meanwhile, some researchers used NG to treat U937 cells. It was found that the secretion of proinflammatory cytokines related to NF-κB increased, and the phagocytic function of macrophages differentiated from U937 cells was also enhanced [13]. Although NG had a good nourishing effect in the known studies, there are still great differences in it before a large amount of clinical application evidence is obtained. Based on this, we use the new animal zebrafish model for the first time to quickly verify the hematopoietic

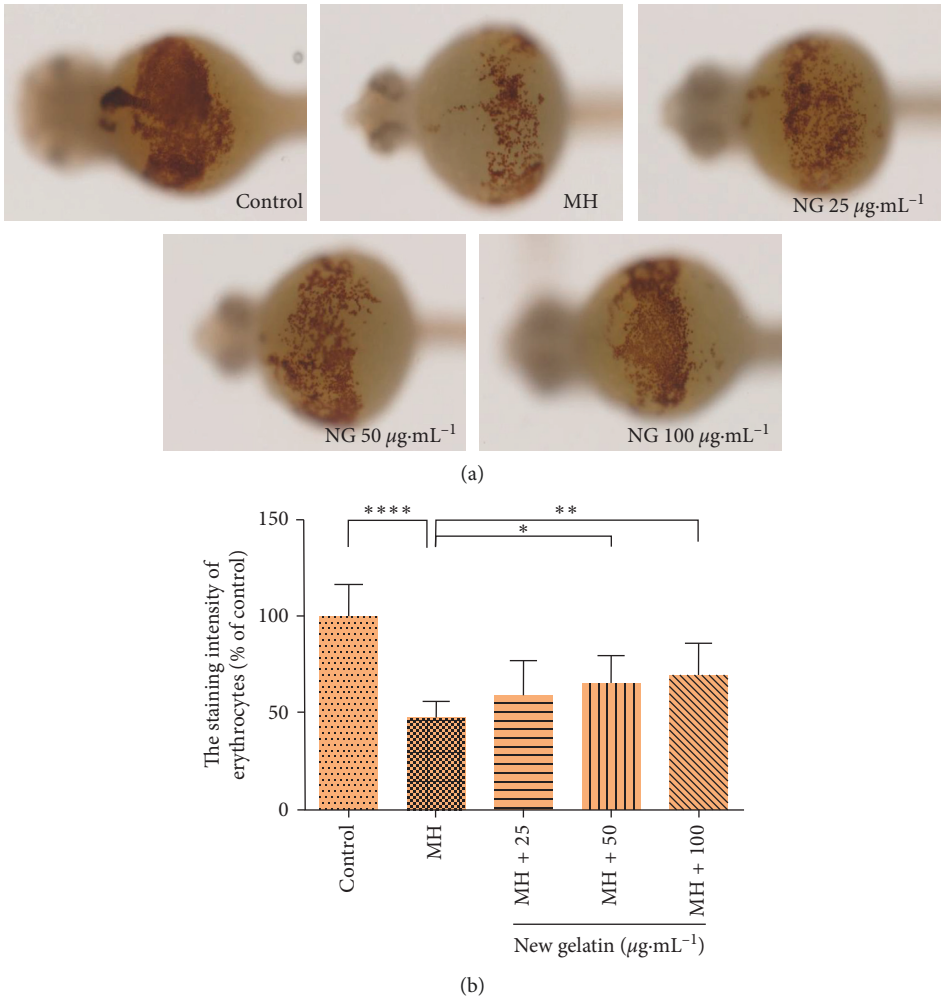

Figure 5: Effect of NG on the number of erythrocytes in zebrafish induced by mechlorethamine hydrochloride (MH). (a) Phenotypes of larvae of wild-type AB lines. (b) The staining intensity of erythrocytes at 48 hpf. The values are expressed as mean ± SEM ($n = 30$). $^{****}P < 0.0001$ versus Ctl, $^{*}P < 0.05$, $^{**}P < 0.01$ versus MH.

effect of the NG and provide experimental basis for the antitumor clinical application of NG.

As a high throughput drug screening model, zebrafish embryos and larvae fill the gap in the transition between cell model and rodent model. In order to find compounds that increase or decrease the number of hematopoietic stem cells (HSCs), North used automatic in situ hybridization to stain HSCs in the aortic-gonadal-mesonephric region of zebrafish embryos and found that PGE2 could increase the number of HSCs. The ability of PGE2 to enhance production of HSCs was later tied to its interaction with WNT signalling [14]. In addition, Jinchao et al. used the zebrafish model and found that platelet number was effectively increased by rhTyrRS (Y341A) via platelet count and reticulated platelets flow cytometry and demonstrated that radiation-induced thrombocytopenia could be prevented by rhTyrRS (Y341A) [15]. The above studies show that the zebrafish model has been increasingly recognized by researchers to explore the mechanism of drug protection.

The hemopoietic system of zebrafish is similar to humans and other advanced mammals. It has complete hematopoietic system, including erythroid, medullary, gonorrhea, and megakaryocyte. Its signal transduction pathway and related transcription factors are highly homologous with human beings. The hematopoietic genetic network is highly conservative in evolution. Primitive hematopoiesis of zebrafish mainly occurs in two extraembryonic regions, intermediate cell mass (ICM) and posterior mesoderm (ALPM) [16, 17]. The former is located between the chorda and trunk mesoderm, which functions in accordance with the islands of yolk sac in mammalian embryonic period, and the latter is the region of origin of early macrophages [18]. The hemopoietic system of humans and zebrafish is divided into primitive hematopoiesis and terminal hematopoiesis. With the beginning of blood circulation, the hematopoiesis in ICM decreases gradually, which indicates the end of primordial hematopoiesis. In the process of terminal hematopoiesis, endothelial cells are separated from peripheral cells through the aorta-gonad-mesonephric region (AGM) to enter the blood circulation, and then the hematopoietic stem cells are formed, which lays the foundation for the production of all kinds of erythrocytes in the hematopoiesis system. In

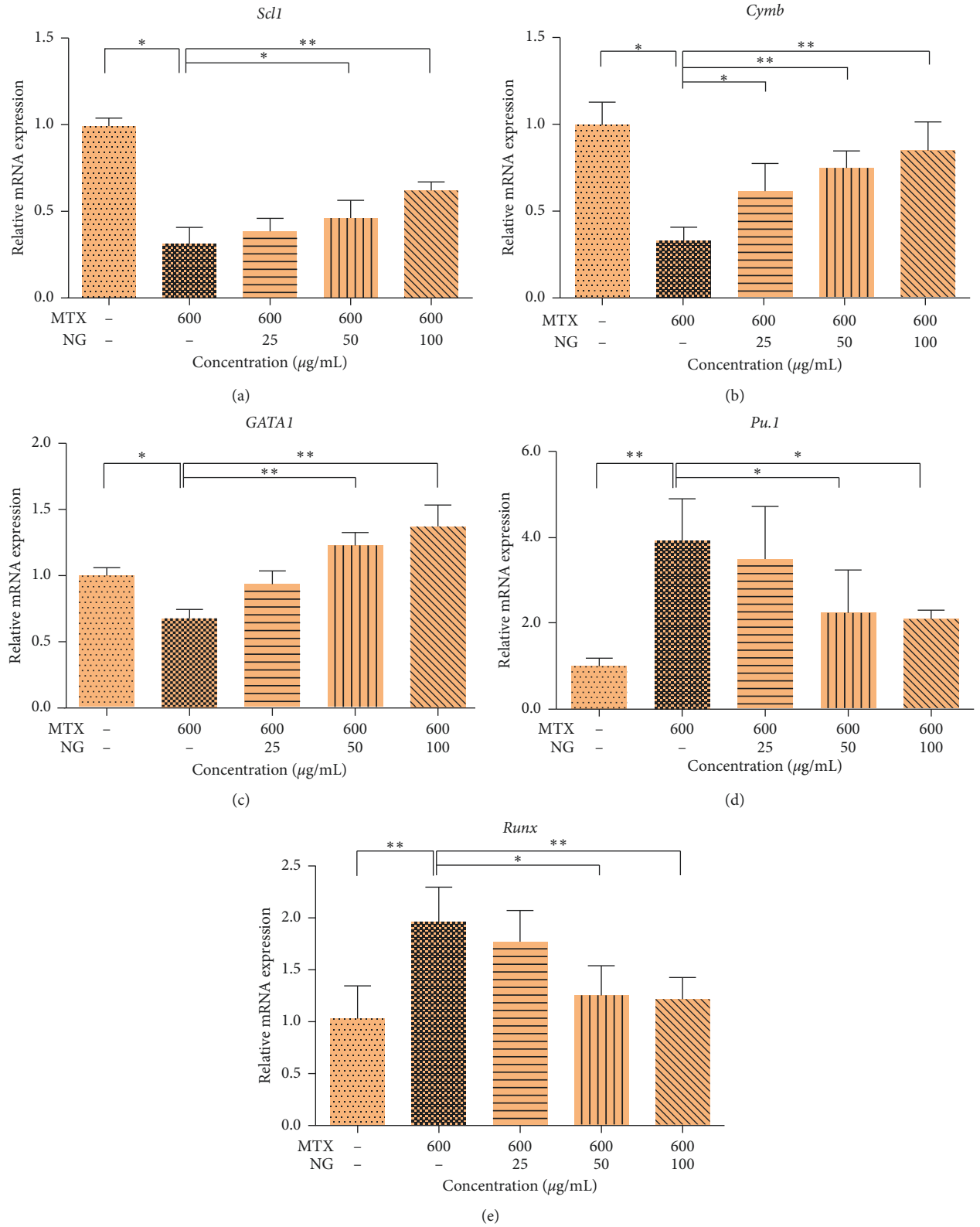

Figure 6: Expression of related genes in zebrafish hematopoietic injury model pretreated by methotrexate (MTX). The mRNA levels of *scl1* (a), *c-myb* (b), *GATA1* (c), *pu.1* (d), and *Runx1* (e). The values are expressed as mean ± SEM ($n = 30$). $^{*}P < 0.05$, $^{**}P < 0.01$ versus Ctl. $^{*}P < 0.05$, $^{**}P < 0.01$, $^{***}P < 0.001$ versus MTX.

addition, zebrafish embryos are transparent and hemoglobin is red, and the circulation of blood can be observed by the naked eye. A transgenic reporter zebrafish using the CD41 promoter to drive enhanced green fluorescent protein (EGFP) expression was previously generated. CD41-GFP$^+$ cells expresses GFP in thrombocytes, thrombocyte precursors, and possibly early hematopoietic stem cells in zebrafish embryos [19]. Among these, CD41-EGFP$^+$ cells' thrombocytes are the largest number ones. Although we are not sure whether CD41-GFP$^+$ cells include hematopoietic stem cells, the results can show that thrombocytes are induced to increase or decrease by the drug. Therefore, we used the zebrafish model to study the protective effect of NG on hemopoietic inhibition.

Vinorelbine, chloramphenicol, methotrexate, doxorubicin, and cyclophosphamide are all first-line antitumor drugs in clinic. However, these chemotherapeutic drugs lead to myelosuppression, which limits the dose enhancement of chemotherapy and hinders the optimal treatment of cancer patients. On the basis of previous research, we found that experimental hematopoietic injury models are usually induced by chemotherapy or irradiation and are widely used in pharmacodynamic evaluation of hematopoiesis [6, 20–24]. Vinorelbine and chloramphenicol can cause hematopoietic disorders and reduce the number of platelets in mice [25, 26]. At the same time, chloramphenicol can produce oxidative stress to induce platelet apoptosis [27, 28]. Cyclophosphamide is an oral inactive prodrug that produces mechlorethamine hydrochloride through metabolism in vivo, which has a toxic effect on the cells of the human hematopoiesis system and easily causes thrombocytopenia, leukopenia, and anemia [29]. Therefore, mechlorethamine hydrochloride was directly used to treat zebrafish larvae to establish the hematopoietic injury model. It has been proved that these chemotherapeutic drugs can cause hematopoietic injury in zebrafish and mice.

In order to further explore the possible protective mechanism of NG on hemopoietic injury in zebrafish, we searched for genes that play an important regulatory role in zebrafish hematopoietic process to verify. *scl1*, *c-myb*, and *runx1* can regulate the differentiation of hematopoietic stem cells, while *pu.1* can regulate the development of myeloid cells and *GATA-1* can regulate the development of erythroid cells [30]. The formation and improvement of hematopoietic system is established by the gradual differentiation of stem cells into different hematopoietic cells under the regulation of hematopoietic transcription factors, and its functional complexity increases with the degree of differentiation [16, 31]. The results showed that methotrexate could affect the expression of *scl1*, *GATA-1*, and *c-myb* in hematopoietic progenitor cells, reduce the production of erythrocyte and megakaryocyte, and significantly increase the expression of *pu.1* and *Runx1* genes, indicating that zebrafish hematopoietic injury model was successfully established. Knockout of *scl1* gene in zebrafish will result in complete loss of primitive erythropoiesis and bone marrow cell production, as well as loss of expression of *c-myb* and *Runx1* in dorsal aorta, which indicates that it is very important in hematopoietic function [32–34]. Burns et al. [35] emphasized the hypothesis that *Runx1* is necessary in primary hematopoiesis, but also in final hematopoiesis. *Runx1* is considered to be one of the earliest markers of HSCs, and *c-myb* acts downstream. The analysis of zebrafish mutants shows that the expression of *c-myb* depends on *Runx1* [36]. The deletion of *c-myb* gene inhibits the development of erythrocyte in mice and then leads to anemia in mice [37]. Some studies have shown that for adult mice, *Runx1* deficiency shows mild myeloproliferative phenotype, and the number of neutrophils and bone marrow progenitor cell group in peripheral blood increases [38], and the composition of mature bone marrow and erythrocyte also increases, which indicates that different hematopoietic factors have different effects at different stages of hematopoietic progenitor cells or hematopoietic lineage development. *GATA1* deficiency will lead to abnormal cell apoptosis in the early proliferation and differentiation of erythrocytes, leading to severe anemia and severe thrombocytopenia [35, 36, 39], and *GATA1* plays an indispensable role in determining the fate of bone marrow-erythrocytic lineage during embryogenesis [40]. Unlike *GATA1*, *pu.1* can regulate the development of hematopoietic stem cells into myeloid cells, forming lymphoid bone marrow progenitor cells, and further differentiate into immune cells such as granulocytes, macrophages, lymphocytes, and so on under the action of downstream regulatory factors. There were antagonistic effects between *GATA1* and *pu.1*, which maintained the dynamic balance of hematopoiesis differentiation [40–42]. Therefore, we selected the above five key genes to study the potential mechanism of the reversal of hematopoietic injury by NG. After treatment with NG, the expression of *scl1*, *GATA1*, and *c-myb* increased with the increase of drug concentration, while the expression of *pu.1* and *runx1* genes showed a decreasing trend, indicating that NG could improve the blood microenvironment, promote the proliferation of hematopoietic stem cells, and inhibit the apoptosis of hematopoietic mother cells, thereby promoting the formation of hematopoietic cells and having the function of hematopoietic protection [43].

5. Conclusion

The zebrafish model provides a huge balance between scale and applicability. Based on this model, NG has the protective effect on hematopoietic injury induced by chemotherapy, which is shown by its reversal effect on thrombocytopenia and erythrocyte reduction induced by chemotherapeutic drugs. Its mechanism may be related to the promotion of the expression of key hematopoietic factors.

Data Availability

The data used to support the findings of this study are available from the corresponding author upon request.

Disclosure

Liwen Han and Haotian Kong are co-first authors.

Conflicts of Interest

The authors declare that there are no conflicts of interest.

Acknowledgments

This study was financially supported by the National Key R&D Program of China (2018YFC1707300), Agricultural Science and Technology Park Industry Improvement Project of Shandong Province (2017YQ001), and Natural Science Foundation of Shandong Province (ZR2019MH037).

References

[1] H. Wu, C. Ren, F. Yang, Y. Qin, Y. Zhang, and J. Liu, "Extraction and identification of collagen-derived peptides with hematopoietic activity from *Colla Corii Asini*," *Journal of Ethnopharmacology*, vol. 182, pp. 129–136, 2016.

[2] P. Mauch, L. Constine, J. Greenberger et al., "Hematopoietic stem cell compartment: acute and late effects of radiation therapy and chemotherapy," *International Journal of Radiation Oncology∗Biology∗Physics*, vol. 31, no. 5, pp. 1319–1339, 1995.

[3] Z. Liu, "Therapeutic effect of traditional Chinese medicine combined with chemotherapy on 78 patients with advanced esophageal cancer," *Guiding Journal of Traditional Chinese Medicine and Pharmacy*, vol. 19, no. 5, pp. 60-61, 2013.

[4] J. Huang, Y. Zhou, and D. Yin, "Ejiao treatment of cancer-related anemia in cancer patients," *Asia-Pacific Traditional Medicine*, vol. 14, no. 07, pp. 167–169, 2018.

[5] C. A. Lessman, "The developing zebrafish (*Danio rerio*): a vertebrate model for high-throughput screening of chemical libraries," *Birth Defects Research Part C: Embryo Today: Reviews*, vol. 93, no. 3, pp. 268–280, 2011.

[6] J. W. Lu, M. S. Hsieh, H. A. Liao, Y. J. Yang, Y. J. Ho, and L. I. Lin, "Zebrafish as a model for the study of human myeloid malignancies," *BioMed Research International*, vol. 2015, Article ID 641475, 9 pages, 2015.

[7] P. Rasighaemi, F. Basheer, C. Liongue, and A. C. Ward, "Zebrafish as a model for leukemia and other hematopoietic disorders," *Journal of Hematology & Oncology*, vol. 8, no. 1, p. 29, 2015.

[8] Y. Chen, P.-D. Chen, B.-H. Bao et al., "Anti-thrombotic and pro-angiogenic effects of *Rubia cordifolia* extract in zebrafish," *Journal of Ethnopharmacology*, vol. 219, pp. 152–160, 2018.

[9] K. J. Livak and T. D. Schmittgen, "Analysis of relative gene expression data using real-time quantitative PCR and the $2^{-\Delta\Delta CT}$ Method," *Methods*, vol. 25, no. 4, pp. 402–408, 2001.

[10] X.-L. Zhu, J.-H. Liu, W. D. Li, and Z.-B. Lin, "Promotion of myelopoiesis in myelosuppressed mice by ganoderma lucidum polysaccharides," *Frontiers in Pharmacology*, vol. 3, p. 20, 2012.

[11] P. Jiang, Z. Zhao, Y. Hu, J. Liu, and Z. Wang, "Comeparative studies on the quality of gelatins from donkey-hide, pig-hide, cattle-hide, horse-hide and mixed animal hides I. ahalysis of amimo acids," *Natural Product Research and Development*, vol. 3, no. 3, pp. 49–59, 1991.

[12] L. Xia, X. He, and Z. Wang, "Therapeutic effect of Ejiao and Xin Ejiao on hematopoietic injury induced by ^{60}Co irradiation in mice," *Chinese Traditional Patent Medicine*, vol. 14, no. 1, p. 30, 1992.

[13] Y.-L. Zhao, Z.-Y. Lu, X. Zhang et al., "Gelatin promotes cell aggregation and pro-inflammatory cytokine production in PMA-stimulated U937 cells by augmenting endocytosis-autophagy pathway," *The International Journal of Biochemistry & Cell Biology*, vol. 95, pp. 132–142, 2018.

[14] W. Goessling, T. E. North, S. Loewer et al., "Genetic interaction of PGE2 and Wnt signaling regulates developmental specification of stem cells and regeneration," *Cell*, vol. 136, no. 6, pp. 1136–1147, 2009.

[15] Y. Jinchao, Z. Yanling, W. Xu et al., "Thrombopoietic stimulating activity of rhTyrRS (Y341A)," *Scientific Reports*, vol. 7, no. 1, article 12184, 2017.

[16] N. Hsia and L. Zon, "Transcriptional regulation of hematopoietic stem cell development in zebrafish," *Experimental Hematology*, vol. 33, no. 9, pp. 1007–1014, 2005.

[17] D. Zizioli, M. Mione, M. Varinelli et al., "Zebrafish disease models in hematology: highlights on biological and translational impact," *Biochimica et Biophysica Acta (BBA)-Molecular Basis of Disease*, vol. 1865, no. 3, pp. 620–633, 2019.

[18] L. Jing and L. I. Zon, "Zebrafish as a model for normal and malignant hematopoiesis," *Disease Models & Mechanisms*, vol. 4, no. 4, pp. 433–438, 2011.

[19] H.-F. Lin, D. Traver, H. Zhu et al., "Analysis of thrombocyte development in CD41-GFP transgenic zebrafish," *Blood*, vol. 106, no. 12, pp. 3803–3810, 2005.

[20] Y. Chen, B. Zhu, S. Yan, L. Zhang, and L. Jing, "Effects of weiganfi on the hemopoietic function of the myelosuppressed anemic mice," *Journal of Traditional Chinese Medicine*, vol. 27, no. 2, pp. 143–147, 2007.

[21] H. Gong, P. Shen, L. Jin, C. Xing, and F. Tang, "Therapeutic effects of *Lycium barbarum* polysaccharide (LBP) on irradiation or chemotherapy-induced myelosuppressive mice," *Cancer Biotherapy and Radiopharmaceuticals*, vol. 20, no. 2, pp. 155–162, 2005.

[22] R. Agarwal, S. Diwanay, P. Patki, and B. Patwardhan, "Studies on immunomodulatory activity of *Withania somnifera* (Ashwagandha) extracts in experimental immune inflammation," *Journal of Ethnopharmacology*, vol. 67, no. 1, pp. 27–35, 1999.

[23] S. E. Lee, H. Oh, J. A. Yang et al., "Radioprotective effects of two traditional Chinese medicine prescriptions: Si-Wu-Tang and Si-Jun-Zi-Tang," *American Journal of Chinese Medicine*, vol. 27, no. 03n04, pp. 387–396, 1999.

[24] T.-H. Kim, S.-J. Lee, H.-K. Rim et al., "In vitro and in vivo immunostimulatory effects of hot water extracts from the leaves of *Artemisia princeps* Pampanini cv. Sajabal," *Journal of Ethnopharmacology*, vol. 149, no. 1, pp. 254–262, 2013.

[25] P. E. I. Tian-xian, J.-j. Wang, T. E. N. G. Jin-ying, C.-m. Guo, G.-s. Gao, and D. Yang, "Long term toxicity of vinorelbine tartrate on immune and hematopoietic systems in rats," *Chinese Journal of Pharmacology and Toxicology*, vol. 28, no. 4, pp. 562–568, 2014.

[26] C. Li, *Comparative Pathlological Study of the Hemotoxicity and Immunotoxicity that Induced by Chloramphenicol, Thiamphenicol and Florfenicol in Mice*, Shandong Agricultural University, Tai'an, China, 2016.

[27] M. Paul, M. Hemshekhar, R. M. Thushara et al., "Methotrexate promotes platelet apoptosis via JNK-mediated mitochondrial damage: alleviation by N-acetylcysteine and N-acetylcysteine amide," *PLoS One*, vol. 10, no. 6, Article ID e0127558, 2015.

[28] E.-J. Kim, K.-M. Lim, K.-Y. Kim et al., "Doxorubicin-induced platelet cytotoxicity: a new contributory factor for doxorubicin-mediated thrombocytopenia," *Journal of Thrombosis and Haemostasis*, vol. 7, no. 7, pp. 1172–1183, 2009.

[29] C. Ponticelli, R. Escoli, and G. Moroni, "Does cyclophosphamide still play a role in glomerular diseases?," *Autoimmunity Reviews*, vol. 17, no. 10, pp. 1022–1027, 2018.
[30] L. Lei, *AGGF1 is Required in the Differentiation of both Hematopoietic and Endothelial Lineages during Zebrafish Embryogenesis*, Huazhong University of Science and Technology, Wuhan, China, 2013.
[31] M. L. Kauts, C. S. Vink, and E. Dzierzak, "Hematopoietic (stem) cell development—how divergent are the roads taken?," *FEBS Letters*, vol. 590, no. 22, pp. 3975–3986, 2016.
[32] K. A. Dooley, A. J. Davidson, and L. I. Zon, "Zebrafish *scl* functions independently in hematopoietic and endothelial development," *Developmental Biology*, vol. 277, no. 2, pp. 522–536, 2005.
[33] L. Robb, N. J. Elwood, A. G. Elefanty et al., "The *scl* gene product is required for the generation of all hematopoietic lineages in the adult mouse," *The EMBO Journal*, vol. 15, no. 16, pp. 4123–4129, 1996.
[34] L. J. Patterson, M. Gering, and R. Patient, "*Scl* is required for dorsal aorta as well as blood formation in zebrafish embryos," *Blood*, vol. 105, no. 9, pp. 3502–3511, 2005.
[35] C. E. Burns, J. L. Galloway, A. C. Smith et al., "A genetic screen in zebrafish defines a hierarchical network of pathways required for hematopoietic stem cell emergence," *Blood*, vol. 113, no. 23, pp. 5776–5782, 2009.
[36] C. Jin and F. Liu, "The research progress of the transcription factor *GATA-1*," *International Journal of Immunology*, vol. 32, no. 1, pp. 47–51, 2009.
[37] M. L. Mucenski, K. McLain, A. B. Kier et al., "A functional *c-myb* gene is required for normal murine fetal hepatic hematopoiesis," *Cell*, vol. 65, no. 4, pp. 677–689, 1991.
[38] J. D. Growney, H. Shigematsu, Z. Li et al., "Loss of *Runx1* perturbs adult hematopoiesis and is associated with a myeloproliferative phenotype," *Blood*, vol. 106, no. 2, pp. 494–504, 2005.
[39] D. Zhao, L. Li, and X. Qian, "The role of *GATA1* in the hematopoietic system," *Journal Developmental Medicine*, vol. 1, no. 1, pp. 57–61, 2013.
[40] J. L. Galloway, R. A. Wingert, C. Thisse, B. Thisse, and L. I. Zon, "Loss of *gata1* but not *gata2* converts erythropoiesis to myelopoiesis in zebrafish embryos," *Developmental Cell*, vol. 8, no. 1, pp. 109–116, 2005.
[41] J. Rhodes, A. Hagen, K. Hsu et al., "Interplay of *pu.1* and *gata1* determines myelo-erythroid progenitor cell fate in zebrafish," *Developmental Cell*, vol. 8, no. 1, pp. 97–108, 2005.
[42] T. Fujiwara, K. Sasaki, K. Saito et al., "Forced FOG1 expression in erythroleukemia cells: induction of erythroid genes and repression of myelo-lymphoid transcription factor *PU.1*," *Biochemical and Biophysical Research Communications*, vol. 485, no. 2, pp. 380–387, 2017.
[43] W. Deng, H. Wu, W. Xu, Y. Zhang, and M. Lu, "Effects of ejiao on hematopoietic microenvironment of bone marrow in anemia mice induced by cyclophosphamide," *Lishizhen Medicine and Materia Medica Research*, vol. 22, no. 10, pp. 2542–2544, 2011.

Hindawi
Evidence-Based Complementary and Alternative Medicine
Volume 2019, Article ID 8512405, 13 pages
https://doi.org/10.1155/2019/8512405

Review Article

Intervention Mechanisms of Xinmailong Injection, a *Periplaneta Americana* Extract, on Cardiovascular Disease: A Systematic Review of Basic Researches

Shan-Shan Lin,[1] **Chun-Xiang Liu**,[2] **Xian-Liang Wang**,[1] **and Jing-Yuan Mao**[1]

[1]*Cardiovascular Department, First Teaching Hospital of Tianjin University of Traditional Chinese Medicine, Tianjin 300381, China*
[2]*Evidence-Based Medicine Center, Tianjin University of Traditional Chinese Medicine, Tianjin 301617, China*

Correspondence should be addressed to Xian-Liang Wang; xlwang1981@126.com and Jing-Yuan Mao; jymao@126.com

Received 12 April 2019; Accepted 25 June 2019; Published 22 July 2019

Guest Editor: Irawan W. Kusuma

Background. At present, the prevention and treatment of cardiovascular disease in the world are facing severe challenges. Xinmailong injection, which is derived from the animal medicine *Periplaneta Americana*, has certain advantages in the clinical treatment of cardiovascular disease. This study systematically evaluated the basic research reports of Xinmailong Injection on cardiovascular disease and made its pharmacological mechanisms more clear. *Methods.* Basic research reports on the intervention mechanisms of Xinmailong Injection on cardiovascular disease in PubMed, EMBASE, Cochrane Library (No. 2, 2019), CNKI, Wan Fang, and VIP databases were searched. The search time limit was from the establishment of the database to February 2019. The literature was screened according to inclusion and exclusion criteria, and then the data were extracted and a descriptive analysis of the pharmacological mechanisms of Xinmailong Injection on cardiovascular disease was performed. *Results.* Finally, twenty-two basic research reports were included. The intervention mechanisms of Xinmailong Injection on cardiovascular disease mainly includes the following: inhibiting oxidative stress and inflammatory reaction; regulating autophagy; promoting Ca^{2+} influx by activating excitability of excitation-contraction coupling (ECC); inhibiting overexpressions of transforming growth factor-β1 (TGF-β1) and connective tissue growth factor (CTGF) to regulate the dynamic balance of matrix metalloproteinases (MMPs) and tissue inhibitors of matrix metalloproteinases (TIMPs); inhibiting the phosphorylation of extracellular regulated protein kinases 1/2 (ERK1/2), protein kinase B (AKT), and glycogen synthase kinase 3β (GSK3β) proteins and overexpression of the downstream transcription factor GATA4 in the nucleus; regulating vascular endothelial factors and so on. *Conclusions.* Xinmailong Injection can protect cardiomyocytes and maintain the normal function of the heart in various ways, thus effectively preventing the development of cardiovascular disease. Therefore, Xinmailong Injection has great potential for clinical application, and more basic researches need to be carried out to explore the medicinal value of Xinmailong Injection.

1. Background

Cardiovascular disease is currently the first cause of death in the world. According to the "China Cardiovascular Disease Report 2017" [1], the number of people suffering from cardiovascular disease in China is about 290 million. At present, the prevention and treatment of cardiovascular disease have achieved initial results, but they still face serious challenges. Animal material medicine is an important part of traditional medicinal resources. A large number of animal material medicine have been developed as important raw materials for modern Chinese patent medicines and western medicines due to their special biological activities. *Periplaneta Americana* is part of them. Due to its rich source and low cost, the medicinal value of *P. Americana* has enormous development potential. Since the 1980s, Chinese pharmacologist Professor Li Shunan has developed a series of new drugs, such as Kangfuxin Liquid, Xinmailong Injection, and Ganlong Capsule, using the *P. Americana* as raw material. They are used in many fields such as fighting tumors, improving heart function, inhibiting liver fibrosis, and protecting the gastrointestinal mucosa [2]. Among them,

Xinmailong Injection is mainly an auxiliary drug for chronic heart failure (CHF), and its main active ingredients are adenosine, inosine, protocatechuic acid, and pyroglutamate dipeptides [3–5]. Xinmailong Injection became the second class of traditional Chinese medicines in the national new drugs in 2006, which was approved by the State Food and Drug Administration (SFDA). Its efficacy in treating cardiovascular disease has been highly recognized since its launch. It has been recommended by many expert consensus and guidelines such as "Expert Consensus on Diagnosis and Treatment of Chronic Heart Failure by Integrative Chinese and Western Medicine" [4] and "Guidelines for the Diagnosis and Treatment of Acute Myocardial Infarction by Integrative Chinese and Western Medicine" [6].

In this study, the basic researches about the intervention mechanisms of Xinmailong Injection on cardiovascular disease were systematically organized. The aim is to provide a reference for further research and clinical application of Xinmailong Injection.

2. Methods

2.1. Inclusion Criteria. The inclusion criteria are the basic researches about the intervention mechanisms of Xinmailong Injection on cardiovascular disease. Experimental models include animals, organs, tissues, and cells associated with cardiovascular disease.

2.2. Exclusion Criteria. Exclusion criteria were (1) to observe the comprehensive efficacy of Xinmailong Injection combined with other interventions; (2) for the repeated publication of the literature, excluding low-quality literature; (3) the full text not obtained; (4) clinical research, case reports, expert consensus, review, systematic review, and meta-analysis.

2.3. Search Strategy. The basic researches about the intervention mechanisms of Xinmailong Injection on cardiovascular disease in PubMed, EMBASE, Cochrane Library (No. 2 of 2019), CNKI, Wan Fang, and VIP databases were searched. The search time was from the database establishment to February 2019. Search terms included *P. Americana*, American cockroach, Xinmailong, heart failure, ventricular dysfunction, blood vessel, artery, heart, cardiac, cardiovascular, myocardium, myocardial, and the like. The search strategy was a combination of subject words and free words. In addition, we screened the reference list of relevant literature to avoid omissions. Take PubMed as an example. The specific search strategy is shown in Table 1.

2.4. Literature Screening and Data Extraction. Literature screening and data extraction were performed according to the inclusion and exclusion criteria. The data extraction includes title, author, publication year, experimental model, observation indicators, and research result, etc. Considering this article is a summary of the intervention mechanisms of Xinmailong Injection on cardiovascular disease, a descriptive analysis was performed.

3. Results

3.1. Literature Screening Process and Results. A total of 1135 pieces of literature were retrieved and 46 pieces of possible related literature were screened out. After reading the full text, twenty-two pieces of literature were finally included. The literature screening process and results are shown in Figure 1.

3.2. Literature Overview. The included literature consists of 4 pieces of English literature and 18 Chinese literature. The literature was published in 1995~2019. The literature published in the past five years accounted for 45.45% (10/22). Experimental models included animals with cardiovascular disease (such as myocardial cell injury, myocardial ischemia-reperfusion injury, myocardial infarction, atherosclerosis, cardiomyopathy, heart failure, or pulmonary hypertension, etc.), isolated rat heart, H9C2 cells, and hypoxic-reoxygenated rat cardiomyocytes, and the like. See Table 2 for details.

3.3. Intervention Mechanism of Xinmailong Injection on Cardiovascular Disease. The main indication for Xinmailong Injection is CHF, which is the terminal stage of the progressive development of various cardiovascular diseases. The early manifestations of heart failure (HF) are myocardial cell damage, hypertrophy, and necrosis, followed by myocardial fibrosis (MF) and ventricular enlargement. Therefore, Xinmailong Injection can also be widely used in the treatment of other cardiovascular diseases. Current researches show that Xinmailong Injection mainly interferes with the cardiovascular system through the following various mechanisms.

3.3.1. Protective Mechanism of Xinmailong Injection on Cardiomyocytes. Studies have shown that myocardial cell damage is closely related to Oxidative Stress (OS) and inflammation [7]. OS refers to an unbalanced state caused by excessive oxidation of the body. In this state, the body's ability to synthesize reactive oxygen species (ROS) increases and the ability to resist oxidation decreases, resulting in damage to the body's tissue function. When OS occurs, the levels of lipid peroxides and ROS are significantly increased. The increase of ROS levels can further increase the expression of proinflammatory factors by activating nuclear factor kappa B (NF-KB) system, thereby promoting the inflammatory response [8, 9].

Wu Jianxin et al. [10] found that Xinmailong Injection can significantly reduce the J-point displacement (increased or lowered) on the electrocardiogram (ECG) of rabbits caused by isoproterenol so that the J-point position is close to the normal equipotential line. This suggests that Xinmailong Injection has a protective effect on isoproterenol-induced myocardial ischemic injury. Xinmailong Injection can also significantly reduce the frequency of ischemic arrhythmias in rabbits. Studies [11] on the rats further confirmed that Xinmailong Injection can correct the J-point displacement on the ECG caused by myocardial ischemia, and Xinmailong Injection can significantly reduce the level of the lipid peroxide malondialdehyde (MDA), reduce the activity of

Table 1: Search Strategy in PubMed.

Search	Query	Items found
#1	Search *Periplaneta Americana*[MeSH Terms]	1191
#2	Search *Periplaneta Americana*[Title/Abstract]	1688
#3	Search American cockroach[MeSH Terms]	1191
#4	Search American cockroach[Title/Abstract]	592
#5	Search Xinmailong[Title/Abstract]	12
#6	#1 or #2 or #3 or #4 or #5	2212
#7	Search heart failure[MeSH Terms]	112410
#8	Search heart failure[Title/Abstract]	158098
#9	Search ventricular dysfunction[Title/Abstract]	16291
#10	Search cardiovascular[MeSH Terms]	1192914
#11	Search cardiovascular[Title/Abstract]	410595
#12	Search heart[Title/Abstract]	793341
#13	Search cardiac[Title/Abstract]	568823
#14	Search myocardium[Title/Abstract]	71660
#15	Search myocardial[Title/Abstract]	322958
#16	Search blood vessel[Title/Abstract]	18964
#17	Search vascular[Title/Abstract]	549712
#18	Search artery[Title/Abstract]	488798
#19	#7 or #8 or #9 or #10 or #11 or #12 or #13 or #14 or #15 or #16 or #17 or #18	2758422
#20	#6 and #19	81

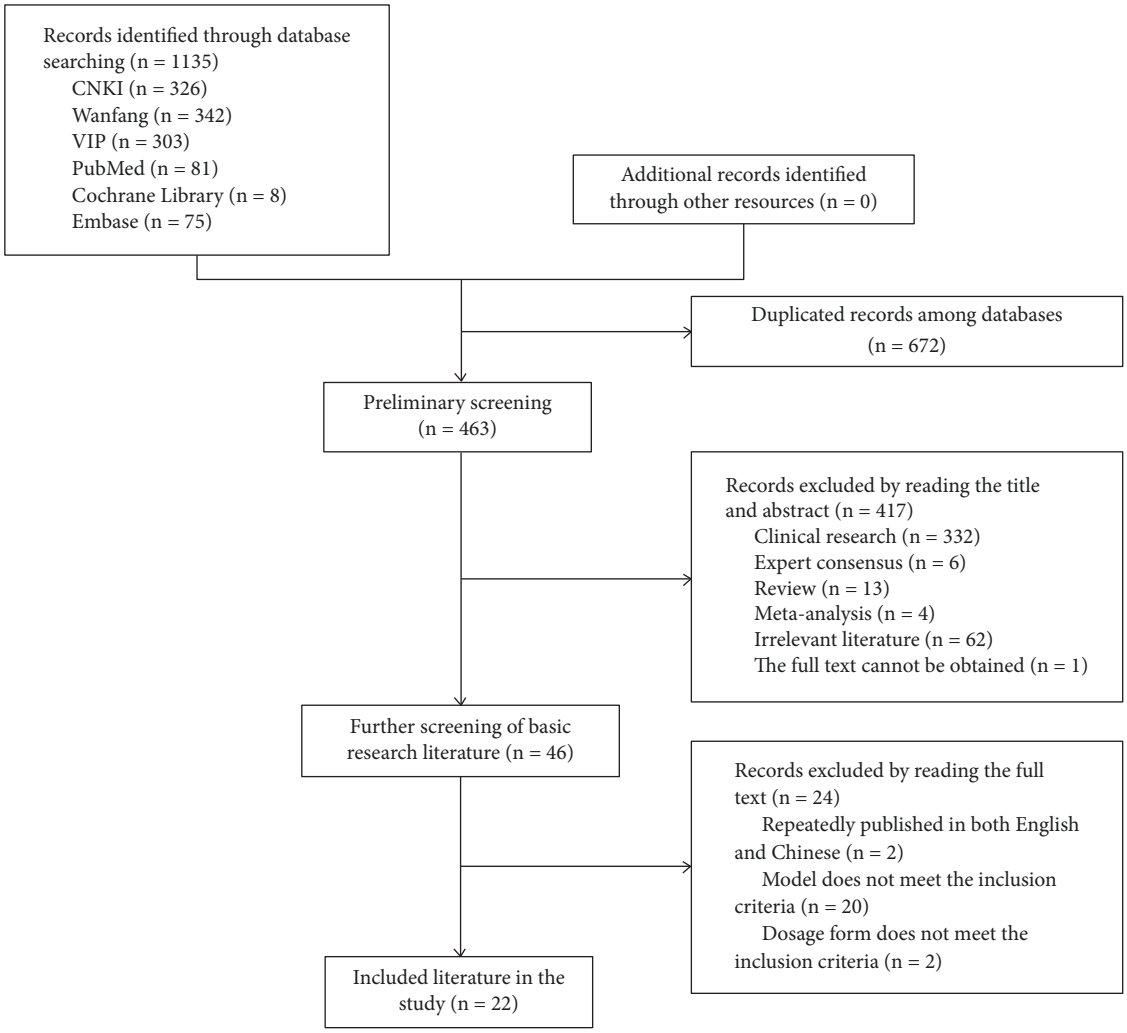

Figure 1: Flowchart of the literature selection process.

creatine phosphokinase (CPK) and lactate dehydrogenase (LDH) in blood, and improve glutathione peroxidase (GSH-PX) and SOD activity in myocardial tissue. Tian Kunlun and Jiang Yu [12] found that Xinmailong Injection can increase SOD activity and NO_2^-/NO_3^- (ratio of nitrite to nitrate) level, correct acidosis, improve circulating blood flow, and increase urine output in rabbits of ischemia-reperfusion injury induced by hypovolemic shock. Li Zhengtao et al. [13] found in the cell experiment that Xinmailong Injection can significantly reduce the production of ROS in H9C2 cells and increase the expression of antioxidant enzymes such as superoxide dismutase- (SOD-) 1, SOD-2, and heme oxygenase (HO)-1, which indicates that the protective effect of Xinmailong Injection on cardiomyocytes is achieved by anti-lipid peroxidation and inhibition of OS.

By observing the protective effect of Xinmailong Injection on myocardial ischemia-reperfusion injury in young rabbits, Cao Hongxiao et al. [14] found that Xinmailong Injection can significantly inhibit the levels of endothelial constitutive nitric oxide synthase (ecNOS), MDA, and creatine kinase (CK) and the infiltration of inflammatory cells after reperfusion. Therefore, the researchers believe that Xinmailong Injection reduces the production of oxygen free radicals by anti-lipid peroxidation, which inhibits the inflammatory response, thereby reducing the damage of vascular endothelial cells and cardiomyocytes caused by reperfusion. Zhang Lijuan et al. [15] found that the levels of serum CK-MB, myocardial NF-κB, and TNF-α reached a peak in neonatal rats after 6 hours of asphyxia. Moreover, the expression of NF-κB and TNF-α was positively correlated ($r=0.979$, $P<0.01$). Xinmailong Injection can significantly inhibit the above changes. This suggests that Xinmailong Injection can reduce the expression of proinflammatory factors by inhibiting the activation of the NF-kB system, thereby protecting the myocardial injury. Xinmailong Injection can significantly inhibit the above myocardial damage. Combined with previous studies, it can be inferred that Xinmailong Injection can reduce the expression of proinflammatory factors by inhibiting the activation of the NF-kB system.

Table 2: Basic information on the included studies.

Research	Experimental model	Observation indicators	Effect of XMLI
Wu et al. 1995[10]	rabbits with myocardial injury induced by isoproterenol	J-point displacement (increased or lowered) on the ECG; frequency of ischemic arrhythmia	After pretreatment with XMLI, the J-point displacement on the ECG caused by isoproterenol can be significantly reduced, so that the J-point position is close to the normal equipotential line. And the frequency of ischemic arrhythmia can be significantly reduced.
Wu et al. 2002[11]	rats with myocardial injury induced by isoproterenol	J-point displacement (increased or decreased) on the ECG; CPK, LDH in serum; MDA, SOD, GSH-PX in myocardial tissue	After pretreatment with XMLI, the J-point displacement on the ECG caused by isoproterenol can be significantly reduced, MDA level be reduced, CPK and LDH activity be reduced, GSH-PX and SOD activity be increased.
Tian and Yang 2010[12]	rabbits with ischemia-reperfusion induced by hypovolemic shock	SOD; NO^{-2}/NO^{-3}; blood pH; urine output	XMLI can increase SOD activity and NO_2^-/NO_3^- level, correct acidosis, increase blood pH, improve circulating blood flow, and increase urine output.
Li et al. 2017[13]	isolated rat heart; H9C2 cells (rat cardiomyocytes)	cardiac function; $[Ca^{2+}]i$ of H9C2 under electrical stimulation; Ca^{2+} influx; intracellular Ca^{2+} store; T-type Ca^{2+} channels; NCX; Na^+/K^+-ATPase activity; ROS; SOD-1; SOD-2; HO-1	XMLI can increase intracellular Ca^{2+} level by activating T-type Ca^{2+} channels and inhibiting Na^+/K^+-ATPase. XMLI can also reduce the production of ROS and enhance the expressions of SOD-1, SOD-2, HO-1.
Cao et al. 2009[14]	young rabbits with myocardial ischemia-reperfusion injury	CPK; iNOS; ecNOS; MDA	XMLI can reduce the ecNOS, MDA, CK activity and inflammatory cell infiltration in the reperfusion injury model.
Zhang et al. 2011[15]	asphyxiating newborn rats	CK-MB; NF-κB; TNF-α	After 6 hours of asphyxia in neonatal rats, serum CK-MB level, myocardial NF-κB, and TNF-α expressions peaked. XMLI can significantly reduce serum CK-MB level, myocardial NF-κB, and TNF-α expressions.
Liu et al. 2014[16]	healthy rats for preparing doxorubicin-induced HF model	LVEF; LVFS; SOD; MDA; BNP; cTnI	XMLI can reduce doxorubicin-induced cardiotoxicity, increase SOD activity and cardiac EF, and decrease MDA activity.
Liu et al. 2016[17]	healthy rats for preparing doxorubicin-induced HF model	LVEF; LVFS; SOD; MDA; BNP	XMLI can reduce doxorubicin-induced cardiotoxicity, increase SOD activity and cardiac EF, and decrease MDA activity.

Table 2: Continued.

Research	Experimental model	Observation indicators	Effect of XMLI
Duan et al. 2018[18]	healthy rats for preparing epirubicin-induced HF model	body weight; LVEF; SOD; MDA; BNP; cTnI	XMLI can reduce epirubicin-induced cardiotoxicity, increase SOD activity and EF, decrease MDA activity and cTnI level, and prevent weight loss.
Yuan and Jiang 2017[19]	H9C2 cells (rat cardiomyocytes)	cardiomyocyte activity; SOD; MDA; Caspase-3 activity; autophagy-associated protein LC3B activity	XMLI can reduce doxorubicin-induced cardiotoxicity, increase cell activity and SOD activity, and decrease MDA level, Caspase-3 activity, and protein LC3B accumulation.
Li et al. 2016[20]	healthy rats for preparing epirubicin-induced HF model	cardiac function; survival rate; body weight; LVPW thickness; EF; ECG; accumulation of collagen; expression of MMPs and TIMP4; expression of TGF-β1 mRNAs; expression of Ace, Ace2, Mas, and Agtr1 mRNAs; autophagy; expression of PI3K and AKT; the phosphorylation of P38 MAPK and ERK1/2	XMLI can enhance the survival rate of rats from epirubicin-induced HF. XMLI can prevent LV dilatation, improve cardiac function. And the treatment of the epirubicin rats with XMLI significantly recovered these changes, such as QT, QTc intervals and QRS duration. Furthermore, XMLI can significantly inhibit the accumulation of collagen, reduce the MMP9 and TGF-β1. XMLI can also decrease Beclin1 and Atg7, activate the PI3K/AKT signaling pathway and inhibit the ERK1/2 and P38 MAPK signaling pathways.
Li et al. 2019[21]	H9C2 cells (rat cardiomyocytes)	IL-1b; IL-6; TNF-α; expression of LC3, PINK1, Parkin, Nix, Beclin-1; Mitofusin1, Mitofusin2, Opa1, Drp1 and P62	XMLI can increase cell viability and the release of LC3 in H9C2 cells. XMLI can reduce the level of cTnI, CK-MB, IL-1b, IL-6, and TNF-α. XMLI can increase the protein and mRNA expression of PINK1, Parkin, Nix, Beclin-1 and decrease expression of Mitofusin1, Mitofusin2, Opa1, Drp1, and P62.
Peng et al. 2002[22]	cardiomyocytes of healthy rats	intracellular Ca^{2+} store	0.19, 0.38 and 0.76g/L XMLI can increase the content of Ca^{2+} in cardiomyocytes. This effect of 0.38g/L XMLI can be slightly inhibited by 40μmol/L verapamil (inhibition rate is 20%), however, this effect of 0.19 and 0.76g/L XMLI cannot be inhibited by 40μmol/L verapamil.
Peng et al. 2003[23]	hypoxia-reoxygenated cardiomyocytes of rats	cardiomyocyte $[Ca^{2+}]$i; MDA; SOD	XMLI can increase $[Ca^{2+}]$i in hypoxia and hypoxia-reoxygenated myocardium, increase SOD level and decrease MDA level. And this effect cannot be inhibited by verapamil.

Table 2: Continued.

Research	Experimental model	Observation indicators	Effect of XMLI
Liu et al. 2017[24]	alcoholic cardiomyopathy rats	myocardial tissue microstructure changes; indicators of cardiac Doppler ultrasound; CTGF	XMLI can reduce CTGF expression and ECM collagen deposition in rats with alcoholic cardiomyopathy.
Qi et al. 2017[3]	HF mice with TAC surgery; H9C2 cells (rat cardiomyocytes)	LVPW thickness; EF; FS; phosphorylation of ERK1/2, AKT, and GSK3β; expression of GATA4 in the nucleus	XMLI can reduce the diastolic thickness of the LVPW, increase EF and FS. XMLI can inhibit the phosphorylation of ERK1/2, AKT, and GSK3β, subsequently inhibiting protein expression of GATA4 in the nucleus.
Wu et al. 2009[25]	pulmonary hypertension rats	mean PAP; ET; NO	XMLI can significantly reduce PAP while increasing plasma NO level and lowering plasma ET level.
Huang and Wu 2009[26]	asphyxiating newborn rats	CK; ET-1; HIF-1α; myocardial histopathological changes	XMLI can reduce the expression of HIF-1α, reduce plasma ET-1 level, and alleviate myocardial hypoxia-ischemic injury.
Zhang et al. 2012[27]	AS rats	NO; ET; PGI2; TXA2	XMLI can significantly increase serum NO level and plasma PGI2, and significantly reduce plasma ET level in AS rats.
Sun and Zhang 2012[28]	AS rats	TC; TG; LDL-C; HDL-C	XMLI can significantly reduce the levels of serum TC, TG and LDL-C and increase the level of HDL-C in AS rats.
Wu et al. 2002[29]	healthy rats for preparing arrhythmia model	survival time; the lethal dose of $BaCI_2$ in rabbits; the rate of sinus rhythm conversion	XMLI can significantly increase the lethal dose of BaCI2 in rabbits and prolong the survival time of rabbits. It prevents and reduces VPB, VT, and VF caused by BaCI2. It can also significantly improve the rate of sinus rhythm conversion.
Li et al. 2018[30]	healthy rabbits for preparing atrial electrical remodeling model	AERP	XMLI can prevent the shortening of AERP200 and AERP150 after 6 hours of rapid pacing.

XMLI: Xinmailong Injection; ECG: electrocardiogram; CPK: creatine phosphokinase; LDH: lactate dehydrogenase; MDA: malondialdehyde; SOD: superoxide dismutase; GSH-PX: glutathione peroxidase; NO_2^-/NO_3^-: ratio of nitrite to nitrate; NCX: Na^+/Ca^{2+} exchanger; ROS: reactive oxygen species; HO: heme oxygenase; iNOS: inducible nitric oxide synthase; ecNOS: endothelial constitutive nitric oxide synthase; CK-MB: creatine kinase-MB; NF-κB; nuclear factor-kappa B; TNF-α: tumor necrosis factor-α; HF: heart failure; LV: left ventricular; EF: ejection fraction; FS: fraction shortening; BNP: brain natriuretic peptide; cTnI: cardiac troponin I; LVPW: left ventricular posterior wall; MMP: matrix metalloproteinase; TIMPs: tissue inhibitors of matrix metalloproteinase; TGF-β1: transforming growth factor-β1; Ace: angiotensin-converting enzyme; Mas: proto-oncogene Mas; PI3K: phosphatidylinositol 3 kinase; AKT: protein kinase B; GSK3β: glycogen synthase kinase 3β; MAPK: mitogen-activated protein kinases; ERK1/2: extracellular regulated protein kinases 1/2; Atg7: autophagy-related gene 7; QTc: corrected QT; IL: interleukin; CTGF: connective tissue growth factor; ECM: extracellular matrix; TAC: transverse aortic coarctation; PAP: pulmonary artery pressure; ET: endothelin; NO: nitric oxide; HIF-1α: hypoxia-inducible factor-1α; AS: atherosclerosis; PGI2: prostacyclin 2; TXA2: thromboxane 2; TC: total cholesterol; TG: triglyceride; LDL-C: low density lipoprotein cholesterol; HDL-C: high density lipoprotein cholesterol; VPB: ventricular premature beat; VT: ventricular tachycardia; VF: ventricular fibrillation; AERP: atrial effective refractory period.

3.3.2. Defensive Mechanism of Xinmailong Injection on Drug Cardiotoxicity. Autophagy refers to the process by which cells use lysosomes to degrade their damaged organelles and macromolecules. This process is regulated by the autophagy-related gene (Atg). The signaling pathways that regulate autophagy are complex. These signaling pathways interact with each other and form a huge regulatory network. Studies have shown that ROS is one of the major intracellular signal transducers that maintain autophagy [31]. At the same time, autophagy, as a protective and defense mechanism widely present in cells, plays an important role in alleviating ROS-mediated cell damage [32].

Liu Wei et al. [16] found that long-term use of doxorubicin significantly reduced the SOD activity and increased the MDA level in rats. While taking doxorubicin, loading and using Xinmailong Injection can increase the SOD activity and MDA level slightly. The results indicate that Xinmailong Injection can alleviate the cardiotoxicity of anthracyclines by activating the endogenous ROS scavenging system. Xinmailong Injection has the same preventive effect on myocardial toxicity induced by doxorubicin and epirubicin [17, 18]. Yuan Lili and Yang Zhihua [19] observed that the activity of H9C2 cells induced by doxorubicin was significantly decreased, the level of SOD in cells decreased and the level of MDA increased, the activity and expression of Caspase-3 in cells increased, and the accumulation of autophagy-related protein LC3B increased. The Xinmailong Injection can obviously reduce the cardiotoxicity induced by doxorubicin. This study suggests that the protective effect of Xinmailong Injection is related to the regulation of autophagy.

Li Hui et al. [20] conducted the autophagy-related studies and found that the increase in PI3K/AKT levels and the inhibition of P38MAPK and ERK1/2 phosphorylation contribute to the enhancement of anti-autophagy activity of Xinmailong Injection. Therefore, the researchers believed that Xinmailong Injection can inhibit autophagy by activating PI3K/AKT signaling pathway and inhibiting ERK1/2 and P38 MAPK signaling pathways, which is an important mechanism for Xinmailong Injection to reduce the cardiotoxicity of drugs.

Li Jie et al. [21] found that Xinmailong Injection significantly inhibited the upregulation of interleukin- (IL-) 1b, IL-6, and tumor necrosis factor- (TNF-) α levels and the decrease of LC3 release in H9C2 cells. However, this effect was inhibited by mitochondrial autophagy inhibitor Mdivi-1 and autophagy-related protein Atg7 siRNA. The study also found that Xinmailong Injection significantly inhibited the expression of PINK1, Parkin, Nix, and Beclin-1 and promoted the expression of Mitofusin1, Mitofusin2, Opa1, Drp1, and P62. This suggests that Xinmailong Injection can reduce the cardiotoxicity of the drug by regulating autophagy mediated by the PINK1/Parkin signaling pathway.

3.3.3. Mechanism of Xinmailong Injection Enhancing Myocardial Contractility. Studies have shown that the enhancement of myocardial contractility can be achieved by activating myocardial excitation-contraction coupling (ECC) excitability to promote Ca^{2+} influx in cardiomyocytes. ECC refers to the signal transduction process of cell membrane depolarization mediated by Ca^{2+}. When ECC excitability is activated, the Ca^{2+} on the cell membrane is transiently increased. At this time, Ca^{2+} and troponin are combined, and the transverse bridge on the thick muscle wire is combined with the thin filament to oscillate, thereby causing the myocardial cells to contract. The transport stability of Ca^{2+} is achieved by adjusting the voltage-dependent Ca^{2+} channel, Ca^{2+}-ATPase, and Na^{+}/Ca^{2+} exchanger.

Peng Fang et al. [22, 23] conducted multiple studies and found that Xinmailong Injection can promote Ca^{2+} influx in rat cardiomyocytes, and this effect cannot be inhibited by verapamil, a Ca^{2+} channel blocker. Therefore, it is concluded that Xinmailong Injection does not promote Ca^{2+} influx through Ca^{2+} channels. However, a further study [13] by Li Zhengtao et al. using Ca^{2+} imaging technology in H9C2 cells revealed that Xinmailong Injection can be inhibited by ML218-HCl (a T-type Ca^{2+} channels antagonist instead of L-type Ca^{2+} channel). Therefore, it is believed that Xinmailong Injection can increase cellular Ca^{2+} influx by activating T-type Ca^{2+} channels. Meanwhile, Li Zhengtao et al. also observed that Xinmailong Injection can inhibit Na^{+}/K^{+}-adenosine triphosphate (ATP) enzyme activity. This process can reduce the transmembrane electrochemical gradient of Na^{+}, weaken the Na^{+}/Ca^{2+} exchange capacity, reduce the Ca^{2+} export, and increase the concentration of Ca^{2+} in the myocardial cells, thereby enhancing the myocardial contractility.

3.3.4. Mechanism of Xinmailong Injection Inhibiting MF. MF is a pathological phenomenon in which cardiac fibroblasts (CFs) abnormally proliferate and collagen deposition in the extracellular matrix (ECM), imbalance of various types of collagen, and disordered collagen arrangement are observed [33]. This process is one of the main causes of ventricular remodeling and cardiac ejection disorders [34, 35].

Transforming growth factor-β (TGF-β) is an important cytokine during MF [36]. It promotes the differentiation of resting fibroblasts into CFs. CFs can synthesize and secrete large amounts of collagen and can also produce matrix metalloproteinases (MMPs) and tissue inhibitors of matrix metalloproteinase (TIMPs) [37]. MMPs are a group of Zn^{2-} dependent proteolytic enzymes that specifically and efficiently degrade ECM. TIMPs can maintain the normal structure and function of ECM by regulating the activity of MMPs. Under physiological conditions, the expression of MMPs was extremely low; under pathological conditions, MMPs expression was significantly upregulated. Studies have shown that the occurrence of MF is related to the upregulation of MMP-2 and MMP-9 expression [38]. Li Hui et al. [20] found that Xinmailong Injection can reduce the levels of TGF-β1 mRNA and MMP-9 in the serum of rats with HF. Clinical studies have also confirmed that Xinmailong Injection can inhibit the upregulation of MMP-1 and MMP-9 expression in serum of HF patients [39, 40] and reduce ECM collagen deposition, thereby counteracting MF.

Connective tissue growth factor (CTGF) is a downstream factor specifically induced by TGF-β. It mediates the profibrotic progression of TGF-β and is an excellent marker of MF. The expression of TGF-β and CTGF increased synchronously during fibrosis, which together promoted ECM collagen deposition [41, 42]. Liu Guohong et al. [24] found that Xinmailong Injection can significantly inhibit the expression of CTGF and decrease the deposition of ECM collagen in cardiomyocytes of rats with alcoholic cardiomyopathy, indicating that Xinmailong Injection can effectively delay the process of MF.

3.3.5. Mechanism of Xinmailong Injection Delaying the Development of Cardiac Hypertrophy. Cardiac hypertrophy is a complex dynamic process that is regulated by multiple factors. Its early change is an adaptive compensatory response. This reaction is caused by pathological factors such as excessive pressure or volume overload. With the long-term existence of pathological stimuli, compensatory cardiac hypertrophy may eventually develop into CHF.

Qi Jianyong et al. [3] found that Xinmailong Injection can effectively improve cardiac structure and function abnormalities in mice with transverse aortic coarctation (TAC) surgery caused by pressure overload and reduce ejection fraction and the thickness of the diastolic left ventricular posterior wall (LVPW). The downstream transcription factor GATA4 is a nuclear transcription factor closely related to cardiac development and plays a key role in the development of cardiomyocyte differentiation, cardiac hypertrophy, and HF [43]. Qi Jianyong et al. further carried out experiments in H9C2 cells and found that Xinmailong Injection can inhibit the phosphorylation of ERK1/2, AKT, and glycogen synthase kinase 3β (GSK3β) associated with cardiac hypertrophy and further inhibit the overexpression of the low downstream factor GATA4 in the nucleus. Therefore, this study supported that Xinmailong Injection can prevent myocardial decompensated hypertrophy from its inhibition of phosphorylation of ERK1/2, AKT/GSK3β pathway, and inhibition of overexpression of GATA4.

3.3.6. Protective Mechanism of Xinmailong Injection on Vascular Structure and Function. Vascular endothelial cells are located between plasma and vascular tissue. It not only completes the exchange of metabolites of plasma and tissue fluids but also synthesizes and secretes a variety of biologically active substances. Bioactive substances can maintain the normal contraction and relaxation of blood vessels, regulate blood pressure (BP), and balance blood coagulation and hemolysis.

Endothelin (ET) and nitric oxide (NO) are a major endothelium-dependent relaxation and contraction vascular substance. ET has the functions of contracting blood vessels, promoting platelet adhesion and aggregation, and damaging the vascular endothelium. NO has the functions of dilating blood vessels, inhibiting blood cell adhesion, and anti-vascular smooth muscle cell proliferation. Wu Jianxin et al. [25] observed the effect of Xinmailong Injection on pulmonary hypertension induced by MCT and found that Xinmailong Injection can significantly reduce pulmonary artery pressure (PAP) and increase plasma NO level and ET level. This indicates that Xinmailong Injection can reduce pulmonary hypertension by regulating vascular endothelial factor.

The expression of endothelin-1 (ET-1) and myocardial hypoxia-inducible factor-1α (HIF-1α) can reflect the hypoxic state of the body. Huang Lixin and Wu Xingheng [26] found that the expression of HIF-1α, ET-1, and CK was significantly increased in neonatal rats with asphyxia, and the expression of HIF-1α was positively correlated with plasma ET-1 level ($r = 0.876$, $P < 0.01$). Xinmailong Injection can effectively inhibit the expression of HIF-1α in the myocardium and decrease the levels of ET-1 and CK in plasma. This indicates that Xinmailong Injection can improve the myocardial ischemia and hypoxia injury by regulating vascular endothelial factor, making the blood vessels patency and blood flow normal, so as to ensure sufficient blood and oxygen supply to the myocardium.

Prostacyclin (PGI2) is an important vasodilator secreted by vascular endothelial cells, and its stable metabolite is 6-keto-prostaglandin F1a (6-Keto-PGF1a). By observing the intervention effect of Xinmailong Injection on vascular endothelial cells in rats with arteriosclerosis, Zhang Wenjing et al. [27] found that Xinmailong Injection can significantly reduce plasma ET levels and increase serum NO levels and plasma 6-Keto-PGF1a levels. In addition, Sun Lin and Zhang Wenjing [28] also found that Xinmailong Injection can significantly reduce total cholesterol (TC), triglyceride (TG), and low-density lipoprotein cholesterol (LDL-C) levels and raise high-density lipoprotein cholesterol (HDL-C) level in the serum of atherosclerotic (AS) rats. It is suggested that Xinmailong Injection can prevent and delay the progression of AS by regulating vascular endothelial factor and improving blood lipid status.

3.3.7. Mechanism of Antiarrhythmia of Xinmailong Injection. Wu Jianxin et al. [29] found that pretreatment of healthy rabbits with an Injection of Xinmailong Injection through the ear vein can significantly prolong the survival time of rabbits during continuous perfusion of $BaCl_2$ solution and reduce the arrhythmia caused by a bolus injection of $BaCl_2$ solution. For rabbit models with arrhythmia, Xinmailong Injection can significantly improve the rate of sinus arrhythmia conversion. Arrhythmias such as atrial fibrillation or rapid atrial stimulation can cause a shortening of the atrial effective refractory period (AERP) [44]. Li Fengde et al. [44] found that continuous injection of 5-day Xinmailong Injection for rabbits can effectively prevent the shortening of AERP200 and AERP150 caused by rapid pacing for 6 hours. This indicates that Xinmailong Injection can effectively prevent atrial electrical remodeling. Li Hui et al. [20] found that Xinmailong Injection can improve the prolongation of QT and QTc on electrocardiogram induced by epirubicin. In addition, prolongation of QT dispersion (QTd) in patients with ischemic heart disease can predict the occurrence of malignant arrhythmia and sudden death. Clinical researches found that Xinmailong Injection can

reduce the prolongation of QTd and prevent the occurrence of arrhythmia.

The researchers considered that the antiarrhythmia function of Xinmailong Injection may be related to the following mechanisms: (1) by regulating the activity of channel proteins transporting Na^+, Ca^{2+}, and K^+ on the cardiomyocyte membrane to ensure the normal cardiac electrical conduction pathway and (2) by improving myocardial cell metabolism and scavenging oxygen free radicals to protect the integrity of myocardial cell membrane structure and function, thereby maintaining the stability of a variety of ion channels. At present, the specific mechanism of antiarrhythmia of Xinmailong Injection is still unclear and needs further exploration [45].

4. Discussion

4.1. Intervention Mechanism of Xinmailong Injection on Cardiovascular Disease. This study shows that the intervention mechanism of Xinmailong Injection on cardiovascular disease mainly includes the following points: (1) Xinmailong Injection inhibits OS by inhibiting the synthesis of ROS and promoting the activity of antioxidant enzymes and reduces the expression of proinflammatory factors by inhibiting the activation of NF-kB system. Therefore, the damage, degeneration, and necrosis of cardiomyocytes are alleviated. (2) Xinmailong Injection protects cardiomyocytes from drug toxicity by activating endogenous ROS clearance systems and regulating cellular autophagy. (3) Xinmailong Injection enhances myocardial contractility by activating ECC excitability and promoting Ca^{2+} influx. Maintaining the normal transport of Na^+, Ca^{2+}, and K^+ on the myocardial cell membrane may also be an important mechanism of antiarrhythmia of Xinmailong Injection. (4) Xinmailong Injection regulates the dynamic balance of MMPs and TIMPs by inhibiting the overexpression of TGF-β1 and CTGF, thereby maintaining the normal structure and function of ECM, inhibiting collagen deposition and MF. (5) Xinmailong Injection delays the development of cardiac hypertrophy by inhibiting the phosphorylation of extracellular regulated protein kinases 1/2, AKT, and GSK3β proteins and overexpression of the downstream factor GATA4 in the nucleus. (6) Xinmailong Injection protects the structure and function of blood vessels by regulating vascular endothelial factor disorder and improving blood lipid status so that the heart muscle can obtain sufficient blood and oxygen supply. (7) The mechanism of antiarrhythmia of Xinmailong Injection is not clear. This may be related to its regulation of the activity of ion transport pathway proteins on the cell membrane to maintain the normal transport of Na^+, Ca^{2+}, and K^+ on the myocardial cell membrane. This may also be related to its ability to scavenge oxygen free radicals to protect cell membrane structure and function.

Excessive activation of the neuroendocrine system is considered to be a key process leading to HF. Among them, the renin-angiotensin-aldosterone system (RAAS) plays a major role and can affect multiple links of the above mechanisms. Clinical studies have found that Xinmailong Injection can inhibit the excitability of the RAAS system. This may be a key intervention mechanism of Xinmailong Injection on cardiovascular disease. It is expected to carry out a large number of relevant basic researches for further exploration.

4.2. Clinical Application Value of Xinmailong Injection in the Treatment of HF. The current conventional drugs for treating HF have certain deficiencies while improving symptoms. Diuretics can cause electrolyte imbalance and hypotension. Beta blockers have a significant negative inotropic effect on the heart and may cause bradycardia or conduction block. Digitalis drugs may cause poisoning due to the narrow treatment width. Meta-analyses [46–48] showed that Xinmailong Injection can significantly improve a variety of clinical indicators related to cardiac function, thereby improving the clinical efficacy of patients with HF. In addition, Xinmailong Injection had the effects of regulating BP, enhancing myocardial contractility, and preventing arrhythmia and thus can prevent the occurrence of the above adverse reactions to a certain extent. However, Xinmailong Injection combined with conventional treatment of western medicine may cause adverse skin reactions [RR=2.04, 95% CI (1.05, 3.96), P=0.03] [49]. In addition, the clinical cost-effectiveness analysis of Xinmailong Injection in the treatment of HF showed that, compared with the conventional treatment group, the combination of Xinmailong and conventional treatment group had low cost, high efficiency, and better economic benefits. In summary, Xinmailong Injection plays an important role in improving the quality of life of patients and reducing the medical burden on families and society. Its medicinal value has great potential for development.

4.3. The Direction and Thinking of the Future Research of Xinmailong Injection. Xinmailong Injection is a multicomponent pharmaceutical preparation whose active ingredients can act on multiple targets of the body through different routes. Clinical studies have shown that Xinmailong Injection can effectively treat a variety of cardiovascular system related diseases, such as pulmonary heart disease (PHD) [50, 51], ischemic cardiomyopathy (IHD) [52], dilated cardiomyopathy (DCM) [53], cardiogenic shock [54], and heart and kidney syndrome [55, 56], etc. Due to the lack of basic research in related fields, the intervention mechanism of Xinmailong Injection is not yet clear. More and more tissue cytology research, molecular biology research, and genetic research are being expected. To study the pharmacological mechanism of Xinmailong Injection, it is necessary to study not only the single active ingredients but also the common pathways, regulatory factors, and targets of the active ingredients in the process of initiation, so as to construct a complete system of intervention mechanisms. This will provide a reference for the formulation of more reasonable clinical prescriptions for Xinmailong Injection and further research and development of new drugs.

5. Conclusion

Xinmailong Injection can protect cardiomyocytes and maintain the normal function of the heart in various ways, thus effectively preventing the development of cardiovascular disease. Therefore, Xinmailong Injection has great potential for clinical application, and more basic researches need to be carried out to explore the medicinal value of Xinmailong Injection.

Conflicts of Interest

The authors declare that there are no conflicts of interest.

Authors' Contributions

Shan-Shan Lin and Chun-Xiang Liu contributed equally to this work. They took part in the design of the study, performed the literature survey, and drafted the manuscript. Xian-Liang Wang and Jing-Yuan Mao took part in the design and implementation of the study. All authors have read and approved the final manuscript.

Acknowledgments

This work was supported by the Tianjin Enterprise Science and Technology Commissioner Project (NO. 18JCTPJC64900), the National Natural Science Foundation of China (NO. 81804218), the Ministry of Education of People's Republic of China "Program for Innovative Research Team in University" (NO. IRT_16R54), and the Tianjin Science and Technology Program (NO. 15ZXLCSY00020).

References

[1] W. W. Chen, R. L. Gao, L. S. Liu et al., "Summary of China cardiovascular disease report 2017," *Chinese Circulation Journal*, vol. 30, no. 1, pp. 1–8, 2018.

[2] H. X. Man, L. Huang, K. G. Na, Q. Y. Tan, Y. S. Yang, and P. Y. Xiao, "Research progress of chemical component and biological activity in medicinal Periplaneta Americana," *Anti-Infection Pharmacy*, vol. 11, no. 5, pp. 403–407, 2014.

[3] J. Y. Qi, J. Yu, Y. F. Tan et al., "Mechanisms of Chinese medicine Xinmailong's protection against heart failure in pressure-overloaded mice and cultured cardiomyocytes," *Scientific Reports*, vol. 7, p. 42843, 2017.

[4] K. J. Chen, Z. G. Wu, M. J. Zhu, J. Y. Mao, and H. Xu, "Expert consensus on diagnosis and treatment of chronic heart failure by integrative Chinese and western medicine," *Chinese Journal of Integrated Traditional Chinese and Western Medicine*, vol. 36, no. 2, pp. 133–141, 2016.

[5] Dali Medical College, *Xinmailong extract and Xinmailong pharmaceutical preparation*, China, 1996.

[6] Doctor Society of Integrative Medicine, Chinese Medical Doctor Association, and ETAL, "Guidelines for the diagnosis and treatment of acute myocardial infarction by integrative Chinese and western medicine," *Chinese Journal of Integrated Traditional Chinese and Western Medicine*, vol. 38, no. 3, pp. 272–284, 2018.

[7] B. Yao, X. He, Y. Lin, and W. Dai, "Cardioprotective effects of anisodamine against myocardial ischemia/reperfusion injury through the inhibition of oxidative stress, inflammation and apoptosis," *Molecular Medicine Reports*, vol. 17, no. 1, pp. 1253–1260, 2018.

[8] A. M. Al-Taweel, M. Raish, S. Perveen et al., "Nepeta deflersiana attenuates isoproterenol-induced myocardial injuries in rats: possible involvement of oxidative stress, apoptosis, inflammation through nuclear factor (NF)-κB downregulation," *Phytomedicine*, vol. 34, pp. 67–75, 2017.

[9] J. Qu, N. Lin, and Q. L. Ding, "ROS-induced NRP3 inflammasome activation and cardiovascular diseases," *Pharmacy Today*, vol. 27, no. 12, pp. 855–858, 2017.

[10] J. X. Wu, Y. G. Zhou, and R. X. Niu, "Protective effect of Xinmailong on myocardial injury induced by isoproterenol in rabbits," *Journal of Dali Medical College*, vol. 4, no. 1, pp. 5–8, 1995.

[11] J. X. Wu, Y. X. Wang, R. X. Niu, Y. G. Zhou, and N. Liang, "Protective effect of Xinmailong on isoproterenol-induced ischemic myocardium in rats," *Chinese Journal of Pathophysiology*, vol. 18, no. 1, pp. 97-98, 2002.

[12] K. L. Tian and Z. H. Yang, "Protective effect of Xinmailong on rabbits with ischemia-reperfusion injury," *Chinese Journal of Ethnomedicine and Ethnopharmacy*, vol. 19, no. 12, pp. 22–25, 2010.

[13] Z. Li, S. Li, L. Hu et al., "Mechanisms underlying action of xinmailong injection, a traditional chinese medicine in cardiac function improvement," *African journal of traditional, complementary, and alternative medicines : AJTCAM*, vol. 14, no. 2, pp. 241–252, 2017.

[14] H. X. Cao, R. M. Zhong, and X. H. Wu, "The protection of Xinmailong against reperfusion injury in immature rabbits myocardial ischemia," *Journal of Jiangxi Medical College*, vol. 49, no. 10, pp. 15–18, 2009.

[15] L. J. Zhang, R. M. Zhong, and X. H. Wu, "Effects of Xinmailong on expression of NF-κB and TNF-a in myocardium of asphyxiated neonatal rats," *Journal of Nanchang University (Medical Science)*, vol. 51, no. 3, pp. 14–17, 2011.

[16] W. Liu, X. B. Duan, and X. Xu, "Preventive effect and mechanism of Xinmailong Injection on cardiotoxicity induced by adriamycin in rats," *Chinese Journal of Integrative Medicine on Cardio-/Cerebrovascular Disease*, vol. 12, no. 2, pp. 210-211, 2014.

[17] W. Liu, Y. H. Wang, and Q. Wang, "Preventive effect and mechanism of Xinmailong Injection on cardiotoxicity induced by adriamycin in rats," *Technology Wind*, vol. 1, no. 29, 2016.

[18] X. B. Duan, W. Liu, and Y. F. Wang, "Experimental study of Xinmailong Injection on cardiotoxicity induced by epirubicin in rats," *Chinese Journal of Integrative Medicine on Cardio/Cerebrovascular Disease*, vol. 16, no. 8, pp. 1038–1040, 2018.

[19] L. L. Yuan and Y. Jiang, "Protective mechanism of Xinmailong Injection on adriamycin-induced cardiomyocyte injury," *Chinese Journal of Integrative Medicine on Cardio/Cerebrovascular Disease*, vol. 15, no. 23, pp. 2977–2980, 2017.

[20] H. Li, Y. Mao, Q. Zhang et al., "Xinmailong mitigated epirubicin-induced cardiotoxicity via inhibiting autophagy," *Journal of Ethnopharmacology*, vol. 192, pp. 459–470, 2016.

[21] J. Li, W. Shi, J. Zhang, and L. Ren, "To explore the protective mechanism of pten-induced kinase 1 (PINK1)/parkin mitophagy-mediated extract of periplaneta americana on lipopolysaccharide-induced cardiomyocyte injury," *Medical Science Monitor*, vol. 25, pp. 1383–1391, 2019.

[22] F. Peng, C. S. Fang, and X. B. Liu, "Effect of Xinmailong Injection on free calcium content in rat myocardial cells,"

Traditional Chinese Drug Research and Clinical Pharmacology, vol. 13, no. 4, pp. 224–269, 2002.

[23] F. Peng, X. B. Liu, C. S. Fang, and Z. K. Yang, "Effect of Xinmailong Injection on cytosolic free calcium and lipid peroxidation in rat heart cells after anoxia and reoxygenation damage," *Journal of Chinese Pharmaceutical Sciences*, vol. 12, no. 1, pp. 33–35, 2003.

[24] G. H. Liu, J. Huang, and Y. S. Liu, "Effect of Xinmailong Injection on myocardial fibrosis in rats with alcoholic cardiomyopathy," *Chinese Journal of Integrative Medicine on Cardio/Cerebrovascular Disease*, vol. 15, no. 10, pp. 1177–1180, 2017.

[25] G. H. Liu, J. Huang, and Y. S. Liu, "Experimental study of the XML injection antagonizing rat pulmonary hypertension by monocrotaline," *Journal of Medical Research*, vol. 38, no. 1, pp. 29–32, 2009.

[26] L. X. Huang and X. H. Wu, "Effect of Xinmailong on hypoxia-inducible factor-1α expression in neonatal rats with asphyxia," *Chinese Journal of Contemporary Pediatrics*, vol. 11, no. 8, pp. 683–686, 2009.

[27] W. J. Zhang, L. L. Wang, and S. Y. Song, "Protective effect of Xinmailong infection vascular endothelial cells of atherosclerosis rats," *Journal of Hebei North University (Natural Science Edition)*, vol. 28, no. 2, pp. 79–81, 2012.

[28] L. Sun and W. J. Zhang, "Effect of Xinmailong (XML) Injection on blood lipids in rats with atherosclerosis," *Journal of Hebei North University (Natural Science Edition)*, vol. 28, no. 1, pp. 67–69, 2012.

[29] J. X. Wu, R. X. Niu, Y. L. Huang, Y. Qin, and X. Q. Huang, "Prevention and treatment effect of Xinmailong on experimental arrhythmias in rabbits," *Medical Journal of Dali College*, vol. 11, no. 2, pp. 18-19, 2002.

[30] J. X. Wu, R. X. Niu, Y. L. Huang, Y. Qin, and X. Q. Huang, "Effect of Xinmailong Injection on atrial electrical remodeling in rabbits with rapid atrial pacing," *Chinese Journal of Integrative Medicine on Cardio/Cerebrovascular Disease*, vol. 16, no. 17, pp. 2489–2491, 2018.

[31] G. Filomeni, D. de Zio, and F. Cecconi, "Oxidative stress and autophagy: the clash between damage and metabolic needs," *Cell Death & Differentiation*, vol. 22, no. 3, pp. 377–388, 2015.

[32] S. Yu and Y. Q. Ni, "Autophagy, oxidative stress and nephropathy," *Progress Physiological Sciences*, vol. 49, no. 4, pp. 275–279, 2018.

[33] M. Gyöngyösi, J. Winkler, I. Ramos et al., "Myocardial fibrosis: biomedical research from bench to bedside," *European Journal of Heart Failure*, vol. 19, no. 2, pp. 177–191, 2017.

[34] R. D. Brown, S. K. Ambler, M. D. Mitchell, and C. S. Long, "The cardiac fibroblast: therapeutic target in myocardial remodeling and failure," *Annual Review of Pharmacology and Toxicology*, vol. 45, pp. 657–687, 2005.

[35] R. Martos, J. Baugh, M. Ledwidge et al., "Diastolic heart failure: evidence of increased myocardial collagen turnover linked to diastolic dysfunction," *Circulation*, vol. 115, no. 7, pp. 888–895, 2007.

[36] K. Y. Goh, L. He, J. Song et al., "Mitoquinone ameliorates pressure overload-induced cardiac fibrosis and left ventricular dysfunction in mice," *Redox Biology*, vol. 21, pp. 1–15, 2019.

[37] W. J. Guang, B. F. Ao, W. W. Ouyang, S. F. Su, and B. Lu, "Effects of TGF-ß1 on myocardial fibrosis due to different reasons," *Science & Technology Review*, vol. 34, no. 2, pp. 221–225, 2016.

[38] S. Fu, Y. L. Li, Y. T. Wu, Y. Yue, and Y. Gao, "Icariside 2 ameliorates myocardial fibrosis in spontaneously hypertensive rats through regulating expression of MMP-2, MMP-9, and TIMP-1," *Science Technology Review*, vol. 34, no. 9, pp. 1253–1257, 2018.

[39] C. M. Zhao, Q. F. Song, X. Z. Wang et al., "Effect of Xinmailong on serum matrix metalloproteinase-1 in patients with congestive heart failure," *Chinese Journal of Gerontology*, vol. 34, no. 12, pp. 3455-3456, 2014.

[40] C. M. Zhao, Q. F. Song, X. Z. Wang et al., "The effect of Xinmailong on matrix metalloproteases-9 in patients with congestive heart failure (CHF)," *Chinese Journal of Coal Industry Medicine*, vol. 17, no. 2, pp. 173–176, 2014.

[41] A. Leask, "Potential therapeutic targets for cardiac fibrosis: TGFβ, angiotensin, endothelin, CCN2, and PDGF, partners in fibroblast activation," *Circulation Research*, vol. 106, no. 11, pp. 1675–1680, 2010.

[42] Y. E. Koshman, N. Patel, M. Chu et al., "Regulation of connective tissue growth factor gene expression and fibrosis in human heart failure," *Journal of Cardiac Failure*, vol. 19, no. 4, pp. 283–294, 2013.

[43] Q. Liang, L. J. de Windt, S. A. Witt, T. R. Kimball, B. E. Markham, and J. D. Molkentin, "The transcription factors GATA4 and GATA6 regulate cardiomyocyte hypertrophy *in vitro* and *in vivo*," *The Journal of Biological Chemistry*, vol. 276, no. 32, pp. 30245–30253, 2001.

[44] M. C. E. F. Wijffels, C. J. H. J. Kirchhof, R. Dorland, and M. A. Allessie, "Atrial fibrillation begets atrial fibrillation: a study in awake chronically instrumented goats," *Circulation*, vol. 92, no. 7, pp. 1954–1968, 1995.

[45] H. Tang, J. Li, Z. H. Huang, Z. Q. Ren, and J. P. Ning, "Effect of Xinmailong on QT dispersion and clinical efficacy in patients with ischemic heart failure," *Chinese Medical Journal*, vol. 8, no. 9, pp. 1211–1213, 2013.

[46] J. M. Zhang, Y. D. Shang, X. R. Wu, Y. J. Fu, and C. Y. Xie, "Clinical efficacy of Xinmailong Injection in the treatment of chronic heart failure: a meta-analysis," *Medica of china family physicians*, vol. 17, no. 12, pp. 1388–1393, 2014.

[47] Y. D. Zuo, X. C. Liu, and M. Li, "A meta-analysis of Xinmailong Injection on treating chronic heart failure," *Clinical Journal of Chinese Medicine*, vol. 7, no. 2, pp. 11–14, 2015.

[48] X. H. Lu, L. Zhang, J. B. Wang et al., "Clinical efficacy and safety of Xinmailong Injection for the treatment of chronic heart failure: a meta-analysis," *Frontiers in Pharmacology*, vol. 9, pp. 1–14, 2018.

[49] Z. Q. Liu, H. B. Liu, and B. L. Wang, "Safety of Xinmailong Injection in the treatment of heart failure:a meta-analysis," *Journal of China Pharmacy*, vol. 29, no. 22, pp. 3152–3157, 2018.

[50] G. H. Liu, H. R. Shi, and J. Huang, "Therapeutic effect of Xinmailong Injection on chronic pulmonary heart disease," *World Latest Medicine Information*, vol. 18, no. 31, pp. 132–136, 2018.

[51] G. H. Liu, H. R. Shi, and J. Huang, "Effect of Xinmailong Injection on blood gas analysis, D-dimer and hemoglobin in patients with chronic pulmonary heart disease," *World Latest Medicine Information*, vol. 18, no. 33, pp. 141–143, 2018.

[52] G. F. Song, F. Shao, and L. Wang, "Therapeutic effect of Xinmailong Injection on patients with ischemic cardiomyopathy," *Chinese Journal of Practical Medicine*, vol. 11, no. 31, pp. 115-116, 2016.

[53] W. Q. Liu, Q. Ao, X. W. Wang, and X. H. Yin, "Effect of Xinmailong Injection on brain natriuretic peptide and high-sensitive C-reactive protein in patients with dilated cardiomyogenic," *Contemporary Medicine*, vol. 21, no. 18, pp. 134-135, 2015.

[54] Z. R. Ge, L. Li, and S. B. Jiang, "Clinical observation on Xinmailong Injection and IABP in the treatment of acute myocardial infarction complicated with cardiac shock," *Chinese Journal of Integrative Medicine on Cardio/Cerebrovascular Disease*, vol. 16, no. 4, pp. 434–436, 2018.

[55] P. Sui, "Clinical curative effect analysis of Xinmailong Infection on I type cardiac-renal syndrome," *Guide of China Medicine*, vol. 14, no. 24, pp. 12-13, 2016 (Chinese).

[56] W. H. Shao, S. X. Wang, C. X. Lv, F. Li, X. Q. Li, and N. Wang, "Effect of Xinmailong Injection on NGAL, hs-cTnT, and RAAS in elderly patients with type 2 cardio-renal syndrome," *The Journal of Practical Medicine*, vol. 35, no. 4, pp. 654–657, 2019.

Hindawi
Evidence-Based Complementary and Alternative Medicine
Volume 2019, Article ID 9746492, 10 pages
https://doi.org/10.1155/2019/9746492

Research Article

Safety and Efficacy of the C-117 Formula for Vulnerable Carotid Artery Plaques (Spchim): A Randomized Double-Blind Controlled Pilot Study

Baoying Gong,[1] **Xiuyan Chen**,[1] **Rongming Lin**,[2] **Feng Zhang**,[3] **Jingxin Zhong**,[4] **Qixin Zhang**,[1] **Yuexiang Zhou**,[1] **Haijun Li**,[1] **Liling Zeng**,[1] **Zonghua Jiang**,[5] **and Jianwen Guo**[4]

[1]*Guangzhou University of Chinese Medicine, No. 232, Waihuan East Road, Guangzhou Higher Education Mega Center, Panyu District, Guangzhou, Guangdong Province 510006, China*
[2]*Guangdong Second Traditional Chinese Medicine Hospital, 60 Hengfu Road, Yuexiu District, Guangzhou, Guangdong Province 510095, China*
[3]*The 6th Affiliated Hospital of Sun Yat-Sen University, 26 Erheng Road, Yuancun, Tianhe District, Guangzhou, Guangdong Province 510655, China*
[4]*The 2nd Teaching Hospital of Guangzhou University of Chinese Medicine (Guangdong Provincial Hospital of Traditional Chinese Medicine), 111 Da'de Road, Yuexiu District, Guangzhou, Guangdong Province 510120, China*
[5]*People's Hospital of Ganzhou City, 17 Hongqi Avenue, Ganzhou City, Jiangxi Province, 341000, China*

Correspondence should be addressed to Zonghua Jiang; gzjzh22@163.com and Jianwen Guo; 306247680@qq.com

Received 10 April 2019; Accepted 27 June 2019; Published 17 July 2019

Guest Editor: Gunhyuk Park

Objective. To investigate the safety and efficacy of the Herbal Medicine C-117 (C-117) formula in the treatment of carotid atherosclerotic vulnerable plaques. *Methods*. This was a prospective, single-centre, randomized, double-blind study. A total of 120 eligible patients were randomly divided into two groups to receive the C-117 formula or placebo. As the basic treatment, both groups were treated according to the *Guidelines for Secondary Prevention of Ischemic Stroke/Transient Ischemic Stroke in China* using statins to regulate blood lipids, blood pressure lowering drugs, drugs for controlling blood sugar, and antiplatelet drugs according to the indications. The primary outcomes were the change in stability, the mean change of the plaque Crouse score, and the area and number of bilateral carotid artery plaques before and after 6 months of treatment. The secondary outcomes were the total number of cardiocerebrovascular events during the treatment and follow-up and the mean changes of lipid levels. *Result*. After 180 days of treatment, the plaque Crouse score(95% CI, 0.39 (0.01-0.77), P=0.046) and plaque area (95% CI, 2.14 (-10.10-14.39), P=0.727) were lower in the C-117 formula group than that before treatment. The plaque Crouse score of the control group (95% CI, 0.17 (-0.24-0.57), P=0.417) was lower than that before treatment, while the plaque area (95% CI, -0.35 (-9.35-8.65), P=0.938) increased, but without statistical significance. There was no significant difference in the reduction of the intima-media thickness (IMT), plaque Crouse score, or plaque area between the two groups after treatment (P>0.05). Subgroup analysis of patients whose Lipitor medication time ≥ 20% of the 6-month treatment showed that the levels of total cholesterol, triglycerides, and low-density lipoprotein were lower in the two groups after treatment than before, and the low-density lipoprotein levels in the C-117 formula group significantly decreased (95% CI, 2.99 (-0.08-0.39), P=0.005), but there was no statistical difference between the two groups after treatment (P>0.05). No serious adverse events occurred in the two groups after 180 days of treatment. *Conclusion*. The C-117 formula may be antiatherosclerotic by strengthening statins to reduce the low-density lipoprotein levels and reducing the carotid plaque Crouse scores. Clinical trials with large sample sizes, long-term interventions, and follow-up are needed to investigate the efficacy of the C-117 formula. *Clinical Trials Registration*. This trial is registered with clinicaltrials.gov identifier: NCT03072225 (registered retrospectively on 1st March 2017).

1. Introduction

Studies have shown that, between 1990 and 2016, global stroke mortality and morbidity gradually declined, but the morbidity in China was still rising and the burden of stroke as worse than before [1]. Stroke is still the leading cause of death and disability in China, and ischemic stroke's incidence rates is the highest among pathological types of stroke [2, 3]. Rupture of carotid atherosclerosis (CAS) plaques is an important cause of ischemic stroke. Studies have shown that, among Chinese symptomatic patients, there were more people with vulnerable carotid artery plaques than those with carotid stenosis (≥50%) [4].

At present, the treatment of CAS plaques mainly includes tertiary drug therapy (antiplatelet, lipid lowering, and blood pressure control) and surgical treatment (carotid endarterectomy; carotid artery stenting) [5, 6]. Vascular stent implantation directly covers unstable plaques, and there is a risk of restenosis after vascular stent surgery, while carotid endarterectomy has not been widely available in China. Statins, the most commonly used lipid-lowering drugs also have shortcomings. The SPARCL study [7] showed that high-dose atorvastatin calcium tablets (80 mg) only reduced the stroke recurrence rate by 16% over 5 years compared with placebo but increased the risk of haemorrhagic stroke. Statins also have other side effects, such as liver damage, muscle damage, and so on [6, 8, 9]. Therefore, there is still a lack of safe and effective drugs for treating CAS-vulnerable plaques.

Traditional Chinese Medicine is widely used as a secondary prevention in various types of chronic diseases in China, including atherosclerosis (AS). In the theory of traditional Chinese Medicine, the plaque is considered to be a tangible pathological factor (tangible evil) that is a pathological product of phlegm and blood stasis. The C-117 formula has been patented (Chinese Patent, application no. 201610326186.9) and consists of four kinds of herbal and insect medicine (*Hirudo* (ShuiZhi), *Atractylodis Rhizoma* (CangZhu), *Curcumae Zedoary* (EZhu), and *Endothelium Corneum Gigeriae Galli* (JiNeiJin)), which might remove blood stasis and clear phlegm, making the meridian smooth again. Traditional Chinese Medicine theory believes that animal medicine has stronger pharmacological activity than botanical medicine. *Hirudo* and *Endothelium Corneum Gigeriae Galli* are animal medicines that have the effect of removing a disease from the deep meridians and making the meridians smooth. Modern pharmacology believes that they can anticoagulation, inhibit endothelial cell proliferation, and antioxidation, and regulate blood lipids [10–13]. Years of clinical practical experience has shown that the Herbal Medicine C-117 formula might stabilize plaques or reduce the area of vulnerable plaques. The preexperiment, a small sample size and nonrandomized controlled study, showed that compared to treatment with atorvastatin calcium tablets alone, combination therapy with the C-117 formula was more effective in reducing the carotid IMT ($F=30.806$, $P\leq0.001$), plaque Crouse score ($F=11.815$, $P=0.001$), and plaque area [14].

However, there is still a lack of well-designed clinical trial evidence. Therefore, we designed a single-centre, prospective, randomized, double-blind, and placebo-controlled clinical trial to evaluate the safety and efficacy of the C-117 formula.

2. Methods

2.1. Setting and Study Population. This study was a single-centre, prospective, randomized, double-blind and placebo-controlled clinical pilot trial with two parallel groups. The study received ethical approval from the Ethics Committee of Guangdong Provincial Hospital of Chinese Medicine (Ethical Review no. Y2016-001) and was registered with ClinicalTrials.gov (ClinicalTrials.gov ID: NCT03072225).

All participants were recruited by posters in the hospital or in the hospital's WeChat official account ads. All patients in the screening session were informed of the protocol and signed a consent form. A total of 120 eligible patients who had hyperlipidaemia and vulnerable carotid plaques (Table 1 shows the detailed eligibility and exclusion criteria) were randomly divided into the C-117 formula group and the placebo group according to a 1:1 ratio and received a 6-month treatment.

2.2. Randomization and Blinding. The participants were assigned at random to one of the two treatment groups at a ratio of 1:1. Block randomization is generated and stratified by the PROC PLAN process using the SAS software version 9.2. The stochastic allocation procedure was saved in the Key Unit of Methodology in Clinical Research of Guangdong Province Hospital of Traditional Chinese Medicine (KYMCRGO-HTCM). Stratified block randomization was concealed using a sequentially numbered and opaque envelope.

Eligible patients were randomized into the C-117 formula group or the placebo group by obtaining medicines associated with the given drug codes in accordance with the order of visits. Participants, investigators, statisticians, and all study staff were blinded. Only the data administrators were permitted access to the unblinded data.

2.3. Interventions. All eligible patients received the basic treatment according to the *Guidelines for Secondary Prevention of Ischemic Stroke/Transient Ischemic Stroke in China 2014* [15], including treatment of basic diseases (control of hypertension, diabetes, hyperlipidaemia, and other diseases) and establishment of a good lifestyle.

For the C-117 group, the C-117 formula is composed of 4 herbal and insect medicines, *Hirudo* (ShuiZhi), *Atractylodis Rhizoma* (CangZhu), *Curcumae Zedoary* (EZhu), and *Endothelium Corneum Gigeriae Galli* (JiNeiJin). For the placebo group, the placebo is composed of dextrin, powdered sugar, starch, and liquid caramel. Its colour, smell and form are consistent with the C-117 formula. Both C-117 and the placebo drugs were prepared by the Kangyuan Pharmaceutical Factory according to Good Manufacturing Practices (GMP). Each pill had a diameter of 4.2 mm and was sealed and packaged in an opaque plastic bag (6 g per bag). Quality control was strictly enforced throughout the trial.

Patients were instructed to take the pills one bag each time, twice a day for 6 months. Only one month's dose could

Table 1: Study inclusion and exclusion criteria.

Inclusion criteria	
1	Meet the diagnostic criteria of carotid artery atherosclerosis
2	Ultrasound of carotid artery atherosclerotic plaque specifies it as an unstable plaque (including malakoplakia and mixed plaque);
3	Can persist on long-term medication
4	Older than 18 and under 80 years old
5	Meet the diagnostic criteria of hyperlipidaemia: Fasting serum total cholesterol ≥ 5.72 mmol/L or triglycerides ≥ 1.70 mmol/L or low density lipoprotein ≥ 1.8 mmol/L;
Exclusion Criteria:	
1	mRS rating higher than or equal to 3 before joining the trial group;
2	Carotid artery stenosis higher than or equal to 50%;
3	Confirmed or suspected vasculitis;
4	Infection, tumour or insufficient heart, liver and kidney functions (renal function higher than twice the upper limit in normal limits, HYHA heart function grading higher than or equal to level 2);
5	Acute myocardial infarction and unstable angina pectoris;
6	Acute cerebral arterial thrombosis;
7	Severe stenosis or occlusion of distal intracranial vessels;
8	Pregnant women or lactating mothers;
9	Known history of allergy to the trial drugs.

be obtained at a time, so each patient had to return to the hospital once a month to receive the drug from the investigators. The investigators were responsible for dispensing the medication and recording the adverse events that occurred during the medication.

2.4. Measurements. The primary outcome measures were the change in stability, the mean change of the plaque Crouse score, and the area and number of bilateral carotid artery plaques before and after 6 months of treatment.

A carotid artery ultrasound was used to the detect carotid artery IMT at the bilateral common carotid artery, bilateral internal carotid artery, bilateral external carotid artery, and its bifurcation 1.0 cm proximal and 1.0 cm distal to the carotid, and the average of the three locations was taken as the carotid IMT. Carotid artery IMT≥1.0 mm is defined as intimal thickening and localized IMT ≥1.5 mm as defined as a plaque [16].

Stability was defined according to the description of the colour ultrasound result: homogeneous hypoechoic plaques and irregular and ulcerated plaques represented unstable plaques, while homogeneous echogenic plaques and strong echogenic plaques represented stable plaques. The sum of the maximum thickness of each plaque in each blood vessel is defined as the plaque Crouse score for that blood vessel, and the sum of the bilateral carotid artery Crouse score was defined as the plaques Crouse score for each patient. To determine the plaque area, 3 diameters of each plaque were measured, and the two largest diameter lines were selected as the length-width multiplication. The sum of the areas of both carotid plaques was the total plaque area of the patient. The number of plaques was the sum of the number of bilateral carotid plaques.

The secondary outcomes were as follows: (1) The total number of cardiocerebrovascular events within 12 months (6 months treatment period and 6 months follow-up): cardiovascular and cerebrovascular events refer to events that cause vascular atherosclerosis and lead to organ lesions, such as coronary heart disease and stroke; (2) the mean changes of lipid levels (including triglyceride, cholesterol, low-density lipoprotein, and high density lipoprotein) before and after the 6-month treatment; (3) the mean changes of bilirubin levels (including the total bilirubin, direct bilirubin, and indirect bilirubin) before and after the 6-month treatment.

All adverse symptoms or adverse events were recorded throughout the study.

2.5. Sample Size. According to the study by Hirayama, A, et al. [17], the most commonly used drug for treatment of hyperlipidaemia, Atorvastatin, could decrease the volume of plaques by 8.7%. We supposed that the basic treatment combined with the C-117 formula could decrease it by 15%. According to this supposition and as calculated by the PASS 11.0 software, a sample size of 210 in each group achieved a 90% power and ruled out a two-sided type I error of 5% to detect a superiority margin difference of 15% in this trial. Considering a 15% loss to follow-up, the total sample size was adjusted to 247 in each group. Our preexperiment enrolled 103 participants, and the results showed that the C-117 formula might stabilize the vulnerable plaques [14], but it was a nonrandomized controlled study that reduced the credibility of the results. This study was designed as a randomized controlled and pilot study, so we reduced the sample size to 120 patients, with 60 patients in each group.

2.6. Statistical Analysis. All the statistical analyses were performed with the Statistical Package for Social Science statistics (SPSS 18.0). The statistical analysis set included Full-Analysis Set, Per-Protocol Population Set, and Safety Set. According to the principle of intention-to-treat analysis, FAS was a randomized group with at least one intervention and included postintervention evaluation data; PPS was in accordance with the inclusion criteria specified in the trial protocol, and compliance was greater than 80%; the outcome of the treatment was complete and there was no outcome evaluation after the last treatment. Drugs or treatments that might affect the efficacy evaluation were not used during the trial. The PPS dataset is the secondary dataset for the efficacy evaluation of this study; SS was all randomized. Grouping was used as long as patients underwent a study treatment and had performed at least one safety assessment. For FAS, this study used the following data-filling method: in the case of 0-180 days of detachment, withdrawal (nondeath): LOCF (last carry-over).

Demographic and baseline data were analyzed with standard, descriptive statistics. The blood lipid levels, number of plaques, plaque area, Crouse score, and bilirubin content are expressed as the mean ± standard deviation. The total cholesterol content, plaque Crouse score, total bilirubin, and indirect bilirubin content were compared before and after treatment with paired design t test. Triglyceride and low-density lipoprotein levels were compared before and after treatment. The independent sample rank sum test was used to compare the block area and posttreatment groups. The statistical description of the qualitative variables included the number of cases per group, the composition ratio (rate), and the chi-square test. All statistical tests were performed by a two-sided test. The test level was defined as α=0.05, and the difference was statistically significant at P<0.05. All statistical analyses were performed on blinded group allocations.

3. Result

From March 1st, 2017, to September 18th, 2018, a total of 270 people entered screening, and 120 cases were included in the study. One case from each group did not meet the inclusion criteria and was excluded. Therefore, a total of 118 patients were treated with medication (see Figure 1), of which 56 were male. More than half of the subjects in the test population were ≥ 60 years old (89 (75.42%), 56.78% of the subjects had hypertension, and 45.76% had diabetes. Of the patients, 79.7% took Lipitor (Atorvastatin calcium tablets 20 mg qn) as a lipid-lowering treatment, and only 4 people did not take lipid-lowering drugs. After 6 months, a total of 17 subjects did not complete the trial (6 in the C-117 formula group and 11 in the placebo group). The two groups were baseline balanced and comparable (Table 2).

3.1. Plaque Characteristics. In the C-117 formula group after 6 months of treatment, the plaque Crouse scores (95% CI, 0.39 (0.01-0.77), P=0.046<0.05) and plaque area (95% CI, 2.14 (-10.10-14.39)), P=0.727) were lower than before treatment, and the change in the plaque Crouse score was statistically significant. The plaque Crouse score of the control group (95% CI, 0.17 (-0.24-0.57), P=0.417) was lower than that before treatment, and the plaque area (95% CI, -0.35 (-9.35-8.65), P=0.938) increased compared with the area pretreatment, though neither of these were statistically significant (Table 3). There was no significant difference in the reduction of IMT, plaque Crouse score, or plaque area between the two groups after treatment (P>0.05).

3.2. Blood Lipid and Bilirubin Changes. To reduce interference, we only analysed lipids levels in patients who were treated with Lipitor. After treatment, the triglycerides and total cholesterol of the two groups were lower than before, and the total cholesterol in the C-117 formula group significantly decreased (P<0.05) (Table 4). There was no significant difference in blood lipids between the two groups after treatment (P>0.05). After sorting out and analyzing the database again, we found that some patients took lipid-lowering drugs only for a very short time, which may cause inaccuracy in the results of analysis. So we divided the patients who had not taken or the lipid-lowering medication time < 20% of the 6-month treatment into one group, a total of 16 people (Table 5). After removing this group of patients, we analyzed the blood lipid levels before and after treatment in patients taking Lipitor again. It showed that the triglyceride, total cholesterol, and low-density lipoprotein (LDL) were found to be reduced in both groups, and the triglyceride change in the control group and the low-density lipoprotein change in the C-117 formula group were statistically significant. There was no statistical difference between two groups after treatment (Table 6).

After treatment, the total bilirubin and direct bilirubin increased in both groups, and the direct bilirubin significantly increased in both groups (P<0.05) (Table 7). There was no statistically significant difference (P>0.05) when comparing bilirubin between the two groups after treatment (Table 7).

3.3. Adverse Events. During the 6-month treatment period, there were 9 cases of a blood pressure drop in the two groups (5 in the C-117 formula group and 4 in the placebo group). There were 2 cases of constipation and 3 cases of diarrhoea, all of which were from the placebo group. There were 9 other adverse events (2 in the C-117 formula group and 7 in the placebo group). A total of 9 patients developed a decrease in blood pressure, and blood pressure returned to normal after the antihypertensive drug was stopped. The blood pressure drop occurred between June and August, which may be related to vasodilation in summer. We think the blood pressure drop was independent of the drug. In the control group, constipation could be alleviated after stopping the drug and may have been related to the drug. Diarrhoea, dizziness, acute cholecystitis, tonsillitis, palpitations, and hyperhidrosis were considered to be unrelated to the test drug. Six patients in the placebo group withdrew from the trial due to adverse events, and 5 were lost to follow-up. Three patients in the C-117 formula group withdrew due to adverse events, and 3 patients were lost to follow-up.

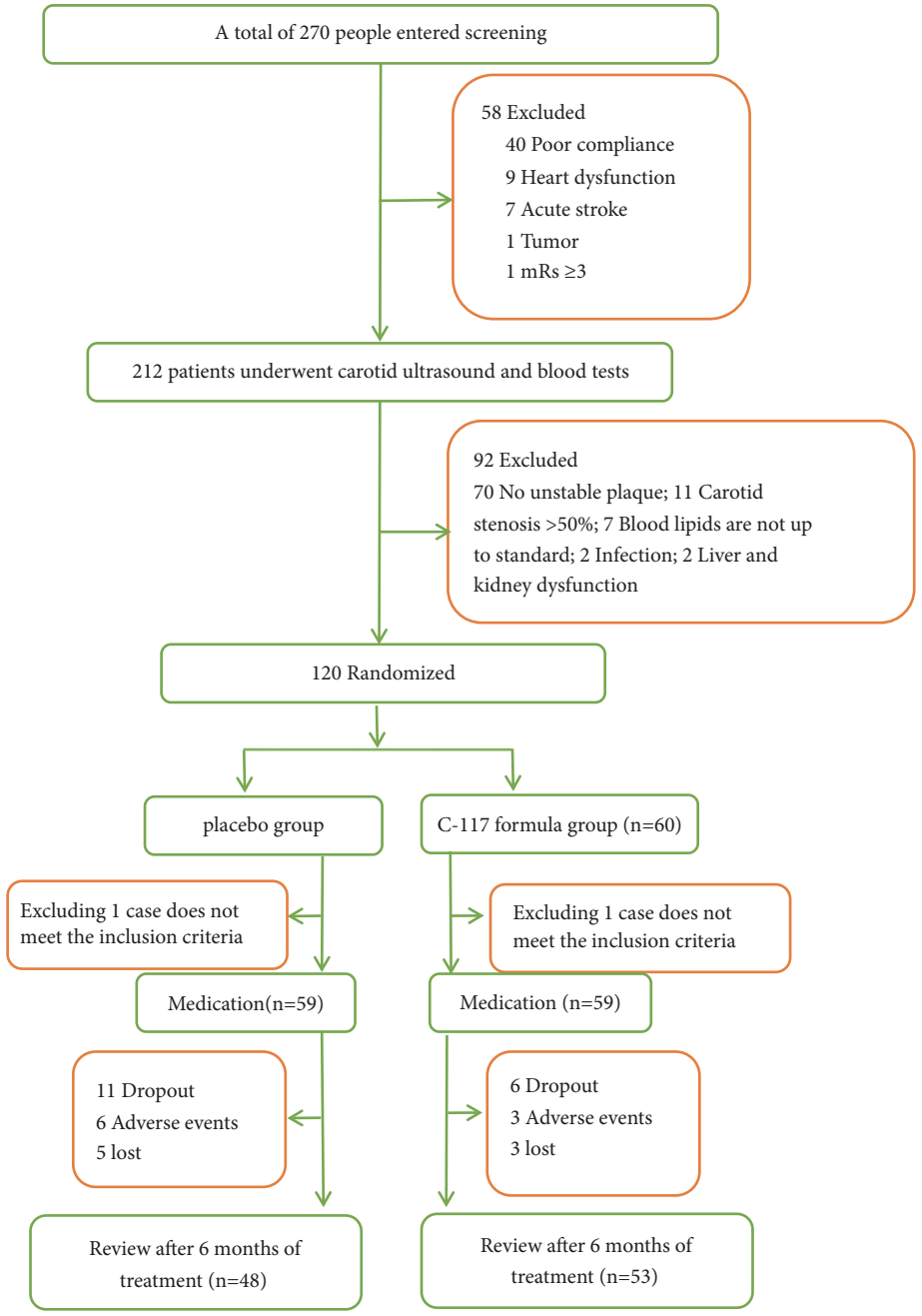

Figure 1: Flowchart of the participants through the trial.

4. Discussion

This study aimed to investigate the safety and efficacy of the C-117 formula in the treatment of CAS-vulnerable plaques. After 180 days of medication, the plaque Crouse scores of the two groups were lower than before and the total cholesterol and blood lipids decreased compared with those before treatment. The change of the C-117 formula group was statistically significant, but no significant differences were found when comparing between groups after treatment. Although adverse events occurred during the 6-month treatment, there was no liver or kidney dysfunction, and all adverse events were associated with a weak correlation with the C-117 formula. We believe that the C-117 formula provided better results.

Studies have found that the serum bilirubin levels in patients with AS are negatively correlated with the TIM thickness. The serum bilirubin levels is one of the risk factors for atherosclerosis. Although all molecular mechanisms behind its biological effects are still unknown, bilirubin is an important prognostic marker and a potential therapeutic target [18–20]. Therefore, we also compared the bilirubin levels of the two groups and found that the total bilirubin and direct bilirubin levels in the two groups were higher than those before treatment, but there was no difference between

Table 2: Baseline characteristics.

	C-117 formula group (n=59)	Placebo group (n=59)
Basic Features		
Age (Yr) $\overline{X} \pm S$	64.76 ± 7.079	63.5 ± 7.691
≥60, n (%)	46(78.0%)	43(72.9%)
Gender		
Female	34(57.6%)	28(47.5%)
Male	25(42.4%)	31(52.5%)
Height (cm) $\overline{X} \pm S$	161.39 ± 7.8	162.46 ± 6.18
Weight (kg) $\overline{X} \pm S$	62.92 ± 11.0	62.13 ± 8.58
Systolic blood pressure, $\overline{X} \pm S$, (mmHg)	126.29 ± 11.33	127.56 ± 13.85
Diastolic blood pressure, $\overline{X} \pm S$, (mmHg)	71.88 ± 8.81	74.32 ± 11.37
Past history, n (%)		
Ischemic stroke or TIA	8(13.6%)	9(15.3%)
Diabetes	14(23.7%)	13(22.0%)
Hypertension	30(50.8%)	37(62.7%)
Hyperuricemia	6(10.2%)	5(8.5%)
Other medical history	30(50.8%)	31(52.5%)
Personal life history, n (%)		
Exercise		
Often	33(55.9%)	36(61.0%)
Occasionally	26(44.1%)	22(37.3%)
Never	0(0%)	1(1.75%)
Eat vegetables every day	55(93.2%)	52(88.1%)
Eat fruit every day	35(59.3%)	34(57.6%)
Smoking history	7(11.9%)	9(15.3%)
Drinking history	19(32.2%)	11(18.6%)
Taking lipid-lowering drugs, n (%)		
Atorvastatin calcium tablets	48(81.4%)	46(78.0%)
Other lipid-lowering drugs	10(16.9%)	10(16.9%)
Not taken	1(1.7%)	3(5.1%)
Combination therapy, n (%)		
Antihypertensive drugs	28(47.5%)	30(50.8%)
Hypoglycaemic agents	10(16.9%)	11(18.6%)
Antiplatelet drug	12(20.3%)	9(15.3%)
Other medication	20(33.9%)	12(20.3%)

the two groups after treatment. Statins, the most commonly used lipid-lowering drug, achieve a lipid-lowering effect by lowering the levels of low-density lipoprotein. The results of this study found that, on the basis of the use of statins, the low-density lipoprotein decreased more significantly after the use of the C-117 formula, suggesting that the C-117 formula may strengthen the effect of statins.

The pathogenesis of AS is unclear, and the "endothelial injury" hypothesis is recognized by most people [21]. AS involves many biological processes, such as the inflammatory response, angiogenesis, and smooth muscle proliferation. Finally, lipids in the intima and proliferated and migrated smooth muscle cells form AS plaques [22]. AS plaques attach to the lumen of the artery, obstruct blood flow, and cause vascular stenosis in severe cases. Because AS is a progressive disease, the current clinical treatment advocates long-term intervention for high-risk patients; controlling blood pressure, blood sugar, and other risk factors; delaying the process; and preventing serious cardiovascular and cerebrovascular diseases [6]. The results of this study did not statistically validate the efficacy of the C-117 formula in the treatment of vulnerable plaques, but we found that the carotid IMT and plaque area in the C-117 formula group were lower than those before treatment, and the degree of change was greater than that of the control group. We speculate that the compound may delay the accumulation of a plaque and have certain lipid-lowering effect, but the effect is relatively mild, and the best therapeutic effect was not achieved in 180 days of treatment.

The C-117 formula consists of four drugs, *Hirudo* (ShuiZhi), *Curcumae Zedoary* (EZhu), *Atractylodis Rhizoma* (CangZhu), and *Endothelium Corneum Gigeriae Galli*

Table 3: Plaque characteristics of the two groups.

	C-117 formula group (n=59)	Placebo group (n=59)	Z/T	P
Bilateral IMT (mm)				
Before treatment	1.88 ± 0.44	1.89 ± 0.41		
After treatment	1.78 ± 0.35∗	1.77 ± 0.33∗	-0.005	0.996
Crouse score (mm)				
Before treatment	4.77 ± 3.06	3.96 ± 2.60		
After treatment	3.96 ± 2.60∗	3.80 ± 2.91	-1.233	0.217
Plaque area (mm^2)				
Before treatment	56.07 ± 71.15	38.13 ± 29.86		
After treatment	53.92 ± 55.58	38.48 ± 46.60	-1.416	0.157
Number of vulnerable plaques (n)				
Before treatment	2.12 ± 1.22	1.80 ± 0.92		
After treatment	2.19 ± 1.27	1.93 ± 1.11	-0.960	0.337
Number of stable plaques (n)				
Before treatment	0.33 ± 0.54	0.25 ± 0.60		
After treatment	0.31 ± 0.56	0.24 ± 0.50	-0.673	0.501
Total number of plaques (n)				
Before treatment	2.46 ± 1.30	2.05 ± 1.11		
After treatment	2.49 ± 1.36	2.17 ± 1.25	-1.295	0.195

M, mean ± standard deviation. P is the P value of the FAS dataset;
∗P<0.05 vs. before treatment.

Table 4: Blood lipid levels of the two groups who had taken Lipitor.

	C-117 formula group (n=48)	*Placebo group (n=46)*	Z/T	P
Lipid levels				
Triglyceride (mmol/L)				
Before treatment	1.33 ± 0.57	1.57 ± 0.89		
After treatment	1.27 ± 0.58	1.30 ± 0.61	-0.983	0.329
Total cholesterol (mmol/L)				
Before treatment	5.02 ± 0.91	4.98 ± 0.86		
After treatment	4.65 ± 1.02∗	4.87 ± 0.95	-0.309	0.757
Low-density lipoprotein (mmol/L)				
Before treatment	3.06 ± 0.79	3.11 ± 0.80		
After treatment	2.89 ± 0.86	3.23 ± 0.81	-1.826	0.720

M, mean ± standard deviation. P is the P value of the FAS dataset;
∗P<0.05 vs. before treatment.

(JiNeiJin), which contains two animal drugs. Hirudo's active ingredient, hirudin, protects endothelial cells by inhibiting thrombin activity, lowering lipids, and regulating the NO/endothelin balance. Hirudin can also inhibit the release of inflammatory factors, the formation of foam cells, and the proliferation of vascular smooth muscle cells [10, 11]. *Curcumae Zedoary's* main component, curcumin, also inhibits endothelial cell proliferation and migration, so the combination of *Curcumae Zedoary* and *Hirudo* can reduce the occurrence of endothelial damage. In addition, *Curcumae Zedoary* can control the risk factors of AS by reducing the local inflammatory response, lower lipid levels, and inhibiting platelet aggregation [23, 24]. *Atractylodis Rhizoma* could control blood pressure by inhibiting the activity of the angiotensin-inhibiting enzyme. it also could inhibits gastric acid secretion, Hypoglycemic and so on [25]. *Endothelium Corneum Gigeriae Galli* is the inner wall of the dry sac of the *Gallus gallus domesticus* Brisson and contains a variety of active proteases, amino acids, and polysaccharides from *Endothelium Corneum Gigeriae Galli*. *Endothelium Corneum Gigeriae Galli* can delay the AS process by antioxidation and improving blood sugar and blood lipid levels and blood rheology parameters [12, 13]. Therefore, we speculate that the combination of the four drugs can help control blood lipids and blood pressure by inhibiting endothelial cells, inhibiting foam cell formation, inhibiting smooth muscle cell proliferation, antioxidation, and improving blood viscosity to delay the development of AS.

The limitations of this study include the following: (1) An insufficient sample size. This study included a total of 120 patients, and the small sample size limited the credibility and extrapolation of the analysis results. (2) A short

Table 5: Taking lipid-lowering drugs, n (%).

	C-117 formula group (n=59)	Placebo group (n=59)
Atorvastatin calcium tablets (Lipitor)	44(74.6%)	42(71.2%)
Other lipid-lowering drugs	7(11.9%)	9(15.3%)
Not taken or the lipid-lowering medication time < 20% of the 6-month treatment	8(13.5%)	8(13.5%)

Table 6: Blood lipid levels of the two groups whose Lipitor medication time ⩾20% of the 6-month treatment.

	C-117 formula group (n=44)	*Placebo group (n=42)*	Z/T	P
Triglyceride (mmol/L)				
Before treatment	1.33 ± 0.58	1.56 ± 0.90		
After treatment	1.25 ± 0.53	1.27 ± 0.56∗	-0.430	0.966
Total cholesterol (mmol/L)				
Before treatment	5.02 ± 0.94	5.01 ± 0.78		
After treatment	4.62 ± 0.96∗	4.74 ± 0.85∗	-0.567	0.572
Low-density lipoprotein (mmol/L)				
Before treatment	3.09 ± 0.81	3.13 ± 0.78		
After treatment	2.86 ± 0.79∗	3.04 ± 0.72	-1.116	0.267

M, mean ± standard deviation. P is the P value of the FAS dataset;
∗P<0.05 vs. before treatment.

research period, the intervention time of this study was too short to realistically reflect the efficacy and safety of the C-117. (3) The diagnostic method of CAS-vulnerable plaques is determination of the carotid artery colour by Doppler ultrasound, and the result is subjectively influenced by the operator. Although we conducted unified training in colour ultrasound examination for doctors before the experiment, we cannot eliminate the existence of subjective deviations. Therefore, there is a certain influence on the judgment of the results. Our follow-up research needs to use more objective examination methods for diagnosis and evaluation.

In summary, the C-117 formula may delay the AS process, but this study is limited by the sample size and study period. The results of this study failed to statistically verify this inference. However, we found that the C-117 formula has a mild effect in delaying the accumulation of plaques and lipid lowering. Clinical trials with large sample sizes, long-term interventions, and follow-up are needed to investigate this effect.

Abbreviations

C-117 formula: The Herbal Medicine C-117 formula
IMT: Intima-media thickness
CAS: Carotid atherosclerosis
AS: Atherosclerosis
KYMCRGOHTCM: The Key Unit of Methodology in Clinical Research of Guangdong Province Hospital of Traditional Chinese Medicine
GMP: Good Manufacturing Practices.

Data Availability

The data used to support the findings of this study are available from the corresponding author upon request.

Ethical Approval

The study received ethical approval from the Ethics Committee of Guangdong Provincial Hospital of Chinese Medicine (Ethical Review no. Y2016-001)

Consent

Consent has been obtained from patients.

Conflicts of Interest

The authors declare that they have no conflicts of interest.

Authors' Contributions

All the authors participated in the study design and performed the trial. The Principle Investigator was Professor Jianwen Guo. Zonghua Jiang participated in the design of the study and the supervision of the study. Baoying Gong and Xiuyan Chen drafted the manuscript. Liling Zeng, Rongming Lin, and Haijun Li supervised and coordinated the clinical trial. Liling Zeng participated in the statistical design. Xiuyan Chen, Feng Zhang, Jingxin Zhong, Qixin Zhang, Yuexiang Zhou, and Baoying Gong were responsible for recruiting the participants. All the authors approved the final manuscript.

Table 7: Bilirubin levels of the two groups.

	C-117 formula group (n=59)	*Placebo group (n=59)*	Z/T	P
Total bilirubin (umol/L)				
Before treatment	10.74 ± 5.58	9.30 ± 2.64		
After treatment	11.08 ± 4.17	9.60 ± 2.32	-1.639	0.101
Direct bilirubin (umol/L)				
Before treatment	3.54 ± 1.56	3.20 ± 0.87		
After treatment	3.90 ± 1.24∗	3.54 ± 0.84∗	-1.561	0.119
Indirect bilirubin (umol/L)				
Before treatment	7.16 ± 4.17	6.06 ± 1.87		
After treatment	7.16 ± 3.10	6.06 ± 1.79	-1.587	0.112

M, mean ± standard deviation. P is the P value of the FAS dataset;
∗P<0.05 vs. before treatment.

Baoying Gong and Xiuyan Chen contributed equally to this study.

Acknowledgments

The authors thank Professor Zehuai Wen for directing the statistics of the data. He is the director of the Key Unit of Methodology in Clinical Research of Guangdong Province Hospital of Traditional Chinese Medicine. The authors are grateful for the research project support by the Guangdong Province Hospital of Traditional Chinese Medicine (Grant no. YN6803 and Grant no. YN2014LN08), the National Platform of Chinese Medicine Clinical Research (Grant no. 2015048), the Science and Technology Department of Guangdong Province of PRC (Grant no. 2014A020221074), the Guangzhou Science Technology and Innovation Commission of PRC (Grant no. 201804010178), and The National Key Research and Development Program of China (Grant no. 2018YFC1704100).

References

[1] V. L. Feigin, G. Nguyen, K. Cercy et al., "Regional, and country-specific lifetime risks of stroke, 1990 and 2016," *The New England Journal of Medicine*, vol. 379, no. 25, pp. 2429–2437, 2018.

[2] W. Longde, L. Jianmin, Y. Yang et al., "The prevention and treatment of stroke still face huge challenges ——brief report on stroke prevention and treatment in China, 2018," *Chinese Circulation Journal*, vol. 34, no. 2, pp. 105–119, 2019.

[3] W. Wang, B. Jiang, H. Sun et al., "Prevalence, incidence and mortality of stroke in china: results from a nationwide population-based survey of 480,687 adults," *Circulation*, vol. 135, no. 8, pp. 759–771, 2017.

[4] X. Zhao, D. Hippe, R. Li et al., "Prevalence and characteristics of carotid artery high-risk atherosclerotic plaques in chinese patients with cerebrovascular symptoms: a chinese atherosclerosis risk evaluation II study," *Journal of the American Heart Association*, vol. 6, no. 8, Article ID e005831, 2017.

[5] A. R. Naylor, J.-B. Ricco, G. J. de Borst, A. Halliday et al., "Management of atherosclerotic carotid and vertebral artery disease, 2017, clinical practice guidelines of the European society for vascular surgery (ESVS)," *European Journal of Vascular and Endovascular Surgery*, vol. 55, pp. 3–81, 2018.

[6] AACE, "American association of clinical endocrinologists and american college of endocrinology guidelines for management of dyslipidemia and prevention of atherosclerosis, Version I," *AACE Clinical Case Reports*, vol. 5, no. 4, 2017.

[7] P. Amarenco, "High-dose atorvastatin after stroke or transient ischemic attack," *Journal of Vascular Surgery*, vol. 44, no. 6, pp. 549–559, 2006.

[8] G. Meiling, Z. Zhendong, H. Zhigang et al., "A reappraisal for the risks of statin therapy," *Chinese Journal of Arteriosclerosis*, vol. 23, no. 3, pp. 310–314, 2015.

[9] C. R. Dormuth, B. R. Hemmelgarn, J. M. Paterson et al., "Use of high potency statins and rates of admission for acute kidney injury: multicenter, retrospective observational analysis of administrative databases," *BMJ*, Article ID f880, p. 346, 2013.

[10] E. Zhang, X. Lixu, Z. Tongde et al., "The research progress of hirudo on the related cells in the progression of atherosclerosis," *Chinese Journal of Arteriosclerosis*, vol. 27, no. 11, pp. 1184–1188, 2017.

[11] X. Liu, M.-F. Gao, and Y. Kong, "Bioactive constituents and pharmacological effects of leech," *Chinese Journal of Pharmaceutical Biotechnology*, vol. 24, no. 1, pp. 76–80, 2017.

[12] J. Changxing, J. Dingyun, X. Qingping et al., "Effects of JiNeiJin's astragalosides on blood lipids, hemorheology, and oxidative stress markers in hyperlipidemic rats," *Pharmacology and Clinics of Traditional Chinese Medicine*, vol. 28, no. 5, pp. 75–78, 2012.

[13] X. Guo, F. Jiguang, H. Kejie et al., "Experimental study on lipid-lowering, anticoagulant and hemorheological effects of JiNeiJin," *Information on Traditional Chinese Medicine*, vol. 4, no. 35, pp. 68-69, 2000.

[14] L. Rongming, *A prospective study to evaluate the safety and efficacy treated with Chinese insects and herbal medicine formula for patients with vulnerable plaques of carotid artery [Master, thesis]*, Guangzhou University of Chinese Medicine, 2016.

[15] Chinese Medical Association Neurology Branch and Chinese Medical Association Neurology Branch Cerebrovascular Disease Group, "Guidelines for secondary prevention of ischemic stroke/transient ischemic stroke in China 2014," *Chinese Journal of Neurology*, vol. 48, no. 4, pp. 258–273, 2015.

[16] Chinese Medical Association Ultrasound Medical Branch, "Carotid ultrasound examination specification for healthy physical examination population," *Chinese Journal of Health Management*, vol. 9, no. 4, pp. 254–260, 2015.

[17] A. Hirayama, S. Saito, Y. Ueda et al., "Plaque-stabilizing effect of atorvastatin is stronger for plaques evaluated as more unstable

by angioscopy and intravenous ultrasound," *Circulation Journal*, vol. 75, no. 6, pp. 1448–1454, 2011.

[18] D. Erdogan, H. Gullu, E. Yildirim et al., "Low serum bilirubin levels are independently and inversely related to impaired flow-mediated vasodilation and increased carotid intima-media thickness in both men and women," *Atherosclerosis*, vol. 184, no. 2, pp. 431–437, 2006.

[19] L. Novotný and L. Vítek, "Inverse relationship between serum bilirubin and atherosclerosis in men: a meta-analysis of published studies," *Experimental Biology and Medicine*, vol. 228, no. 5, pp. 568–571, 2003.

[20] L. Vítek, "Bilirubin and atherosclerotic diseases," *Physiological Research*, vol. 66, pp. S11–S20, 2017.

[21] R. Ross, "Cell biology of atherosclerosi," *Annual Review of Physiology*, vol. 57, pp. 791–804, 1995.

[22] A. J. Lusis, "Atherosclerosis," *Nature*, vol. 407, no. 6801, pp. 233–241, 2000.

[23] Y.-Y. Cui, J.-G. Liu, F.-H. Zhao, and D.-Z. Shi, "Advances in studies on pharmacological action of mainchemical constituent of curcumae zedoary in preventing in-stent restenosis," *China Journal of Chinese Materia Medica*, vol. 40, no. 7, pp. 1230–1234, 2015.

[24] W. Qian, Z. Fuhai, and S. Dazhuo, "Advances in cardiovascular pharmacology research of rhizoma curcumae and its extracts," *Chinese Journal of Integrated Traditional Chinese and Western Medicine*, vol. 32, no. 4, pp. 575-576, 2012.

[25] D. Aiping, L. Ying, W. Zhitao et al., "Advances in studies on chemical compositions of Atractylodes lancea and their biological activities," *China Journal of Chinese Materia Medica*, vol. 41, no. 21, pp. 3904–3913, 2016.

Hindawi
Evidence-Based Complementary and Alternative Medicine
Volume 2019, Article ID 4674190, 12 pages
https://doi.org/10.1155/2019/4674190

Research Article

Scolopendra subspinipes mutilans L. Koch Ameliorates Rheumatic Heart Disease by Affecting Relative Percentages of $CD4^+CD25^+$FoxP3 Treg and $CD4^+$IL17 T Cells

Tiechao Jiang,[1,2] Qini Zhao,[1,2] Hongyan Sun,[3] Lirong Zhang,[3] Shanshan Song,[4] Hongli Chi,[5] and Hui Zhou[6]

[1]*Department of Cardiovascular Medicine, China-Japan Union Hospital of Jilin University, Changchun 130033, China*
[2]*Jilin Provincial Precision Medicine Key Laboratory for Cardiovascular Genetic Diagnosis, Changchun 130033, China*
[3]*Department of Pathology, China-Japan Union Hospital of Jilin University, Changchun 130033, China*
[4]*Department of Radiology, College of Public Health, Jilin University, Changchun 130021, China*
[5]*Department of EICU, The First Hospital of Jilin University, Changchun 130021, China*
[6]*Department of Anesthesiology, China-Japan Union Hospital of Jilin University, Changchun 130033, China*

Correspondence should be addressed to Hongli Chi; chihl@jlu.edu.cn and Hui Zhou; zhouhuijlu@126.com

Received 9 April 2019; Accepted 28 May 2019; Published 14 July 2019

Guest Editor: Gunhyuk Park

Scolopendra subspinipes mutilans L. Koch. (SSLK) helps reduce the risk of coronary heart disease (CHD) but its effects on rheumatic heart disease (RHD) patients remain unclear. 80 RHD patients were recruited and randomly assigned into SG (to receive SSLK treatment) and CG (to receive placebo) groups, and the intervention lasted for 3 months. The following cardiac indexes were measured, including mean arterial pressure (MAP), heart rate (HR), central venous pressure (CVP), blood lactate, fatigue, shortness of breath, palpitation, and chest pain. ELISA kits were used to analyze creatine kinase isoenzyme (CK-MB), serum troponin T (cTnT), CRP, IL-1β, IL-6, and TNF-α, malondialdehyde (MDA), and superoxide dismutase (SOD). Relative percentages of $CD4^+CD25^+$FoxP3 regulatory (Treg) and $CD4^+$IL-17 T cells were measured using flow cytometry. After 3-month therapy, SSLK intervention improved MAP, HR, CVP, fatigue, palpitation, and shortness breath of CHD patients, reduced the levels of blood lactate, CK-MB, cTnT, CRP, IL-1β, IL-6, TNF-α, MDA, and increased SOD level ($p < 0.05$). Meanwhile, SSLK treatment increased the percentages of $CD4^+CD25^+$FoxP3 Treg cells and reduced relative percentages of $CD4^+$IL-17 T cells in a dose-dependent way ($p < 0.05$). Relative percentage of $CD4^+CD25^+$FoxP3 Treg cells had negative relationship while $CD4^+$IL17 T cells had positive relationship with CK-MB, cTnT, CRP, and TNF-a ($p < 0.01$). SSLK ameliorated RHD by affecting the balance of $CD4^+CD25^+$FoxP3 Treg and $CD4^+$IL17 T cells.

1. Introduction

Rheumatic heart disease (RHD) is a sequel of acute rheumatic fever (ARF) [1, 2] and an autoimmune disease caused by the damage to heart valves [3] or hemolytic streptococcal infection [4]. According to statistics, there are more than 15.6 million RHD patients in the world [5]. The prevention and treatment of RHD is still a common public health issue and causes a global burden. Antibiotics are often used in the treatment of RHD to prevent infection and the inflammation of the heart and other symptoms [6, 7]. However, a frequent and distressing complication often occurs after the treatment. Some pathogen can develop antibiotic resistance and make the treatment ineffective [8]. Furthermore, antibiotics produce toxicity [9] and cause drug-drug interaction [10], which will further contribute to RHD progression. It is highly needed to explore new effective medicine with fewer side effects.

Scolopendra subspinipes mutilans L. Koch (SSLK), ancient antipyretic traditional Chinese medicine, can improve blood circulation, relieve blood stasis [11], and prevent heart failure by attenuating postinfarct remodeling [12]. SSLK has been

reported to control vascular disease via its anti-inflammatory activities [13]. SSLK can reduce the risk of heart disease by improving the biochemical indices of patients [14]. More work indicates that SSLK can regulate fatty acids metabolism by exerting antiadipogenic activity via the inhibition of the expression of C/EBPβ, C/EBPα, and PPARγ and the Akt signaling pathway in adipocytes [15].

It has been reported that $CD4^+$T cells are the major effector cells in the heart valve of RHD patients, and the number of these cells is increased in the peripheral blood of RHD patients [16]. There are approximately 5% to 10% of $CD4^+$T cells in peripheral blood and spleen tissues of healthy persons. CD25, TGF-beta, and forkhead box protein P3 (FoxP3) are highly expressed in T cells [17]. These proteins play crucial roles in the immunosuppressive functions of regulatory T (Treg) cells [18]. $CD4^+CD25^+$Treg cells are generated in the thymus and have been reported to mitigate autoimmune myocarditis [19]. The dysfunction of $CD4^+CD25^+$Treg cells may lead to RHD occurrence and FoxP3 regulates Treg cell development and function [20, 21]. $CD4^+$IL-17 T cells have been reported to be associated with bacterial infection and inflammatory responses [22, 23].

SSLK reduces the risk of coronary heart disease (CHD) [24]. However, the effects of SSLK on RHD remain unknown and related molecular mechanisms are unclear. High-level Th17/Treg ratio has been found to be associated with the risk and progression of RHD [25]. $CD4^+$IL17 T cells are the main Th17 cell subsets [26] and $CD4^+CD25^+$FoxP3 Treg cells are the main Treg cell subsets [27]. Thus, SSLK may exert beneficial effects on RHD patients by affecting the levels of $CD4^+CD25^+$FoxP3 Treg and $CD4^+$IL17 T cells. Therefore, in this study, peripheral blood samples were collected from RHD patients to investigate the effects of SSLK on regulatory T lymphocytes. To investigate the changes of relative percentages of $CD4^+CD25^+$Treg and $CD4^+$IL-17 T cells induced by SSLK, the study may provide new molecular mechanism for RHD treatment.

2. Materials and Methods

2.1. Materials. FITC mouse anti-human CD4 (Clone RPA-T4), an isotype control mouse IgG1-FITC (Clone MOPC-21), APC mouse anti-human CD25 (Clone M-A251), an isotype control anti-APC mouse IgG1 (Clone MOPC-21), PE Mouse anti-Human FoxP3 (Clone 259D/C7), and an isotype control PE mouse IgG1 (Clone MOPC-21) were purchased from BD eBioscience (BD Bioscience, San Jose, CA, USA). Ficoll-Paque was purchased from Sigma (Louis, MO, USA). M-MLV First Strand Kit was purchased from Invitrogen (Shanghai, China). Power SYBR Green PCR Master Mix was purchased from ABI (Foster, CA, USA).

2.2. Participants. The study was approved by the Human Research Ethics Committee of China-Japan Union Hospital of Jilin University (Changchun, China, approval no. 2015NXY) and all participants signed informed consent. From November 2015 to July 2016, 227 CHD patients were recruited at our hospital. All patients were diagnosed with RHD based on clinical symptoms, rheumatic fever history, and cardiac ultrasonography.

2.3. Inclusion Criteria. All patients were diagnosed with rheumatic mitral valve disease by medical history, physical examination, laboratory examination, echocardiography, and surgery.

2.4. Exclusion Criteria. The patients would be excluded if they had the following symptoms: acute myocardial infarction and severe heart failure; psychiatric abnormalities and being unable to correctly describe their symptoms and other autoimmune system diseases (such as rheumatoid arthritis); or systemic lupus erythematosus.

2.5. Patient Grouping. After applying inclusion criteria and exclusion criteria, a total of 80 RHD patients entered the present study at China-Japan Union Hospital of Jilin University. SSLKs were purchased from Beijing Tongrentang Pharmacy (Beijing, Chin) to make fine powder. The patients were evenly and randomly assigned into two groups: SSLK (SG, orally given 100-mg SSLK powder every morning) and control (CG, orally given 100-mg placebo every morning). The whole duration of the treatment was three months. Liver function was measured using liver function monitoring system (LiMON Leberfunktionsmonitor, Pulsion Medical Systems AG, Munich, Germany). Renal function was measured using blood urea nitrogen, serum creatinine, and estimated glomerular filtration rate according to previous reports [28]. Meanwhile, side effects (dry mouth, diarrhea, dizziness, weakness, no appetite or nausea, headache, fatigue, nightmares, and so on) were measured according to self-reported physical activity.

2.6. Hemodynamics and Arterial Blood Gas Index. Dopamine would be considered when the severe condition of RHD occurred. Mean arterial pressure (MAP), heart rate (HR), central venous pressure (CVP, evaluated by ultrasound of the internal jugular vein), partial pressure of oxygen (PaO_2), and blood lactate levels were measured at 0 months, 1 month, 2 months, and 3 months.

2.7. Serum Levels of Inflammatory Cytokines. The serum concentrations of C-reactive protein (CRP, Cat. No. ab136176), tumor necrosis factor-a (TNF-a, Cat. No. ab9348), IL-1β (Cat. No. ab46052), IL-6 (Cat. No. ab178013), IL-10 (Cat. No. ab46034), and TGF-β (Cat. No. ab100647) were measured using the ELISA kits from Abcam (Shanghai, China).

2.8. Cardiac Biomarker Levels. After 0-, 1-, 2- and 3-month treatment, the creatine kinase isoenzyme (CK-MB), serum cardiac troponin T (cTnT), malondialdehyde (MDA), and superoxide dismutase (SOD) were detected by an automatic biochemical analyzer (Hitachi 7600P, Hitachi, Japan).

2.9. The Measurement of $CD4^+CD25^+$FoxP3 Treg and $CD4^+$IL-17 T Cells. Five-mL venous blood was taken aseptically from each subject at 0 months and 3 months

Table 1: Clinical characteristics of all participants.

	SSLK group (N=40)	Control group (N=40)	t/χ2 values	P values
Age, (years)	47.85 ± 9.95	45.20 ± 9.99	0.984	0.324
Female, n (%)	31(77.5)	28(70)	0.581	0.446
BMI, kg/m^2	23.92 ± 2.26	23.32 ± 2.47	0.157	0.873
Smoking, n (%)	8 (20)	4 (10)	1.569	0.210
Diabetes, n (%)	5 (12.5)	6(15)	0.105	0.745
Hypertension, n (%)	32(78)	33(82.5)	0.082	0.775
Ongoing treatment				
Digoxin, n (%)	10(25)	8(20)	0.287	0.592
Aspirin, n (%)	22(55)	23(57.5)	0.051	0.822
NYHA classification				
II, n (%)	34(85)	35(87.5)	0.626	0.731
III, n (%)	6(15)	8(20)		
AF, n (%)	38(95)	33(82.5)		
Mitral stenosis,				
Moderate, n (%)	20(50)	23(57.5)	0.188	0.664
Severe, n (%)	15(37.5)	14(35)		
Aortic stenosis,				
Moderate, n (%)	3(7.5)	4(10)		
Severe, n (%)	2(5)	3(7.5)		
Tricuspid incompetence				
Mild, n (%)	28(70)	29(72.5)	0.583	0.747
Moderate, n (%)	6(15)	8(20)		
Severe, n (%)	2(5)	1(2.5)		
Plasma measurements,				
Triglycerides,	2.16 ± 1.24	1.94 ± 1.77	0.763	0.482
Total cholesterol (mmol/L),	5.33 ± 1.36	4.67 ± 1.41	1.639	0.163
LDL-C (mmol/L),	3.31 ± 0.89	3.46 ± 0.99	0.652	0.561
HDL-C (mmol/L),	1.59 ± 0.67	1.68 ± 0.39	0.758	0.478

Note: *SSLK, Scolopendra subspinipes mutilans L. Koch.* BMI, body mass index. NYHA, the New York Heart Association; AF, atrial fibrillation; LDL-C, low-density lipoprotein cholesterol; HDL-C, high-density lipoprotein cholesterol.

and heparinized anticoagulated. The blood samples were processed within 2 h. Five-mL venous blood and equal volume of sterile saline were used to dilute the venous blood and mixed thoroughly to extract peripheral blood mononuclear cells (PBMCs). PBMCs were prepared using Ficoll-Paque density gradient centrifugation. $CD4^+$ cells were gated on forward and side scatter for lymphocyte purity in the gate. Relative percentages of $CD4^+CD25^+$FoxP3 Treg and $CD4^+$IL-17 T cells were analyzed by flow cytometry.

2.10. The Effects of SSLK on Relative Percentages of $CD4^+CD25^+$FoxP3 Treg and $CD4^+$IL-17 T Cells. Above PBMCs were cultured in DMEM medium with fetal bovine serum (Cat. No. TM999) to a final concentration of 10% and penicillin/streptomycin at 1%. The cells were adjusted to a density of 1×10^5 cells/mL, added to a 96-cell plate (100 μL/per cell), and cultured at 95% air, 5% CO_2, and 37°C. SSLK powder was added to the medium with final concentration from 0 to 10 μg/mL. After 48 h, PBMCs were stained by surface marker CD4 and CD25 antibodies firstly. After fixation and permeabilization, PBMCs were then stained by Foxp3 and IL-17 antibodies. Relative percentages of $CD4^+CD25^+$FoxP3 Treg and $CD4^+$IL-17 T cells were analyzed by flow cytometry.

2.11. Statistical Analysis. SPSS18.0 statistical software was used for data analysis. Quantitative variables were expressed as mean values ± S.D. (standard derivative). Independent samples T-test and one-way analysis of variance (ANOVA) were used to compare the data difference between CG and SG groups. Chi-square test was used to compare the number difference between two groups. The correlation between two variables was analyzed using Pearson correlation coefficient test. $p < 0.05$ indicates the difference was statistically significant.

3. Results

3.1. Clinical Characteristics. The baseline clinical characteristics of RHD patients from two groups were shown in Table 1. There was no significant difference in age, body mass

Table 2: The complications of rheumatic heart disease (RHD) patients between two groups.

Parameters	CG	SG	p values
0 months			
Fatigue, cases	35	33	0.531
Palpitation, cases	30	31	0.793
Dyspnea, cases	29	27	0.626
Chest pain grades, cases			
0	0	0	
1	4	3	
2	5	7	
3	9	8	
4	8	7	
5	6	4	1.000
6	5	6	
7	2	3	
8	1	2	
9	0	0	
10	10	0	
3 months			
Fatigue, cases	36	19	0.001
Palpitation, cases	30	21	0.036
Dyspnea, cases	28	16	0.007
Chest pain grades, cases			
0	3	8	
1	6	10	
2	9	7	
3	8	5	
4	6	2	
5	5	3	0.935
6	1	3	
7	2	1	
8	0	0	
9	0	0	
10	0	0	

Note: The pain grade scores (0-10) were analyzed and higher pain grades with higher scores were associated with more serious pain. The significant difference was analyzed by using a Chi-square test or one-way ANOVA. SG, SSLK group and CG, control group. There was significant difference if $p < 0.05$ vs. a control group.

index, triglyceride, total cholesterol, low density lipoprotein cholesterol, and high-density lipoprotein cholesterol between the two groups ($p > 0.05$). At the same time, there were more female patients in the case group.

3.2. SSLK Consumption Improved the Complications of CHD Patients. The statistical difference for the cases of fatigue, chest pain, palpitation, and short breathing was insignificant between the CG and SG groups (Table 2, $p > 0.05$). After 3-month therapy, the symptoms were improved in SG when compared with CG group except chest pain (Table 2, $p < 0.05$). SSLK treatment improved the complications of CHD patients.

3.3. SSLK Treatment Reduced the Level of Blood Lactate. The statistical differences for the levels of MAP, HR, CVP, arterial PaO2, and blood lactate content were insignificant between two groups at 0 months and 1 month (Table 3, $p > 0.05$); MAP, HR, CVP, Pao2, and blood lactate content in the SG were lower than in the CG group after 2 months (Table 3, $p < 0.05$). The results suggested that SSLK treatment could not affect MAP, HR, CVP, PaO_2, and blood lactate in a short term.

3.4. SSLK Treatment Reduced the Inflammatory Cytokines Levels. The statistical differences for the levels of CRP, TNF-a, IL-1β, and IL-6 levels were insignificant between the two groups at 0 months (Table 4, $p > 0.05$). The concentrations of CRP, TNF-a, IL-1β, and IL-6 in the SG group were lower than in the CG group (Table 4, $p < 0.05$). The results suggested that SSLK reduced the inflammatory cytokines levels.

3.5. SSLK Treatment Improved Myocardial Enzyme Levels. The statistical differences of CK-MB, cTnT, MDA, and SOD levels were insignificant between the two groups (P<0.05, Table 3). The concentrations of CK-MB, cTnT, and MDA in the SG group were lower than in the CG group while SOD had reverse results (Table 5, $p < 0.05$). The results suggested that SSLK treatment improved myocardial enzyme levels.

3.6. SSLK Treatment Improved Serum Levels of Inflammatory Factors. ELISA analysis showed that SSLK treatment reduced the serum levels of IL-1β (Figure 1(a)) and IL-6 (Figure 1(b)) and increased the levels of IL-10 (Figure 1(c)) and TGF-β (Figure 1(d)) when compared with the CG group ($p < 0.05$). SSLK treatment improved serum levels of inflammatory factors.

3.7. SSLK Treatment Affected Relative Percentages of $CD4^+CD25^+FoxP3$ Treg and $CD4^+$IL-17 T Cells in PBMCs. Before SSLK intervention, the average percentages of $CD4^+CD25^+$FoxP3 Treg cells (Figure 2(a)) and $CD4^+$IL-17 T cells (Figure 2(b)) were 3.5% and 7.2% in CG group, respectively. The average percentages of $CD4^+CD25^+$FoxP3 Treg cells (Figure 2(c)) and $CD4^+$IL-17 cells (Figure 2(d)) were 3.7% and 6.9%. The statistical differences for the percentages of $CD4^+CD25^+$FoxP3 Treg cells and $CD4^+$IL-17 T cells were insignificant ($p > 0.05$). After 3-month SSLK intervention, the average percentages of $CD4^+CD25^+$FoxP3 Treg cells (Figure 2(e)) and $CD4^+$IL-17 T cells (Figure 2(f)) were 3.2% and 6.5% in CG group, respectively. The average percentages of $CD4^+CD25^+$FoxP3 Treg cells (Figure 2(g)) and $CD4^+$IL-17 cells (Figure 2(h)) were 5.8% and 3.4% in the SG group, respectively. SSLK treatment increased the percentages of $CD4^+CD25^+$FoxP3 Treg cells (from 3.2 ± 0.5 to 5.8 ± 0.7) and reduced the percentages of $CD4^+$IL-17 T cells (from 6.5 ± 0.9 to 3.4 ± 0.6). The results suggested that SSLK consumption affected the percentages of $CD4^+CD25^+$FoxP3 Treg cells and $CD4^+$IL-17 T cells in PBMCs.

3.8. The Effects of SSLK on the Percentage of $CD4^+CD25^+FoxP3$ Treg and $CD4^+$IL-17 T Cells in PBMCs. Figure 3 showed that SSLK increased the percentage of $CD4^+CD25^+$FoxP3 Treg

Table 3: Comparison of hemodynamic parameters and arterial blood gas between two groups.

Parameters		0 months	1 month	2 months	3 months
MAP/mmHg	CG	73.65 ± 4.16	77.49 ± 6.23	78.21 ± 6.48	78.92 ± 7.25
	SG	75.12 ± 3.85	73.20 ± 5.76	70.33 ± 7.16	70.93 ± 7.64
F		0.245	0.268	2.495	2.996
p values		0.687	0.612	0.035	0.027
HR (times/min)	CG	76.48 ± 13.54	81.26 ± 15.37	80.38 ± 15.89	81.32 ± 15.71
	SG	77.62 ± 12.36	76.34 ± 9.18	70.96 ± 12.53	70.13 ± 13.99
F		0.109	0.436	3.168	3.656
p values		0.853	0.375	0.039	0.024
CVP/cmH_2O	CG	15.41 ± 2.12	13.42 ± 3.84	14.61 ± 4.23	14.58 ± 4.35
	SG	15.65 ± 2.05	11.95 ± 4.13	10.36 ± 4.38	9.87 ± 4.69
F		0.063	1.169	4.219	5.324
p values		0.869	0.082	0.012	0.003
PaO_2/mmHg	CG	156.26 ± 62.35	138.52 ± 40.24	130.44 ± 42.19	134.48 ± 43.01
	SG	168.23 ± 59.35	130.78 ± 35.17	111.36 ± 40.14	114.53 ± 42.38
F		0.246	0.835	3.237	3.064
p values		0.627	0.102	0.027	0.031
Blood lactate /mmol/L	CG	0.47 ± 0.10	0.85 ± 0.26	1.36 ± 0.36	1.34 ± 0.21
	SG	0.51 ± 0.16	0.73 ± 0.39	1.21 ± 0.30	1.22 ± 0.33
F		0.878	1.943	2.053	2.246
p values		0.126	0.051	0.042	0.039

Note: MAP, mean arterial pressure; HR, heart rate; CVP, central venous pressure and PaO2, Partial Pressure of Oxygen. SG, SSLK group and CG, control group. There was significant difference if $p < 0.05$ vs. a control group.

Table 4: The concentrations of CRP, TNF- a, IL-1, and IL-6 between two groups.

Parameters		0 months	1 month	2 months	3 months
CRP (μg/mL)	CG	9.81 ± 1.32	79.36 ± 8.57	76.15 ± 9.25	56.23 ± 5.26
	SG	10.12 ± 1.26	62.21 ± 6.29	45.62 ± 3.26	39.58 ± 3.54
F		0.563	2.140	14.363	12.072
p values		0.451	0.022	0.001	0.001
TNF-α (pg/mL)	CG	11.32 ± 3.24	45.31 ± 5.26	24.15 ± 5.05	22.23 ± 4.25
	SG	10.29 ± 3.18	34.18 ± 2.95	18.23 ± 3.12	12.68 ± 2.52
F		1.027	9.741	13.981	15.327
p values		0.068	0.003	0.002	0.001
IL-6/(ng/L)	CG	21.15 ± 3.26	53.62 ± 11.05	68.29 ± 10.26	35.21 ± 9.26
	SG	20.59 ± 3.52	34.26 ± 5.62	23.46 ± 3.52	17.62 ± 4.76
F		0.217	12.451	22.461	38.972
p values		0.822	0.001	0.001	0.001
IL-1/(ng/L)	CG	18.26 ± 4.26	67.59 ± 8.26	59.26 ± 7.52	43.26 ± 5.21
	SG	18.15 ± 4.31	53.26 ± 6.05	31.25 ± 6.20	21.36 ± 4.74
F		0.116	8.642	12.673	36.519
p values		0.824	0.003	0.001	0.001

Note: CRP, C-creative protein; TNF-a, tumor necrosis factor; IL-1, interleukin-1 and IL-6, interleukin-6. SG, SSLK group and CG, control group. There was significant difference if $p < 0.05$ vs. a control group.

cells (Figure 3(a)) and reduced the percentage of $CD4^+$IL-17 T cells (Figure 3(b)) in a dose-dependent way in PBMCs. The results showed that SSLK intervention regulated the percentages of $CD4^+CD25^+$FoxP3 Treg and $CD4^+$IL-17 T cells in PBMCs.

3.9. The Percentage of $CD4^+CD25^+$FoxP3 Treg Cells Had Negative Relationship with CK-MB, cTnT, CRP, and TNF-a. Pearson correlation coefficient test showed that, with the increase in the percentage of $CD4^+CD25^+$FoxP3 Treg cells, the levels of CK-MB (Figure 4(a)), cTn1 (Figure 4(b)), CRP

Table 5: Comparison of cardiac marker between two groups.

Parameters		0 months	1 month	2 months	3 months
CK-MB/	CG	7.61 ± 1.52	41.35 ± 12.20	52.26 ± 13.36	33.65 ± 8.26
(ng/mL)	SG	7.26 ± 1.46	26.58 ± 10.54	34.69 ± 11.25	21.26 ± 7.26
F		0.098	32.147	22.654	18.761
p values		0.912	0.001	0.001	0.001
cTnl/(ng/mL)	CG	0.01 ± 0.01	0.61 ± 0.23	1.38 ± 0.51	0.84 ± 0.35
	SG	0.01 ± 0.01	0.41 ± 0.28	0.76 ± 0.21	0.28 ± 0.12
F		0	16.423	25.349	45.678
p values		1.000	0.002	0.001	0.001
MDA/	CG	3.51 ± 0.89	7.68 ± 0.65	7.34 ± 0.58	6.84 ± 0.48
(nmol/mL)	SG	3.48 ± 0.79	5.87 ± 0.79	5.74 ± 0.83	4.26 ± 0.36
F		0.082	9.856	10.154	15.483
p values		0.947	0.002	0.002	0.001
SOD/	CG	120.35 ± 18.26	66.82 ± 17.65	78.52 ± 23.15	84.51 ± 26.03
(UN/mL)	SG	119.45 ± 17.36	88.26 ± 13.62	95.62 ± 24.58	108.26 ± 25.15
F		0.085	14.872	16.485	20.163
p values		0.793	0.002	0.001	0.001

Note: CK-MB, creatine kinase isoenzyme; cTnT, cardiac troponin T; MDA, malondialdehyde and SOD, superoxide dismutase. SG, SSLK group and CG, control group. There was significant difference if $p < 0.05$ vs. a control group.

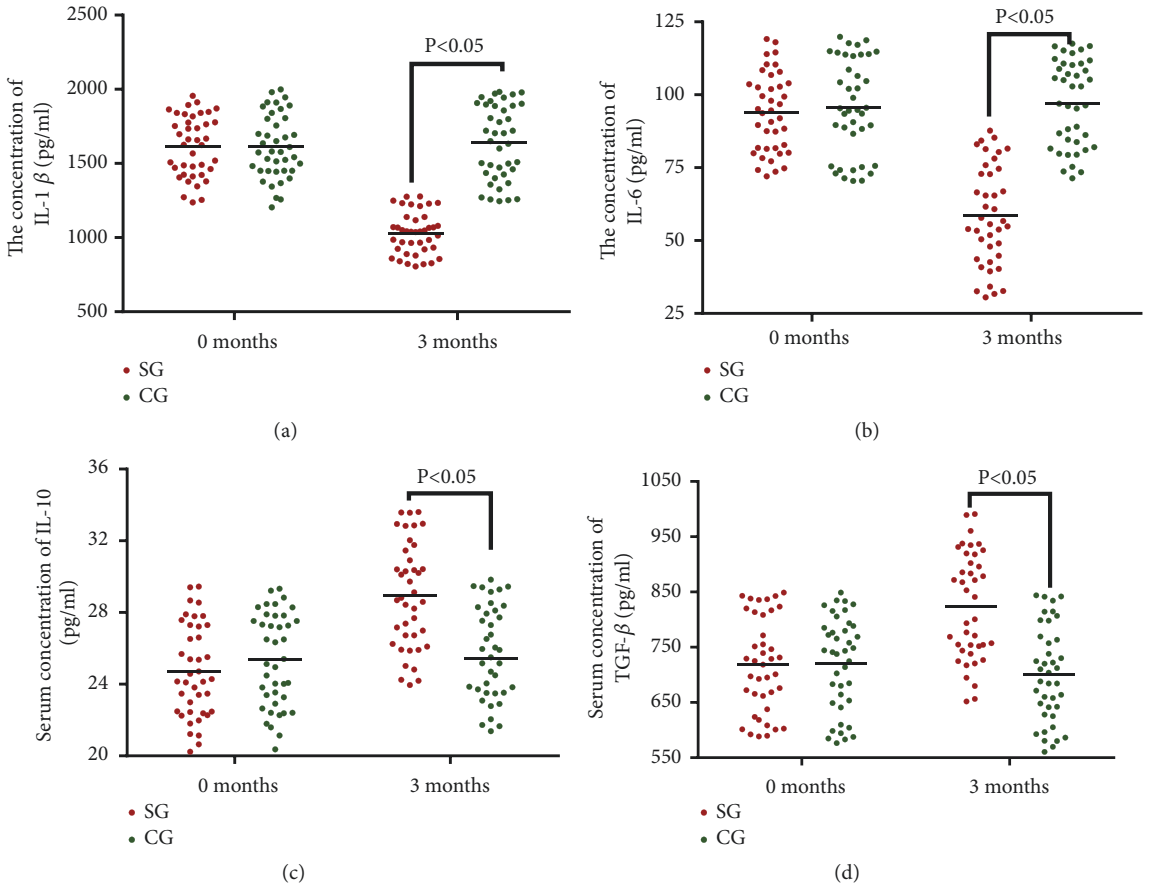

Figure 1: ELISA analysis of the effects of SSLK on the levels of cytokines and transcription factor. (a), the effects of SSLK on serum levels of IL-1β. (b), the effects of SSLK on serum levels of IL-6. (c), the effects of SSLK on serum levels of IL-10. (d), the effects of SSLK on the levels of TGF-β. In the SG group, the patients took SSLK and in the CG group, the patients took placebo (n = 40 for each group).$*p < 0.05$ via a control group.

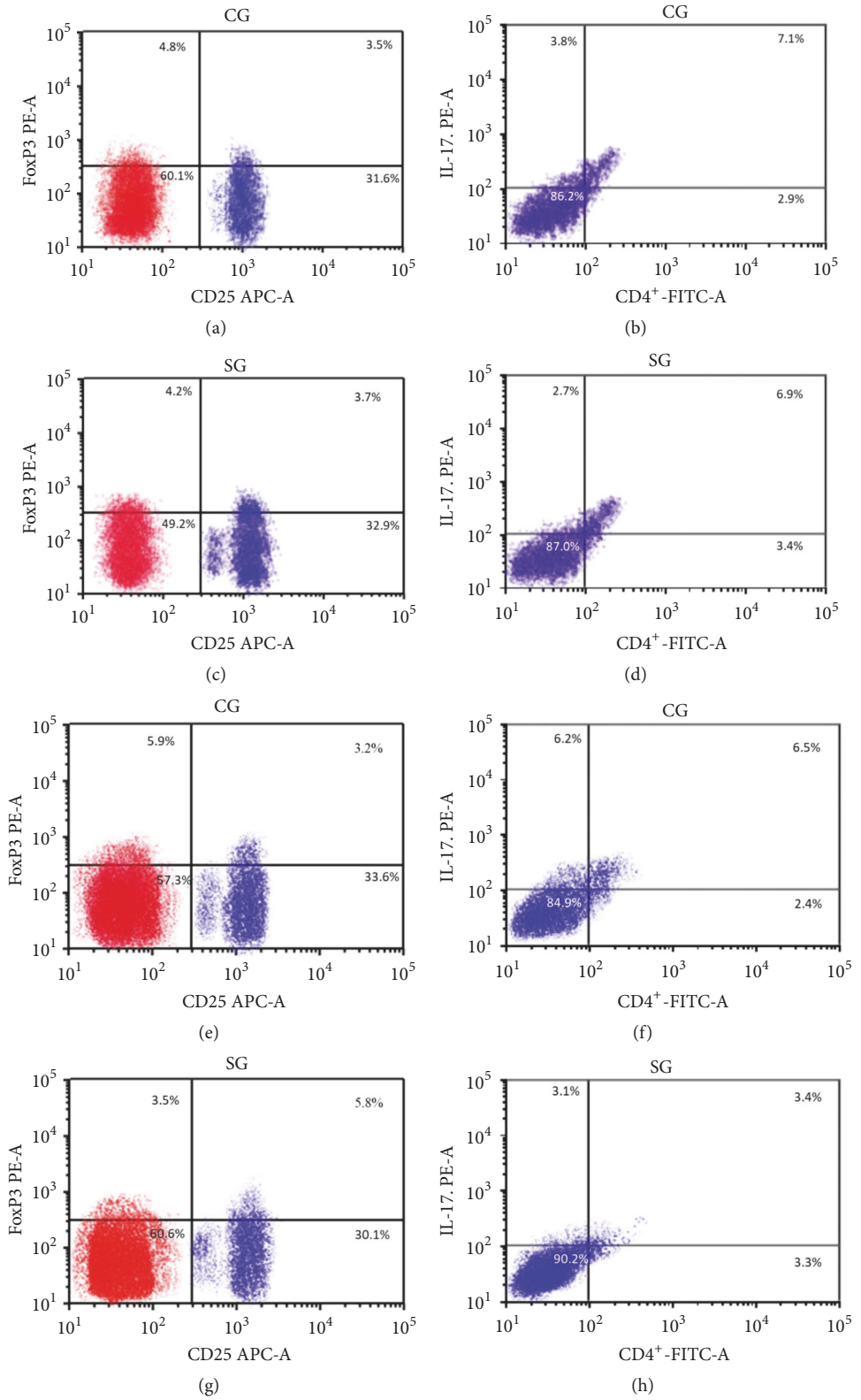

Figure 2: Flow cytometry analysis of the percentage of $CD4^+CD25^+$FoxP3 Treg and $CD4^+$IL-17 T cells in PBMCs. (a), the percentage of $CD4^+CD25^+$FoxP3 Treg cells in the CG group before placebo intervention. (b), the percentage of CD4+IL-17 T cells in the CG group before placebo intervention. (c), the percentage of $CD4^+CD25^+$ FoxP3 Treg cells in the SG group before SSLK intervention. (d), the percentage of $CD4^+$IL-17 T cells in the SG group before SSLK intervention. (e), the percentage of $CD4^+CD25^+$FoxP3 Treg cells in the CG group after 3-month placebo intervention. (b), the percentage of CD4+IL-17 T cells in the CG group after 3-month placebo intervention. (c), the percentage of $CD4^+CD25^+$ FoxP3 Treg cells in the SG group after 3-month SSLK intervention. (d), the percentage of $CD4^+$IL-17 T cells in the SG group after 3-month SSLK intervention. In the SG group, the patients took SSLK and in the CG group, the patients took placebo.

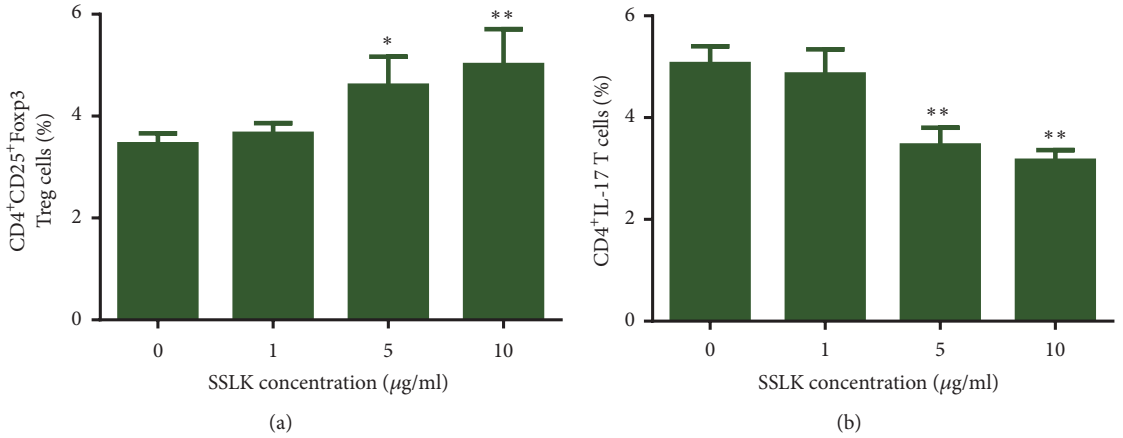

Figure 3: The effects of SSLK on the percentage of $CD4^+CD25^+$FoxP3 Tregs and $CD4^+$IL-17 T cells in PBMCs. (a), The effects of SSLK on the percentage of $CD4^+$IL-17 T cells in PBMCs. (b), the effects of SSLK on the percentage of $CD4^+CD25^+$FoxP3 Treg cells in PBMCs. $*p$ <0.05 and $**p$ <0.01 via the 0-μg/ml group.

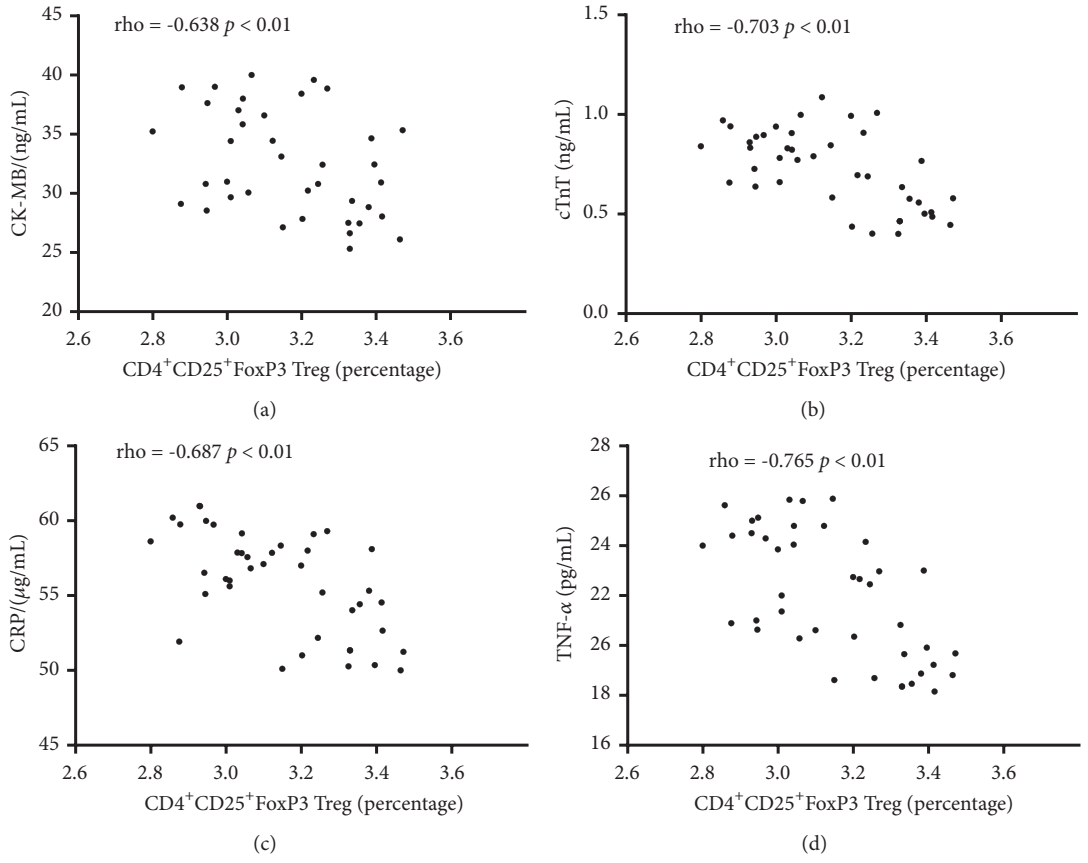

Figure 4: The relationship between the percentage of $CD4^+CD25^+$FoxP3 Tregs and CK-MB,cTn1, CRP and TNF-α. (a), the relationship between the percentage of $CD4^+CD25^+$FoxP3 Tregs and CK-MB. (b), the relationship between the percentage of $CD4^+CD25^+$FoxP3 Tregs and cTn1. (c), the relationship between the percentage of $CD4^+CD25^+$FoxP3 Tregs and CRP. (d), the relationship between the percentage of $CD4^+CD25^+$FoxP3 Tregs and TNF-α. There was a strong negative relationship between two variables if rho values < -0.5.

(Figure 4(c)), and TNF-a (Figure 4(d)) were reduced. The percentage of $CD4^+CD25^+$FoxP3 Treg cells had negative relationship with the levels of CK-MB, cTnT, CRP, and TNF-a since rho < -0.5 and p < 0.01.

3.10. The Percentage of $CD4^+$IL-17 T Cells Had Positive Relationship with CK-MB, cTnT, CRP, and TNF-a. Pearson correlation coefficient test showed that, with the increase in the percentage of $CD4^+$IL-17 T cells, the levels of CK-MB

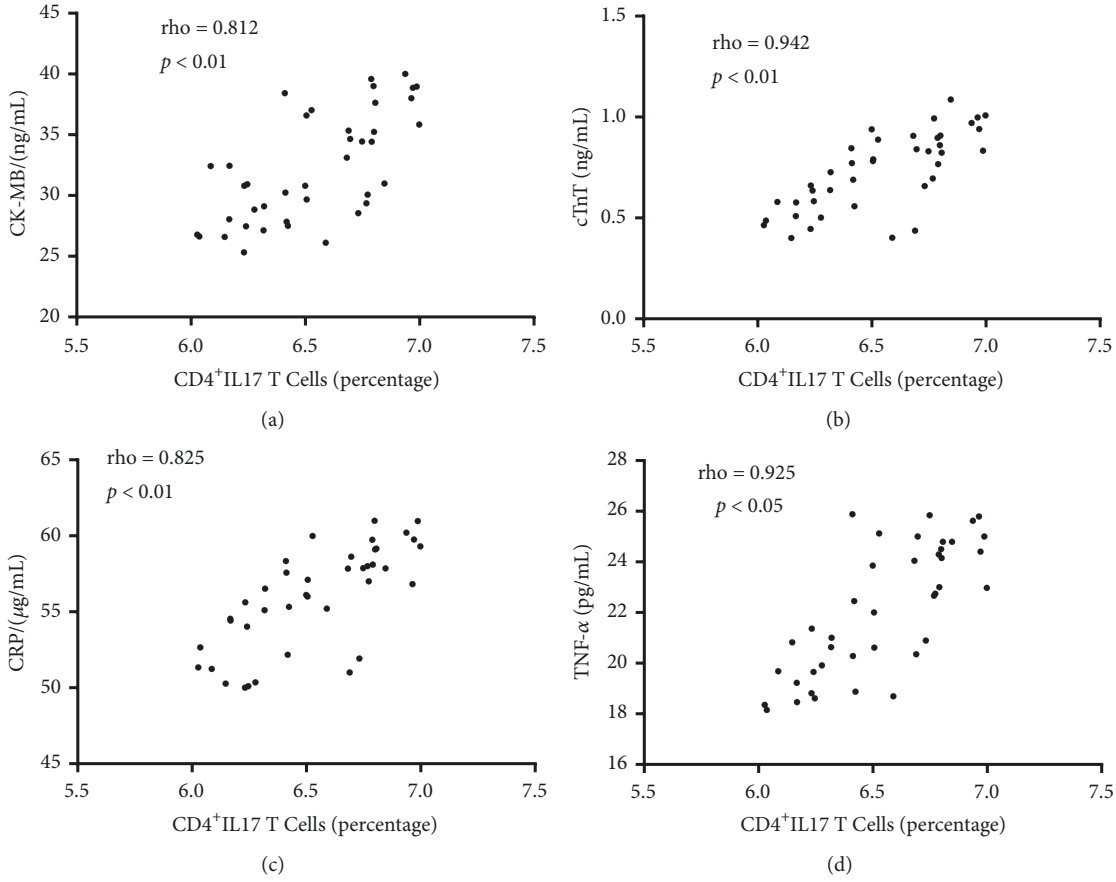

Figure 5: The relationship between the percentage of $CD4^+$IL-17 T cells and CK-MB,cTn1, CRP, and TNF-α. (a), the relationship between the percentage of $CD4^+$IL-17 T cells and CK-MB. (b), the relationship between the percentage of $CD4^+$IL-17 T cells and cTn1. (c), the relationship between the percentage of $CD4^+$IL-17 T cells and CRP. (d), the relationship between the percentage of $CD4^+$IL-17 T cells and TNF-α. There was a strong negative relationship between two variables if rho values > 0.5.

(Figure 5(a)), cTn1 (Figure 5(b)), CRP (Figure 5(c)), and TNF-a (Figure 5(d)) were increased. The percentage of $CD4^+$IL-17 T cells had positive relationship with the levels of CK-MB, cTnT, CRP, and TNF-a since rho > 0.5 and $p < 0.01$.

4. Discussion

SSLK reduced the levels of cardiac biomarkers (CK-MB and cTnT) and inflammatory cytokines in RHD patients (Table 4 and Figure 1), suggesting it can regulate inflammatory activity of patients. The reduction of $CD4^+CD25^+$FoxP3 Treg cells and the increase in $CD4^+$IL-17 cells in PBMCs may be associated with poor prognosis of RHD. $CD4^+CD25^+$Tregs [29] and $CD4^+CD25^+$FoxP3 Treg cells [30] regulated the immune activity in heart disease. Relative percentages of $CD4^+CD25^+$Tregs and $CD4^+CD25^+$FoxP3 Treg cells in PBMCs in the SG group were higher than in the CG group (Figure 2, P<0.05). SSLK has antibacterial [31], anticoagulant [32], and anti-inflammatory [33] properties. SSLK intervention may improve CHD symptoms of the patients by increasing the percentage of $CD4^+CD25^+$FoxP3 Treg cells and reducing the percentage of $CD4^+$IL-17 cells in PBMCs and maintained their balance (Figure 6). The immunomodulatory function of Treg cells is also closely related to the secretion of cytokines in peripheral blood plasma. IL-10 and TGF-β are secreted by Treg T cells, control inflammation, and regulate immunosuppression [34, 35]. In addition, TGF-β1 can induce the FoxP3 gene expression, participate in the accurate differentiation of Treg cells, and promote the survival of natural Treg cells [36]. Previous studies have demonstrated that TGF-β, which bind to cell membranes, increased the number of $CD4^+CD25^+$Treg cells and also affected Treg function [37, 38]. SSLK intervention increased the serum levels of IL-10 and TGF-β in RHD patients (Figures 1(c) and 1(d)). A decrease in the secretion of IL-10 and TGF-β in the serum of RHD patients may affect the number of Treg cells and impair their functions. IL-10 polymorphism has been found to be associated with progression of RF/RHD, suggesting its important role in controlling CHD risk [39]. SSLK treatment reduced the levels of IL-1 β and IL-6 and effectively controlled inflammation responses.

There is significant deficiency of Tregs ($CD4^+$CD25(med-high)CD127(low) Foxp3(high)) in patients of chronic RHD [40] while increased percentage of Th17 cell-associated cytokines plays crucial roles in the progression of RHD [41].

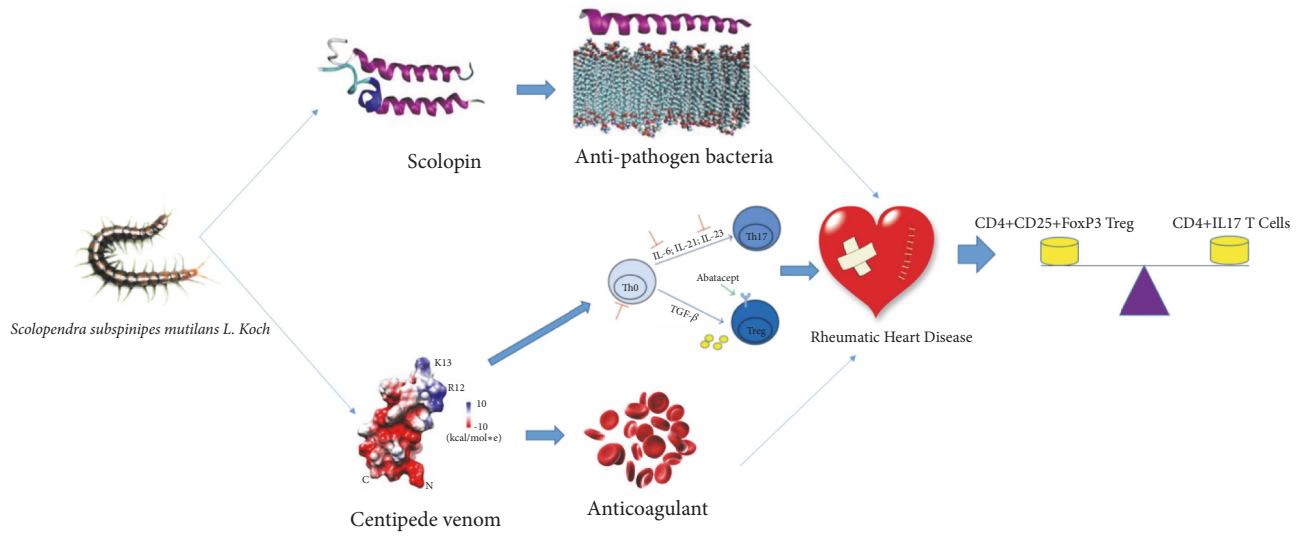

Figure 6: Schematic diagram of the effects of SSLK on CHD patients.

The present work showed that SSLK treatment increased the percentages of $CD4^+CD25^+$FoxP3 Treg cells and reduced the percentages of $CD4^+$IL-17 T cells in a dose-dependent way ($p < 0.05$). The percentage of $CD4^+CD25^+$FoxP3 Treg cells had negative relationship with CK-MB, cTnT, CRP, and TNF-a (Figure 4). The percentage of $CD4^+$IL-17 T cells had positive relationship with CK-MB, cTnT, CRP, and TNF-a (Figure 5). CK-MB and cTnT are the important cardiac biomarkers associated with RHD risk [42]. CRP [43] and TNF-a [44] are related to the inflammation of CHD. Thus, SSLK ameliorated RHD by affecting $CD4^+CD25^+$FoxP3 Treg and $CD4^+$IL17 T cells.

Notably, to reduce inflammation, low-dose aspirin (50 mg/daily) was orally administrated in both group [45]. Although aspirin has been reported to increase the numbers of Treg cells, its effects on the control group were not found when compared with before treatment [46]. On the other hand, in the present study, the normal percentages of Treg and Th17 cells were not found in CHD patients, which may be caused by the small size (40 subjects in each group). The effects of SSLK on the CHD patients with normal percentages of $CD4^+CD25^+$FoxP3 Treg and $CD4^+$IL-17 cells remain unclear. However, according to another report, the normal percentage of Treg cells should be existing even in severe gastrointestinal inflammation [47]. Much work needs to address these important issues in the future.

The cases of fatigue, chest pain, palpitation, and short breathing are the common complications of RHD. In the present study, the symptoms of fatigue and palpitation were all improved after SSLK intervention (Table 2, $p < 0.05$). Adverse reaction of SSLK was also analyzed, 2 patients had dizziness, weakness (1 case), and headache (1 case), and there were no liver, or kidney dysfunction, and/or other clinical abnormalities in the SSLK group. Notably, a SSLK treatment duration was 3 months. Traditional Chinese medicine is quite different with normal drug and cannot exert its function in human body immediately, and several months will be considered [48].

There are some limitations to the present work. The subsequent clinical characteristics were not investigated further after stopping taking SSLK. In addition, $CD4^+CD25^+$Treg cells was only detected in PBMCs from peripheral blood, and our results would be affected by the fact that Treg cells were a small fraction in RHD patients. An additional marker FoxP3 was used to distinguish between functional Treg cells and immature nonfunctional Treg cells. Therefore, further study should be performed to observe FOXP3 gene expression in the $CD4^+CD25^+$ Treg cells. The epigenetic regulation of $CD4^+CD25^+$Treg cells is closely related to human heart diseases. Therefore, it is very important to evaluate the epigenetic regulation of FoxP3 gene in RHD patients. The small sample size of this study should be further expanded to a larger population of RHD patients and follow-up period should be longer in order to gain the key advantages of SSLK. In Figure 1(d), the treatment seems to induce a separation for TGF-β between two different patient populations in the SG group (the median cuts sharply between two groups of red dots). The problem may be caused by small population size. To address these issues, further work is highly demanded in the future.

5. Conclusions

SSLK treatment improved MAP, HR, CVP, fatigue, palpitation, and shortness breath in the CHD patients. Meanwhile, SSLK intervention reduced the levels of blood lactate, CK-MB, cTnT, CRP, IL-1β, IL-6, TNF-α, and MDA and increased SOD level. SSLK treatment reduced the levels of IL-1β and IL-6 and increased the levels of IL-10 and TGF-β. SSLK had better anti-inflammatory effects. No increased risk of serious adverse reactions such as bleeding was found. SSLK treatment increased the percentage of $CD4^+CD25^+$FoxP3

Treg cells and reduced the percentage of $CD4^+$IL-17 T cells. SSLK ameliorated RHD by affecting the percentage of $CD4^+CD25^+$FoxP3 Treg and $CD4^+$IL17 T cells.

Data Availability

The data used to support the findings of this study are available from the corresponding author upon request.

Conflicts of Interest

The authors declare that they have no competing interests.

Authors' Contributions

Tiechao Jiang and Qini Zhao equally contributed to the work.

References

[1] M. Yacoub, B. Mayosi, A. ElGuindy, A. Carpentier, and S. Yusuf, "Eliminating acute rheumatic fever and rheumatic heart disease," *The Lancet*, vol. 390, no. 10091, pp. 212-213, 2017.

[2] Z. M. Makrexeni and L. Pepeta, "Clinical presentation and outcomes of patients with acute rheumatic fever and rheumatic heart disease seen at a tertiary hospital setting in Port Elizabeth, South Africa," *Cardiovascular Journal of Africa*, vol. 28, no. 4, pp. 248–250, 2017.

[3] E. Teker, A. B. Akadam-Teker, O. Ozturk et al., "Association between the interferon gamma 874 T/A polymorphism and the severity of valvular damage in patients with rheumatic heart disease," *Biochemical Genetics*, vol. 56, no. 3, pp. 225–234, 2018.

[4] T. Suzuki, M. Mawatari, T. Iizuka et al., "An ineffective differential diagnosis of infective endocarditis and rheumatic heart disease after streptococcal skin and soft tissue infection," *Internal Medicine*, vol. 56, no. 17, pp. 2361–2365, 2017.

[5] U. Abdullahi, S. Kana, M. Yakasai et al., "Update on rheumatic heart disease in Kano: data from the Aminu Kano Teaching Hospital echocardiography registry," *Nigerian Journal of Basic and Applied Sciences*, vol. 14, no. 2, pp. 127–130, 2017.

[6] D. Engelman, R. L. Mataika, J. H. Kado et al., "Adherence to secondary antibiotic prophylaxis for patients with rheumatic heart disease diagnosed through screening in Fiji," *Tropical Medicine & International Health*, vol. 21, no. 12, pp. 1583–1591, 2016.

[7] N. Zegeye, D. Asrat, Y. Woldeamanuel et al., "Throat culture positivity rate and antibiotic susceptibility pattern of beta-hemolytic streptococci in children on secondary prophylaxis for rheumatic heart disease," *BMC Infectious Diseases*, vol. 16, no. 1, pp. 510–517, 2016.

[8] T. Ikebe, R. Okuno, M. Sasaki et al., "Molecular characterization and antibiotic resistance of Streptococcus dysgalactiae subspecies equisimilis isolated from patients with streptococcal toxic shock syndrome," *Journal of Infection and Chemotherapy*, vol. 24, no. 2, pp. 117–122, 2018.

[9] U. Kamensek, N. Tesic, G. Sersa, and M. Cemazar, "Clinically usable interleukin 12 plasmid without an antibiotic resistance gene: Functionality and toxicity study in murine melanoma model," *Cancers*, vol. 10, no. 3, article E60, 2018.

[10] L. Mizera, T. Geisler, K. Mörike, M. Gawaz, and M. Steeg, "Problems in anticoagulation of a patient with antibiotic treatment for endocarditis: interaction of rifampicin and vitamin K antagonists," *BMJ Case Reports*, vol. 2018, no. 2, Article ID bcr-2016-215155, 2018.

[11] Y. Wu, J. Li, J. Wang et al., "Anti-atherogenic effects of centipede acidic protein in rats fed an atherogenic diet," *Journal of Ethnopharmacology*, vol. 122, no. 3, pp. 509–516, 2009.

[12] Z. Zhao, J. Li, and Y. Jiang, "Influence of centipede acidic protein on cardiac function in rats with acute heart failure," *Journal of Beijing University of Traditional Chinese Medicine*, vol. 31, no. 2, pp. 106–112, 2008.

[13] H. Zeng, S. Su, X. Xiang et al., "Comparative analysis of the major chemical constituents in Salvia miltiorrhiza roots, stems, leaves and flowers during different growth periods by UPLC-TQ-MS/MS and HPLC-ELSD methods," *Molecules*, vol. 22, no. 5, article 771, 2017.

[14] A. H. Mohamed, E. Zaid, N. M. El-Beih, and A. Abd El-Aal, "Effects of an extract from the centipede Scolopendra moristans on intestine, uterus and heart contractions and on blood glucose and liver and muscle glycogen levels," *Toxicon*, vol. 18, no. 5-6, pp. 581–589, 1980.

[15] H. J. Park, B. Y. Chung, M.-K. Lee et al., "Centipede grass exerts anti-adipogenic activity through inhibition of C/EBPbeta, C/EBPalpha, and PPARgamma expression and the AKT signaling pathway in 3T3-L1 adipocytes," *BMC Complementary and Alternative Medicine*, vol. 12, no. 230, pp. 1–9, 2012.

[16] D. Gorton, S. Sikder, N. L. Williams et al., "Repeat exposure to group A streptococcal M protein exacerbates cardiac damage in a rat model of rheumatic heart disease," *Autoimmunity*, vol. 49, no. 8, pp. 563–570, 2016.

[17] R. Chu, S. Y. Liu, A. C. Vlantis et al., "Inhibition of Foxp3 in cancer cells induces apoptosis of thyroid cancer cells," *Molecular and Cellular Endocrinology*, vol. 399, no. 1, pp. 228–234, 2015.

[18] J. Y. Hong, M. Kim, I. S. Sol et al., "Chitotriosidase inhibits allergic asthmatic airways via regulation of TGF-β expression and Foxp3+ Treg cells," *Allergy: European Journal of Allergy and Clinical Immunology*, vol. 73, no. 8, pp. 1686–1699, 2018.

[19] R. Torii, T. Yamashita, C. Furutani, H. Nakayama, and Y. Fujio, "CD4+CD25+regulatory T cells (Treg cells) migrate into hearts in experimental autoimmune myocarditis (EAM)," *Journal of Pharmacological Sciences*, vol. 121, no. 1, pp. 96-97, 2013.

[20] J. L. Hwang, S.-Y. Park, H. Ye et al., "FOXP3 mutations causing early-onset insulin-requiring diabetes but without other features of immune dysregulation, polyendocrinopathy, enteropathy, X-linked syndrome," *Pediatric Diabetes*, vol. 19, no. 3, pp. 388–392, 2018.

[21] C. Griswold, A. R. Durica, L. G. Dennis, and A. F. Jewell, "Prenatal bowel findings in male siblings with a confirmed FOXP3 mutation," *Journal of Ultrasound in Medicine*, vol. 37, no. 4, pp. 1033–1037, 2018.

[22] M. Cavalcanti-Neto, R. Prado, A. Piñeros et al., "Improvement of the resistance against early Mycobacterium tuberculosis-infection in the absence of PI3Kgamma enzyme is associated with increase of CD4+IL-17+ cells and neutrophils," *Tuberculosis*, vol. 113, pp. 1–9, 2018.

[23] A. Barczyk, W. Pierzchala, G. Caramori et al., "Decreased percentage of CD4+Foxp3+TGF-β+ and increased percentage of CD4+IL-17+ cells in bronchoalveolar lavage of asthmatics," *Journal of Inflammation*, vol. 11, no. 1, pp. 1–9, 2014.

[24] M. Ozsarac, O. Karcioglu, C. Ayrik, F. Somuncu, and S. Gumrukcu, "Acute coronary ischemia following centipede envenomation: Case report and review of the literature," *Wilderness & Environmental Medicine*, vol. 15, no. 2, pp. 109–112, 2004.

[25] H. D. Bas, K. Baser, E. Yavuz et al., "High Th17/Treg ratio in rheumatic heart disease," *European Heart Journal*, vol. 34, pp. 697-698, 2013.

[26] C. J. Neely, R. Maile, M.-J. Wang, S. Vadlamudi, A. A. Meyer, and B. A. Cairns, "Th17 (IFNγ- IL17+) CD4+ T cells generated after burn injury may be a novel cellular mechanism for postburn immunosuppression," *Journal of Trauma - Injury Infection and Critical Care*, vol. 70, no. 3, pp. 681–690, 2011.

[27] X. Yang, W. Wang, J. Xu et al., "Significant association of CD4+CD25+Foxp3+ regulatory T cells with clinical findings in patients with systemic lupus erythematosus," *Annals of Translational Medicine*, vol. 7, no. 5, p. 93, 2019.

[28] A. Murata, T. Kasai, Y. Matsue et al., "Relationship between blood urea nitrogen-to-creatinine ratio at hospital admission and long-term mortality in patients with acute decompensated heart failure," *Heart and Vessels*, vol. 33, no. 8, pp. 877–885, 2018.

[29] R. Bascom, K. Tao, S. Tollenaar, and L. West, "Injected allogeneic CD4(+) CD25(+) Tregs regulate the neonatal immune system and prolong heart allograft survival," *American Journal of Transplantation*, vol. 13, pp. 362-362, 2013.

[30] P. Kanellakis, T. N. Dinh, A. Agrotis, and A. Bobik, "CD4+ CD25+Foxp3+ regulatory T cells suppress cardiac fibrosis in the hypertensive heart," *Journal of Hypertension*, vol. 29, no. 9, pp. 1820–1828, 2011.

[31] W. G. You, J. H. Lee, Y. Shin et al., "Antimicrobial peptides in the centipede Scolopendra subspinipes mutilans," *Functional & Integrative Genomics*, vol. 14, no. 2, pp. 275–283, 2014.

[32] Z.-C. Liu, R. Zhang, F. Zhao et al., "Venomic and transcriptomic analysis of centipede scolopendra subspinipes dehaani," *Journal of Proteome Research*, vol. 11, no. 12, pp. 6197–6212, 2012.

[33] Y. Wang, X. Li, M. Yang et al., "Centipede venom peptide SsmTX-I with two intramolecular disulfide bonds shows analgesic activities in animal models," *Journal of Peptide Science*, vol. 23, no. 5, pp. 384–391, 2017.

[34] Z. Yang, Y. Qi, N. Lai et al., "Notch1 signaling in melanoma cells promoted tumor-induced immunosuppression via upregulation of TGF-beta1," *Journal of Experimental & Clinical Cancer Research*, vol. 37, no. 1, p. 1, 2018.

[35] K. Torres-Poveda, M. Bahena-Roman, C. Madrid-Gonzalez et al., "Role of IL-10 and TGF-β1 in local immunosuppression in HPV-associated cervical neoplasia," *World Journal of Clinical Oncology*, vol. 5, no. 4, pp. 753–763, 2014.

[36] E. Elkord, S. Sharma, D. J. Burt, and R. E. Hawkins, "Expanded subpopulation of FoxP3+ T regulatory cells in renal cell carcinoma co-express helios, indicating they could be derived from natural but not induced Tregs," *Clinical Immunology*, vol. 140, no. 3, pp. 218–222, 2011.

[37] L. Islas-Vazquez, H. Prado-Garcia, D. Aguilar-Cazares et al., "LAP TGF-beta subset of CD4+CD25+CD127- Treg cells is increased and overexpresses LAP TGF-beta in lung adenocarcinoma patients," *BioMed Research International*, vol. 2015, Article ID 430943, 11 pages, 2015.

[38] Z. F. Chen, Q. Xu, J. B. Ding, Y. Zhang, R. Du, and Y. Ding, "CD4+CD25+Foxp3+ Treg and TGF-beta play important roles in pathogenesis of Uygur cervical carcinoma," *European Journal of Gynaecological Oncology*, vol. 33, no. 5, pp. 502–507, 2012.

[39] N. Sharma and D. Toor, "Interleukin-10: Role in increasing susceptibility and pathogenesis of rheumatic fever/rheumatic heart disease," *Cytokine*, vol. 90, pp. 169–176, 2017.

[40] S. Mukhopadhyay, S. Varma, H. N. Mohan Kumar et al., "Circulating level of regulatory T cells in rheumatic heart disease: an observational study," *Indian Heart Journal*, vol. 68, no. 3, pp. 342–348, 2016.

[41] Y. Wen, Z. Zeng, C. Gui, L. Li, and W. Li, "Changes in the expression of Th17 cell-associated cytokines in the development of rheumatic heart disease," *Cardiovascular Pathology*, vol. 24, no. 6, pp. 382–387, 2015.

[42] C. Wei, S. Zhang, J. Liu, R. Yuan, and M. Liu, "Relationship of cardiac biomarkers with white matter hyperintensities in cardioembolic stroke due to atrial fibrillation and/or rheumatic heart disease," *Medicine*, vol. 97, no. 33, p. e11892, 2018.

[43] A. Attar, P. Marzban, A. Moaref, and K. Aghasadeghi, "The association of plasma high-sensitivity C-reactive protein level with rheumatic heart disease: the possible role of inflammation," *Indian Heart Journal*, vol. 70, no. 3, pp. 346–349, 2018.

[44] U. Gupta, S. S. Mir, N. Garg, S. K. Agarwal, S. Pande, and B. Mittal, "Association study of inflammatory genes with rheumatic heart disease in North Indian population: A multi-analytical approach," *Immunology Letters*, vol. 174, pp. 53–62, 2016.

[45] J. Chen, J. Zhao, J. Huang, S. Su, B. Qiang, and D. Gu, "717A>G polymorphism of human C-reactive protein gene associated with coronary heart disease in ethnic Han Chinese: the Beijing atherosclerosis study," *Journal of Molecular Medicine (Berlin)*, vol. 83, no. 1, pp. 72–78, 2005.

[46] J. Zhu and B. Gao, "Simvastatin combined with aspirin increases the survival time of heart allograft by activating $CD4^+CD25^+$ Treg cells and enhancing vascular endothelial cell protection," *Cardiovascular Pathology*, vol. 24, no. 3, pp. 173–178, 2015.

[47] E. Janssen, M. Tohme, S. Ullas, and R. Geha, "DOCK8 associates with STAT5 and promotes regulatory T cell function," *Arthritis & Rheumatology*, vol. 68, 2016.

[48] M. Hong, C. Hong, H. Chen et al., "Effects of the Chinese herb formula Yufeining on stable chronic obstructive pulmonary disease: A randomized, double-blind, placebo-controlled trial," *Medicine*, vol. 97, no. 39, p. e12461, 2018.

Hindawi
Evidence-Based Complementary and Alternative Medicine
Volume 2019, Article ID 9817949, 6 pages
https://doi.org/10.1155/2019/9817949

Research Article

Neuroprotective Effects of Musk of Muskrat on Transient Focal Cerebral Ischemia in Rats

Donghun Lee[1], **Young-Sik Kim**[2], **Jungbin Song**[2] **and Hocheol Kim**[2]

[1]*Department of Herbal Pharmacology, College of Korean Medicine, Gachon University, 1342 Seongnamdae-ro, Sujeong-gu, Seongnam-si, Gyeonggi-do 13120, Republic of Korea*
[2]*Department of Herbal Pharmacology, College of Korean Medicine, Kyung Hee University, 26 Kyungheedae-ro, Dongdaemun-gu, Seoul 02447, Republic of Korea*

Correspondence should be addressed to Jungbin Song; jbsong@khu.ac.kr and Hocheol Kim; hckim@khu.ac.kr

Received 12 April 2019; Accepted 11 June 2019; Published 25 June 2019

Guest Editor: Yong-Ung Kim

Musk of musk deer has been one of the most precious traditional medicinal materials for treatment of stroke, but trading is prohibited. Musk of muskrat, *Ondatra zibethicus*, is an accessible substitute for musk of musk deer. However, neuroprotective effects of the musk of muskrat on stroke model are so far unclear. Aim of the study is to determine neuroprotective effects of the musk of muskrat on focal cerebral ischemia. The protective effects against focal cerebral ischemia were evaluated using a model of middle cerebral artery occlusion (90-minute occlusion followed by 24-hour reperfusion). Musk of muskrat was collected from scent bag of muskrat and orally administered at doses of 100 and 300 mg/kg twice at times of 0 and 90 min after occlusion. The effects on sensorimotor dysfunction were investigated by using balance beam test and rotarod test after brain ischemia. The expression of cyclooxygenase-2 (COX-2) was investigated by immunohistochemistry. Oral administration of musk at 300 mg/kg significantly reduced ($p<0.001$) the infarct volume by 32.4% compared with a vehicle-treated group. Oral administration of musk at 300 mg/kg also ameliorated ischemia-induced spontaneous and vestibule sensorimotor dysfunction in balance beam test and rotarod test compared with control group and COX-2 upregulation. Musk of muskrat may have neuroprotective effects against transient focal cerebral ischemia with recovery of sensorimotor dysfunction. Regarding the immunohistochemistry, the effects of muskrat may be due to anti-inflammatory properties through inhibition of COX-2 expressions.

1. Introduction

Musk is a collective name for a substance with a penetrating odor obtained from a gland of musk animals including African civet, sperm whale, or muskrat. But, in general, when it is called musk, it is known as secretions from preputial gland of the male musk deer. Musk of musk deer is essential component of Woohwangcheongsimwon as one of the representative medicinal materials for stroke treatment [1]. Its traditional use for stroke treatment has also been checked with focal ischemia animal model [2, 3]. However, there has been a growing need for an alternative of musk deer due to the restriction of its trade by Convention on International Trade in Endangered Species of Wild Fauna and Flora (CITES) since 1973.

Substances such as civet of African civet, ambergris of sperm whale, and musk of muskrat are known substitutes for musk of musk deer [4]. Among them, citvet was proved to be the main vector of severe acute respiratory syndrome (SARS), and as a result breeding citvet became impossible. Ambergris of cachalot is restricted item by CITES like musk of musk deer. On the other hand, musk of muskrat is the easiest securable alternative as muskrats are easy to breed and manage and very prolific [5].

The use of musk of muskrat, secretions of hypogastric scent bag of *Ondatra zibethicus*, has never been recorded in traditional medicinal references. In 1996, it was first recorded in Zhongguodongwuyaozhi that musk of muskrat could treat stroke, abscess, and swelling as it reduces inflammation, relieves pain, activates blood, and opens the orifices with aroma. It is also recorded in Zhongyaoxue that musk of muskrat could be used for both external and internal use as a substitute for musk of musk deer. Musk of muskrat consists of

similar ingredients with musk of musk deer. It is known that musk of muskrat contains l-muscone, a key component, and macrocyclic musk compounds like civetone, cycloheptadecanone, cyclopentadecanone, cyclododecanone, and 22 kinds of C19-C26 fatty acids, sterol compounds, 19 kinds of esters, et cetera [6–8]. But Kim et al. reported that musk of muskrat contains cyclohexadecanone, which is a constitutional isomer of l-muscone, instead of l-muscone itself [5].

As musk of muskrat gets more interest for an alternative medicine for musk of musk deer, pharmacological effects are reported to possess anti-inflammatory, anticoagulant, analgesic, and hypotensive effects [5, 6, 9, 10], like musk of musk deer. However, there has been no report about whether it is effective on focal cerebral ischemia, which mimics ischemic stroke.

The aim of present study is to determine the neuroprotective effects of musk of muskrat on stroke animal model. To achieve this, we estimated the effect of musk of muskrat on brain infarct volume, sensorimotor dysfunction, and the expression of COX-2 involved in inflammation on middle cerebral artery occlusion (MCAo) rat model.

2. Materials and Methods

2.1. Sample. Musk of muskrat was bought from Muskland Co. (Jochiwon, Korea) and was kept in refrigerator as oil form for being used at this research. Muskland collected scent bag of muskrat, *Ondatra zibethicus*, and found that it contained 8.46% moisture, 87.0% crude fat, 0.01% ash, 0.024% total carbohydrate, and 1% protein.

2.2. Animals. Male Sprague-Dawley rats (300 ± 10 g) were obtained from Samtako Co. (Osan, Korea). Rats were housed under consistent temperature (23 ± 1°C) and humidity (55 ± 10%) on a 12-h light/dark cycle (light on at 07:00). Food and water were available *ad libitum*. The experiments were carried out in accordance with the Principle of Laboratory Animal Care (NIH Publication #85-23, revised 1985) and Kyung Hee University's Institutional Animal Care and Use Committee.

2.3. Surgery. Focal cerebral ischemia was induced by transient MCAo [11]. Briefly, rats were anesthetized under 2% isoflurane in a mixture of N_2O/O_2 (7:3) throughout the surgery. Left branch of carotid artery was exposed through a midline incision. The external carotid artery (ECA) was ligated and cut near the junction of the proximal ECA junction. The common carotid artery (CCA) and internal carotid artery (ICA) were temporarily blocked by vascular clips. A 4-0 nylon monofilament (diameter 370 ± 5 μm) with a round silicone head was inserted into the ECA. Exact location of the suture was determined when the suture was inserted at a minimum of 18 mm from the CCA/ ICA junction. After 90 minutes of MCAo, the suture was removed to allow reperfusion. Rats in the sham operated group received the same surgical procedure except for a probe insertion. The rectal temperature was maintained at 37 ± 0.5°C until 6 hours after ischemia with a heating lamp and blanket system (Harvard Apparatus, Holliston, MA, USA). Occlusion of the MCA was confirmed by the presence of characteristic behavioural deficits, such as paralyzed forelimb flexion, torso twist, and spontaneous circling after reperfusion. Rats that failed to meet these criteria were excluded from the study.

2.4. Sample Treatment. Musk of muskrat was dissolved in aqueous solution of tween 20 (5%, w/v) and administered orally twice at doses of 100 and 300 mg/kg at 0 and 90 min after occlusion. The rats in the vehicle-treated group were given aqueous solution of tween 20 (5%, w/v). Treatment was blinded.

2.5. Balance Beam Test. The balance beam test was performed at 22 hours after ischemia by modifying the previously described [12]. The rats were placed in the middle of a wooden square bar (width 2.5 cm, length 122 cm, and height 42 cm) and scored as follows: 0 = the rat was not able to stay on the beam; 1 = the rat did not move, but was able to stay on the beam; 2 = the rat tried to traverse the beam, but fell; 3 = the rat traversed the beam with more than 50% footslips of the affected hindlimb; 4 = the rat traversed the beam with more than one footslip, but less than 50%; 5 = the rat had only one slip of the hindlimb; and 6 = the rat traversed the beam without any slips of the hindlimb.

2.6. Rotarod Test. The rotarod test was performed at 22 hours after ischemia. Rats were placed onto an accelerating rotarod (from 0 to 40 rpm; Ugo Basile, Milan, Italy) and the time from when the rats fell of the rotarod was measured. For each rat, latency times were recorded in five separate trials. The highest and lowest values were excluded and the mean of the remaining three trial results was used for the analysis.

2.7. Tissue Preparation. Twenty-four hours after MCAo, the rats were anesthetized and decapitated. For measuring infarct volume, the decapitated rat brain was carefully removed and cut into 6 coronal sections of 2 mm thickness. The sections were stained with 2% TTC (2,3,5-triphenyltetrazolium chloride; Sigma, USA) in saline at 37°C for 30 minutes. Immunohistochemical staining was performed by perfusion with 4% paraformaldehyde after 24 hours of ischemia and heparinized 5% sodium nitrite saline solution. The brain was removed and cut into 4 μm sections using a cryocut (3050s; Leica, Germany).

2.8. Measurement of Infarct Volume. TTC-stained sections were analysed for infarct volume using a computerized image analysis system (Image ProPlus, Media Cybernetics, USA). Correlated infarct volume (mm3) was calculated from the total volume of the contralateral hemisphere minus the unimpaired volume of the ipsilateral hemisphere. The infarct volume (%) was calculated by dividing the correlated infarct volume with the total volume of the opposite hemisphere.

2.9. Immunohistochemistry. Immunohistochemistry was performed by modifying the previously described [13]. Brains were removed, fixed, and cut into 40-μm sections

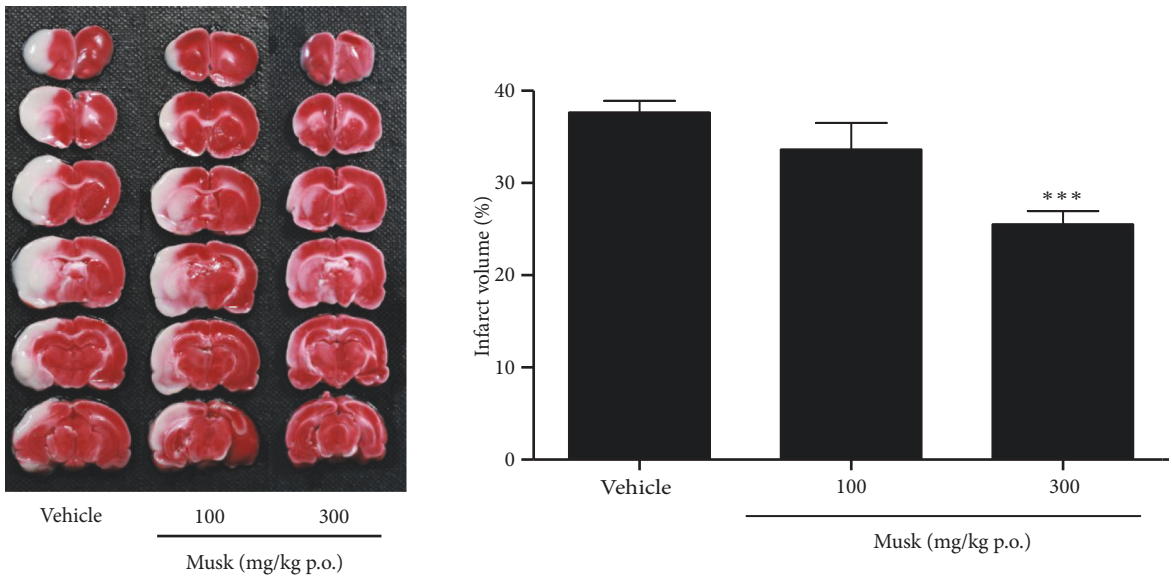

Figure 1: Dose-dependent effect of musk of muskrat on infarct volume induced by MCAo. N=12 per group; ∗ ∗ ∗p<0.001 vs. Vehicle-treated control by one-way ANOVA with *post hoc* Dunnett's test.

using a cryostat (Cell Signaling, USA). Free-floating sections were reacted with a rabbit polyclonal antibody against COX-2 (1:100; Abcam, UK) overnight at room temperature. Subsequently, the sections were reacted with biotinylated rabbit antibody (1:200; Sigma Aldrich, USA) and incubated with avidin-biotin complex reagent (Vector Laboratories, USA) for 1 h. The sections were visualised with 0.05% 3,3-diaminobenzidine solution (Sigma Aldrich) containing hydrogen peroxide.

2.10. Statistics. Statistical difference between three groups was analyzed using one-way analysis of variance (ANOVA) followed by Dunnett's post hoc test. Difference between two groups was analysed using independent t-test (GraphPad Prism 5.0, GraphPad Software, USA). Statistical significance was accepted at $p<0.05$ in Dunnett's test. Data were expressed as mean ± standard error of the mean.

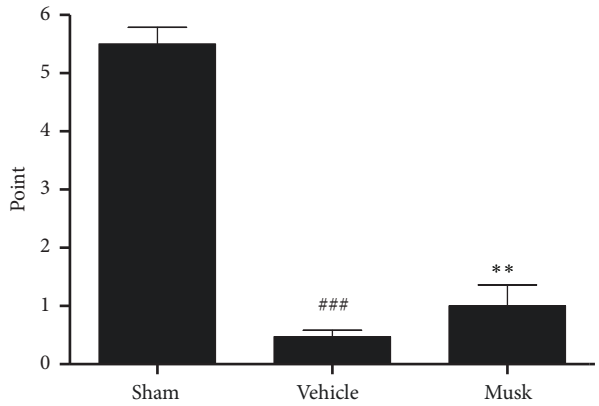

Figure 2: The effect of musk of muskrat on balance beam test after MCAo. Musk; oral administration of musk of muskrat at dose of 300 mg/kg. N=5 per group; ### $p < 0.001$ vs. Sham group, ∗∗ $p < 0.01$ vs. vehicle-treated group.

3. Results

3.1. Effects on Infarct Volume. To determine the neuroprotective effect of musk of muskrat, coronal sections were obtained after 24 h of induction. The white area indicates the infarct area in the bottom (Figure 1). It extended from the caudoputamen, parietal cortex, and temporal cortex to the penumbral region after MCAo. The vehicle-treated group showed 36.69±1.42% of infarct volume, while musk-treated group showed 33.37±2.93% and 25.18±1.64% at 100 and 300 mg/kg, respectively. Oral administration of musk of muskrat at 300 mg/kg significantly reduced the infarct volume by 32.4% compared with vehicle-treated group, respectively. Oral administration of musk of muskrat at 100 mg/kg showed moderate tendency to decrease but there was no significant difference because of its high deviation.

3.2. Effects on Balance Beam and Rotarod Tests. To see whether the protective effects of musk of muskrat associate with any functional recovery, we investigated balance beam test and rotarod test which are commonly used to determine the ameliorating effect on motor coordination, sensory motor integration, and spontaneous locomotion.

Rats in the vehicle-treated group scored significantly lower on the balance beam test than did those in the sham-operated group (0.5 ± 0.1 vs. 5.5 ± 0.3 points; $p<0.001$); however, rats that received 300 mg/kg musk of muskrat scored higher than those in the vehicle-treated group (1.0 ± 0.4 points vs. 0.5 ± 0.1 points; $p < 0.01$; Figure 2). In the rotarod test, vehicle-treated group significantly decreased compared with sham-operated group (11.0 ± 2.9 s vs. 78.5 ± 4.7 s); however, rats received 300 mg/kg of musk of muskrat

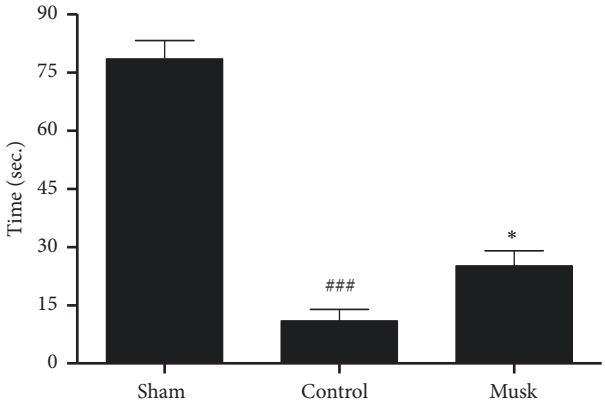

Figure 3: The effect of musk of muskrat on rotarod test after MCAo. Musk; oral administration of musk of muskrat at dose of 300 mg/kg. N=5 per group; ### $p < 0.001$ vs. Sham group, $* p < 0.05$ vs. vehicle-treated group.

significantly prolonged the latency time to 25.2 ± 3.9 s ($p < 0.05$; Figure 3).

3.3. Effects on COX-2 Expression. To define early change in COX-2, immunohistochemistry was performed at 24 hours after induction. COX-2 expressions in the peri-infarct cortex were increased in vehicle-administered group compared with sham group. In the group treated with musk of muskrat, COX-2 expression was remarkably decreased and restricted to the core part of the ipsilateral hemisphere. The peripheral part was hardly stained (Figure 4).

4. Discussions

Oral administration of musk of muskrat at doses of 300 mg/kg at 0 min and 90 min after MCAo reduced the infarct volume significantly and ameliorated spontaneous and vestibule sensorimotor dysfunction in balance beam test and rotarod test compared with control group, respectively. Also it was found that it restrained COX-2 expression markedly when measuring after 24 h.

MCAo model is known as the most suitable model for stroke treatment research because it induces focal cerebral ischemia by occluding proximal of middle cerebral artery where ischemic stroke occurs most frequently [14, 15]. Because there is the coexistence of necrosis of ischemic core and apoptosis spreading to penumbra region in MCAo model, it is the most analogous model with clinical stoke patients' pathophysiological and behavior pattern including extracellular edema and blood circulatory system intervention [16]. Both in clinical stroke and in MCAo model, necrosis at ischemic core cannot be protected without reperfusion therapy within 3 h; nevertheless it is known to be almost clinically unfeasible [16]. Meanwhile, in apoptosis arising in penumbra region neurons, death of neurons can be inhibited by neuroprotective substances [17, 18]. The brain infarct volume is the most important index to confirm the medicinal effects on injury of necrosis or apoptosis from focal ischemic stroke induced by MCAo model [19] and estimation of 90 min of MCAo-induced brain infarct volume after 24 h by TTC staining is known to be one of the most suitable conditions for evaluating the effects of sample due to its clear induction and low variation [20]. In this study, oral administration of musk of muskrat at doses of 300 mg/kg at 0 min and 90 min after MCAo significantly reduced brain infarct volume and infarct area was mostly restricted to ischemic core region. This result suggests that musk of muskrat can inhibit neuronal damage at penumbra region, which means it could be neuroprotective substance at focal cerebral ischemia.

To define whether neuroprotective effects of musk of muskrat associate with protective effects on sensorimotor dysfunction from brain damage, balance beam test and rotarod test were conducted. Brain injury is a form of physical impairment, accompanied by sensorimotor dysfunction [21], and whether the sample ameliorates sensorimotor dysfunction is important to determine whether to conduct clinical trials [22]. The balance beam and rotarod tests are both commonly used to assess motor coordination and balance alterations following MCAo [12, 23]. These tests are also known to have considerable correlation with evaluation of locomotion by MCAo brain damage [24]. In this study, the reduction in infarct volume was accompanied by elevated balance beam score and prolonged rotarod latency after musk of muskrat treatment. The results suggest that the protective effect of musk of muskrat in cerebral cortex and corpus striatum injury is associated with a restoration of the ischemia-induced sensorimotor dysfunction, suggesting that musk of muskrat could help functional restoration after ischemia.

Herein, musk of muskrat inhibited COX-2 upregulation induced by MCAo in ipsilateral neocortex. Focal cerebral ischemia triggers an inflammatory reaction, which is known as the main factor to accelerate brain damage [25]. After several hours from ischemic stroke, blood brain barrier is collapsed and leukocytes invade in large scale in succession and mass production of inflammatory cytokine accelerates tissue damage, brain edema, and glial activation [26]. COX-2 is rate-limiting enzyme in charge of inflammatory reaction by transforming arachidonic acid into prostaglandin endoperoxide H2 [27]. COX-2 expression increases as of the activation of NMDA receptor from excessive glutamate release [28] and the production of inflammatory cytokine in focal cerebral ischemia [29]. It is known that this increase of COX-2 expression is one of the main reasons of secondary damage at ischemic stroke and, also, it has proved that selective COX-2 inhibitor or COX-2 gene deletion shows neuroprotective effect [30–33]. These results suggest that neuroprotective effects of musk of muskrat after focal cerebral ischemia might be attributable to interrupting inflammatory reaction by the inhibition of COX-2 expression.

5. Conclusion

Musk of muskrat protects neurons against focal cerebral ischemia in rats with functional restoration. In relation to the immunohistochemical studies, the effects of musk of

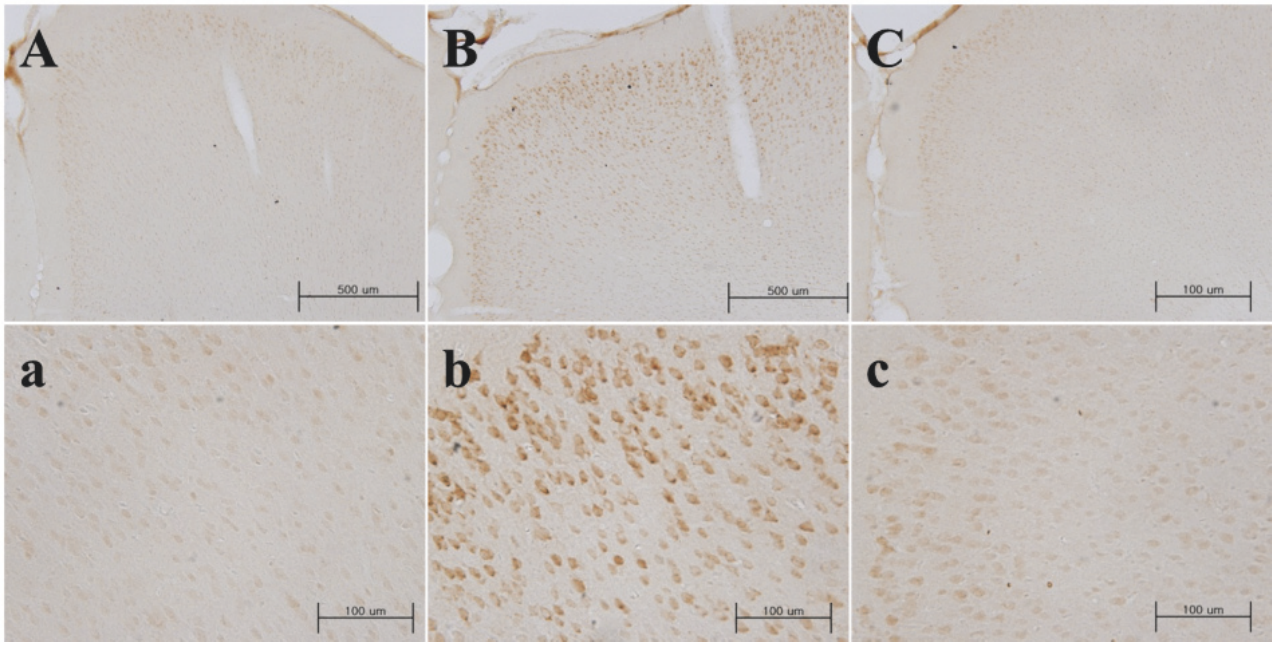

Figure 4: Inhibitory effect of musk of muskrat on COX-2 expressions (A, B, C) in the peri-infarct cortex, 24 hours after 90 minutes of MCAo. Sham (A, a), vehicle administered group (B, b), musk of musk rat administered group (300 mg/kg, p.o.; C, c). Boxed regions in A, B, and C (x40) are shown in a, b, and c (x400), respectively.

muskrat may be due to their anti-inflammatory properties by inhibiting COX-2 expression. Based on these findings, it is tempting to suppose that musk of muskrat could be considered as a substitute for musk of musk deer in view of the traditional use of stroke treatment.

Data Availability

The experimental data used to support the findings of this study are available from the corresponding author upon request.

Conflicts of Interest

The authors have no conflicts of interest to declare.

Acknowledgments

This work was supported by the Bio-Synergy Research Project (NRF-2012M3A9C4048795) of the Ministry of Science, ICT and Future Planning through the National Research Foundation.

References

[1] J. Heo, *Dongeuibogam (1613)*, Dongeuibogam Publishing Company, Seoul, Republic of Korea, 2006.

[2] W. Li, Y. Yin, X. Cao, and W. Li, "Protective effects of Shexiang Xingnaonin on focal cerebral ischemia/reperfusion injury and mechanism," *Zhongguo Zhong Yao Za Zhi= Zhongguo Zhongyao Zazhi= China Journal of Chinese Materia Medica*, vol. 33, no. 10, pp. 1195–1199, 2008.

[3] X. Xin-hua, "Effect of musk with borneol on brain water content and blood-brain barrier permeability in the rat model of cerebral focal ischemia with reperfusion," *Chinese Journal of Experimental Traditional Medical Formulae*, vol. 2, 2009.

[4] E. Choi, K. Kim, S. Shin, M. Cho, and W. Mar, "The comparative effects of civet-containing and musk-containig woohwangchungsimwon on the central nervous system," *Yakhak Hoeji*, vol. 44, no. 5, pp. 470–477, 2000.

[5] Y.-X. Jin, S. J. Choi, E.-J. Jung et al., "Analysis of volatile components of the musk of Ondatra zibethicus by gas chromatography-mass spectrometry," *Korean Journal of Pharmacognosy*, 2009.

[6] X.-Z. Chen, Z.-D. Qiu, Y.-H. Zhang, and H. Zhang, "Comparison of anti-inflammation and analgesia between muskrat and moschus," *Journal of Jilin University Medicine Edition*, vol. 31, no. 3, pp. 414–416, 2005.

[7] D. A. van Dorp, R. Klok, and D. H. Nugteren, "New macrocyclic compounds from the secretions of the civet cat and the musk rat," *Recueil des Travaux Chimiques des Pays-Bas*, vol. 92, no. 8, pp. 915–928, 1973.

[8] B. Li, C. Li, F. Sun, L. Zhang, and F. Song, "Determination of chemical composition of muskrat musk," *Chinese Pharmaceutical Journal-Beijing*, vol. 29, pp. 396-396, 1994.

[9] G. Jingtai, "Anti-inflammation and anti-coagulation effects of the muskrat musk," *Heilongjiang Medicine and Pharmacy*, vol. 6, 2000.

[10] M. Zhang, S. Yang, M. Shi et al., "Regulatory roles of peroxisomal metabolic pathways involved in musk secretion in muskrats," *The Journal of Membrane Biology*, vol. 252, no. 1, pp. 61–75, 2019.

[11] E. Z. Longa, P. R. Weinstein, S. Carlson, and R. Cummins, "Reversible middle cerebral artery occlusion without craniectomy in rats," *Stroke*, vol. 20, no. 1, pp. 84–91, 1989.

[12] K. Puurunen, J. Jolkkonen, J. Sirviö, A. Haapalinna, and J. Sivenius, "An α2-adrenergic antagonist, atipamezole, facilitates behavioral recovery after focal cerebral ischemia in rats," *Neuropharmacology*, vol. 40, no. 4, pp. 597–606, 2001.

[13] D. Lee, J. Park, J. Yoon, M. Kim, H. Choi, and H. Kim, "Neuroprotective effects of eleutherococcus senticosus bark on transient global cerebral ischemia in rats," *Journal of Ethnopharmacology*, vol. 139, no. 1, pp. 6–11, 2012.

[14] P. J. Crack and J. M. Taylor, "Reactive oxygen species and the modulation of stroke," *Free Radical Biology & Medicine*, vol. 38, no. 11, pp. 1433–1444, 2005.

[15] A. Durukan and T. Tatlisumak, "Acute ischemic stroke: overview of major experimental rodent models, pathophysiology, and therapy of focal cerebral ischemia," *Pharmacology Biochemistry & Behavior*, vol. 87, no. 1, pp. 179–197, 2007.

[16] F. Liu and L. D. McCullough, "Middle cerebral artery occlusion model in rodents: methods and potential pitfalls," *Journal of Biomedicine and Biotechnology*, vol. 2011, Article ID 464701, 9 pages, 2011.

[17] M. D. Ginsberg, "Neuroprotection for ischemic stroke: past, present and future," *Neuropharmacology*, vol. 55, no. 3, pp. 363–389, 2008.

[18] H. Kim, "Neuroprotective Herbs for Stroke Therapy In Traditional Eastern Medicine," *Neurological Research*, vol. 27, no. 3, pp. 287–301, 2013.

[19] L. C. Hoyte, M. Papadakis, P. A. Barber, and A. M. Buchan, "Improved regional cerebral blood flow is important for the protection seen in a mouse model of late phase ischemic preconditioning," *Brain Research*, vol. 1121, no. 1, pp. 231–237, 2006.

[20] F. Liu, D. P. Schafer, and L. D. McCullough, "TTC, Fluoro-Jade B and NeuN staining confirm evolving phases of infarction induced by middle cerebral artery occlusion," *Journal of Neuroscience Methods*, vol. 179, no. 1, pp. 1–8, 2009.

[21] A. Tamura, D. I. Graham, J. McCulloch, and G. M. Teasdale, "Focal Cerebral Ischaemia in the Rat: 1. Description of Technique and Early Neuropathological Consequences following Middle Cerebral Artery Occlusion," *Journal of Cerebral Blood Flow & Metabolism*, vol. 1, no. 1, pp. 53–60, 2016.

[22] A. DeVries, R. J. Nelson, R. J. Traystman, and P. D. Hurn, "Cognitive and behavioral assessment in experimental stroke research: will it prove useful?" *Neuroscience & Biobehavioral Reviews*, vol. 25, no. 4, pp. 325–342, 2001.

[23] T. N. Luong, H. J. Carlisle, A. Southwell, and P. H. Patterson, "Assessment of Motor Balance and Coordination in Mice using the Balance Beam," *Journal of Visualized Experiments*, no. 49, 2011.

[24] A. Williams, T. Myers, S. Cohn et al., "Recovery from ischemic brain injury in the rat following a 10 h delayed injection with MLN519," *Pharmacology Biochemistry & Behavior*, vol. 81, no. 1, pp. 182–189, 2005.

[25] U. Dirnagl, "Inflammation in stroke: the good, the bad, and the unknown," *ErnstScheringResFoundWorkshop*, no. 47, pp. 87–99, 2004.

[26] C. Iadecola and J. Anrather, "The immunology of stroke: from mechanisms to translation," *Nature Medicine*, vol. 17, no. 7, pp. 796–808, 2011.

[27] J. R. Vane, Y. S. Bakhle, and R. M. Botting, "Cyclooxygenases 1 and 2," *AnnuRevPharmacolToxicol*, vol. 38, pp. 97–120, 1998.

[28] J. Koistinaho and P. H. Chan, "Spreading depression-induced cyclooxygenase-2 expression in the cortex," *NeurochemRes*, vol. 25, no. 5, pp. 645–651, 2000.

[29] W. L. Smith, D. L. DeWitt, and R. M. Garavito, "Cyclooxygenases: structural, cellular, and molecular biology," *Annual Review of Biochemistry*, vol. 69, pp. 145–182, 2000.

[30] E. Araki, C. Forster, J. M. Dubinsky, M. E. Ross, and C. Iadecola, "Cyclooxygenase-2 Inhibitor NS-398 Protects Neuronal Cultures From Lipopolysaccharide-Induced Neurotoxicity," *Stroke*, vol. 32, no. 10, pp. 2370–2375, 2001.

[31] E. Candelario-Jalil, "Nimesulide as a promising neuroprotectant in brain ischemia: New experimental evidences," *Pharmacological Research*, vol. 57, no. 4, pp. 266–273, 2008.

[32] C. Iadecola, K. Niwa, S. Nogawa et al., "Reduced susceptibility to ischemic brain injury and N-methyl-D-aspartate-mediated neurotoxicity in cyclooxygenase-2-deficient mice," *Proceedings of the National Acadamy of Sciences of the United States of America*, vol. 98, no. 3, pp. 1294–1299, 2001.

[33] S. Nogawa, F. Zhang, M. Elizabeth Ross, and C. Iadecola, "Cyclo-oxygenase-2 gene expression in neurons contributes to ischemic brain damage," *The Journal of Neuroscience*, vol. 17, no. 8, pp. 2746–2755, 1997.

Hindawi
Evidence-Based Complementary and Alternative Medicine
Volume 2019, Article ID 1453612, 12 pages
https://doi.org/10.1155/2019/1453612

Research Article

A New Flavanone as a Potent Antioxidant Isolated from *Chromolaena odorata* L. Leaves

Devi Anggraini Putri and Sri Fatmawati

Laboratory of Natural Products and Synthetic Chemistry, Department of Chemistry, Faculty of Science, Institut Teknologi Sepuluh Nopember, Surabaya 60111, Indonesia

Correspondence should be addressed to Sri Fatmawati; fatma@chem.its.ac.id

Received 29 December 2018; Accepted 20 May 2019; Published 18 June 2019

Guest Editor: Irawan W. Kusuma

Chromolaena odorata L. (Asteraceae) is one of the tropical plants which is widely used as traditional medicines for diabetes and soft tissue wounds treatment in some regions in East Indonesia. The present study was aimed at determining the bioactive compounds of *C. odorata* leaves. The methanol and ethyl acetate extracts of *C. odorata* leaves have the inhibitory activity against 2,2-diphenyl-1-picryl-hydrazyl (DPPH) and 2,2'-azinobis-(3-ethylbenzothiazoline-6-sulfonic acid) (ABTS) radicals as well as α-glucosidase rat intestine enzyme. A new flavanone was isolated from the methanol extract and elucidated as 5,3'-dihydroxy-7,6'-dimethoxyflavanone or, namely, odoratenin **(1)** together with two known compounds: isosakuranetin **(2)** and subscandenin **(3)**. The antioxidant activity of odoratenin **(1)** exhibited very potent ABTS radical inhibitory activity with IC_{50} value of 23.74 μM which is lower than that of trolox (IC_{50} 31.32 μM) as a positive control. The result showed that a new flavanone, odoratenin **(1)**, should be potential as an antioxidant source.

1. Introduction

Antioxidant is a bioactive substance preventing the oxidation of the harmful chemicals. That oxidation is caused by free radicals that have unpaired electrons. So, those free radicals are very reactive to damage molecules in cell [1]. During the past decade, a lot of antioxidant products are consumed by people in the world as the synthetic drugs, supplements, or traditional medicines. The traditional medicines have been taken by people in the world derived from the natural sources like medicinal plants according to World Health Organization (WHO) data. 65% of population in India consume the medicinal plants as a primary health. The 40% of prescription drugs in China are also based on the component of medicinal plants. In addition, 70% of Canadians have also used the medicinal plants as both a health supplement and an alternative therapeutic product [2]. In Indonesia, the medicinal plants are recognized as jamu. Approximately 85% of jamu's ingredients are the extract of medicinal plants. Hence, a number of modern or synthetic medicines are made from the isolation of natural sources based on the traditional plant medicines [3]. One of the natural sources that has been used as a medicinal plant is *Chromolaena odorata* L.

C. odorata (Asteraceae) is one of the species of *Chromolaena* genus that has been identified by King and Robinson in 1970. *C. odorata* is recognized as siam weed. It is one of the invasive species with a rapid growth forming the thick bushes as high as about two meters. Besides, it spreads rapidly on the open areas such as grasslands, roadsides, forests, nature reserves, and wildlife sanctuaries [4]. Actually, *C. odorata* is used as a medicinal plant by people lived in the tropic and subtropic areas. For example, in Vietnam, this plant is used as a treatment of leech bites, soft tissue injuries, burns, and skin infections [5]. Furthermore, a leaf water extract is widely used as a diarrhea, malaria, and diabetes drug [6]. Additionally, this leaf is also used as the treatment of wounds because the leaf's contents are protein, carbohydrate, and fiber source [7].

The previous studies have reported that most of the *Chromolaena* genus contains the flavonoids group. Based on a review information by Oliveira *et al.* (2017), they reported that about 40 flavonoids have been identified from this genus. One of species from this genus, *C. hirsuta*, has been reported

to contain quercetin and kaempferol derivatives which belong to flavonoids group [8]. Some researchers also reported that *C. odorata* contains the flavonoid compounds [9–15]. In addition, the qualitative phytochemical properties of *C. odorata* leaves extract also showed the presence of secondary metabolite compounds such as coumarins, flavonoids, tannins, and sterols [16]. Currently, this preceding research aims to isolate and identify other secondary metabolite compounds of *C. odorata* leaves. Furthermore, the antioxidant activity of the compounds will be assayed.

Recently, some researchers reported that *C. odorata* showed bioactivity as an antibacterial [17], antifungal [18, 19], anti-inflammatory [20, 21], anticancer [11, 13, 22], antiplasmodial [9], antidiabetic [23, 24], and antioxidant [6, 25–28]. Rao *et al*. (2010) reported *in vitro* antioxidant activity of chloroform extract of *C. odorata* leves. The antioxidant activity was presented by using 2,2'-azinobis-(3-ethylbenzothiazoline-6-sulfonic acid) (ABTS) assay. The result showed a good inhibition with value of IC_{50} (1.32 mg/mL) compared to standard ascorbic acid (1.00 mg/mL) [28]. Furthermore, the antioxidant activity was also reported by ABTS assay from ethanol extract of *C. odorata*. The result showed a good amount of activity inhibition about 29.92-63.34% [26]. In addition, the significant activity was also obtained with polysaccharide fraction of *C. odorata* (91.91 ± 0.9%) by the same assay method [6]. However, its IC_{50} value, both research of Parameswari & Suriyavathana (2013) and Boudjeko *et al*. (2015), is not reported yet. Based on these studies, *C. odorata* has been recognized potentially as an antioxidant source. In the present study, the further research aims to identify the compounds of methanol extract from *C. odorata* leaves as an antioxidant.

2. Materials and Methods

2.1. Chemicals. The chemicals used were 2,2-diphenyl-1-picryl-hydrazyl (DPPH) (TCI, 1898-66-4), 2,2'-azinobis-(3-ethylbenzothiazoline-6-sulfonic acid) (ABTS) (Wako), pottasium peroxydisulphate ($K_2S_2O_8$), Folin-Ciocalteu's phenol reagent (FCR) (Merck), anhydrous sodium carbonate (Na_2CO_3), rat intestinal acetone powder (Sigma, 1639), glucose kit liquor (HUMAN), acarbose, gallic acid, 6-hydroxy-2,5,7,8-tetramethylchromen-2-carboxylate acid (trolox) (Wako), and dimethylsulfoxide (DMSO) (Merck). Solvents (*n*-hexane, dichroloromethane, ethyl acetate, methanol, and ethanol) were purchased from Anhui Fulltime specialized solvents & reagents Co., Ltd. (Anhui, China).

2.2. General Experimental Procedures. The purity of the compounds was determined by column chromatography (CC) using silica gel 60 G (Merck), silica gel 60 (0,063-0,200 mm), and Sephadex LH-20. For thin layer chromatography (TLC) analysis, silica gel $60F_{245}$ aluminium sheets (Merck) were used. Spots were visualized under UV light and sprayed with $CeSO_4$ in H_2SO_4 solution followed by heating. Fisher-Johns was used as melting point apparatus. The IR data were obtained on a Shimadzu FT-IR-8400S spectrometer using the KBr method. The 1D- and 2D-NMR, including ^1H and ^{13}C-NMR, HMBC (*Heteronuclear Multiple Bond Correlation*), and HMQC (*Heteronuclear Multiple Quantum Coherence*) spectra, were measured on a DELTA2_NMR spectrometer (JEOL, 400 MHz) with tetramethylsilane as a standard in $CDCl_3$. The molecular formula was confirmed by using Xevo G2-XS QTof LC-MS-MS with ESI for type of ionization. The absorbance data were measured on UV-Vis Genesys Thermo Scientific 10S spectrophotometer.

2.3. Plant Material. The leaves of *C. odorata* were collected on August 2017 at Ambon, Maluku Province, Indonesia. The plant was identified with a voucher specimen (48) by Pamela Papila, a botanist at the Fundamental Biology Laboratory, Pattimura University, Indonesia.

2.4. Extraction. The dried leaves of *C. odorata* (30 g) were extracted with various solvents for the bioactivity preparation assay. The leaves were dried in room temperature. They were extracted by using *n*-hexane, dichloromethane, ethyl acetate, methanol, and water in 200 mL of solvent for each extract at room temperature for 24 hours. The solvent was removed from the extracts by rotary evaporator to obtain the five crude extracts.

2.5. Fractionation. The dried leaves of *C. odorata* (2.76 kg) were extracted during 3 × 24 hours at room temperature in 10 L MeOH for each time. The solvent was removed from the extract by rotary evaporator to yield 832 g of extract (30.15% yield). 90 g of methanol extract was then fractionated by CC vacuum on silica gel 60 G (480 g) with a gradient elution of CH_2Cl_2 (100%), EtOAc (100%), and MeOH (100%), each 5.4 L to obtain three fractions (A-C). Fraction A (25.6 g) was further subjected to CC vacuum (Si gel 60 G, 180 g) with a step gradient elution of *n*-hexane:EtOAc (99:1, 97:3, 93:7, 90:10, 75:25, 50:50, 25:75, and 0:100, *v/v*, each 900 mL) and MeOH to obtain five subfractions (A1-A5). Subfraction A3 (6.4 g) was subjected to CC vacuum (Si gel 60 G, 92 g) with a step gradient elution of *n*-hexane:EtOAc (93:7, 92:8, 91:9, 90:10, 88:12, 86:14, 82:18; 80:20, 50:50, 20:80, and 0:100, *v/v*, each 500 mL) and MeOH, respectively, to obtain eight subfractions (A3A-A3H). Furthermore, subfraction A3E (1.7 g) was subjected to Sephadex LH-20 CC eluted with CH_2Cl_2:MeOH (1:1, *v/v*) to yield five subfractions (A3E1-A3E5). Subfraction A3E4 (0.6 g) was subjected to Sephadex LH-20 CC eluted with CH_2Cl_2:MeOH (1:1, *v/v*) to obtain four subfractions (A3E4A-A3E4D). A compound **(2)** (29.8 mg) was obtained by purification of subfraction A3E4C (100 mg) with recrystallization technique. Furthermore, subfraction A3E4B (400 mg) was separated by using silica gel 60 CC (50 g) eluted with CH_2Cl_2 (100%) to afford compound **(1)** (54.1 mg) and six subfractions (A3E4B1-A3E4B6). The compound of **(1)** was obtained by purification of subfraction A3E4B1 (100 mg). And compound **(3)** (5 mg) was obtained by purification of subfraction A3E4B2B2B3 (80 mg).

2.6. Antioxidant Activity

2.6.1. Determination of Total Phenolic Contents. The total phenolic content of various *C. odorata* extracts (the *n*-hexane, dichloromethane, ethyl acetate, methanol, and water extracts)

was determined according to the procedure of Qassabi *et al.* (2018) with slight modifications [29]. The total phenolic content was determined by applying gallic acid calibration curve and expressed in mg of gallic acid equivalents (GAE)/g crude extracts. Each extract (1 mg/mL) was dissolved in methanol to prepare a sample solution. The absorbance of sample solution was determined by using UV-Vis Genesys Thermo Scientific 10S spectrophotometer with those following steps. First, the mixture solution between 66 μL of sample solution and 500 μL of 10% FCR solution was mixed and incubated in a dark place for 5 minutes. Then, 500 μL of 6% Na_2CO_3 was added into the solution, mixed well, and left for 90 minutes in the dark place. Finally, the absorbance of sample solution was measured by UV-Vis spectrophotometer at λ 750 nm.

2.6.2. DPPH Radical Scavenging Assay. DPPH assay was performed based on the method published previously [30]. First, DPPH solution (6×10^{-5} M) was separated by dissolving 2.37 mg of DPPH in 100 mL of methanol to obtain a working solution. Then, 1 mL the working solution was mixed with 33 μL of samples (*n*-hexane, dichloromethane, ethyl acetate, methanol, and water extracts) at maximum dissolved concentration in methanol and mixed well. Finally, the mixed sample solution was incubated for 20 minutes at room temperature. Then, the absorbance (A_s) of the reaction mixture was measured by UV-Vis spectrophotometer at 517 nm. The mixed solution between methanol and the working solution was used as blank to give the blank absorbance (A_b). Gallic acid was used as a standard. The inhibitory activity was calculated by (1). The IC_{50} value is expressed as a quantity of an extract inhibitory concentration against a half of DPPH radicals.

$$\text{Inhibition (\%)} = \left[\frac{(A_b - A_s)}{A_b}\right] \times 100 \quad (1)$$

2.6.3. ABTS Radical Cation Scavenging Assay. Free radical scavenging by ABTS radical was based on the method described previously by us [30]. First, ABTS solution (7 mM) was prepared by dissolving 19.2 mg of ABTS in 5 mL of water and, then, 140 mM $K_2S_2O_8$ in 88 μL of water. Those two solutions were mixed and incubated for 12-16 hours to obtain ABTS radical cation solution which is a dark blue solution. It was added with ± 274 mL of ethanol to give an absorbance of 0.7 ± 0.02 units at 734 nm for making a working solution. 1 mL of working solution was mixed with 10 μL of samples (*n*-hexane, dichloromethane, ethyl acetate, methanol, and water extracts) at maximum dissolved concentration in DMSO and mixed well. Finally, the mixed sample solution was incubated for four minutes at room temperature; then, the absorbance (A_s) of the reaction mixture was measured by UV-Vis spectrophotometers at 734 nm. The mixed solution between DMSO and the working solution was used as blank to give the blank absorbance (A_b). Trolox was used as a standard. The inhibitory activity was calculated by (1). The IC_{50} value was expressed as a quantity of an extract inhibitory concentration against a half of ABTS radicals.

2.7. α-Glucosidase Inhibitory Activity Assay. The α-glucosidase inhibitory assay was performed based on the procedure from Ayinampudi *et al.*, (2012) with some modifications [31]. First, rat intestinal acetone powder (1 g) was suspended in 30 mL of normal saline. This suspended solution was sonicated for five minutes at 4°C. After centrifugation (12,000 rpm, 30 minutes, 4°C), the resulting supernatant was used for the assay. Briefly, a mixture of 10 μL samples, 30 μL of 0.1 M phosphate buffer (pH 6.9), 20 μL of 10 mM maltose, 80 μL glucose kit, and 20 μL of enzyme supernatant were incubated in 96-well plates at 37°C for 10 minutes. Acarbose was used as a standard. The absorbance was recorded at 490 nm by microplate reader (Biotek ELx800UV). The inhibitory activity was determined from the formula as follows:

$$\text{Inhibition (\%)} = \left[\frac{\left(A_{\text{blank}} - A_{\text{sample}}\right)}{A_{\text{blank}}}\right] \times 100 \quad (2)$$

where $A_{\text{blank}} = A_{\text{enzyme reaction}} - A_{\text{blank of enzyme reaction}}$ and $A_{\text{sample}} = A_{\text{sample reaction}} - A_{\text{blank of sample reaction}}$.

3. Results

3.1. Extraction. The five crude extracts from *C. odorata* leaves have been obtained. The methanol extract has the highest yield of all extracts. From 30 g dried leaves in 200 mL of each solvent, the yields of the five extracts were obtained such as 4.33% yield of *n*-hexane, 6.77% yield of dichloromethane, 7.33% yield of ethyl acetate, 10.00% yield of methanol, and 7.33% yield of water extract.

3.2. Total Phenolic Content. The total phenolic content of different extracts of *C. odorata* leaves was determined by using FCR according to the procedure of Qassabi *et al.* (2018) with slight modifications. The tested extracts are *n*-hexane, dichloromethane, ethyl acetate, methanol, and water extracts at concentration 61.91 μg/mL. The evaluated result of total phenolic content of each extract is showed in Table 1. Gallic acid was used as a standard for calibration curve to determine the amount of total phenolic content. Based on study, the total phenolic content of different extracts varied from 14.65 to 104.08 μgGAE/mg of extract. The ethyl acetate extract is the highest amount of total phenolic content of all the extracts with value of 104.08 μgGAE/mg of ethyl acetate extract.

3.3. DPPH Radical Scavenging Activity. DPPH radical scavenging activity of the five extracts and gallic acid as a standard are presented in Figure 1 and summarized in Table 1. Based on these IC_{50} values, the dichloromethane, ethyl acetate, and methanol extracts are potential antioxidant against DPPH radicals with IC_{50} value of 90.83, 57.26, and 188.61 μg/mL, respectively. According to this result, the ethyl acetate extract is the highest inhibitory activity against DPPH radicals among other extracts. The minimum of IC_{50} value indicates a good free radical scavenging activity.

3.4. ABTS Radical Cation Scavenging Activity. ABTS radical cation scavenging activity of the five extracts, compounds

Table 1: Antioxidant and α-glucosidase activities of the extracts and compounds from *C. odorata*.

Samples	Total phenolic contents (μg GAE/mg of sample) ± SD[1]	DPPH IC_{50} (μg/mL) ± SD[1]	ABTS IC_{50} (μg/mL) ± SD[1]	α-Glucosidase inhibition IC_{50} (μg/mL) ± SD[1]
Samples (Extracts of *C. odorata*)				
n-Hexane	14.65 ± 0.98	>319.46	>99.01	>1250
Dichloromethane	74.84 ± 2.11	90.83 ± 0.31	13.97 ± 0.22	>1250
Ethyl acetate	104.08 ± 3.87	57.26 ± 1.07	24.43 ± 0.09	779.54 ± 6.16
Methanol	57.11 ± 4.85	188.61 ± 3.31	46.80 ± 2.91	1329.31 ± 2.68
Water	27.49 ± 1.41	>319.46	21.37 ± 0.89	>1250
Samples (the compounds isolated from *C. odorata*)				
Odoratenin (**1**)	NS[2]	NS[2]	7.51 ± 1.57	>62.5
Isosakuranetin (**2**)	NS[2]	NS[2]	>9.9	>312.5
Subscandenin (**3**)	NS[2]	NS[2]	NS[2]	NS[2]
Standard				
Gallic acid	as a standard curve	1.11 ± 0.42	NS[2]	NS[2]
Trolox	NS[2]	NS[2]	7.84 ± 0.45	NS[2]
Acarbose	NS[2]	NS[2]	NS[2]	7.67 ± 1.86

[1]values represent the means ± standard deviations for triplicate experiments.
[2]not studied.

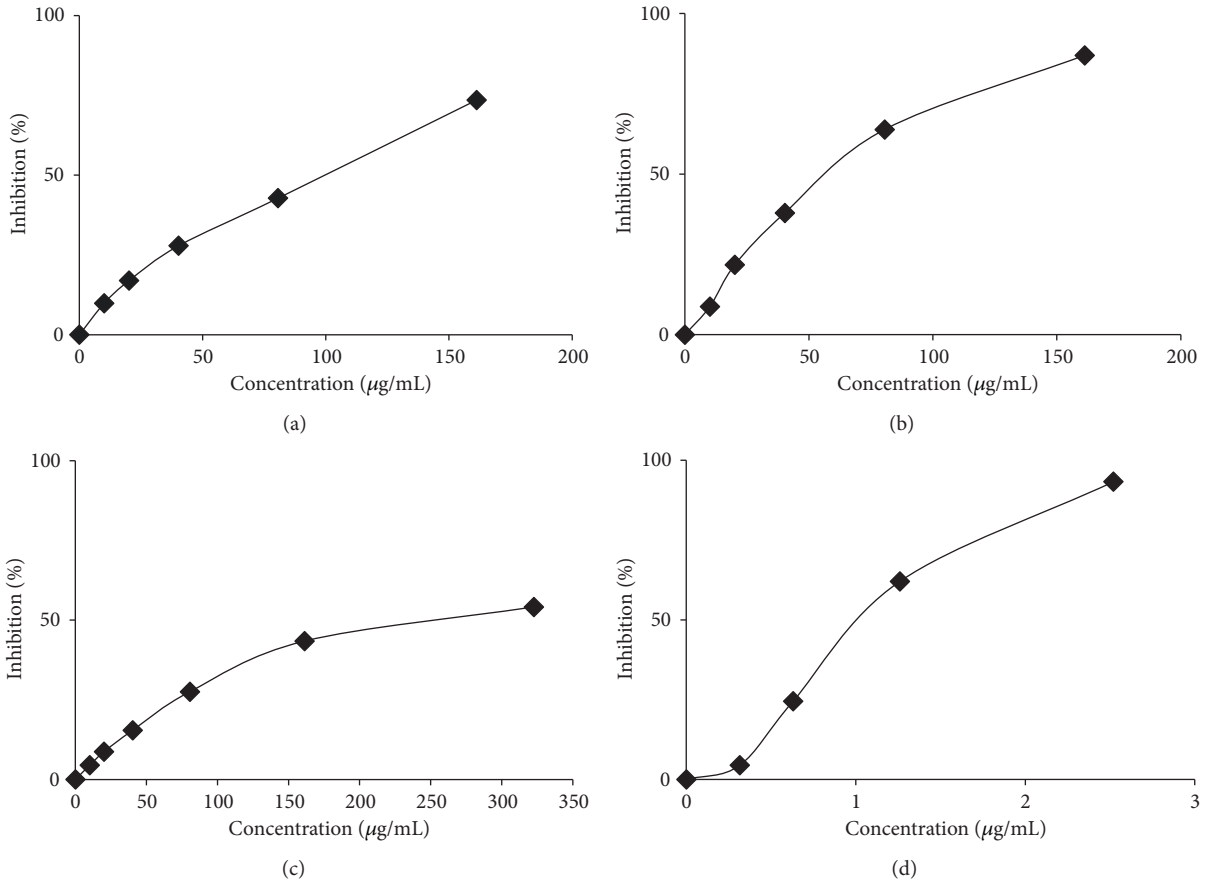

Figure 1: DPPH radical scavenging activity of *C. odorata* (a) dichloromethane, (b) ethyl acetate, (c) methanol extracts, and (d) gallic acid as a standard.

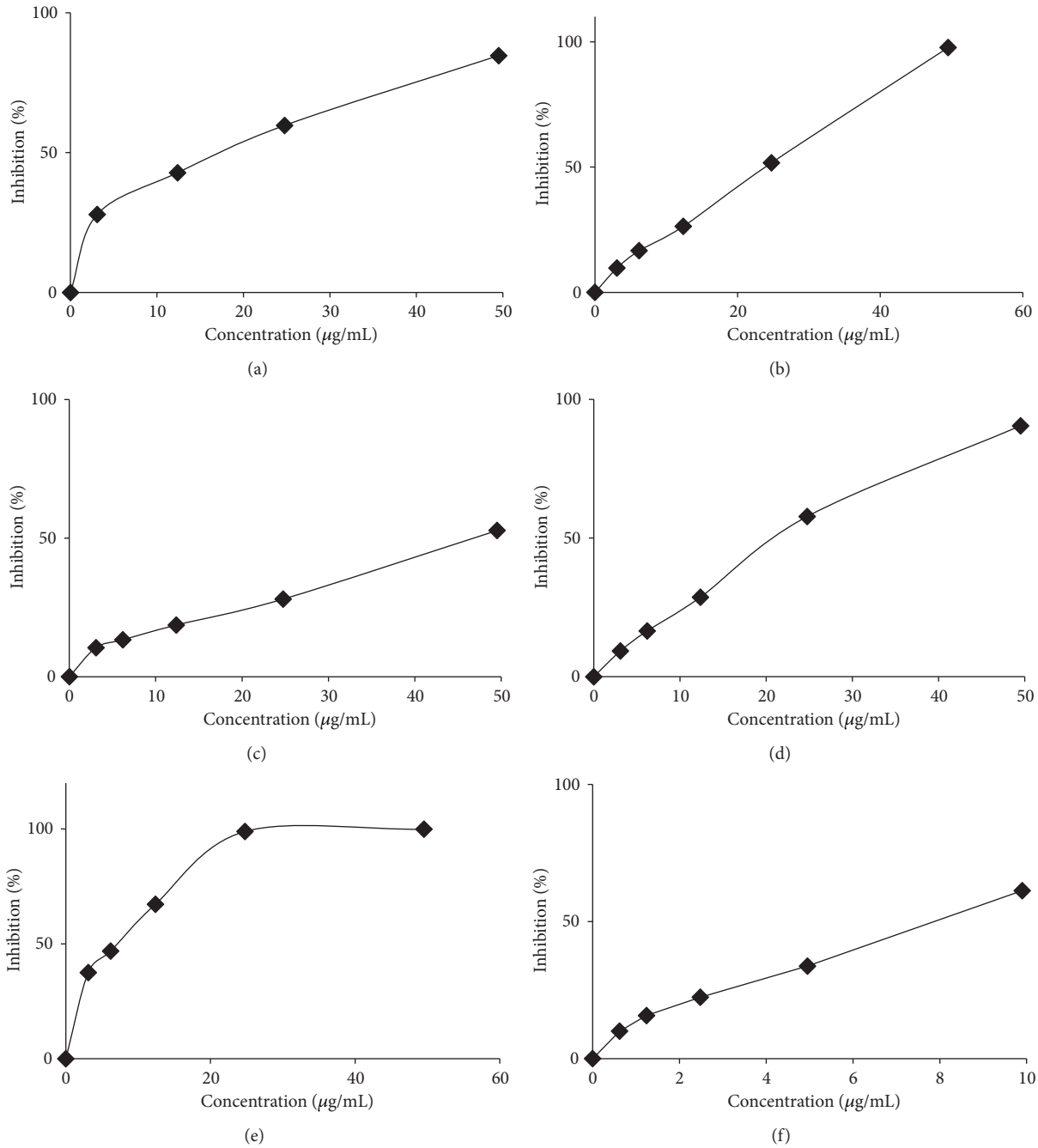

Figure 2: ABTS scavenging activity of *C. odorata* (a) dichloromethane, (b) ethyl acetate, (c) methanol, (d) water extracts, (e) trolox as a standard, and (f) odoratenin **(1)**.

isolated from *C. odorata*, and trolox as a standard are presented in Figure 2 and summarized in Table 1. According to these IC_{50} values, both the extracts and compounds are potential antioxidant against ABTS radical cations. The IC_{50} values of dichloromethane, ethyl acetate, methanol, and water extracts are 13.97, 24.43, 46.79, and 21.37 μg/mL, respectively. Interestingly, odoratenin (**1**) is higher free radical scavenging activity than that of the various extracts with IC_{50} value of 7.51 μg/mL (23.74 μM) also compared with trolox as a standard with IC_{50} value of 31.32 μM.

3.5. α-Glucosidase Inhibitory Activity. Rat intestinal acetone powder was used in this assay system. The five extracts, compounds isolated from *C. odorata*, and acarbose as a standard are showed in Figure 3 and summarized in Table 1. In this assay system, the ethyl acetate extract was found to be slightly more active than that of the methanol extract. In contrast, the *n*-hexane, dichloromethane, water, and the compounds **(1-2)** had a weak effect on the enzyme activity. The ethyl acetate extract presented the inhibitory activity with an IC_{50} value of 779.54 μg/mL. Acarbose, which is known as

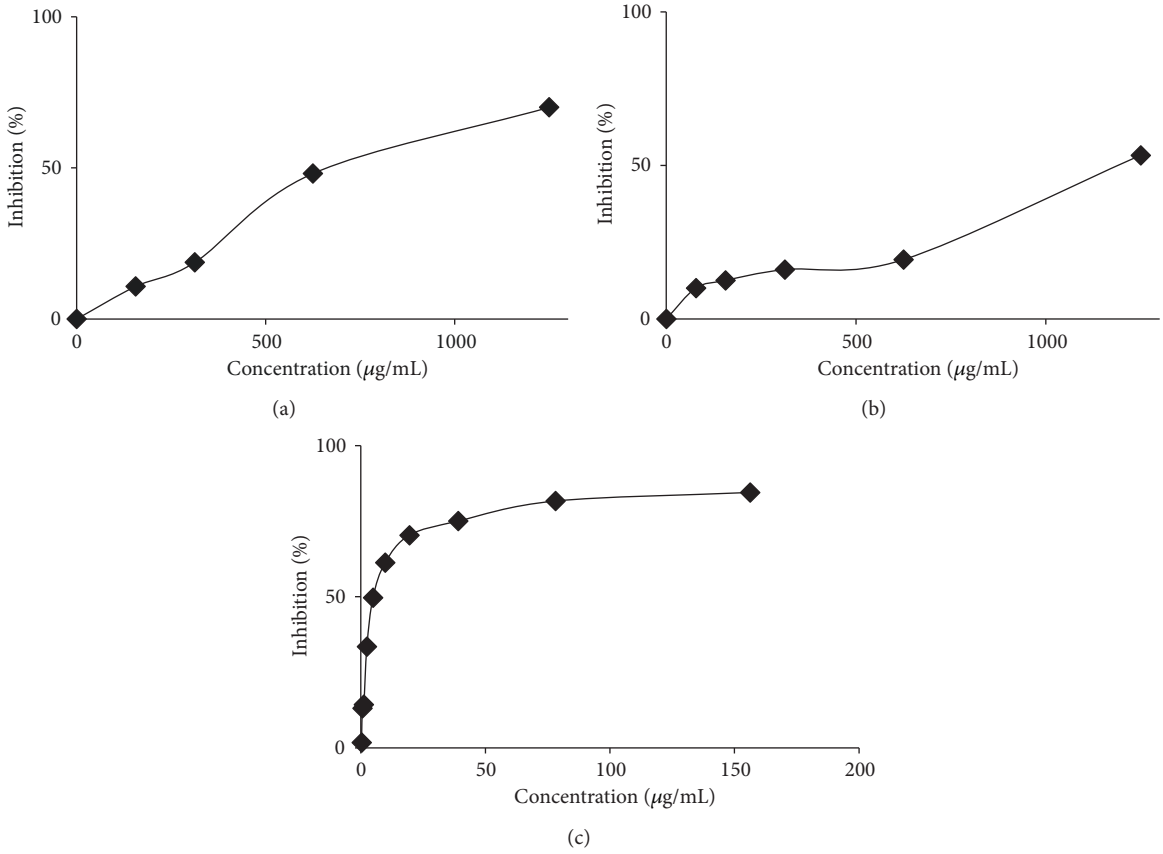

Figure 3: α-Glucosidase inhibitory activity of *C. odorata* (a) ethyl acetate, (b) methanol extracts, and (c) acarbose as a standard.

a potent α-glucosidase inhibitor, was used as a standard and showed an IC_{50} of 7.67 μg/mL in our assay system.

*3.6. Odoratenin (**1**).* White crystal; mp: 144-145°C; $[\alpha]_{25}^{D}$ -16.0° ($CHCl_3$; c = 0.001); IR ν_{max} (KBr): 3518, 2943, 1629, 1593, 1519, 1442, 1300, 1278, 1201, 810 cm^{-1}; for ^1H (400 MHz, $CDCl_3$), ^{13}C NMR (400 MHz, $CDCl_3$), HMQC, and HMBC spectroscopic data are presented in Figure 4 and summarized in Table 2; and HR-ESI-MS *m/z* 339.0831 $[M + Na]^+$ (cald. for $C_{17}H_{16}O_6Na$, 339.3090).

*3.7. Isosakuranetin (**2**).* White needles; mp: 173-174°C; IR ν_{max} (KBr): 3504, 2955, 1639, 1599, 1518, 1492, 1302, 1253, 1163, 833 cm^{-1}; for ^1H (400 MHz, $CDCl_3$) and ^{13}C NMR (400 MHz, $CDCl_3$) spectroscopic data are presented in Table 2.

*3.8. Subscandenin (**3**).* Yellow needles; mp: 174-175°C; for ^1H (400 MHz, $CDCl_3$), ^{13}C NMR (400 MHz, $CDCl_3$) and HMBC spectroscopic data are presented in Table 2.

4. Discussion

4.1. Antioxidant Activities of C. odorata. C. odorata is a species of the genus *Chromolaena* which is one of the largest genera of the family Eupatorieae (Asteraceae) [8]. In Indonesia, *C. odorata,* known as sungga-sungga, was collected from Ambon, Maluku, East Indonesia. This plant is a popular folk medicine widely used as alternative herbal treatment for diabetes and soft tissue wounds in East Indonesia. Besides, in Vietnam, this plant is used as a treatment of leech bites, soft tissue injuries, burns, and skin infections [5]. Furthermore, a leaf water extract is widely used as a diarrhea, malaria, and diabetes drug [6]. In the past 40 years, this plant has been reported in phytochemical studies in the United States [14, 15]. Recently, *C. odorata* was described for its beneficial attributes in some Asia-Africa countries, especially the pharmacological effects of this plant. The specific reported attributes of *C. odorata* include being antibacterial [17], antifungal [18, 19], anti-inflammatory [20, 21], anticancer [11, 13, 22], antiplasmodial [9], antidiabetic [23, 24], and antioxidant [6, 25–28]. However, the antioxidant activity of the isolated compound from *C. odorata* has never been reported.

This present study demonstrated the antioxidant activity of the isolated compound from *C. odorata* for the first time. Related to this study, the antioxidant effect from this plant has been done by two radical scavenging assays supported with the total phenolic content data. As we know, there are a lot of free radical types caused of reactive oxygen species (ROS) [32]. They are the dangerous free radicals against the human body. These free radicals come from either the body itself or the external factors. The free radicals are by products

Table 2: 1D- and 2D NMR spectroscopic data of compounds (**1-3**) in $CDCl_3$.

Position	Isosakuranetin (**2**)		Odoratenin (**1**)			Subscandenin (**3**)		
	δ_H (J in Hz)	δ_c	δ_H (J in Hz)	δ_c	HMBC	δ_H (J in Hz)	δ_c	HMBC
2	5.36 (dd; J=13.2, 3.2 Hz, 1H)	79.10	5.32 (dd; J=12.8, 3.2 Hz, 1H)	79.06	-	5.34 (dd; J=13.2, 3.2 Hz, 1H)	79.13	-
3a	2.78 (dd; J=17.8, 3.2 Hz, 1H)	43.20	2.78 (dd; J=17.0, 3.2 Hz, 1H)	43.30	C-4	2.77 (dd; J=17.2, 3.2 Hz, 1H)	43.29	C-4
3b	3.09 (dd; J=17.0, 13.2 Hz, 1H)		3.07 (dd; J=17.2, 12.8 Hz, 1H)		C-2, 4	3.07 (dd; J=17.2, 12.8 Hz, 1H)		C-2, 4
4	-	196.18	-	196.07	-		196.96	-
5	12.04 (s; 1H)	164.43	12.01 (s; 1H)	162.93	C-6, 7, 8, 10	12.19 (s; 1H)	158.78	-
6	5.97 (d; J=2.4 Hz, 1H)	96.76	6.06 (d; J=2.8 Hz, 1H)	95.19	C-4, 7, 9, 10	6.10 (s; 1H)	94.66	C-5, 8, 9, 10
7	5.76 (br s; 1H)	164.59	-	164.19		6.46 (br s; 1H)	154.43	-
7-OMe	-	-	3.82 (s; 3H)	55.79	C-9	-	-	-
8	5.99 (d; J=2.4 Hz, 1H)	95.54	6.04 (d; J=2.4 Hz, 1H)	94.33	C-6, 9, 10	-	128.38	-
8-OMe	-	-	-	-	-	3.94 (s; 3H)	61.09	C-4, 8
9	-	163.36	-	168.05	-	-	157.50	-
10	-	103.20	-	103.20	-	-	103.19	-
1’	-	130.36	-	147.06	-	-	130.36	-
2’	7.37 (d; J=8.8 Hz, 1H)	114.33	7.04 (d; J=2,0 Hz, 1H)	112.73	C-2, 1’, 4’	6.95 (d; J=10 Hz, 1H)	127.81	C-1’, 3’, 4’, 5’
3’	6.95 (d; J=8.4 Hz, 1H)	127.85	5.69 (s; 1H)	145.99	-	7.37 (d; J=9,2 Hz, 1H)	114.30	C-1’, 2’, 4’, 6’
4’	-	160.14	6.91 (d, J=1.6 Hz, 1H)	118.26	C-1’	-	160.13	-
4’-OMe	3.83 (s; 3H)	55.48	-	-	-	3.82 (s; 3H)	55.46	C-4’
5’	6.95 (d; J=8.4 Hz, 1H)	127.85	6.88 (d; J=8.4 Hz, 1H)	110.72	C-2, 2’, 3’, 6’	7.37 (d; J=9.2 Hz, 1H)	114.30	C-1’, 2’, 4’, 6’
6’	7.37 (d; J=8.8 Hz, 1H)	114.33	-	131.59	-	6.95 (d; J=10 Hz, 1H)	127.81	C-1’, 3’, 4’, 5’
6’-OMe	-	-	3.92 (s; 3H)	56.14	C-1’	-	-	-

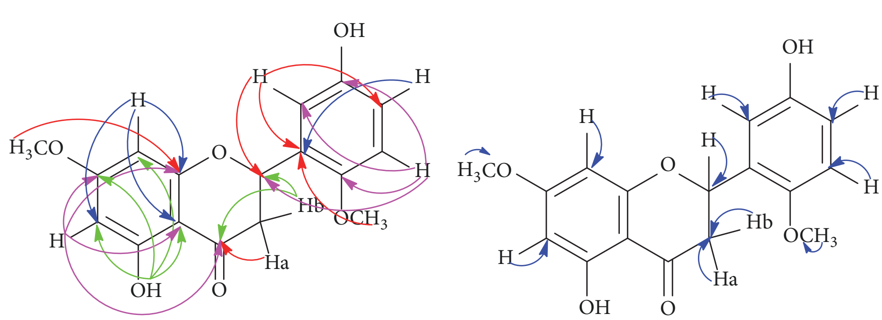

(a) (b)

Figure 4: (a) HMBC and (b) HMQC correlations of odoratenin (**1**).

of energy production by mitochondria which are energy-producing cells as adenosine triphosphate (ATP), while the external factors come from the pollutions, ultraviolet radiation, diet, or lifestyle. Furthermore, the free radicals have an unpaired electron so this condition makes them to be reactive with other molecules around them [33]. Then, the molecules in cells are attacked by free radicals. Normally, the body’s antioxidant defence system can block the free radicals before they become harmful to the body. Unfortunately, because of the old age or a lot of toxin that accumulate inside, the defence system works slowly and then the free radicals start to cause cell damage. The cell damage caused by free radicals is called

oxidative stress. On the long term, the danger of free radicals inside is related to aging and chronic diseases such as cancer, diabetes, and neurodegenerative and cardiovascular diseases.

In the body, free radicals are superoxide anion (SOA) from 2.5% oxygen (O_2). The using of O_2 in the body as a distributor of energy products changes because of free radicals of SOA. Because of that, the body is protected from those free radicals by its antioxidant defence system with these following steps [34]. First, SOA is neutralized by the antioxidant enzyme superoxide dismutase (SOD) changed as hydrogen peroxide (H_2O_2). H_2O_2 is a weak free radical which is used as an immune compound to inhibit the pathogen bacteria or to treat the broken cell tissue. However, the large amounts of H_2O_2 will be toxic for the body. So, there is the second step from the body's defence system that helped with glutathione peroxidase (GPO) enzyme. Two GPOs covert H_2O_2 into two water molecules (H_2O). Certainly, H_2O is safer than that of H_2O_2. Those two steps are very important to protect the cell body. Unfortunately, there is not enough amount of SOD and GPO in the body. So, the amount of free radicals of SOA and H_2O_2 will increase in the cell. The SOA and H_2O_2 might not be worse. But in excess, they will react with each other into more dangerous free radicals, namely, hydroxyl radicals (•OH). Hence, an antioxidant is needed as a resistance support from the outside of the body's defence system [35].

Studies are in our laboratory to identify the antioxidant compound present in *C. odorata*. The determination of the antioxidant effect was assayed by using DPPH and ABTS radicals. As we described previously, there are a lot of free radical types caused by ROS including DPPH and ABTS radicals. DPPH radicals are expressed as the free radical with high reactivity at room temperature. The high reactivity is caused by delocalization of electrons around the molecules. The mechanism of radical scavenging is hydrogen donors. When the DPPH radical is reacted with a substance that donates a hydrogen atom, DPPH radical is reduced into a nonradical DPPH. In the assay, this reaction is characterized by decolorization of the solution. It changes its colour solution from purple to yellow. At room temperature, ABTS radical is more stable and has higher reactivity than that of DPPH. The ABTS radicals are expressed as cation radical with high reactivity ability [36]. The radical cation is formed from the oxidation reaction between ABTS and buffer solution especially using $K_2S_2O_8$. Furthermore, the mechanism of radical scavenging as well as DPPH's mechanism is hydrogen donors [35]. Thus, the antioxidant activity for both of the two assays is evaluated by using UV-Vis Genesys Thermo Scientific spectrophotometer.

According to this study, there is a linear relationship between the antioxidant activity and total phenolic content. This evidence means that the higher the total phenolic content, the higher the antioxidant activity. Among the five tested extracts, the ethyl acetate extract exhibited the highest antioxidant activity against either DPPH or ABTS because of the high amount of total phenolic content. Not only the ethyl acetate extract, but also the dichloromethane, methanol, and water extracts, showed fine antioxidant activity as well as the ethanol and chloroform extracts reported previously [27, 28]. However, there was only weak activity in the *n*-hexane extract. These results suggest the presence of phenolic compounds could be major contributor to antioxidant activity. The phenolic compounds including xanthone [37] or stilbene [38] have been reported as a potent antioxidant activity. Based on this study, the phenolic compounds of *C. odorata* could be extracted by the polar and semipolar solvents very well. When the methanol extract was fractionated and elucidated, the major secondary metabolite came from flavanone compounds which is one of the phenolic groups. The finding of a new flavanone, odoratenin **(1)**, indicates the presence of two hydroxyls and two methoxyl group. They might be donated and the hydrogen atom also supported the electron conjugation system from the phenolic ring for stabilizing the free radicals. Interestingly, the new compound odoratenin **(1)** has higher antioxidant activity than that of trolox as a standard. The present study and these results reveal odoratenin **(1)** isolated from *C. odorata* as a potent antioxidant source.

4.2. α-Glucosidase Inhibitory Activity of C. odorata. Diabetes mellitus is a metabolic disorder caused by a lack of insulin [39]. Insulin helps the blood glucose level to be a normal circumstance and not turn into hyperglycemia or hypoglycaemia. According to the type of an abnormal insulin, diabetes mellitus is divided into two types [40]. The first type is known as insulin dependent diabetes mellitus (IDDM) caused by a genetic factor such as the destruction of pancreatic β-cells which produce insulin and type 2 is non-insulin dependent diabetes (NIDDM) caused by a wrong lifestyle especially on diet. This study focuses on the effective treatment for type 2. As we know, carbohydrates are the major components of our daily foods, for instance, polysaccharides or disaccharides. After carbohydrates intake, the amount of polysaccharides is transformed into monosaccharides as known as the simple sugars, and then they are transferred through the bloodstream system for energy [41]. However, before they are transferred, they are absorbed on the intestine. In the small intestinal tissue, there is a catalyse of the cleavage of polysaccharides to glucose, namely, α-glucosidase. It makes the total of glucose too large. Certainly, the increasing of glucose level as known as hyperglycemia in the blood is not good enough for health [42, 43]. Related to hyperglycemia, α-glucosidase inhibitor is recommended as antidiabetic [44].

In this assay system, the rat intestinal acetone powder has been used as enzyme to determine the antidiabetic inhibitory activity of *C. odorata* extracts. The tested extracts might inhibit or compete with maltose as a substrate. Based on our work, there is a linear correlation between α-glucosidase inhibition and antioxidant activity. The ethyl acetate and methanol extracts performed a fine inhibitory activity. This result as well as the antioxidant activity screening previously reported that these two extracts have a good radical scavenging activity also against both DPPH and ABTS radicals. Furthermore, the isolated compound from *C. odorata* reported a significantly higher α-glucosidase inhibitory activity than that of deoxynojirimycin and acarbose as the standards in previous research [24]. From this study, it should be noted that the α-glucosidase inhibitory effect of the ethyl acetate

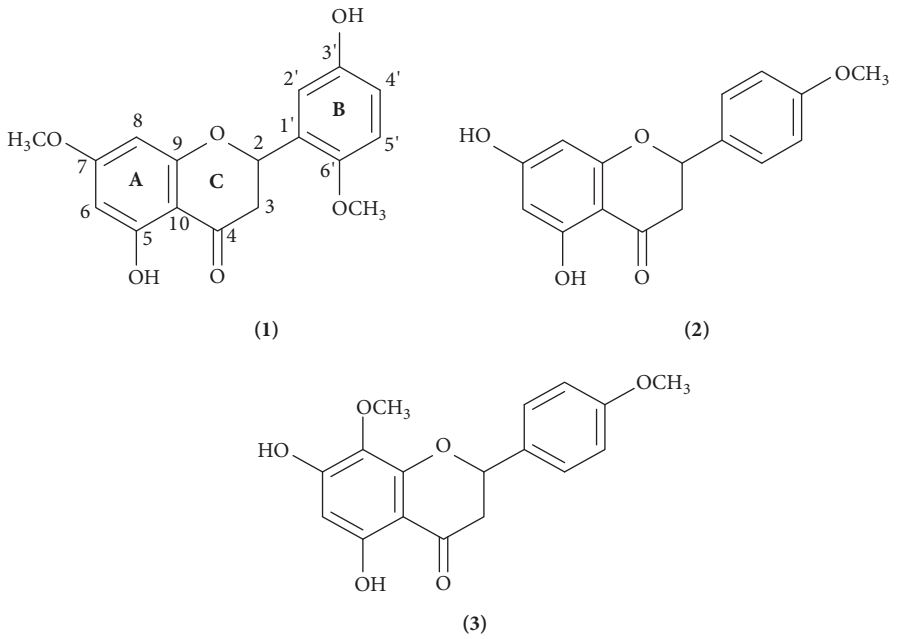

Figure 5: The structures of odoratenin **(1)**, isosakuranetin **(2),** and subscandenin **(3)** isolated from the leaves of *C. odorata* methanol extract.

extract from *C. odorata* was almost the same as that of the methanol extract.

4.3. The Flavanones Isolated from C. odorata. Antioxidant evaluation of the methanol extract from the leaves of *C. odorata* led to finding of a bioactive compound as well as a new flavanone, odoratenin **(1)**, along with two known compounds: isosakuranetin **(2)** and subscandenin **(3)**. The structure of a new compound **(1)** was elucidated by using 1D- and 2D-NMR spectroscopy analysis and the structures of the known compounds **(2)** and **(3)** were determined and compared with the published NMR spectroscopic data previously.

Odoratenin **(1)** was obtained as a white crystal. Its molecular formula was determined as 5,3'-dihydroxy-7,6'-dimethoxyflavanone ($C_{17}H_{16}O_6$) by HR-ESI-MS measurement through the hydrogen ion at *m/z* 317.1013 $[M + H]^+$ and the sodium ion at *m/z* 339.0831 $[M + Na]^+$ (calcd. for $C_{17}H_{16}O_6Na$, 339.3090). The IR spectrum showed characteristic absorption bands for hydroxyl chelated carbonyl stretching bonds at 3518 and 1629 cm^{-1}, indicating the presence of a flavonoid group. The NMR assignments were made by applying 1D- and 2D-NMR experiments (^1H NMR, ^{13}C NMR, HMBC, and HMQC; $CDCl_3$, 400 MHz). The ^1H NMR spectrum (Table 2) showed signal for a hydrogen-bonded hydroxyl proton at δ_H 12.01 (s, 1H, 5-OH); two aromatic protons at δ_H 6.06 (d, *J*=2.8 Hz, 1H, H-6) and 6.04 (d, *J*=2.4 Hz, 1H, H-8); three pyrone vicinal-geminal protons at δ_H 5,32 (dd, *J*=12.8; 3.2 Hz, 1H, H-2), 3.07 (dd, *J*=17.2; 12.8 Hz, 1H, H-3b), and 2.77 (dd, *J*=17.0; 3.2 Hz, 1H, H-3a) indicating the presence of a flavanone which are similar to the ^1H NMR spectrum of known compound, isosakuranetin **(2)**; three aromatic protons with abx-system at δ_H 7.04 (d, *J*=2.0 Hz, 1H, H-2'), 6.91 (dd, *J*=1.6 Hz, 1H, H-4'), and 6.88 (d, *J*=8.4 Hz, 1H, H-5'); and six methoxy protons at δ_H 3.92 (s, 3H, 6'-OMe) and 3.82 (s, 3H, 7-OMe). Based on the ^{13}C NMR spectrum, there are 17 carbon signals of this compound **(1)** including a carbonyl group of C-4 (δ_C 196.07), one chiral carbon of C-2 (δ_C 79.06) with $[\alpha]_{25}^{D}$ -16.0° as the absolute configuration, two carboxyl groups (-C-OH) of C-5 and C-3' (δ_C 162.93 and 145.99), and two methoxy carbons (-OCH$_3$) of 7-OCH$_3$ and 6'-OCH$_3$ (δ_C 55.79 and 56.14). However, there is the only one methoxy carbon of 4'-OCH$_3$ (δ_C 55.48) in isosakuranetin **(2)**. The long-range hydrogen to carbon correlations were assigned and confirmed by two-dimensional NMR (HMBC and HMQC) as Figures 4(a) and 4(b). The HMBC correlations showed that a hydrogen-bonded hydroxyl proton at δ_H 12.01 (5-OH) correlated with C-6 (δ_C 95.19), C-7 (δ_C 164.19), C-8 (δ_C 94.33), and C-10 (δ_C 103.20) showing that the hydroxyl group was attached to C-5. Two vicinal-geminal protons at δ_H 3.07 (3-Hb) and 2.77 (3-Ha) were attached to carbon carbonyl (C-4, δ_C 196.07). Besides, the 3-Hb proton correlated with C-2 (δ_C 79.06) showing that the vicinal-geminal protons were attached to C-3. Furthermore, five aromatic protons were placed at C-6, C-8, C-2', C-4', and C-5'. They have hydrogen-to-carbon correlations between H-6/C-4, C-7, C-9, C-10; H-8/C-6, C-7, C-9, C-10; H-2'/C-2, C-1', C-4'; H-4'/C-1'; H-5'/C-2, C-2', C-3', C-6' which were also confirmed by HMQC spectrum as Figure 4(b). Accordingly, both hydroxyl and methoxy substituents were assigned as 3'-hydroxy [9, 13] and 8-methoxy [14] at C-3' and C-8. Interestingly, although more than 79 flavonoid compounds have been isolated from the genus *Chromolaena* [8], the methoxy substituent at C-6' has not been reported yet before. Accordingly, the compound of **(1)** is a new flavanone named odoratenin **(1)** as in Figure 5 **(1)**.

Isosakuranetin **(2)** is a white needles solid powder with a melting point of 173-174°C. The elucidation process of isosakuranetin **(2)** was determined as these following steps. First, the FT-IR data showed the strong intensity of peaks as follows, ν_{maks} (KBr): 3504, 2955, 1639, 1599, 1518, 1492, 1302, 1253, 1163, and 833 cm^{-1}. The peaks of 3504 cm^{-1} with medium intensity and 1639 cm^{-1} with strong intensity revealed the presence of a hydroxyl (-OH) group chelated with carbonyl group (-C=O). In addition, the peaks of 1518, 1492, and 833 cm^{-1} with medium to weak intensities indicated the presence of a conjugated aromatic group. Furthermore, this information was confirmed by data ^{1}H and ^{13}C-NMR ($CDCl_3$, 400 MHz) presented in Table 2. Based on the presented data, there are a number of detected chemical shifts as 14 protons and 16 carbons. The 14 proton signals including the singlet signal of δ_H 12.04 ppm with integration in the downfield area indicated the presence of one proton as 5-O<u>H</u>. This proton is deshielded because it bonds with O atom which has more electrons directly to be a hydroxyl group and also as a typical signal at the same time. The typical signal means a hydroxyl proton chelated with a carbonyl group. So, the proton has a far chemical shift. Next, a strong singlet signal of δ_H 3.83 ppm with three integration processes in the upfield area showed three protons as 4'-OC<u>H</u>$_3$. They are shielded because they do not bond with O atom directly. So, these three protons have near chemical shifts and also they are suspected strongly to be protons from the methoxy group. Furthermore, three signals with doublet multiplicity at δ_H 5.36 (H-2), 2.78 (H-3a), and 3.09 ppm (H-3b) coupling with the vicinal-geminal proton system indicated the presence of a pyran group [45]. This proton system indicated strongly that compound **(2)** is one of the flavanone groups which is similar to a previous known compound reported by Suksamrarn *et al.* (2004) [13]. In addition, the doublet signals of δ_H 7.37 (H-2'/6') and 6.95 ppm (H-3'/5') coupling with each other with double intensity showed four proton signals indicating the protons of an aromatic group. Based on our results, compound **(2)** has a flavanone skeleton with an ABC ring system substituted with the methoxy and hydroxyl groups as Figure 5 **(2)**. Furthermore, two signal doublets of δ_H 5.97 and 5.99 ppm also coupling with each other are strongly suspected as two signals of aromatic potons as H-6 and H-8 on ring A. The determination of the structure of compound **(2)** is confirmed with ^{13}C-NMR data. Based on our ^{13}C-NMR data, there are 16 carbons including a carbon carbonyl group which is strongly expected as a position of C-4 (δ_C 196.18 ppm), one chiral carbon assumed as a position of C-2 (δ_C 79.10 ppm), one carbon methoxy at position of C-4' (δ_C 55.48 ppm), and the aromatic carbon expected as the position of C-2'/6' (δ_C 114.33 ppm) and C-3'/5' (δ_C 127.85 ppm) with double intensity, respectively. And the other aromatic carbons including δ_C 95.54, 96.76, 103.20, 130.36, 160.14, 163.36, 164.53, and 164.59 ppm. Based on this elucidation study, compound **(2)** is an isosakuranetin **(2)** as in Figure 5 **(2)** which was also isolated by Suksamrarn *et al.* (2004).

Subscandenin **(3)** is yellow needles solid powder with a melting point of 174-175°C. Compound **(3)** is strongly expected as subscandenin which is one of the derivatives from flavanone compounds with a skeleton similar to compounds **(1-2)**. The structure is confirmed by the interpretation of ^{1}H, ^{13}C-NMR, and HMBC data ($CDCl_3$, 400 MHz) presented in Table 2. The results of the NMR characterization showed characters that are similar to the NMR characterization of compounds **(1-2)**. Based on the presented data, there are a number of detected chemical shifts as 16 protons and 17 carbons. This total of protons and carbons is equal to the total of compound **(1)**. The ^{1}H NMR spectrum (Table 2) showed signal for a hydrogen-bonded hydroxyl proton at δ_H 12.19 (s, 1H, 5-OH); two aromatic protons at δ_H 6.10 (s, 1H, H-6) and 6.46 (br s, 1H, H-7); three pyrone vicinal-geminal protons at δ_H 5.34 (dd, *J*=13.2; 3.2 Hz, 1H, H-2), 3.07 (dd, *J*=17.2; 12.8 Hz, 1H, H-3b), and 2.77 (dd, *J*=17.2; 3.2 Hz, 1H, H-3a) indicating the presence of a flavanone which are similar to the ^{1}H NMR spectrum of the known compounds, odoratenin **(1)** and isosakuranetin **(2)**; four aromatic protons at δ_H 6.95 (d, *J*=10 Hz, 2H, H-2'/6') and 7.37 (d, *J*=9.2 Hz, 2H, H-3'/5'); and six methoxy protons at δ_H 3.94 (s, 3H, 8-OMe) and 3.82 (s, 3H, 4'-OMe). Based on the ^{13}C NMR spectrum, there are 17 carbon signals of compound **(3)** including a carbonyl group (δ_C 196.96), one chiral carbon (δ_C 79.13), two carboxyl groups (δ_C 158.78 and 114.30), and two methoxy carbons (δ_C 61.09 and 55.46). The long-range hydrogen to carbon correlations were assigned and confirmed by HMBC spectrum presented in Table 2. The HMBC correlation data confirmed the existence of 18 correlations between protons and carbons. These results showed the structure of compound **(3)** is different from either compound **(1)** or compound **(2)**. The signal correlation showed a relationship between proton methoxy of 4'-OC<u>H</u>$_3$ (δ_H 3.82 ppm) with carbon of C-4 (δ_c 160.13 ppm) and other proton methoxy of 8-OC<u>H</u>$_3$ (δ_H 3.94 ppm) with two carbons of C-4 (δ_c 196.96 ppm) and C-8 (δ_c 128.38 ppm). This signal correlation revealed the position of the methoxy of 4'-OC<u>H</u>$_3$ (δ_H 3.82 ppm) on ring B and other methoxy group of 8-OC<u>H</u>$_3$ (δ_H 3.94 ppm) on ring A. Furthermore, there are four correlations between protons and aromatic carbon on ring B, namely, proton of H-3'/5' (δ_H 7.37 ppm) correlating with four carbons of C-1 (δ_c 130.36 ppm), C-2'/6' (δ_c 127.81 ppm with double integrations), and C-4' (δ_c 160.13 ppm). The same thing happened to proton of H-2'/6/ (δ_H 6.95 ppm) which also correlated with four carbons of C-1' (δ_c 130.36 ppm), C-3'/5' (δ_c 114.30 with double integrations), and C-4' (δ_c 160.13 ppm). These correlation evidences assumed strongly that the O-methoxy binds directly to carbon of C-4'. In addition, there are four correlations between a proton and the aromatic carbons on ring A, namely, proton of H-6 (δ_H 6.10 ppm) correlating with four carbons of H-5 (δ_c 158.78 ppm), H-8 (δ_c 128.38 ppm), H-9 (δ_c 157.50 ppm), and H-10 (δ_c 103.19 ppm). These correlation evidences assumed strongly that the O-methoxy binds directly to carbon of C-8. Based on our elucidation study, the compound of **(3)** is a subscandenin **(3)** as in Figure 5**(3)** which was also isolated by Amaro-Luis & Delgado-Mendez (1993). However, they reported isolated subscandenin **(3)** from a different species, namely, *C. subscandens* [14].

5. Conclusion

C. odorata, collected from East Indonesia, contributes to drug discovery and healthcare. This is the first report on the antioxidant activity of a new flavanone isolated from the *C. odorata* leaves methanol extract. Among the tested five extracts, the ethyl acetate extract exhibited the highest inhibitory effect against ABTS radical and α-glucosidase rat intestinal enzyme. Further investigations will focus on the identification of the other active flavanone compounds responsible for the antioxidant as well as α-glucosidase inhibitory activity of *C. odorata* leaves ethyl acetate extract.

Data Availability

The data used to support the findings of this study are available from the corresponding author upon request.

Conflicts of Interest

All authors declare that there are no conflicts of interest regarding the publication of this article.

Acknowledgments

This work was supported by a grant from Directorate General of Higher Education, Ministry of Research, Technology & Higher Education, Indonesia. This work was also supported by the financial support for Putri, D. A. from Indonesia Endowment Fund for Education Scholarship (LPDP-RI), Ministry of Finance, Indonesia.

References

[1] W. Brand-Williams, M. E. Cuvelier, and C. Berset, "Use of a free radical method to evaluate antioxidant activity," *LWT - Food Science and Technology*, vol. 28, no. 1, pp. 25–30, 1995.

[2] WHO, "Traditional medicine," Fifty-sixty world health assembly, 2003.

[3] O. Tebboub, R. Cotugno, F. Oke-Altuntas et al., "Antioxidant potential of herbal preparations and components from *Galactites elegans* (All.) Nyman ex Saldano," *Evidence-Based Complementary and Alternative Medicine*, vol. 2018, Article ID 9294358, 7 pages, 2018.

[4] CABI, "Invasive Species Compendium," 2017, http://www.cabi.org/isc/datasheet/23248.

[5] T.-T. Phan, L. Wang, P. See, R. J. Grayer, S.-Y. Chan, and S. T. Lee, "Phenolic compounds of *Chromolaena odorata* protect cultured skin cells from oxidative damage: implication for contaneous wound healing," *Biological & Pharmaceutical Bulletin*, vol. 24, no. 12, pp. 1373–1379, 2001.

[6] T. Boudjeko, R. Megnekou, A. L. Woguia et al., "Antioxidant and immunomodulatory properties of polysaccharides from *Allanblackia floribunda* Oliv stem bark and *Chromolaena odorata* (L.) King and H.E. Robins leaves," *BioMed Central*, vol. 8, no. 1, article no 759, 2015.

[7] A. G. Omokhua, L. J. McGaw, J. F. Finnie, and J. Van Staden, "Chromolaena odorata (L.) R.M. King and H. Rob. (Asteraceae) in sub-Saharan Africa: A synthesis and review of its medicinal potential," *Journal of Ethnopharmacology*, vol. 183, pp. 112–122, 2016.

[8] J. A. M. de Oliveira, D. I. Bernardi, R. B. Balbinot et al., "Chemotaxonomic value of flavonoids in Chromolaena congesta (Asteraceae)," *Biochemical Systematics and Ecology*, vol. 70, pp. 7–13, 2017.

[9] I. C. Ezenyi, O. A. Salawu, R. Kulkarni, and M. Emeje, "Antiplasmodial activity-aided isolation and identification of quercetin-4'-methyl ether in *Chromolaena odorata* leaf fraction with high activity against chloroquine-resistant *Plasmodium falciparum*," *Parasitology Research*, vol. 113, no. 12, pp. 4415–4422, 2014.

[10] M.-L. Zhang, D. Irwin, X.-N. Li et al., "PPARγ agonist from chromolaena odorata," *Journal of Natural Products*, vol. 75, no. 12, pp. 2076–2081, 2012.

[11] T. M. Hung, T. D. Cuong, N. H. Dang et al., "Flavonoid glycosides from Chromolaena odorata leaves and their in vitro cytotoxic activity," *Chemical & Pharmaceutical Bulletin*, vol. 59, no. 1, pp. 129–131, 2011.

[12] N. Pisutthanan, B. Liawruangrath, S. Liawruangrath, and J. B. Bremner, "A new flavonoid from Chromolaena odorata," *Natural Product Research (Formerly Natural Product Letters)*, vol. 20, no. 13, pp. 1192–1198, 2006.

[13] A. Suksamrarn, A. Chotipong, T. Suavansri et al., "Antimycobacterial activity and cytotoxicity of flavonoids from the flowers of *Chromolaena odorata*," *Archives of Pharmacal Research*, vol. 27, no. 5, pp. 507–511, 2004.

[14] J. M. Amaro-Luis and P. Delgado-Méndez, "Flavonoids from the leaves of chromolaena subscandens," *Journal of Natural Products*, vol. 56, no. 4, pp. 610–612, 1993.

[15] R. N. Barua, R. P. Sharma, G. Thyagarajan, and W. Hertz, "Flavonoids of Chromolaena odorata," *Phytochemistry*, vol. 17, no. 10, pp. 1807-1808, 1978.

[16] E. Wollenweber, M. Dörr, and R. Muniappan, "Exudate flavonoids in a tropical weed, Chromolaena odorata (L.) R. M. King et H. Robinson," *Biochemical Systematics and Ecology*, vol. 23, no. 7-8, pp. 873-874, 1995.

[17] M. Atindehou, L. Lagnika, B. Guérold et al., "Isolation and identification of two antibacterial agents from Chromolaena odorata L. active against four diarrheal strains," *Advances in Microbiology*, vol. 03, no. 01, pp. 115–121, 2013.

[18] K. K. Naidoo, R. M. Coopoosamy, and G. Naidoo, "Screening of Chromolaeana odorata (L.) king and robinson for antibacterial and antifungal properties," *Journal of Medicinal Plant Research*, vol. 5, no. 19, pp. 4859–4862, 2011.

[19] A. N. Ngane, R. E. Etame, F. Ndifor, L. Biyiti, P. H. A. Zollo, and P. Bouchet, "Antifungal activity of Chromolaena odorata (L.) King & Robinson (Asteraceae) of Cameroon," *Chemotherapy*, vol. 52, no. 2, pp. 103–106, 2006.

[20] H. Pandith, X. Zhang, S. Thongpraditchote, Y. Wongkrajang, W. Gritsanapan, and S. J. Baek, "Effect of Siam weed extract and its bioactive component scutellarein tetramethyl ether on anti-inflammatory activity through NF-κB pathway," *Journal of Ethnopharmacology*, vol. 147, no. 2, pp. 434–441, 2013.

[21] T. T. H. Hanh, D. T. T. Hang, C. Van Minh, and N. T. Dat, "Anti-inflammatory effects of fatty acids isolated from Chromolaena odorata," *Asian Pacific Journal of Tropical Medicine*, vol. 4, no. 10, pp. 760–763, 2011.

[22] P. B.-K. Kouamé, C. Jacques, G. Bedi et al., "Phytochemicals isolated from leaves of chromolaena odorata: Impact on viability and clonogenicity of cancer cell lines," *Phytotherapy Research*, vol. 27, no. 6, pp. 835–840, 2013.

[23] M. Onkaramurthy, V. P. Veerapur, B. S. Thippeswamy, T. N. Madhusudana Reddy, H. Rayappa, and S. Badami, "Anti-diabetic and anti-cataract effects of *Chromolaena odorata*Linn. in streptozotocin-induced diabetic rats," *Journal of Ethnopharmacology*, vol. 145, no. 1, pp. 363–372, 2013.

[24] P. Wafo, R. S. T. Kamdem, Z. Ali et al., "Kaurane-type diterpenoids from Chromoleana odorata, their X-ray diffraction studies and potent α-glucosidase inhibition of 16-kauren-19-oic acid," *Fitoterapia*, vol. 82, no. 4, pp. 642–646, 2011.

[25] M. Madhavan, "Quantitative Estimation of total phenols and antibacterial studies of leaves extracts of *Chromolaena odorata* (L.) King & H. E. Robins," *International Journal of Herbal Medicine*, vol. 3, no. 2, pp. 20–23, 2015.

[26] G. Parameswari and M. Suriyavathana, "In-vitro antioxidant activity chromolaena odorata (L.) king and robinson," *International Research Journal of Pharmacy*, vol. 3, no. 1, pp. 187–192, 2013.

[27] D. Bhargava, C. Mondal, J. Shivapuri, S. Mondal, and S. Kar, "Antioxidant properties of the leaves of Chromolaena odorata linn," *Journal of Institute of Medicine*, vol. 35, no. 1, pp. 53–56, 2013.

[28] K. Srinivasa Rao, P. K. Chaudhury, and A. Pradhan, "Evaluation of anti-oxidant activities and total phenolic content of Chromolaena odorata," *Food and Chemical Toxicology*, vol. 48, no. 2, pp. 729–732, 2010.

[29] J. S. A. Al-Qassabi, A. M. Weli, and M. A. Hossain, "Comparison of total phenols content and antioxidant potential of peel extracts of local and imported lemons samples," *Sustainable Chemistry and Pharmacy*, vol. 8, pp. 71–75, 2018.

[30] D. A. Putri, A. Ulfi, A. S. Purnomo, and S. Fatmawati, "Antioxidant and antimicrobial activities of Ananas comosus peel extracts," *Malaysian Journal of Fundamental and Applied Sciences*, vol. 14, no. 2, pp. 307–311, 2018.

[31] S. R. Ayinampudi, R. Domala, R. Merugu, S. Bathula, and M. R. Janaswamy, "New icetexane diterpenes with intestinal α-glucosidase inhibitory and free-radical scavenging activity isolated from Premna tomentosa roots," *Fitoterapia*, vol. 83, no. 1, pp. 88–92, 2012.

[32] T. H. Bang, H. Suhara, K. Doi et al., "Wild mushrooms in Nepal: some potential candidates as antioxidant and ACE-inhibition sources," *Evidence-Based Complementary and Alternative Medicine*, vol. 2014, Article ID 195305, 11 pages, 2014.

[33] W. D. Fitriana, T. Ersam, K. Shimizu, and S. Fatmawati, "Antioxidant activity of Moringa oleifera extracts," *Indonesian Journal of Chemistry*, vol. 16, no. 3, pp. 297–301, 2016.

[34] N. A. Kristanti, S. N. Aminah, M. Tanjung, and B. Kurniadi, *Fitokimia*, Airlangga University Press, Surabaya, Indonesia, 1st edition, 2008.

[35] M. D. Hidayati, T. Ersam, K. Shimizu, and S. Fatmawati, "Antioxidant activity of Syzygium polynthum extracts," *Indonesian Journal of Chemistry*, vol. 17, no. 1, pp. 49–53, 2017.

[36] E. A. Shalaby and S. M. M. Shanab, "Antioxidant compounds, assays of determination and mode of action," *African Journal of Pharmacy and Pharmacology*, vol. 7, no. 10, pp. 528–539, 2013.

[37] E. R. Sukandar, T. Ersam, S. Fatmawati, P. Siripong, T. Aree, and S. Tip-Pyang, "Cylindroxanthones A-C, three new xanthones and their cytotoxicity from the stem bark of Garcinia cylindrocarpa," *Fitoterapia*, vol. 108, pp. 62–65, 2016.

[38] T. Ersam, S. Fatmawati, and D. N. Fauzia, "New prenylated stilbenes and antioxidant activities of Cajanus cajan (L.) millsp. (Pigeon pea)," *Indonesian Journal of Chemistry*, vol. 16, no. 2, pp. 151–155, 2016.

[39] Z. Yin, W. Zhang, F. Feng, Y. Zhang, and W. Kang, "α-Glucosidase inhibitors isolated from medicinal plants," *Food Science and Human Wellness*, vol. 3, no. 3-4, pp. 136–174, 2014.

[40] S. Fatmawati, K. Kurashiki, S. Takeno et al., "The inhibitory effect on aldose reductase by an extract of Ganoderma lucidum," *Phytotherapy Research*, vol. 23, no. 1, pp. 28–32, 2009.

[41] S. Fatmawati, K. Shimizu, and R. Kondo, "Ganoderic acid Df, a new triterpenoid with aldose reductase inhibitory activity from the fruiting body of Ganoderma lucidum," *Fitoterapia*, vol. 81, no. 8, pp. 1033–1036, 2010.

[42] S. Fatmawati, T. Ersam, and K. Shimizu, "The inhibitory activity of aldose reductase in vitro by constituents of Garcinia mangostana Linn," *Phytomedicine*, vol. 22, no. 1, pp. 49–51, 2015.

[43] S. Fatmawati, T. Ersam, H. Yu, C. Zhang, F. Jin, and K. Shimizu, "20(S)-Ginsenoside Rh2 as aldose reductase inhibitor from Panax ginseng," *Bioorganic & Medicinal Chemistry Letters*, vol. 24, no. 18, pp. 4407–4409, 2014.

[44] S. Fatmawati, K. Shimizu, and R. Kondo, "Ganoderol B: a potent α-glucosidase inhibitor isolated from the fruiting body of *Ganoderma lucidum*," *Phytomedicine*, vol. 18, no. 12, pp. 1053–1055, 2011.

[45] T. Robinson, *Kandungan organik tumbuhan tinggi*, ITB Publisher, Bandung, Indonesia, 6th edition, 1995.

Hindawi
Evidence-Based Complementary and Alternative Medicine
Volume 2019, Article ID 2607086, 9 pages
https://doi.org/10.1155/2019/2607086

Research Article

Chemical Composition and Antiproliferative Effects of a Methanol Extract of *Aspongopus chinensis* Dallas

Jun Tan,[1,2] Ying Tian,[1] Renlian Cai,[1,2] Rui Luo ,[3] and Jianjun Guo [1]

[1]*Provincial Key Laboratory for Agricultural Pest Management of Mountainous Region, Institute of Entomology, Guizhou University, Guiyang, Guizhou 550025, China*
[2]*Department of Histology and Embryology, Zunyi Medical University, Zunyi, Guizhou 563000, China*
[3]*College of Life Science, Guizhou University, Guiyang, Guizhou 550025, China*

Correspondence should be addressed to Rui Luo; rluo1@gzu.edu.cn and Jianjun Guo; jjguo@gzu.edu.cn

Received 12 March 2019; Accepted 9 May 2019; Published 30 May 2019

Guest Editor: Yong-Ung Kim

Natural products from insects can be potent sources for developing a variety of pharmaceutical products. *Aspongopus chinensis* Dallas has been used as a traditional Chinese medicine and there are several clinical evidences to support its anticancer activity. However, the anticancer active ingredients present in *A. chinensis* remain unidentified. In the present study, we investigated the anticancer effects of a methanol extract of *A. chinensis* (AME). Gas chromatography mass spectrometry was used to analyse the chemical composition of AME. The cell viability of MDA-MB-453 and HCC-1937 cells treated with different concentrations of AME was detected by MTT assay and the ratio of cells in different cell cycle phases was analysed by flow cytometry. The expression of genes associated with cell cycle was analysed by real-time PCR assay. The results showed that oleic acid (25.39%) and palmitic acid (21.798%) are the main anticancer compounds present in AME. There was a concentration-dependent decrease in the proliferation of MDA-MB-453 and HCC-1937 cells. Moreover, treatment with AME induced a S-phase arrest in the cells. Real-time PCR assay demonstrated that AME could significantly downregulate the expression of *CDC20*, *AURKB*, *PLK1*, *CCNB2*, and *TOP2A* mRNAs and upregulate the expression of *GADD45A* mRNA. We demonstrate that the methanol extract of *A. chinensis* could be a potential natural alternative or complementary therapy for breast cancer.

1. Introduction

Breast cancer is the most common malignancy in women and accounts for around 18% of all cancers in females [1]. In the United States, about 63,960 cases of female breast carcinoma were diagnosed in 2018. In women, the three most common types of cancers are breast, lung, and colorectal cancer. Breast cancer alone accounts for 30% of new cancer diagnoses in women [2]. Such cases are particularly on the rise in some Asian countries. In the past decade, the incidence of breast cancer in China has increased by 27%, and 40% of the diagnosed patients died within 5 years. The incidence of breast cancer in Chinese women and the mortality associated with it has increased sharply [3]. The treatment of cancer with traditional Chinese medicine (TCM) has attracted extensive attention, as chemotherapeutic agents have more side effects [4].

Aspongopus chinensis Dallas (Dinidoridae, Insecta) is a TCM [5]. Owing to its anticancer, antibacterial, and anticoagulant functions, much attention has been focused on *A. chinensis* [6]. It can be used to treat gastric and oesophageal cancers. Trichloromethane extracts and water extracts from *A. chinensis* could inhibit the proliferation of human gastric (SGC-7901) and liver (HepG2) cancer cells [7–10]. Serum containing *A. chinensis* could inhibit the proliferation of SW480 [11]. Our previous findings revealed that the haemolymph from *A. chinensis* had a significant inhibitory effect on the proliferation of SGC-7901, BGC-823, and MCF-7 cells [12–15] and that the apoptosis of SGC-7901 and MCF-7 cells induced by the haemolymph might be through mitochondrial signalling pathway [16]. Excellent anticancer effects of *A. chinensis* have been supported by an increasing body of evidence; however, the effective ingredients present in it have not been identified as yet.

In the current study, the chemical composition of an *A. chinensis* methanol extract (AME) and its anticancer activities were investigated. The results of this study support the opinion that *A. chinensis* is a valuable insect resource that can be investigated further for potential medicinal uses.

2. Materials and Methods

2.1. Chemicals and Reagents. The 3-(4,5-dimethylthiazol-2-yl)-2,5-diphenyltetrazolium bromide (MTT) and cell cycle detection kit were obtained from Beyotime (Beyotime Institute of Biotechnology, Shanghai, China). L-15 medium, RPMI-1640 medium, and fetal bovine serum (FBS) were purchased from Hyclone (GE Healthcare, Logan, UK). Dimethyl sulfoxide (DMSO) was obtained from Sigma company.

2.2. Materials. Specimens of *A. chinensis* (known by its name in Chinese as Jiuxiangchong) were collected in Zunyi, Guizhou Province, China (27°42′15″ N latitude, 106°55′22″ E longitude, 1161 m a.s.l. altitude). The specimens were authenticated by Prof. Zizhong Li (Institute of Entomology, Guizhou University, Guiyang, China). They were shade dried and ground into a fine powder, which was then extracted with 5 × the volume of methanol for 48 h at 25°C. The insoluble particles were removed by centrifugation at 12,000 × *g* for 10 min at 4°C and by filtration through a 0.22-μm membrane (Millipore, Merck Millipore Ltd., Germany). The bulk methanol extracts were vacuum dried in a freeze dryer (Chaist, Alpha 1-2 LD plus, Germany) and quantified. For *in vitro* cellular assay, DMSO was used to redissolve the dried methanol extracts, which were stored at −80°C until use. The final concentration of DMSO in the cell culture studies was maintained at 0.1%.

2.3. Cell Culture. Human breast cancer cell lines MDA-MB-453 and HCC-1937 were kindly provided by the Stem Cell Bank, Chinese Academy of Sciences. The cells were cultured in L-15 and RPMI-1640 media (GE Healthcare, Logan, UK), supplemented with 2 mM L-glutamine and 10% FBS (Life Technology, Shanghai, China), containing penicillin (100 U/mL) and streptomycin (100 μg/mL, Life Technology, Shanghai, China). The HCC-1937 cells were cultured in an incubator with 5% CO_2 at 37°C and MDA-MB-453 cells were cultured in an incubator at 37°C without CO_2 (air, 100%).

2.4. Cell Viability Assay. The MDA-MB-453 and HCC-1937 cells (5×10^3/well) were seeded into 96-well plates and incubated for 24 h. After treatment with AME (0.5, 1, or 1.5 mg/mL) or an equivalent concentration (1%) of DMSO for 48 h, the cell viability was determined by MTT assay. MTT solution (20 μL, 5 mg/mL) was added to the wells, and the cells were incubated for 4 h. Thereafter, the MTT solution was removed and DMSO (150 μL) was added to each well. The absorbance was measured at 570 nm using an automated microplate reader (Bio-Rad, Hercules, CA, USA). The control values for DMSO were deducted from the absorbance values obtained for all the groups. The 50% growth inhibition value (IC50) of AME was calculated. The experiment was repeated five times. The cell survival rate was calculated on the basis of the percentage of cell survival in the drug-treated group versus that in the control group. The formula used for calculation was as follows: cell viability (%) = absorbance (treated)/absorbance (control) × 100.

2.5. Morphological Study. The MDA-MB-453 and HCC-1937 cells were grown on coverslips (1×10^5 cells/cover slip) and incubated with different concentrations (0.5, 1, or 1.5 mg/mL) of AME or with 0.1% DMSO for 48 h, and then fixed in a solution of ethanol: acetic acid (3:1, v/v). The cover slips were mounted on glass slides for morphometric analysis. Three monolayers per experimental group were photographed. Morphological changes in MDA-MB-453 and HCC-1937 cells were determined using a Nikon bright-field inverted light microscope (Tokyo, Japan) at 200× (for MDA-MB-453 cells) or 400× (for HCC-1937 cells) magnification.

2.6. Cell Cycle Assay. Cell cycle analysis was performed using a cell cycle detection kit (Beyotime Biotechnology, Shanghai, China), according to the manufacturer's instructions. Briefly, the MDA-MB-453 and HCC-1937 cells were seeded in 6-well plates (1×10^5/well) and cultured for 24 h. The cells were starved by culturing them in serum-free medium for 12 h. After treatment with AME (0 and 2.57 mg/mL for MDA-MB-453 cells; 0 and 3.64 mg/mL for HCC-1937 cells), the cells were further cultured for 48 h. Thereafter, the cells were collected by trypsinization with EDTA-free trypsin, washed with ice-cold PBS three times, and fixed in 70% ice-cold ethanol for 12 h at 4°C. Subsequently, the cells were washed thrice with PBS and stained using a solution containing PI and RNase A for 30 min in the dark. The cell cycle distribution was determined using a flow cytometer (Beckman Coulter Epics XL, USA). Each experiment was performed in triplicate.

2.7. RNA Extraction and Real-Time RCR Analysis. After AME treatment, differences in the expression of genes in MDA-MB-453 were detected by real-time PCR assay. Total RNA was extracted from MDA-MB-453 cells after 48 h of treatment with AME (0 and 2.57 mg/mL) using TRIzol reagent (Ambion), according to the manufacturer's protocol. The cDNA synthesis reaction was done using 0.5 μg total RNA for each sample, using the cDNA SuperScript First-Strand Synthesis kit (Takara Biotechnology Co., Ltd.). Real-time PCR was performed using the SYBR Green PCR kit (Takara Biotechnology Co., Ltd.). qPCR mixture included the following: 10.0 μL SYBR Green Mix, 10 μL of 5 M forward and reverse primers, 1.0 μL template cDNA, and 8 μL ddH_2O. The reaction conditions were as follows: 95°C for 30 s, 40 cycles of denaturation at 95°C for 5 s, annealing at 65°C for 30 s, and extension at 72°C for 35 s. The sequences of the primers for the tested genes are presented in Table 1. GAPDH was used as the reference gene and the threshold cycle number (CT) was recorded for each reaction.

2.8. Gas Chromatography Mass Spectroscopy (GC-MS). GC-MS analysis was performed to determine the molecular composition of AME. The filtered AME was analysed using Agilent 6890 Gas Chromatograph with a 5975C Mass-selective Detector (Agilent, Palo Alto, CA, USA). The column used was

Table 1: Primer sequences used for real-time RCR analysis.

Gene	Forward primer	Reverse primer
GAPDH	5′-CCACTCCTCCACCTTTG-3′	5′-CACCACCCTGTTGCTGT-3′
GADD45A	5′-CGAGAACGACATCAACA-3′	5′-CGGCAAAAACAAATAAG-3′
CDC20	5′-TCTGGTCTCCCCATTACA-3′	5′-ATAGCCTCAGGGTCTCAT-3′
AURKB	5′-AGAGATGATTGAGGGGCG-3′	5′-GATTGAAGGGCAGAGGGA-3′
PLK1	5′-TAAGTCTCTGCTGCTC-3′	5′-ATAACTCGGTTTCGGT-3′
CCNB2	5′-CAACCCACCAAAACAACA-3′	5′-GCAAGGCATCAGAAAAAG-3′
TOP2A	5′-ATAGGAGCAGTGACGA-3′	5′-GGAAATGTGTAGCAGG-3′

ZB-5 MSI (30 m × 0.25 mm × 0.25 μm) and the mobile phase was 5% phenyl/95% dimethylpolysiloxane. Helium was used as the carrier gas at a constant flow rate of 1 mL/min. The initial oven temperature was 40°C and it was maintained at this temperature for 1.5 min; the temperature was gradually increased to 230°C at a rate of 4°C/min and was maintained for 8 min. The temperature of the injection port was 250°C and the flow rate of helium was 1 mL/min. The compounds discharged from the column were detected by a quadrupole mass detector. The ions were generated by electron ionization method. The temperatures of the MS quadrupole and source were 150 and 230°C, respectively, electron energy was 70 eV, temperature of the detector was 230°C, the emission current multiplier voltage was 1624 V, the interface temperature was 280°C, and the mass range was from 20 to 460 u. The relative mass fraction of each chemical component was determined by peak area normalization method. The National Institute Standard and Technology Library was used to analyse the spectrum and identify the compounds detected.

2.9. Data Analysis. All results were expressed as means ± SD. SPSS 18.0 software (IBM, Chicago, IL, USA) was used for one-way ANOVA to evaluate the significance of the differences between groups. A value of $P < 0.05$ was defined as significant.

3. Results

3.1. AME Inhibits the In Vitro Growth of MDA-MB-453 and HCC-1937 Cells. Morphological characterization of MDA-MB-453 and HCC-1937 cells was performed after treatment with AME. The extent of cell shrinkage at 48 h of treatment with different concentrations of the AME was evaluated by light microscopy. The results were compared with those obtained for untreated breast cancer cells. The MDA-MB-453 cells appeared to be more susceptible to AME; the most recognizable morphological changes in AME-treated MDA-MB-453 cells were cytoplasmic condensation and shrinkage of cell membrane (Figure 1(a)). In contrast, the HCC-1937 cells showed no distinct morphological changes upon treatment and only a decrease in the number of cells was observed (Figure 2(a)).

The results of viability assay for MDA-MB-453 and HCC-1937 cells treated with different concentrations (0.5, 1, or 1.5 mg/mL) of AME or DMSO (0.1%) for 48 h are shown in Figures 1(b) and 2(b). The viability of MDA-MB-453 cells at 0.5, 1, and 1.5 mg/mL doses was 96.39% ± 3.06%, 75.42% ± 1.40%, and 68.50% ± 3.65%, respectively (Figure 1(b)). The viability of HCC-1937 cells at 0.5, 1, and 1.5 mg/mL doses was 97.14% ± 0.65%, 91.61% ± 1.58%, and 82.96 ± 1.98%, respectively (Figure 2(b)). A significant reduction in the survival of both the cell lines was observed at 1 and 1.5 mg/mL doses. The results revealed that AME reduced the survival of both the cells in a concentration-dependent manner ($P < 0.01$), although MDA-MB-453 (IC50 = 2.57 mg/mL) was more sensitive than HCC-1937 cells (IC50 = 3.64 mg/mL).

3.2. AME Induces S-Phase Arrest of MDA-MB-453 and HCC-1937 Cells. To investigate the factors contributing to the growth inhibition of MDA-MB-453 and HCC-1937 cells, we studied the effect of AME on cell cycle distribution in both the cell lines. We found that treatments of both the cell lines with AME resulted in cell cycle arrest in the S-phase (Figure 3). For MDA-MB-453 cells, the percentage of cells in the S-phase increased from 2.83% for untreated cells to 17.13% for cells treated with 2.57 mg/mL AME (Figure 3(a)). For HCC-1937 cells, the percentage of cells in the S-phase increased from 10.43% to 21.40% for cells treated with 3.64 mg/mL AME (Figure 3(b)). The increase in the percentage of cells in the S-phase also caused a significant reduction in the percentage of cells in the G1-phase (Figure 3).

3.3. AME Downregulates the Expression of CDC20, AURKB, PLK1, CCNB2, and TOP2A mRNAs. The relative expression levels of target genes modulated by AME were determined by qPCR assay. As shown in Figure 4, AME could significantly downregulate the expression of *CDC20*, *AURKB*, *PLK1*, *CCNB2*, and *TOP2A* mRNAs ($P < 0.01$) and upregulated the expression of *GADD45A* mRNA ($P < 0.05$) in MDA-MB-453 cells compared to the expression levels of the respective genes in the untreated group (Figure 4).

3.4. GC-MS Analysis of A. chinensis Extracts. The GC-MS analysis was performed to determine the presence of potential anticancer or medicinally important compounds in the *A. chinensis* extract. A total of 16 compounds were identified (Figure 5), among which seven were esters, based on their peak area, retention time, and molecular formula. These esters were of oleic acid (25.39%), palmitic acid (21.798%), z-11-hexadecenoic acid (8.08%), threitol (6.74%),

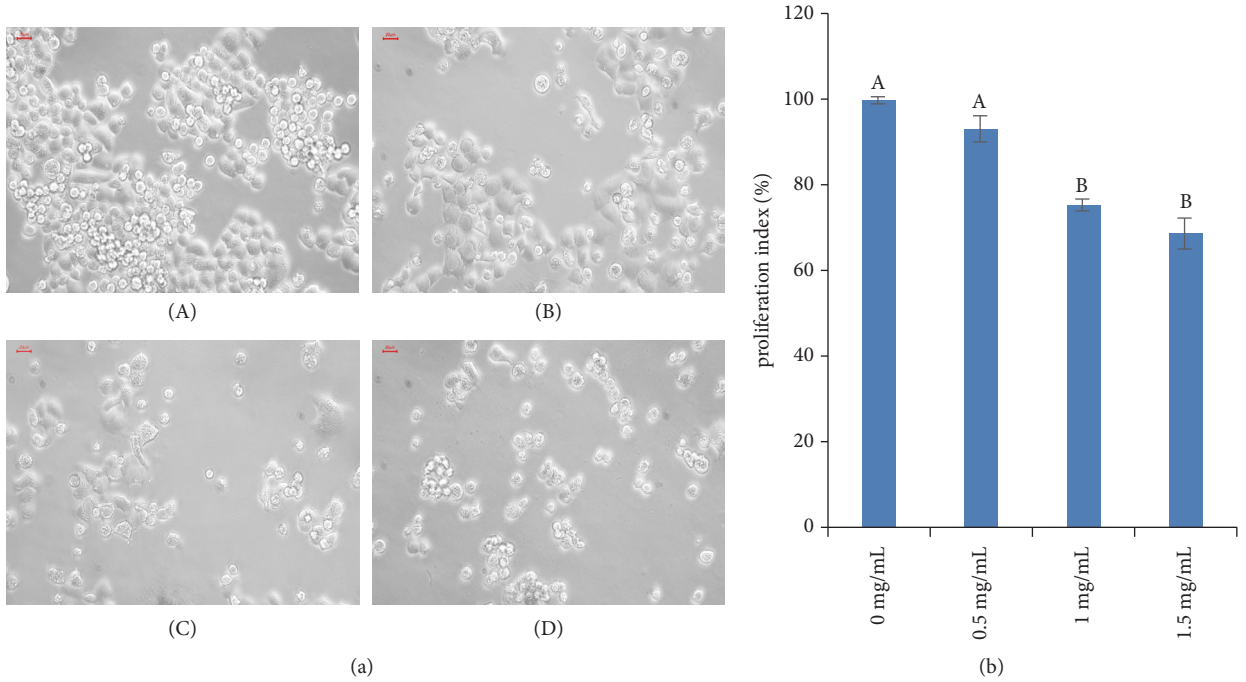

Figure 1: Effect of *Aspongopus chinensis* methanol extract (AME) on the proliferation of breast cancer MDA-MB-453 cells. (a) Morphologic characterization of MDA-MB-453 cells treated with different concentrations of AME (0, 0.5, 1, or 1.5 mg/mL (A-D), respectively; 200×). (b) Viability of MDA-MB-453 cells treated with 0 (control), 0.5, 1, or 1.5 mg/mL AME. Values are presented as the mean ± SD of five independent experiments. Different upper case letters indicate significant difference between groups (Fisher's LSD, $P<0.01$).

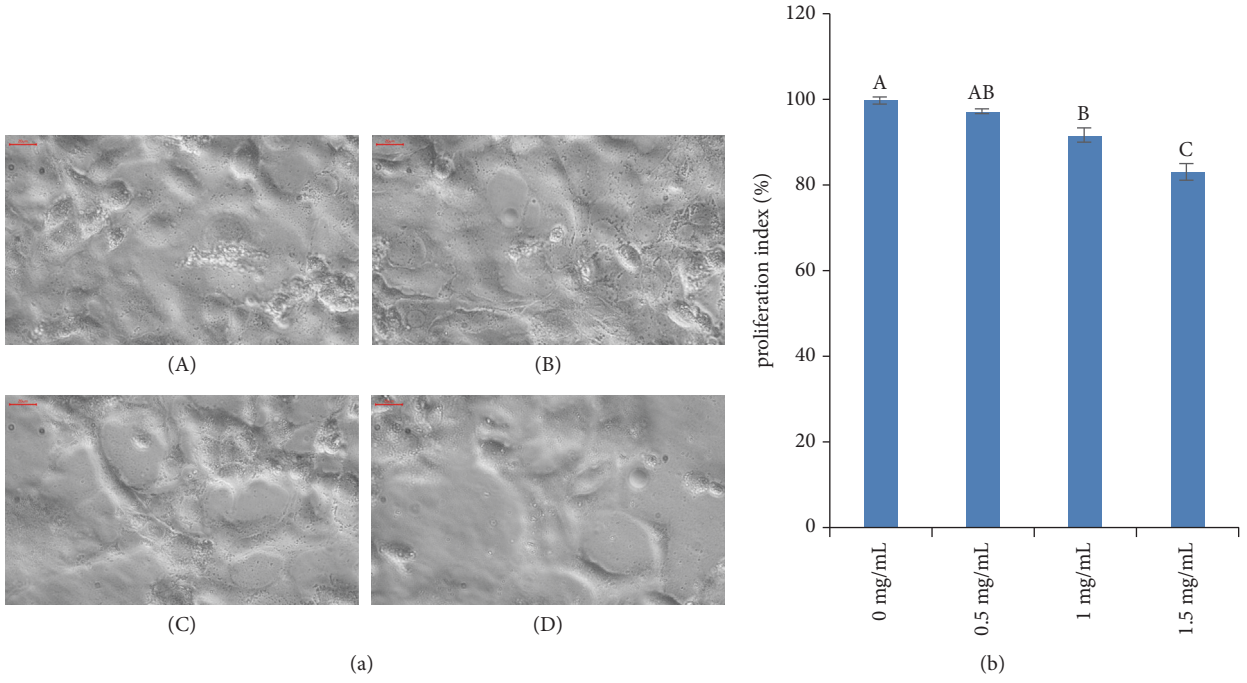

Figure 2: Effect of *Aspongopus chinensis* methanol extract (AME) on the proliferation of breast cancer HCC-1937 cells. (a) Morphologic characterization of HCC-1937 cells treated with different concentrations of AME (0, 0.5, 1, or 1.5 mg/mL (A-D), respectively; 400×). (b) Viability of HCC-1937 cells treated with 0 (control), 0.5, 1, or 1.5 mg/mL AME. Values are presented as the mean ± SD of five independent experiments. Different upper case letters indicate significant difference between groups (Fisher's LSD, $P<0.01$).

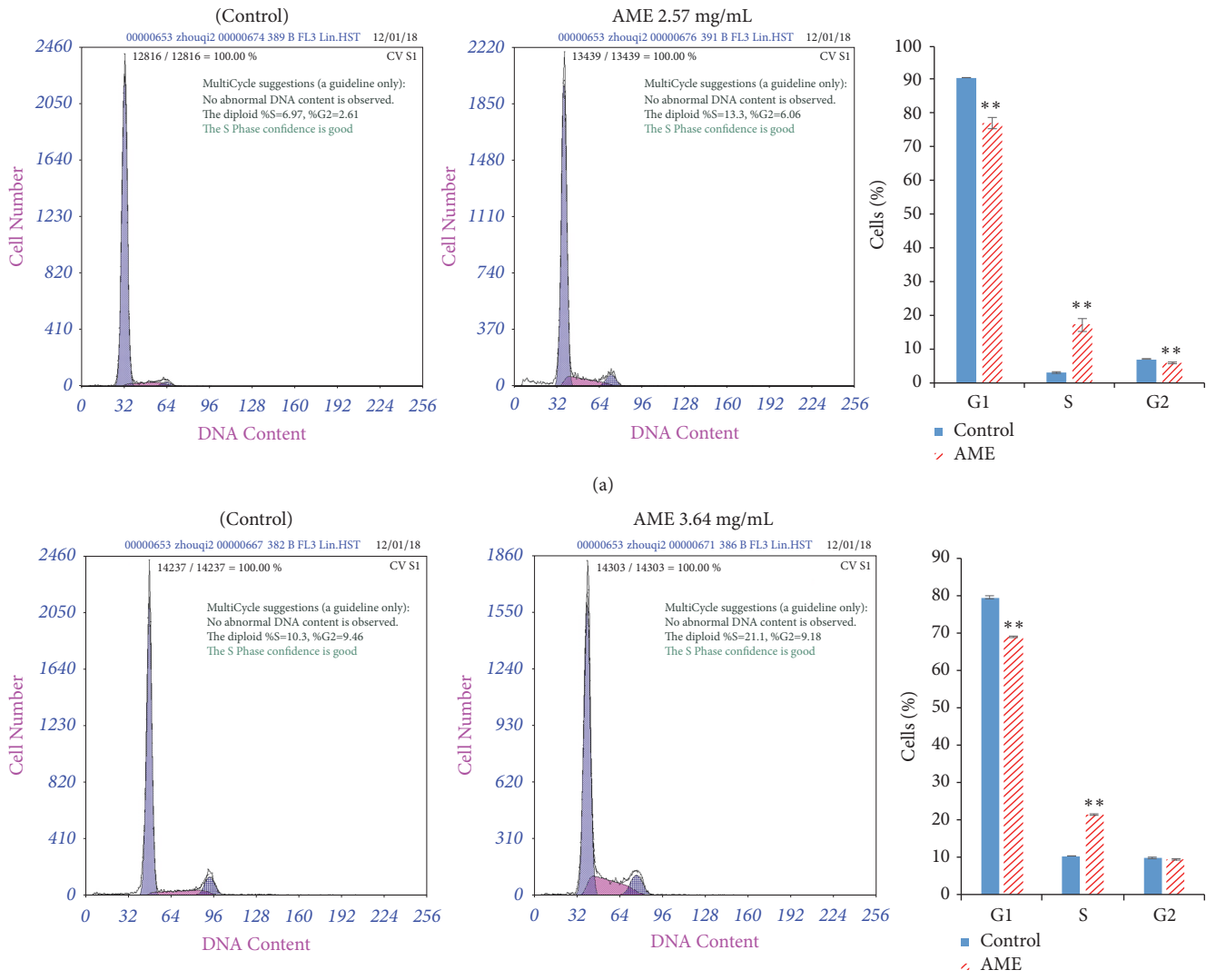

Figure 3: Cell cycle arrest in the S-phase in MDA-MB-453 and HCC-1937 cells treated with *Aspongopus chinensis* methanol extract (AME). (a) MDA-MB-453 cells were treated with 2.57 mg/mL AME for 48 h; (b) HCC-1937 cells were treated with 3.64 mg/mL AME for 48 h. Data are representative of three independent experiments. $^{**}P < 0.01$.

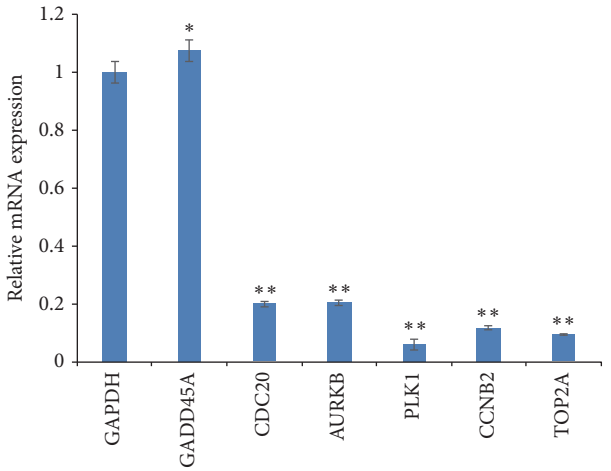

Figure 4: Relative mRNA expression of target genes in MDA-MB-453 cells treated with AME at 2.57 mg/mL for 48 h. Data are representative of three independent experiments. $^{**}P < 0.01$; $^{*}P < 0.05$.

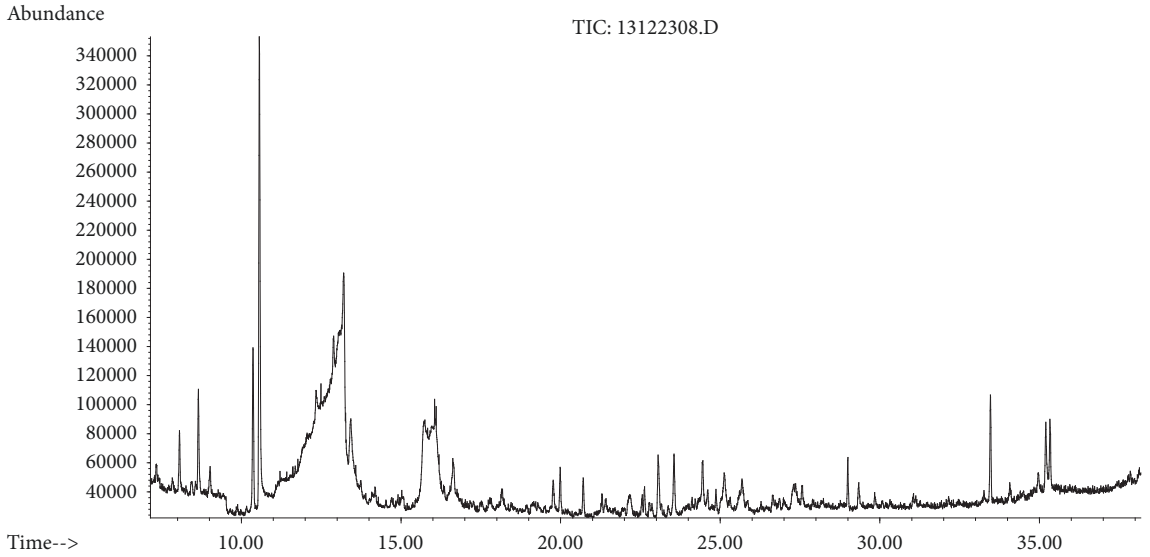

Figure 5: GC-MS chromatogram of compounds presents in the methanol extract of *Aspongopus chinensis* Dallas.

Table 2: Compounds detected by GC-MS analysis of methanol extracts from *Aspongopus chinensis* Dallas.

Sample NO.	RT (min)	Name of compounds	MF	CS	MW	Area (%)
1	38.678	oleic acid	$C_{18}H_{34}O_2$		282.461	25.39
2	35.348	palmitic acid	$C_{16}H_{32}O_2$		256.424	21.798
3	34.924	z-11-Hexadecenoic acid	$C_{16}H_{30}O_2$		254.408	8.077
4	37.327	threitol, acetylated	$C_{12}H_{18}O_8$		290.267	6.739
5	39.008	Stearic acid	$C_{18}H_{36}O_2$		284.477	3.036
6	11.745	2-Hexenoic acid	$C_6H_{10}O_2$		114.142	2.491
7	45.873	1-(14-methylhexadecanoyl) pyrrolidine	$C_{21}H_{41}NO$		323.556	0.344

RT, retention time; MF, molecular formula; CS, chemical structure; MW, molecular weight. The chemical structure was made using the National Institute of Standard and Technology (NIST) Library.

stearic acid (3.04%), 2-hexenoic acid (2.49%), and 1-(14-methylhexadecanoyl) pyrrolidine (0.34%) (Table 2); the percentage content of fatty acids in AME was 61.337%. The oleic acid and palmitic acid were determined to be the major compounds present in the *A. chinensis* extracts, and these have medically important functions (Table 2). Oleic acid is a fatty acid found in animal and vegetable oils; it is the major component of olive oil responsible for a healthy Mediterranean diet, and is especially effective for the prevention of breast cancer [17]. Palmitic acid, one of the most common saturated fatty acids in animals and plants, has been reported to induce apoptosis in exocrine pancreatic AR42J cells [18].

4. Discussion

Breast cancer is a major public health problem worldwide [1]. The traditional methods for breast cancer treatment mainly

include surgery, chemotherapy, radiotherapy, and drug therapy. Among these, surgery is the preferred method. However, because of its high recurrence and metastasis rate, surgical resection of solid tumours is unable to achieve a radical effect. Chemotherapy and radiotherapy can cause vomiting, baldness, thrombocytopenia, and other adverse reactions. Therefore, searching for noncytotoxic anticancer drugs is an important area of research [4]. *A. chinensis* has been used as a TCM and has been shown to have good clinical anticancer effects in China. Previous investigations have shown that *A. chinensis* possess anticancer, anticoagulant, and antibacterial effects [6]. However, the anticancer active ingredients present in it have remained undiscovered.

In recent years, a lot of attention has been given to the isolation of natural products from *A. chinensis* [5, 19–21]. Four kinds of small molecules extracted from *A. chinensis* (a new oxazole and three known N-acetyldopamines) have been identified and were proven to inhibit the proliferation of cancer cells *in vitro* [22]. In a previous study, we determined that the content of proteins and fatty acids in *A. chinensis* were 23.68% and 27.72%, respectively, and unsaturated fatty acids occupied about 64.03% of the total fatty acid content. Our studies further showed that the proteins extracted from *A. chinensis* could inhibit the proliferation of SGC-7901 and MCF-7 cells [5, 13–16]. However, there is not much information on the effects of fatty acids present in *A. chinensis*.

Fatty acids are components of cell membranes. Altering the components of fatty acids in the membrane can inhibit DNA synthesis in cancer cells [23]. In the present study, oleic acid and palmitic acid were found to be the main compounds in the AME (Table 2). In recent years, palmitic acid has attracted wide attention because of its therapeutic roles in some chronic diseases, such as metabolic syndrome, diabetes, and inflammation [24]. Byberg *et al*. analysed the ratio of fatty acids in the blood of Swedish cancer population; the results showed that the imbalance of palmitic and palmitoleic acid metabolism would result in the death of cancer cells [25]. Unsaturated fatty acids have inhibitory effects on the occurrence, growth, metastasis, and proliferation of tumour cells [26, 27]. In the present study, we determined that the percentage content of fatty acids in AME was 61.337%. Moreover, we observed that AME could inhibit the proliferation of MDA-MB-453 and HCC-1937 cells (Figures 1 and 2). The proliferation of treated cells was reduced in a dose-dependent manner ($P < 0.01$); however, MDA-MB-453 (IC50 = 2.57 mg/mL) cells were more sensitive than HCC-1937 (IC50 = 3.64 mg/mL) cells. The MDA-MB-453 cells are HER-2 positive, and the overexpression of HER2/neu is associated with tumour classification and poor prognosis [28]. Moreover, oleic acid is reported to inhibit the HER-2/neu overexpression and promote apoptosis [17].

The regulation of cell cycle is very important for cell growth [29]. In the present study, we found that treatment of MDA-MB-453 and HCC-1937 cells with AME resulted in cell cycle arrest in the S-phase (Figure 3). Similar results have been reported for Berberine, Tanshinone I, and the ethanol extracts of *Ganoderma lucidum,* which could inhibit the proliferation of breast cancer MCF-7 cells and induce cell cycle arrest [30–32]. Elm Indican II and Berberine could inhibit the proliferation of breast cancer cells and induce cell cycle arrest in the G0/G1 and S-phase [33, 34]. Based on the results of these studies and our findings in the present study, we speculate that TCM may contain components that can induce cell cycle arrest in breast cancer cells. In addition, the expression levels of *CDC20, AURKB, PLK1, CCNB2*, and *TOP2A* were found to be downregulated by AME (Figure 4). CDC20 is a cell cycle protein and its overexpression can promote the proliferation and inhibit the apoptosis of cancer cells [35]. PLK1 is highly expressed in tumour cells [36] and is involved in almost all the processes of mitosis [37]. PLK1 can inhibit the activity of anaphase promoting complex by phosphorylating CDC20, which can promote cytokinesis. The inhibition of the activity of PLK1 can prevent cells from completing mitosis and eventually leads to cell death [38]. AURK family proteins are highly expressed in tumour cells, and their inhibition can decrease the proliferation of tumour cells [39]. CCNB2 is a cell cycle protein, which is highly expressed in cancer tissues [40]. TOP2A is a target of anticancer drugs; its downregulation can inhibit chromosome aggregation and assembly [41]. In the present study, we found that AME can cause S-phase arrest of breast cancer cells, downregulate the expression of *CDC20*, *AURKB*, *PLK1*, *CCNB2*, and *TOP2A*, and upregulate the expression of *GADD45A*, eventually inhibiting the proliferation of breast cancer cells. Although *A. chinensis* has been used as a TCM for hundreds of years in China and the long-term clinical application suggests its anticancer effects [8, 10], several questions about the ingredients with anticancer properties remain unanswered. The present study is important as a first step in screening the anticancer activity of methanol extract of *A. chinensis.* We further intend to isolate these active ingredients and decipher their anticancer mechanisms.

In conclusion, the methanolic extract of *A. chinensis* can inhibit the proliferation of MDA-MB-453 and HCC-1937 cells by inducing cell cycle arrest; the oleic acid and palmitic acid were found to be the main compounds in AME. These results suggest that AME can be a potential natural alternative or can provide a complementary therapy for breast cancer. Further evaluation of the anticancer properties of AME *in vivo* is needed to ensure its efficacy and long-term safety.

Data Availability

The data used to support the findings of this study are available from the corresponding author upon request.

Conflicts of Interest

The authors declare that they have no conflicts of interest.

Authors' Contributions

Jianjun Guo, Rui Luo, and Jun Tan participated in the study design. Jun Tan, Ying Tian, and Renlian Cai participated in the experimental work; Jun Tan wrote the paper. Jianjun Guo and Rui Luo critically revised the manuscript. Jun Tan and Ying Tian contributed equally to this work.

Acknowledgments

This work was supported by the National Natural Science Foundation of China (81803968; 81360612); Special Funds for Excellent Young Scientific Talent in Guizhou ([2015]25); the Master's Start-Up Foundation of Zunyi Medical University (F-672); Graduate Education Innovation Project of Guizhou Province (Qian Jiao He YJSCXJH, no. (2018)044).

References

[1] E. Gupta, S. Kaushik, S. Purwar, R. Sharma, A. K. Balapure, and S. Sundaram, "Anticancer potential of steviol in MCF-7 human breast cancer cells," *Pharmacognosy Magazine*, vol. 13, no. 51, pp. 345–350, 2017.

[2] R. L. Siegel, K. D. Miller, and A. Jemal, "Cancer statistics, 2018," *CA: A Cancer Journal for Clinicians*, vol. 68, no. 1, pp. 7–30, 2018.

[3] Y. Zheng, C. X. Wu, and M. L. Zhang, "The epidemic and characteristics of female breast cancer in China," *China Oncology*, vol. 23, no. 8, pp. 561–569, 2013.

[4] M. Trendowski, "Recent advances in the development of antineoplastic agents derived from natural products," *Drugs*, vol. 75, no. 17, pp. 1993–2016, 2015.

[5] J. Tan, Y. Tian, R. L. Cai et al., "Antiproliferative and proapoptotic effects of a protein component purified from *Aspongopus chinensis* Dallas on cancer cells *in vitro* and *in vivo*," *Evidence-Based Complementary and Alternative Medicine*, vol. 2019, Article ID 8934794, 12 pages, 2019.

[6] L. Zhang and J. J. Guo, "Review on research and application on the resource of *Aspongopus chinensis* Dallas," *Journal of Southwest China Normal University (Natural Science)*, vol. 1, no. 5, pp. 151–155, 2011.

[7] M. L. Wu and D. C. Jin, "The antibacterial activity of the haemolymph and the purified haemo-protein from *Asporgopus chinesis*," *Chinese Bulletin of Entomology*, vol. 42, pp. 315–318, 2005.

[8] B. Xu, G.-H. Zhu, J.-T. Xia, and S. H. Li, "Influence of Chinese herb aitongke on the proliferation, apoptosis and Rb gene expression of hepatoma carcinoma cells HepG2," *Journal of Clinical Rehabilitative Tissue Engineering Research*, vol. 11, no. 12, pp. 2253–2256, 2007.

[9] Y. Gao, J. W. Chen, P. Li et al., "Study on the effects of blood anticoagulation from *Aspongopus chinensis* Dallas," *Research and Practice of Chinese Medicines*, vol. 24, pp. 34–36, 2010.

[10] Q. J. Yang, L. W. Lei, X. X. Pang et al., "Study on apoptosis of human gastric cancer cells induced by Xianglong powder (containing serum)," *Journal of Hubei College of Traditional Chinese Medicine*, vol. 1, no. 1, pp. 43–45, 1999.

[11] Q. Fan, H. Wei, H. B. Cai et al., "Effects of the serum containing Aspongopus chinensis Dallas on the expression of SW480 apoptosis-associated factors, FADD and p53," *Journal of Anhui Agriculture Science*, vol. 39, no. 13, pp. 7828–7831, 2011.

[12] M. L. Cao, Y. F. Wu, and J. J. Guo, "Effect of Aspongopus chinesis Dallas by different treatments on human gastric cancer SGC-7901 cells in vitro and its antitumor component distribution," *Biotic Resources*, vol. 39, pp. 328–332, 2017.

[13] J. Tan, J. J. Guo, C. Wei et al., "The inhibitory effects of haemolymph from Aspongopus chinensis Dallas on in vitro proliferation of gastric carcinoma cell SGC -7901," *Journal of Mountain Agriculture and Biology*, vol. 32, no. 2, pp. 119–122, 2013.

[14] R. L. Cai, J. Tan, D. T. Fan et al., "Research on medicinal and edible value of Aspongopus chinensis Dallas after being novelly processed," *Journal of Zunyi Medical University*, vol. 39, no. 4, pp. 345–349, 2016.

[15] J. Q. Yang, J. Tan, M. L. Cao et al., "The inhibitory effect of haemolymph from Aspongopus chinensis Dallas on growth of human breast cancer MCF-7 by CCK-8," *Journal of Environmental Entomology*, vol. 39, no. 1, pp. 193–197, 2017.

[16] J. Q. Yang, J. L. Long, J. Tan et al., "Effects of haemolymph of Aspongopus chinensis Dallas on the expression of apoptosis related proteins in tumour cells," *Biotic Resources*, vol. 39, no. 5, pp. 360–365, 2017.

[17] D. T. Win, "Oleic acid-The anti-breast cancer component in olive oil," *AU Journal of Technology*, vol. 9, no. 2, pp. 75–78, 2005.

[18] J. H. Ahn, M. H. Kim, H. J. Kwon, S. Y. Choi, and H. Y. Kwon, "Protective effects of oleic acid against palmitic acid-induced apoptosis in pancreatic AR42J cells and its mechanisms," *Korean Journal of Physiology & Pharmacology*, vol. 17, no. 1, pp. 43–50, 2013.

[19] Y. N. Shi, Z. C. Tu, X. L. Wang et al., "Bioactive compounds from the insect Aspongopus chinensis," *Bioorganic & Medicinal Chemistry Letters*, vol. 24, no. 22, pp. 5164–5169, 2014.

[20] Y. M. Yan, J. Ai, Y. N. Shi et al., "(±)-Aspongamide A, an N-acetyldopamine trimer isolated from the insect Aspongopus chinensis, is an inhibitor of p-Smad3," *Organic Letters*, vol. 16, no. 2, pp. 532–535, 2014.

[21] L. Di, Y. N. Shi, Y. M. Yan et al., "Nonpeptide small molecules from the insect Aspongopus chinensis and their neural stem cell proliferation stimulating properties," *RSC Advances*, vol. 5, no. 87, pp. 70985–70991, 2015.

[22] X.-W. Lu and Y. Wu, "On the structure of aspongopusin recently isolated from *Aspongopus chinensis*," *Fitoterapia*, vol. 84, no. 1, pp. 318–320, 2013.

[23] C. desBordes and M. A. Lea, "Effects of C18 fatty acid isomers on DNA synthesis in hepatoma and breast cancer cells," *Anticancer Research*, vol. 15, no. 5B, pp. 2017–2021, 1995.

[24] H. Cao, K. Gerhold, J. R. Mayers, M. M. Wiest, S. M. Watkins, and G. S. Hotamisligil, "Identification of a lipokine , a lipid hormone linking adipose tissue to systemic metabolism," *Cell*, vol. 134, no. 6, pp. 933–944, 2008.

[25] L. Byberg, L. Kilander, E. W. Lemming, K. Michaëlsson, and B. Vessby, "Cancer death is related to high palmitoleic acid in serum and to polymorphisms in the SCD-1 gene in healthy Swedish men," *American Journal of Clinical Nutrition*, vol. 99, no. 3, pp. 551–558, 2014.

[26] M. Noguchi, D. P. Rose, M. Earashi, and I. Miyazaki, "The role of fatty acids and eicosanoid synthesis inhibitors in breast carcinoma," *Oncology*, vol. 52, no. 4, pp. 265–271, 1995.

[27] J. Hofmanová, N. Straková, A. H. Vaculová et al., "Interaction of dietary fatty acids with tumour necrosis factor family cytokines during colon inflammation and cancer," *Mediators of Inflammation*, vol. 2014, Article ID 848632, 17 pages, 2014.

[28] T.-D. Way, M.-C. Kao, and J.-K. Lin, "Apigenin induces apoptosis through proteasomal degradation of HER2/neu in HER2/neu-overexpressing breast cancer cells via the phosphatidylinositol 3-kinase/Akt-dependent pathway," *The Journal of Biological Chemistry*, vol. 279, no. 6, pp. 4479–4489, 2004.

[29] R. Agami and R. Bernards, "Distinct initiation and maintenance mechanisms cooperate to induce G1 cell cycle arrest in response to DNA damage," *Cell*, vol. 102, no. 1, pp. 55–66, 2000.

[30] G. Wu, Z. Qian, J. Guo et al., "Ganoderma lucidum extract induces G1 cell cycle arrest, and apoptosis in human breast cancer cells," *American Journal of Chinese Medicine*, vol. 40, no. 3, pp. 631–642, 2012.

[31] L. Wang, J. Wu, J. Lu, R. Ma, D. Sun, and J. Tang, "Regulation of the cell cycle and PI3K/Akt/mTOR signaling pathway by tanshinone I in human breast cancer cell lines," *Molecular Medicine Reports*, vol. 11, no. 2, pp. 931–939, 2015.

[32] E. Barzegar, S. Fouladdel, T. K. Movahhed et al., "Effects of berberine on proliferation, cell cycle distribution and apoptosis of human breast cancer T47D and MCF7 cell lines," *Iranian Journal of Basic Medical Sciences*, vol. 18, no. 4, pp. 334–342, 2015.

[33] X. Zhu, K. Wang, K. Zhang et al., "Ziyuglycoside II inhibits the growth of human breast carcinoma MDA-MB-435 cells via cell cycle arrest and induction of apoptosis through the mitochondria dependent pathway," *International Journal of Molecular Sciences*, vol. 14, no. 9, pp. 18041–18055, 2013.

[34] J. B. Kim, J. H. Yu, E. Ko et al., "The alkaloid berberine inhibits the growth of anoikis-resistant MCF-7 and MDA-MB-231 breast cancer cell lines by inducing cell cycle arrest," *Phytomedicine*, vol. 17, no. 6, pp. 436–440, 2010.

[35] M. F. Gayyed, N. M. R. A. El-Maqsoud, E. R. Tawfiek, S. A. A. El Gelany, and M. F. A. Rahman, "A comprehensive analysis of CDC20 overexpression in common malignant tumors from multiple organs: its correlation with tumor grade and stage," *Tumor Biology*, vol. 37, no. 1, pp. 749–762, 2016.

[36] B. T. Gjertsen and P. Schöffski, "Discovery and development of the Polo-like kinase inhibitor volasertib in cancer therapy," *Leukemia*, vol. 29, no. 1, pp. 11–19, 2015.

[37] D. Yan and T. Lampkin, "Targeting polo-like kinase in cancer therapy," *Clinical Cancer Research*, vol. 16, no. 2, pp. 384–389, 2010.

[38] J.-E. Park, N.-K. Soung, Y. Johmura et al., "Polo-box domain: a versatile mediator of polo-like kinase function," *Cellular and Molecular Life Sciences*, vol. 67, no. 12, pp. 1957–1970, 2010.

[39] G. Bertolin, F. Sizaire, G. Herbomel, D. Reboutier, C. Prigent, and M. Tramier, "A FRET biosensor reveals spatiotemporal activation and functions of aurora kinase A in living cells," *Nature Communications*, vol. 7, Article ID 12674, p. 16, 2016.

[40] D. Stav, I. Bar, J. Sandbank et al., "Usefulness of CDK5RAP3, CCNB2, and RAGE genes for the diagnosis of lung adenocarcinoma," *The International Journal of Biological Markers*, vol. 22, no. 2, pp. 108–113, 2007.

[41] R. Tubbs, W. E. Barlow, G. T. Budd et al., "Outcome of patients with early-stage breast cancer treated with doxorubicin-based adjuvant chemotherapy as a function of HER2 and TOP2A status," *Journal of Clinical Oncology*, vol. 27, no. 24, pp. 3881–3886, 2009.

Hindawi
Evidence-Based Complementary and Alternative Medicine
Volume 2019, Article ID 7824146, 12 pages
https://doi.org/10.1155/2019/7824146

Research Article

Analytical Method Validation of Gamijakyakgamchobuja-Tang (KCHO-1, Mecasin) Preparation

Tingting Wang,[1] **Seongjin Lee**,[1,2] **Muhack Yang**,[1,2] **Eunhye Cha**,[1,2] **Jongwon Jang**,[1,2] **and Sungchul Kim**[1,2]

[1]*Department of Acupuncture & Moxibustion Medicine, Wonkwang University Gwangju Korean Medicine Hospital, Gwangju 61729, Republic of Korea*
[2]*Nervous & Muscular System Disease Clinical Research Center of Wonkwang University Gwangju Korean Medical Hospital, Gwangju 61729, Republic of Korea*

Correspondence should be addressed to Sungchul Kim; kscndl@hanmail.net

Received 6 January 2019; Accepted 24 April 2019; Published 22 May 2019

Guest Editor: Irawan W. Kusuma

Previous studies have confirmed that KCHO-1 (Mecasin) was developed to alleviate the symptoms of Amyotrophic Lateral Sclerosis (ALS). And its toxicity test has also been carried out. The aim of this study is confirming the validation and stability of concentration analysis method of the Mecasin preparations using HPLC. As a conclusion, we found that the preparations at the concentrations of 50mg/ml and 200mg/ml in sterilized distilled water were homogeneous and it was stable for 4 hours at room temperature and 7 days refrigerated condition (2~8°C). And this method for analyzing the concentration of the Mecasin preparations has been found to be suitable. This study is helpful to promote development of reliable manufacturing medicine and good researches through definitive quality control of Mecasin as complex herbal medicine, aiming to provide help for the treatment of ALS.

1. Introduction

Gamijakyakgamchobuja-tang (KCHO-1, Mecasin) is a new prescription reported to have anti-inflammatory and antioxidant properties [1]. The constituents of Mecasin are Radix Paeoniae Alba, Radix Glycyrrhizae, Radix Aconiti Lateralis Preparata, Radix Salviae Miltiorrhizae, Rhizoma Gastrodiae, Radix Polygalae, Curcuma Root, Fructus Chaenomelis, and Rhizoma Atractylodis Japonicae (Table 1) [2]. This medicine has been used mainly for alleviating pain, muscle spasms, and cold syndrome due to blood deficiency for centuries in traditional oriental medicine [3]. In recent years of medical research, we have found that it has a role in reducing pain, GABA neuron regeneration and NO reduction in neuropathic pain rats [1], antiseizure, analgesic, antipyretic, anti-inflammatory, and antiulcer effects, suppressing the progress of osteoarthritis, neuroprotective, and antineuroinflammatory effects and safety in both in vitro and in vivo trials [4–12]. More concretely, in the first mechanism of action of Mecasin, KCHO-1 increases cellular resistance to glutamate or H2O2-induced oxidative injury in HT22 cells, presumably through ERK and p38 pathways and Nrf2/ARE-dependent HO-1 expression (Figure 1) [2]. And in the second mechanism of action of Mecasin, KCHO-1 upregulated HO-1 expression by promoting the nuclear translocation of Nrf2 in mouse BV2 microglia, and it suppressed the production of proinflammatory mediators and cytokines through suppression of IκB-α phosphorylation and degradation and NF-κB nuclear translocation in LPS-stimulated microglia (Figure 2) [2, 7].

In addition, several studies have been conducted on the compositions of KCHO-1 and its toxicity. Now it is time to advance the study of KCHO-1, and the ultimate goal is to apply it to the clinic to help the treatment of ALS. And for quality control of Mecasin, confirming the validation and stability of concentration analysis method of the Mecasin preparations has become a major issue. We could promote development of reliable manufacturing medicine and good researches through definitive quality control of Mecasin as

Table 1: The constituents of Mecasin.

	Scientific Names	Parts
1	*Curcuma longa*	Radix
2	*Salvia miltiorrhiza*	Radix
3	*Gastrodia elata*	Rhizoma
4	*Pseudocydonia sinensis*	Fructus
5	*Paeonia lactiflora*	Radix
6	*Polygala tenuifolia*	Radix
7	*Glycyrrhiza uralensis*	Radix
8	*Atractylodes japonica*	Rhizoma
9	*Aconitum carmichaeli*	Radix Preparata

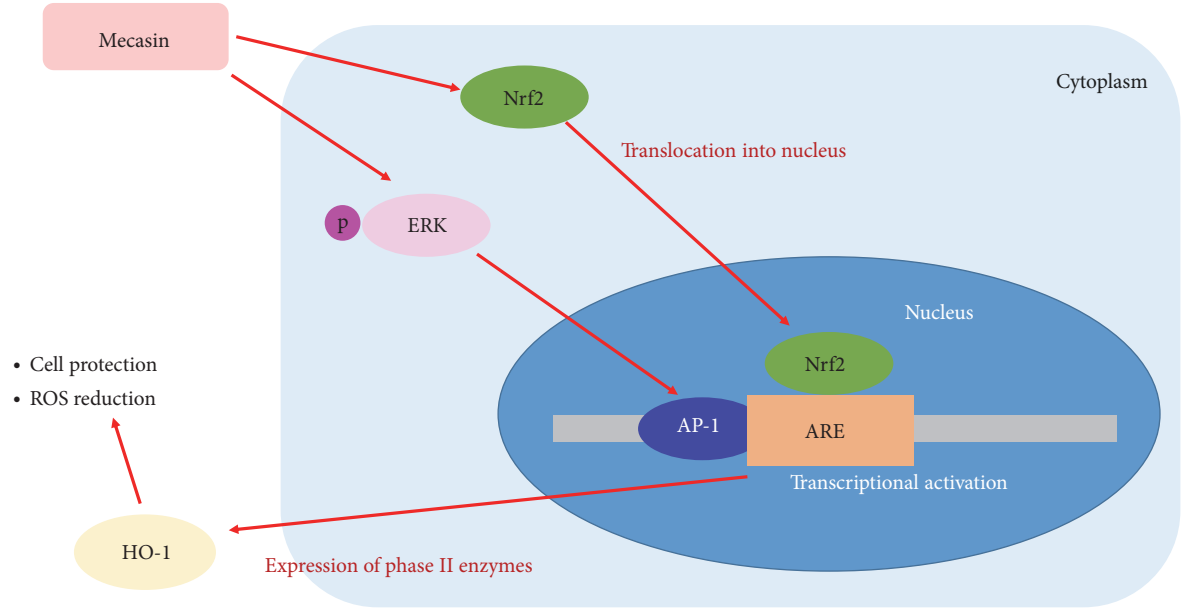

Figure 1: 1st mechanism of action of Mecasin.

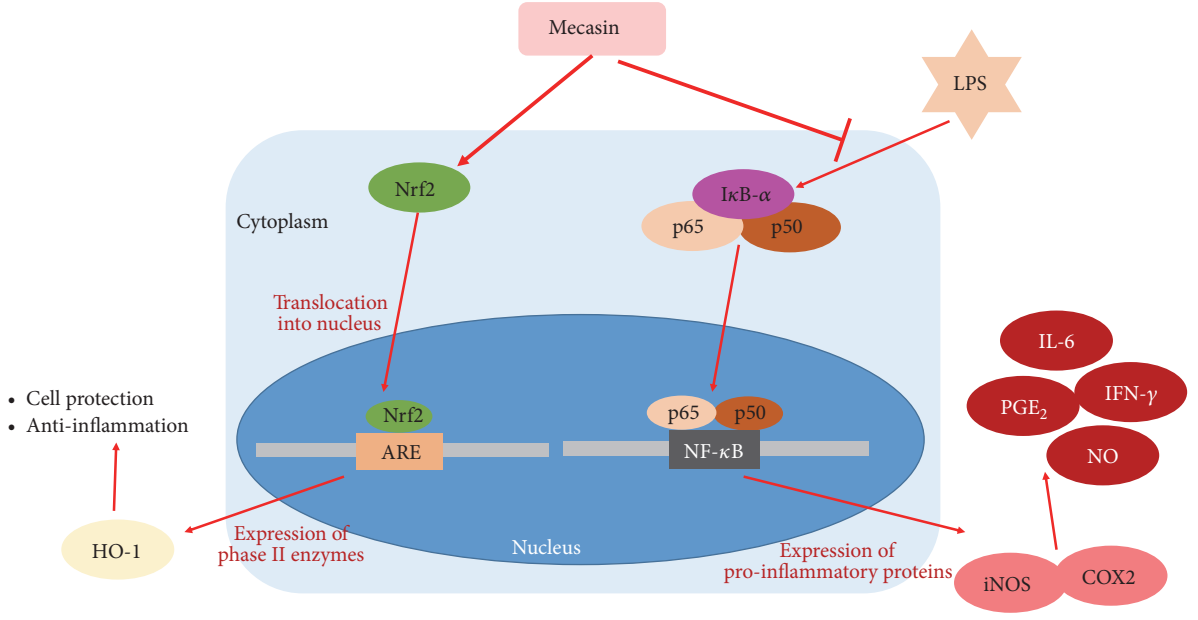

Figure 2: 2nd mechanism of action of Mecasin.

Table 2: Analytical conditions of KCHO-1 using HPLC.

	Time (min)	Water (%)	Acetonitrile (%)
Mobile phase	0	90	10
	30	90	10
	70	13	87
	72	13	87
	73	90	10
	85	90	10
Flow rate	1.0 mL/min		
Injection volume	20 μL		
Column	CAPCELLPAK 5 C18, 250 × 2.6 mm, 5 μm		
Column oven temperature	40°C		
Detector wavelength (PDA)	254 (Glycyrrhizic acid), 280 (Salvianolic acid B), 420 (Curcumin) nm		
Run time	85 min		

complex herbal medicine by the validation and stability studies.

The experiments for this research were conducted at the Korea Testing & Research Institute (KTR), an institution authorized to perform nonclinical studies under the GLP regulations.

2. Materials and Methods

2.1. Analytical Method Validation

(1) Test Article and Vehicle Control. The test article was KCHO-1, which was provided by the Nervous & Muscular System Disease Clinical Research Center of Wonkwang University Gwang-ju Korean Medicine Hospital and stored at room temperature (1~30°C). The vehicle control was sterilized distilled water manufactured by Korean Sci. Standard substances were Curcumin, Glycyrrhizic Acid, and Salvianolic Acid B. All were provided by ChromaDex, with assay of 97.7, 93.3, and 96.7%, respectively.

(2) Reagents and Equipment. The reagents were acetonitrile, purified water, methanol, ethanol (Burdick and Jackson, USA). Balance (KG-EQM-042) and micropipette (KG-EQM-359) were used as equipment. Shimadzu HPLC (KG-EQM-352(8)) was used as the analytical instrument and the analysis conditions were as follows (Table 2).

(3) Preparation of Solvents and Methods

(i) Mobile Phase

A line: water

B line: acetonitrile

The mobile phase was used within 7 days.

(ii) Diluent. Ethanol: methanol (50:50, v/v) was used as diluent solvent.

(iii) Standard Solution

(a) Curcumin. 20mg of the standard substance was weighed and placed in a 10mL volumetric flask, and diluted solvent was added to the line. This was used as a stock solution. The stock solution was diluted to 1, 5, 10, 50, and 100μg/mL with dilution solvent and used as a standard solution.

(b) Glycyrrhizic Acid. 20mg of the standard substance was weighed and placed in a 10mL volumetric flask, and diluted solvent was added to the line. This was used as a stock solution. The stock solution was diluted to 5, 25, 50, 250, and 500μg/mL with dilution solvent and used as a standard solution.

(c) Salvianolic Acid B. 20mg of the standard substance was weighed and placed in a 10mL volumetric flask, and diluted solvent was added to the line. This was used as a stock solution. The stock solution was diluted to 5, 25, 50, 250, and 500μg/mL with dilution solvent and used as a standard solution.

(4) QC Sample

(a) Curcumin. A 50μg/mL concentration of the standard solution was used.

(b) Glycyrrhizic Acid. A 250μg/mL concentration of the standard solution was used.

(c) Salvianolic Acid B. A 250μg/mL concentration of the standard solution was used.

(5) Preparation of Test Article and Treatment of Preparation. 1500 mg and 6000 mg of the test article were weighed and added with a vehicle (sterilized distilled water), shaken, and adjusted to 30mL. Concentrations of preparations for homogeneity and stability tests were 50mg/mL and 200mg/mL. 1mL of the preparation at a concentration of 50mg/mL and 200mg/mL was diluted with a diluting solvent and injected in 20 mL each into HPLC within the calibration curve range.

(6) Quantitation. The quantitative value of the preparation was calculated by the following equation after substituting the

peak area of the measured value into the calibration curve (y = ax + b).

(i) The quantitative value of the preparation: the measured value × dilution factor

The coefficient of variation, accuracy, and rate of variation were calculated as follows.

(i) The coefficient of variation: (Standard deviation of quantitative values ÷ Average of quantitative values) × 100

(ii) The accuracy: (Average of quantitative values ÷ Theoretical concentration) × 100

(iii) The rate of variation: [(Average of Quantitative value after storage - Quantitative value average immediately after sample preparation) ÷ Quantitative value average immediately after sample preparation]) × 100

(4) Preparation Analysis

(i) System Suitability. The coefficient of variation was calculated by repeatedly measuring QC samples 5 times. The criterion was that the coefficient of variation of peak area and retention time was less than 3%.

(ii) Linearity. The concentration of the standard solution was measured once each time, and the correlation coefficient between the concentration of the standard solution and the peak area was calculated. The criterion was that the correlation coefficient r was 0.9950 or more. The results used for linearity validation were used as calibration curves for stability analysis.

(iii) Specificity. Blank samples were measured and the presence or absence of interference peaks was confirmed at the same position as the retention time of the test substance. The criterion is that the peaks of the test substance exhibit sufficient shape for quantification and that there is no interference peak at the same retention time as the test substance.

(iv) Intraday. The preparation was sampled three times in the middle layer and measured once per sample. The criterion was that the variation coefficient of the quantitative value was 15% or less and the accuracy was 75 to 125%.

(v) Stability in Autosampler. In order to confirm the stable time in the autosampler, the samples used in the intraday were left in the autosampler for a certain time and then remeasured. The criterion was that the variation coefficient of the quantitative value was 15% or less and the variation rate with respect to the initial concentration was within ±25%.

(vi) Homogeneity. The preparation was sampled each three times in the upper, middle, and lower layers and measured once per sample. The results of the middle layer were used as a result of intraday. The criterion was that the variation coefficient of the quantitative value was 15% or less and the accuracy was 75 to 125%.

(vii) Stability

(a) Room Temperature for 4 Hours. The preparation for each dose was left at room temperature for 4 hours, sampled three times in the middle layer, and measured once per sample; the stability was confirmed. The criterion was that the variation coefficient of the quantitative value was 15% or less and the variation rate with respect to the initial concentration was within ±25%.

(b) Refrigeration for 7 Days. The preparation for each dose was left at refrigerated condition (2~8°C) for 7 days, sampled three times in the middle layer, and measured once per sample; the stability was confirmed. The criterion was that the variation coefficient of the quantitative value was 15% or less and the variation rate with respect to the initial concentration was within ±25%.

(8) QC (Quality Control). The qc samples were measured three times at the end of the analysis. The criterion was that the coefficient of variation of the analysis result was less than 10% and the accuracy was 80~120%.

3. Results

3.1. Analytical Method Validation

(1) System Suitability. The coefficient of variation of the peak area and retention time measured five times repeatedly at a concentration of 50μg/ mL of the QC sample of the Curcumin was 0.20% and 0.03%.

The coefficient of variation of the peak area and retention time measured five times repeatedly at a concentration of 250μg/ mL of the QC sample of the Glycyrrhizic Acid was 0.32% and 0.04%.

The coefficient of variation of the peak area and retention time measured five times repeatedly at a concentration of 250μg/ mL of the QC sample of the Salvianolic Acid B was 0.37% and 0.02%. The results are shown in Table 3.

(2) Linearity. The correlation coefficient r of the calibration curve measured at the concentration range of 1 to 100 μg /mL of the standard solution of the Curcumin was 1.0000 on day 0 and 0.9999 on day 7.

The correlation coefficient r of the calibration curve measured at the concentration range of 5 to 500 μg /mL of the standard solution of the Glycyrrhizic Acid was 1.0000 on day 0 and 1.0000 on day 7.

The correlation coefficient r of the calibration curve measured at the concentration range of 5 to 500 μg /mL of the standard solution of the Salvianolic Acid B was 0.9998 on day 0 and 1.0000 on day 7. The results are shown in Tables 4 and 5.

(3) Specificity. The preparation exhibited sufficient shape for analysis and no component that affected the peak of the test substance during the analysis was detected. The results are shown in Figures 3, 4, and 5.

Table 3: System suitability.

(a) Curcumin

Concentration of standard solution (μg/mL)	Classification	No.1	No.2	No.3	No.4	No.5	Mean	SD	CV (%)
50	Peak area	4524661	4514684	4516341	4517396	4499824	4514581	9089	0.20
	R/Time	58.43	58.42	58.41	58.45	58.41	58.43	0.02	0.03

(b) Glycyrrhizic Acid

Concentration of standard solution (μg/mL)	Classification	No.1	No.2	No.3	No.4	No.5	Mean	SD	CV (%)
50	Peak area	3923859	3913992	3910725	3923579	3893235	3913078	12516	0.32
	R/Time	55.37	55.36	55.35	55.39	55.35	55.36	0.02	0.04

(c) Salvianolic Acid B

Concentration of standard solution (μg/mL)	Classification	No.1	No.2	No.3	No.4	No.5	Mean	SD	CV (%)
50	Peak area	2079298	2079339	2082767	2064939	2068935	2075056	7675	0.37
	R/Time	46.47	46.46	46.45	46.48	46.45	46.46	0.01	0.02

Table 4: Accuracy of calibration curves (Day 0).

(a) Curcumin

No.	Concentration of standard solution (μg/mL)	Peak Area	Measured concentration (μg/mL)
1	1	85263.00	1.15
2	5	433268.00	4.97
3	10	888555.00	9.98
4	50	4511765.00	49.81
5	100	9086517.00	100.10

y=90965.1551x − 18969.5488, r=1.0000

(b) Glycyrrhizic Acid

No.	Concentration of standard solution (μg/mL)	Peak Area	Measured concentration (μg/mL)
1	5	78714.00	5.30
2	25	382923.00	24.61
3	50	788267.00	50.33
4	250	3928115.00	249.56
5	500	7878090.00	500.20

y=15759.4853x − 4852.7604, r=1.0000

(c) Salvianolic Acid B

No.	Concentration of standard solution (μg/mL)	Peak Area	Measured concentration (μg/mL)
1	5	32793.00	8.51
2	25	177058.00	25.17
3	50	384874.00	49.17
4	250	2073814.00	244.24
5	500	4313601.00	502.92

y=8658.3059x − 40850.7837, r=0.9998

(4) Intraday. The coefficient of variation of the test substance was 0.82% and 1.66% and the accuracy was 116.99% and 116.32% at a concentration of Curcumin of 50mg/mL and 200mg/mL of the preparation by each dose.

The coefficient of variation of the test substance was 2.07% and 0.64% and the accuracy was 78.64% and 79.02% at a concentration of Glycyrrhizic Acid of 50mg/mL and 200mg/mL of the preparation by each dose.

The coefficient of variation of the test substance was 0.86% and 1.30% and the accuracy was 95.61% and 94.70% at a concentration of Salvianolic Acid B of 50mg/mL and 200mg/mL of the preparation by each dose. The results are shown in Table 6.

(5) Stability in Autosampler. As a result of confirming the stability of the Curcumin concentration in the autosampler

Table 5: Accuracy of calibration curves (Day 7).

(a) Curcumin

No.	Concentration of standard solution (μg/mL)	Peak Area	Measured concentration (μg/mL)
1	1	99129.00	0.66
2	5	573255.00	4.97
3	10	1110862.00	9.85
4	50	5642990.00	51.01
5	100	10983038.00	99.51

y=110099.9926x + 26535.0464, r=0.9999

(b) Glycyrrhizic Acid

No.	Concentration of standard solution (μg/mL)	Peak Area	Measured concentration (μg/mL)
1	5	70795.00	5.45
2	25	361460.00	25.03
3	50	736343.00	50.29
4	250	3679238.00	248.53
5	500	7422854.00	500.70

y=14845.4655x – 10159.4707, r=1.0000

(c) Salvianolic Acid B

No.	Concentration of standard solution (μg/mL)	Peak Area	Measured concentration (μg/mL)
1	5	36633.00	6.23
2	25	197146.00	25.21
3	50	409263.00	50.30
4	250	2069324.00	246.63
5	500	4225420.00	501.63

y=8455.2959x – 16021.9262, r=1.0000

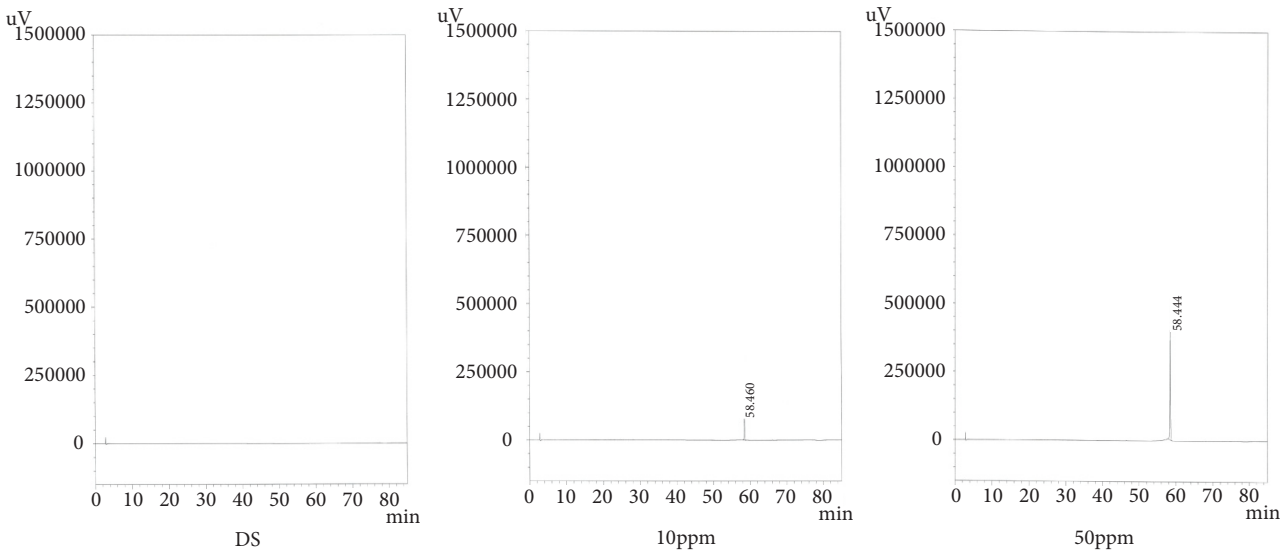

Figure 3: Chromatogram of specificity (Curcumin).

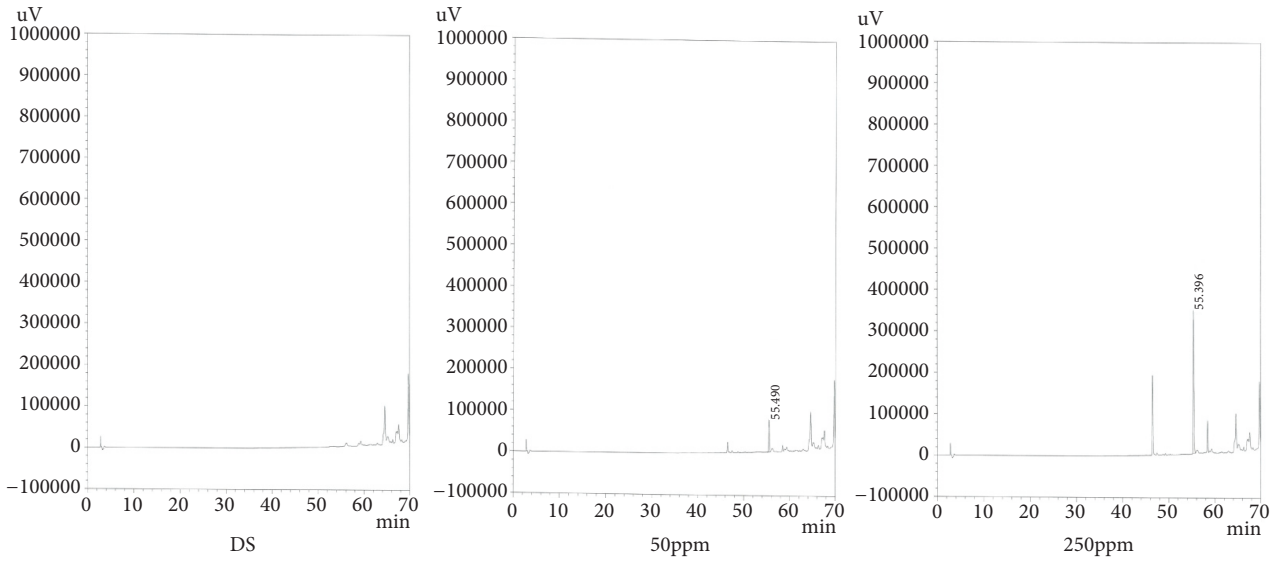

Figure 4: Chromatogram of specificity (Glycyrrhizic Acid).

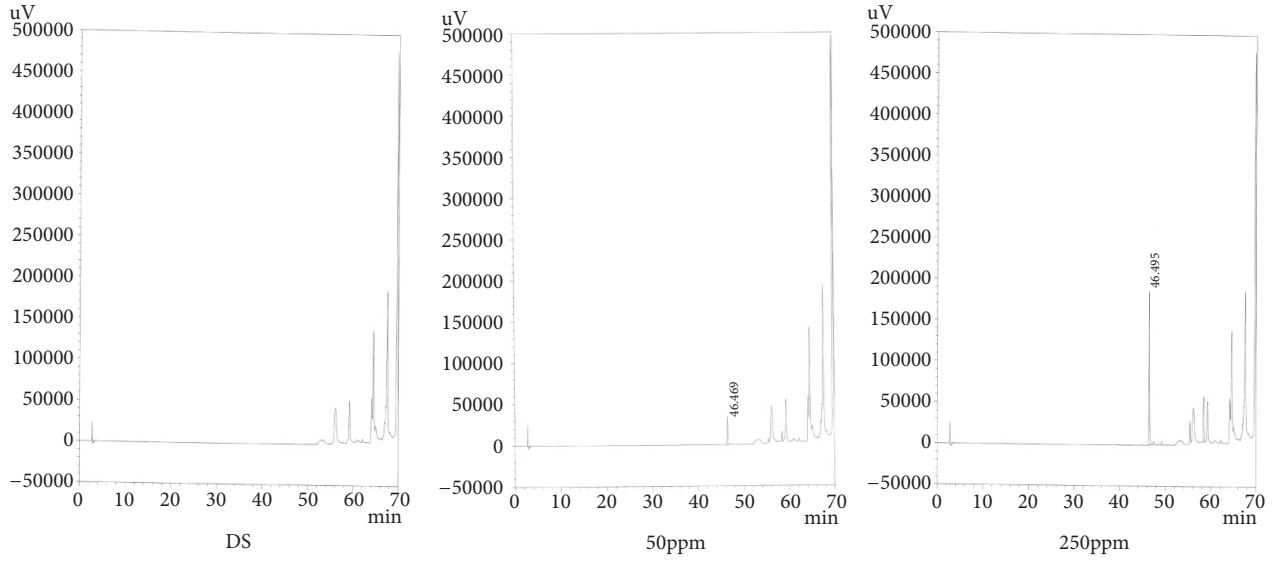

Figure 5: Chromatogram of specificity (Salvianolic Acid B).

at 50mg/mL and 200mg/mL for each dose, the variation rates with respect to the initial concentration were 1.15% and 0.85%, and the coefficient of variation was 0.59% and 0.88%.

As a result of confirming the stability of the Glycyrrhizic Acid concentration in the autosampler at 50mg/mL and 200mg/mL for each dose, the variation rates with respect to the initial concentration were 0.99% and 1.85%, and the coefficient of variation was 0.42% and 0.95%.

As a result of confirming the stability of the Salvianolic Acid B concentration in the autosampler at 50mg/mL and 200mg/mL for each dose, the variation rates with respect to the initial concentration were 1.31% and 0.22%, and the coefficient of variation was 1.08% and 0.45%. The results are shown in Table 7.

(6) Homogeneity. The homogeneity of the upper, middle, and lower layers at the concentrations of Curcumin at 50mg/mL and 200mg/mL of the preparations was confirmed. The coefficient of variation was 2.52% and 1.73%, and the accuracy was 117.65% and 115.91%.

The homogeneity of the upper, middle, and lower layers at the concentrations of Glycyrrhizic Acid at 50mg/mL and 200mg/mL of the preparations was confirmed. The coefficient

Table 6: Accuracy and precision of intraday variation.

(a) Curcumin

Concentration of dosing formulation (μg/mL)	Measured concentration (μg/mL)			Mean (μg/mL)	SD	CV (%)	Accuracy (%)
	No.1	No.2	No.3				
39.5	46.52	45.79	46.33	46.21	0.38	0.82	116.99
158.0	186.52	180.49	184.37	183.79	3.06	1.66	116.32

(b) Glycyrrhizic Acid

Concentration of dosing formulation (μg/mL)	Measured concentration (μg/mL)			Mean (μg/mL)	SD	CV (%)	Accuracy (%)
	No.1	No.2	No.3				
305.0	234.75	240.17	244.67	239.86	4.97	2.07	78.64
1220.0	961.40	959.78	971.12	964.10	6.13	0.64	79.02

(c) Salvianolic Acid B

Concentration of dosing formulation (μg/mL)	Measured concentration (μg/mL)			Mean (μg/mL)	SD	CV (%)	Accuracy (%)
	No.1	No.2	No.3				
985.0	932.67	944.18	948.37	941.74	8.13	0.86	95.61
3940.0	3762.21	3675.21	3755.96	3731.13	48.53	1.30	94.70

Table 7: Stability of treated sample in the autosampler.

(a) Curcumin

Title	Concentration of the dosing formulation (μg/mL)	Measured concentration (μg/mL)			Mean (μg/mL)	SD	CV (%)	Accuracy (%)	Variation (%)
		No.1	No.2	No.3					
Start	39.5	46.52	45.79	46.33	46.21	0.38	0.82	116.99	-
	158.0	186.52	180.49	184.37	183.79	3.06	1.66	116.32	-
End	39.5	47.06	46.57	46.59	46.74	0.28	0.59	118.33	1.15
	158.0	186.74	183.55	185.76	185.35	1.63	0.88	117.31	0.85

(b) Glycyrrhizic Acid

Title	Concentration of the dosing formulation (μg/mL)	Measured concentration (μg/mL)			Mean (μg/mL)	SD	CV (%)	Accuracy (%)	Variation (%)
		No.1	No.2	No.3					
Start	305.0	234.75	240.17	244.67	239.86	4.97	2.07	78.64	-
	1220.0	961.40	959.78	971.12	964.10	6.13	0.64	79.02	-
End	305.0	241.22	242.24	243.27	242.24	1.03	0.42	79.42	0.99
	1220.0	943.30	956.29	939.06	946.22	8.98	0.95	77.56	-1.85

(c) Salvianolic Acid B

Title	Concentration of the dosing formulation (μg/mL)	Measured concentration (μg/mL)			Mean (μg/mL)	SD	CV (%)	Accuracy (%)	Variation (%)
		No.1	No.2	No.3					
Start	985.0	932.67	944.18	948.37	941.74	8.13	0.86	95.61	-
	3940.0	3762.21	3675.21	3755.96	3731.13	48.53	1.30	94.70	-
End	985.0	945.25	965.36	951.74	954.12	10.26	1.08	96.86	1.31
	3940.0	3758.11	3726.34	3733.48	3739.31	16.67	0.45	94.91	0.22

Table 8: Homogeneity of dosing formulation.

(a) Curcumin

Concentration of dosing formulation (μg/mL)		Measured concentration (μg/mL)			Mean (μg/mL)	SD	CV (%)	Accuracy (%)
		No.1	No.2	No.3				
39.5	Upper	46.67	47.97	46.87	46.47	1.17	2.52	117.65
	Middle	46.66	46.08	46.08				
	Lower	43.99	47.82	46.06				
158.0	Upper	177.77	182.59	187.16	183.13	3.17	1.73	115.91
	Middle	186.58	182.00	184.79				
	Lower	183.97	179.00	184.33				

(b) Glycyrrhizic Acid

Concentration of dosing formulation (μg/mL)		Measured concentration (μg/mL)			Mean (μg/mL)	SD	CV (%)	Accuracy (%)
		No.1	No.2	No.3				
305.0	Upper	252.52	260.77	261.73	248.68	8.32	3.35	81.53
	Middle	238.85	248.52	245.37				
	Lower	243.74	247.37	239.27				
1220.0	Upper	975.53	947.51	962.39	963.45	20.06	2.08	78.97
	Middle	938.64	955.67	954.80				
	Lower	951.83	980.93	1003.77				

(c) Salvianolic Acid B

Concentration of dosing formulation (μg/mL)		Measured concentration (μg/mL)			Mean (μg/mL)	SD	CV (%)	Accuracy (%)
		No.1	No.2	No.3				
985.0	Upper	966.20	1001.76	988.87	960.32	22.91	2.39	97.49
	Middle	934.32	958.07	945.25				
	Lower	938.01	964.54	945.84				
3940.0	Upper	3739.49	3721.20	3813.87	3749.74	52.53	1.40	95.17
	Middle	3759.39	3704.46	3731.31				
	Lower	3694.78	3728.22	3854.97				

of variation was 3.35% and 2.08%, and the accuracy was 81.53% and 78.97%.

The homogeneity of the upper, middle, and lower layers at the concentrations of Salvianolic Acid B at 50mg/mL and 200mg/mL of the preparations was confirmed. The coefficient of variation was 2.39% and 1.40%, and the accuracy was 97.49% and 95.17%. The results are shown in Table 8.

(7) Stability

(i) Room Temperature for 4 Hours. As a result of confirming the stability of the concentration of Curcumin at 50mg/mL and 200mg/mL of the preparation at room temperature for 4 hours, the variation rates with respect to the initial concentration immediately after preparation was -1.04% and -0.39%, and the coefficient of variation was 1.66% and 2.78%.

As a result of confirming the stability of the concentration of Glycyrrhizic Acid at 50mg/mL and 200mg/mL of the preparation at room temperature for 4 hours, the variation rates with respect to the initial concentration immediately after preparation were 1.19% and -0.76%, and the coefficient of variation was 4.36% and 1.49%.

As a result of confirming the stability of the concentration of Salvianolic Acid B at 50mg/mL and 200mg/mL of the preparation at room temperature for 4 hours, the variation rates with respect to the initial concentration immediately after preparation were -0.30% and 0.52%, and the coefficient of variation was 2.69% and 1.63%. The results are shown in Table 9.

(ii) Refrigeration for 7 Days. As a result of confirming the stability of the concentration of Curcumin at 50mg/mL and 200mg/mL of the preparation at refrigerated condition (2~8°C) for 7 days, the variation rates with respect to the initial concentration immediately after preparation were -18.39% and -18.53%, and the coefficient of variation was 2.80% and 3.37%.

As a result of confirming the stability of the concentration of Glycyrrhizic Acid at 50mg/mL and 200mg/mL of the preparation at refrigerated condition (2~8°C) for 7 days, the variation rates with respect to the initial concentration immediately after preparation were 13.18% and 17.02%, and the coefficient of variation was 2.48% and 2.99%.

As a result of confirming the stability of the concentration of Salvianolic Acid B at 50mg/mL and 200mg/mL of the preparation at refrigerated condition (2~8°C) for 7 days, the variation rates with respect to the initial concentration immediately after preparation were 4.18% and 7.01%, and the

Table 9: Stability of the dosing formulations for 4 hours at room temperature.

(a) Curcumin

Time (hr)	Concentration of the dosing formulation (μg/mL)	Measured concentration (μg/mL)			Mean (μg/mL)	SD	CV (%)	Accuracy (%)	Variation (%)
		No.1	No.2	No.3					
0	39.5	46.52	45.79	46.33	46.21	0.38	0.82	116.99	-
	158.0	186.52	180.49	184.37	183.79	3.06	1.66	116.32	-
4	39.5	46.37	45.93	44.89	45.73	0.76	1.66	115.77	-1.04
	158.0	178.89	181.59	188.74	183.07	5.09	2.78	115.87	-0.39

(b) Glycyrrhizic Acid

Time (hr)	Concentration of the dosing formulation (μg/mL)	Measured concentration (μg/mL)			Mean (μg/mL)	SD	CV (%)	Accuracy (%)	Variation (%)
		No.1	No.2	No.3					
0	305.0	234.75	240.17	244.67	239.86	4.97	2.07	78.64	-
	1220.0	961.40	959.78	971.12	964.10	6.13	0.64	79.02	-
4	305.0	254.16	240.70	233.31	242.72	10.57	4.36	79.58	1.19
	1220.0	947.84	973.20	949.28	956.77	14.24	1.49	78.42	-0.76

(c) Salvianolic Acid B

Time (hr)	Concentration of the dosing formulation (μg/mL)	Measured concentration (μg/mL)			Mean (μg/mL)	SD	CV (%)	Accuracy (%)	Variation (%)
		No.1	No.2	No.3					
0	985.0	932.67	944.18	948.37	941.74	8.13	0.86	95.61	-
	3940.0	3762.21	3675.21	3755.96	3731.13	48.53	1.30	94.70	-
4	985.0	964.42	938.51	913.89	938.94	25.27	2.69	95.32	-0.30
	3940.0	3680.07	3779.39	3791.90	3750.45	61.27	1.63	95.19	0.52

coefficient of variation was 2.26% and 2.91%. The results are shown in Table 10.

(8) QC (Quality Control). When the concentration of 50μg/mL of the QC sample of Curcumin was measured three times at the end of the analysis, the coefficient of variation was 0.41% and the accuracy was 101.78%.

When the concentration of 250μg/mL of the QC sample of Glycyrrhizic Acid was measured three times at the end of the analysis, the coefficient of variation was 0.46% and the accuracy was 101.21%.

When the concentration of 250μg/mL of the QC sample of Salvianolic Acid B was measured three times at the end of the analysis, the coefficient of variation was 0.39% and the accuracy was 96.92%. The results are shown in Table 11.

4. Discussion

Validation was performed to quantitate the concentration of the preparation to be used in the efficiency and toxicity test. As a result of the validation analysis, the peak area and the coefficient of variation of the retention time, which were measured QC samples 5 times repeatedly, satisfied all of the criteria. The linearity measured in the concentration range of the standard solution also satisfied criteria of both the correlation coefficient and the accuracy. The peak of the preparation showed a sufficient shape for analysis, and no ingredient that affected the peak of the test article was detected in the blank sample. As a result of intraday, the coefficient of variation and accuracy of the test articles in the preparations at concentrations of 50mg/mL and 200mg/mL satisfied all the criteria. 50mg/mL and 200mg/mL of the preparation were allowed to left in autosampler for a certain time and then their stability was confirmed. As a result, the variation rate and the coefficient of variation for the initial concentration of the test article for 5 hours satisfied all the criteria. The homogeneity of the upper, middle, and lower layers in the preparations at concentrations of 50mg/mL and 200mg/mL was checked. The coefficient of variation and accuracy were all satisfied the criteria. To confirm the stability, the preparation at 50mg/mL and 200mg/mL was maintained at room temperature for 4 hours and at refrigerated condition (2~8°C) for 7 days. The variation rate of the initial concentration immediately after preparation and the coefficient of variation were all satisfied with the criterion. In addition, the coefficient of variation and accuracy at the QC sample concentration satisfied all the criteria.

Table 10: Stability of the dosing formulations for 7 days under refrigeration.

(a) Curcumin

Day	Concentration of the dosing formulation (μg/mL)	Measured concentration (μg/mL)			Mean (μg/mL)	SD	CV (%)	Accuracy (%)	Variation (%)
		No.1	No.2	No.3					
0	39.5	46.52	45.79	46.33	46.21	0.38	0.82	116.99	-
	158.0	186.52	180.49	184.37	183.79	3.06	1.66	116.32	-
7	39.5	37.92	38.65	36.57	37.71	1.06	2.80	95.48	-18.39
	158.0	143.93	152.77	152.53	149.74	5.04	3.37	94.77	-18.53

(b) Glycyrrhizic Acid

Day	Concentration of the dosing formulation (μg/mL)	Measured concentration (μg/mL)			Mean (μg/mL)	SD	CV (%)	Accuracy (%)	Variation (%)
		No.1	No.2	No.3					
0	305.0	234.75	240.17	244.67	239.86	4.97	2.07	78.64	-
	1220.0	961.40	959.78	971.12	964.10	6.13	0.64	79.02	-
7	305.0	277.24	273.06	264.09	271.46	6.72	2.48	89.00	13.18
	1220.0	1099.67	1165.43	1119.48	1128.19	33.73	2.99	92.47	17.02

(c) Salvianolic Acid B

Day	Concentration of the dosing formulation (μg/mL)	Measured concentration (μg/mL)			Mean (μg/mL)	SD	CV (%)	Accuracy (%)	Variation (%)
		No.1	No.2	No.3					
0	985.0	932.67	944.18	948.37	941.74	8.13	0.86	95.61	-
	3940.0	3762.21	3675.21	3755.96	3731.13	48.53	1.30	94.70	-
7	985.0	996.37	991.24	955.72	981.11	22.14	2.26	99.61	4.18
	3940.0	3879.51	4111.82	3986.46	3992.60	116.28	2.91	101.34	7.01

Table 11: Accuracy and precision of QC sample.

(a) Curcumin

Concentration of total catechins (μg/mL)	Measured concentration (μg/mL)			Mean (μg/mL)	SD	CV (%)	Accuracy (%)
	No.1	No.2	No.3				
50	50.66	51.07	50.93	50.89	0.21	0.41	101.78

(b) Glycyrrhizic Acid

Concentration of total catechins (μg/mL)	Measured concentration (μg/mL)			Mean (μg/mL)	SD	CV (%)	Accuracy (%)
	No.1	No.2	No.3				
250	251.68	253.84	253.55	253.02	1.17	0.46	101.21

(c) Salvianolic Acid B

Concentration of total catechins (μg/mL)	Measured concentration (μg/mL)			Mean (μg/mL)	SD	CV (%)	Accuracy (%)
	No.1	No.2	No.3				
250	242.70	242.95	241.21	242.29	0.94	0.39	96.92

5. Conclusion

This method for analyzing the concentration of KCHO-1 preparations has been found to be suitable. The preparations at the concentrations of 50mg/ml and 200mg/ml in sterilized distilled water were homogeneous and it was stable for 4 hours at room temperature and 7-day refrigerated condition (2~8°C).

Data Availability

The data used to support the findings of this study are available from the corresponding author upon request.

Conflicts of Interest

The authors declare that there are no conflicts of interest.

Authors' Contributions

Tingting Wang, Seongjin Lee, and Muhack Yang equally contributed (co-first authors) to this work.

Acknowledgments

This research was supported by a grant of the Korea Health Technology R&D Project through the Korea Health Industry Development Institute (KHIDI), funded by the Ministry of Health & Welfare, Korea (Grant no. HI11C2142).

References

[1] D. H. Kim, *Effect of Gamijakyakgamchobuja-Tang on Neuropathic Pain in Rats*, Wonkwang University, Jeollabuk-do, South Korea, 2015.

[2] D.-S. Lee, W. Ko, B.-K. Song et al., "The herbal extract KCHO-1 exerts a neuroprotective effect by ameliorating oxidative stress via heme oxygenase-1 upregulation," *Molecular Medicine Reports*, vol. 13, no. 6, pp. 4911–4919, 2016.

[3] L. Guo, S. Y. Cho, S. S. Kang, S. H. Lee, H. Y. Baek, and Y. S. Kim, "Orthogonal array design for optimizing extraction efficiency of active constituents from Jakyak-Gamcho Decoction, the complex formula of herbal medicines, Paeoniae Radix and Glycyrrhizae Radix," *Journal of Ethnopharmacology*, vol. 113, no. 2, pp. 306–311, 2007.

[4] J. W. Yu, *Study on the Ingredient of Jakyakgamchotang*, Wonkwang University, Jeollabuk-do, South Korea, 2010.

[5] B. W. Kim, "Anti-inflammatory effect of Jakyakgamcho-tang," *The Korean Journal of Internal Medicine*, vol. 31, no. 2, pp. 365–371, 2010.

[6] J. M. Lee, S. Y. Hong, and M. S. Oh, "Effects of Jakyak-kamchobuja-tang on Papain-induced osteoarthritis in mice," *Journal of Korean Oriental Medicine*, vol. 34, no. 1, pp. 116–135, 2013.

[7] D.-S. Lee, W. Ko, C.-S. Yoon et al., "KCHO-1, a novel anti-neuroinflammatory agent, inhibits lipopolysaccharide-induced neuroinflammatory responses through Nrf2-mediated heme oxygenase-1 expression in mouse BV2 microglia cells," *Evidence-Based Complementary and Alternative Medicine*, vol. 2014, Article ID 357154, 11 pages, 2014.

[8] E. Cha, J. Lee, S. Lee et al., "A 4-week repeated dose oral toxicity study of Mecasin in Sprague-Dawley rats to determine the appropriate doses for a 13-week, repeated toxicity test," *Journal of Pharmacopuncture*, vol. 18, pp. 45–50, 2015.

[9] H. Jeong, J. Lee, E. Cha et al., "A study on the oral toxicity of mecasin in rats," *Journal of Pharmacopuncture*, vol. 17, no. 4, pp. 61–65, 2014.

[10] E. Cha, H. Jeong, J. Lee, S. Lee, M. Park, and S. Kim, "A study on single dose toxicity of mecasin pharmacopuncture injection in muscle," *Journal of Korean Medicine*, vol. 36, no. 2, pp. 36–42, 2015.

[11] S. J. Lee, H. H. Jeong, J. C. Lee et al., "A study on single dose toxicity of intravenous injection of mecasin herbal acupuncture," *The Acupuncture*, vol. 33, no. 1, pp. 1–7, 2016.

[12] M. G. Kook, S. W. Choi, Y. Seo et al., "KCHO-1, a novel herbal anti-inflammatory compound, attenuates oxidative stress in an animal model of amyotrophic lateral sclerosis," *Journal of Veterinary Science*, vol. 18, no. 4, pp. 487–497, 2017.

Hindawi
Evidence-Based Complementary and Alternative Medicine
Volume 2019, Article ID 6180236, 6 pages
https://doi.org/10.1155/2019/6180236

Research Article

Two-Week Repeated Oral Dose Toxicity Study of Mantidis Ootheca Water Extract in C57BL/6 Mice

Hye-Sun Lim, Yun Soo Seo, Seung Mok Ryu, Byeong Cheol Moon, Goya Choi, and Joong-Sun Kim

Herbal Medicine Resources Research Center, Korea Institute of Oriental Medicine, 111Geonjae-ro, Naju-si, Jeollanam-do 58245, Republic of Korea

Correspondence should be addressed to Joong-Sun Kim; centraline@kiom.re.kr

Received 27 February 2019; Accepted 26 March 2019; Published 7 April 2019

Guest Editor: Yong-Ung Kim

Background. Mantidis Ootheca (MO), described as the ootheca of *Hierodula patellifera* Serville, 1839, *Tenodera angustipennis* (Saussure, 1869), or *Statilia maculate* (Thunberg, 1784) in Korean Herbal Pharmacopoeia, is an important herbal material that has been traditionally used for treating several medical conditions including renal failure, spermatorrhea, and pediatric enuresis in Korea. *Objective.* The present study investigated the potential subacute toxicity of MO water extract during a 2-week repeated oral administration of doses of 0, 50, 150, or 450 mg/kg/day to C57BL/6 male mice by gavage. *Methods.* The following parameters were examined during the study period: mortality, clinical signs, body weight, hematology, serum biochemistry, gross findings, organ weight, and histopathology. All the mice were euthanized at the end of the treatment period. *Results.* No treatment-related changes in mortalities, clinical signs, body weight, gross finding, and organ weight change were detected after 14 days of oral MO extract administration. In addition, no meaningful MO extract treatment-related changes were observed in the hematological, serum biochemical, and histopathological parameters compared with the normal control group following treatment with doses of up to 450 mg/kg/day. *Conclusion.* Based on these findings, we concluded that treatment of mice with the water extract of MO did not result in significant toxicity and, therefore, it could be considered safe for further pharmacological studies.

1. Introduction

Insects have been commonly used as a source of food and drug resources worldwide [1]. Animal-based therapeuticals including insects have remained a component of traditional medicine and are increasingly gaining interest and attention as part of animal-based medicine [2]. Korean history provides the most well-known historical record of animal-based medicinal in the medical book entitled "Donguibogam" written by Heo Jun, an Eastern physician (1546–1615). Dr. Heo recorded the use of 95 different varieties of animal-based medicines including insects for the effective treatment of certain illnesses [3]. For example, grasshoppers have been used to heal bronchitis and asthma, and crickets have been used to alleviate symptoms related to liver diseases and fever [4]. Recently, the focus of drug-related research has shifted to insect-based products with a potential to be used as medicines to treat a variety of diseases. In this regard, several insect varieties to species have been tested by pharmaceutical companies as potential sources of modern drugs [5]. However, despite the increasing popularity of insect-based medicines, limited research is available on the safety of these products. Therefore, toxicological assessment of insect-based drugs is crucial for safe use and regulation of doses to achieve maximum benefits.

The authentic Mantidis Ootheca (MO) refers to the dried ootheca of *Hierodula patellifera* Serville, 1839, *Tenodera angustipennis* (Saussure, 1869), and *Statilia maculate* (Thunberg, 1784) which belongs to the insects of the Mantidae family in Korea. It has been widely used as a traditional medicine to treat kidney-related complications such as frequent urination, incontinence, and cloudy urine [6]. In addition, results from the electronic databases research related to MO using the Oriental Medicine Advanced Searching Integrated System (OASIS) reveal MO to have been used as an effective drug in treating sterility and premature

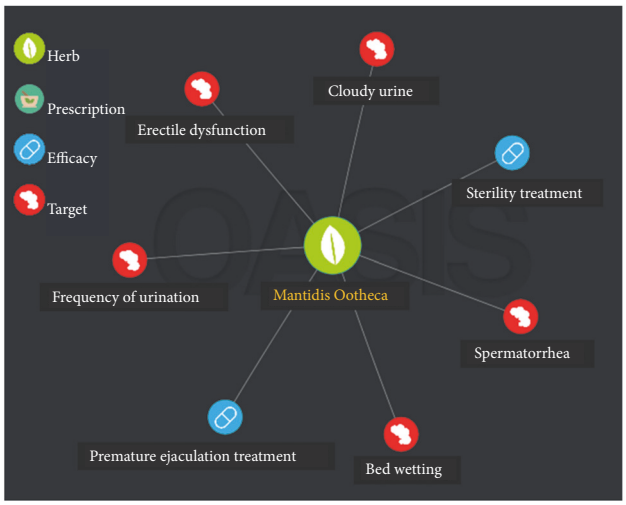

Figure 1: Oriental Medicine Advanced Searching Integrated System (OASIS) analysis of MO.

ejaculation (Figure 1). Pharmacological studies reported that MO increased the index of testis and thymus gland, and exerted an antidiuretic effect, and decreased lipid peroxidation in the liver of hypercholesterolemia rats [7]. Despite these studies and the widespread use of MO in traditional medicine, no study on its toxicological profile has been reported. With this background, we investigated the possible toxic effects of oral administration of MO water extract in mice in a 2-week study.

2. Materials and Methods

2.1. Preparation of MO Extract. MO was purchased from a medicinal herb shop in Kwong Mungdang (Ulsan, Korea) in June 2017 and was authenticated by Dr. Goya Choi (Herbal Medicine Resources Research Center, Korea Institute of Oriental Medicine, Naju, Korea). A voucher specimen (accession number: 2-18-0123) was deposited at the Herbal Medicine Resources Research Center, Korea Institute of Oriental Medicine. MO (2.0 kg) was extracted in distilled water (5 × 5 L) for 3 h under reflux (100 ± 2°C). After filtrating and evaporating the solvent *in vacuo*, the remaining liquid was removed by freeze drying to obtain a distilled water-soluble powder extract (23.6 g).

2.2. Experimental Animals. Twenty, specific pathogen-free, 7-week-old C57BL6 male mice (20 ± 2 g) were purchased from DooYeol Biotech (Seocho-gu, Seoul, Korea). After 1 week of quarantine and acclimatization to the animal care facility, mice were randomly divided into four groups (n = 5 per group): one normal control (0 mg/kg/day) and three MO extract groups (50, 150, and 450 mg/kg/day). The experiment design is outlined in Figure 2(a). All mice were housed in a room maintained at a temperature of 23 ± 3°C with a relative humidity of 50 ± 10%, an air ventilation frequency of 10 to 20 times/h, and a light intensity of 150 to 300 Lux with artificial lighting from 08:00 to 20:00. The animals were

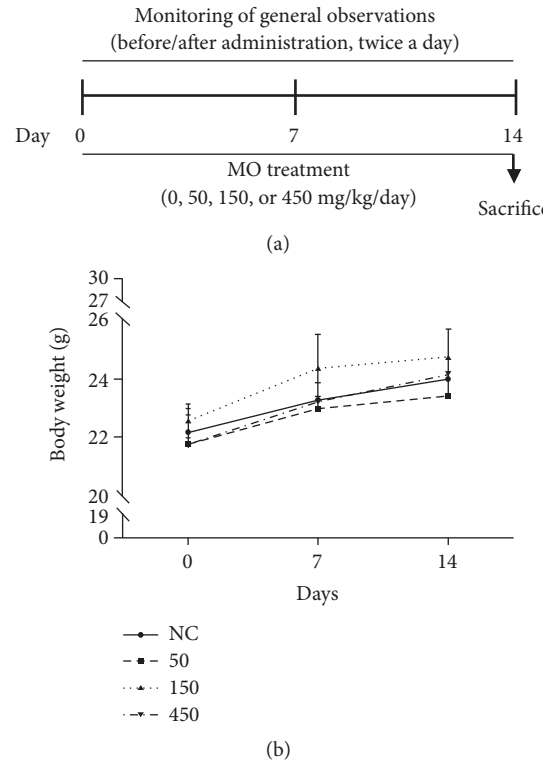

Figure 2: Toxicological evaluation of MO extract in mice. (a) Schematic diagram of drug treatment, tissue preparation, and toxicological evaluation. (b) Mean body weights of mice exposed to repeated doses of 0, 50, 150, and 450 mg/kg/day of MO extract. Values are expressed as means ± SD. SD, standard deviation.

kept in stainless wire cages and fed a commercial pellet diet (Nestlé Purina Pet Care Company; Bundang-gu, Seongnam, Korea) and sterilized tap water was provided ad libitum. All experimental procedures were conducted in accordance with the National Institutes of Health (NIH) Guidelines for the Care and Use of Laboratory Animals. The study was approved by the Institutes of Animal Care and Use Committee of the Korean Institute of Oriental Medicine (Approval number: 18-041). Animal handling was performed in accordance with the dictates of the National Animal Welfare Law of Korea.

2.3. General Observations. Characteristics such as mortality, clinical signs, and body weight of mice were monitored for 14 days. Mortality and clinical signs were recorded twice a day (before and after administration) during the study period. The body weight of each mouse was measured at the initiation of administration of the extract and once a week throughout the study period.

2.4. Necropsy. At the end of experiments, all animals that survived were anesthetized using ethyl ether and euthanized by exsanguination via the aorta. Complete gross postmortem examinations were performed with special attention to all vital organs and tissues. Absolute organ weights were measured, and relative organ weights were calculated for the lungs, liver, spleen, kidneys, and testis.

Table 1: Mortality in male mice after 2 weeks of repeated oral administration of MO.

Group (mg/kg/day)	Days after treatment													
	1	2	3	4	5	6	7	8	9	10	11	12	13	14
0	*0/5	0/5	0/5	0/5	0/5	0/5	0/5	0/5	0/5	0/5	0/5	0/5	0/5	0/5
50	0/5	0/5	0/5	0/5	0/5	0/5	0/5	0/5	0/5	0/5	0/5	0/5	0/5	0/5
150	0/5	0/5	0/5	0/5	0/5	0/5	0/5	0/5	0/5	0/5	0/5	0/5	0/5	0/5
450	0/5	0/5	0/5	0/5	0/5	0/5	0/5	0/5	0/5	0/5	0/5	0/5	0/5	0/5

∗Number of dead mice/total mice.

Table 2: Clinical signs in male mice after 2 weeks of repeated oral administration of MO.

Group (mg/kg/day)	Days after treatment													
	1	2	3	4	5	6	7	8	9	10	11	12	13	14
0	*0/5	0/5	0/5	0/5	0/5	0/5	0/5	0/5	0/5	0/5	0/5	0/5	0/5	0/5
50	0/5	0/5	0/5	0/5	0/5	0/5	0/5	0/5	0/5	0/5	0/5	0/5	0/5	0/5
150	0/5	0/5	0/5	0/5	0/5	0/5	0/5	0/5	0/5	0/5	0/5	0/5	0/5	0/5
450	0/5	0/5	0/5	0/5	0/5	0/5	0/5	0/5	0/5	0/5	0/5	0/5	0/5	0/5

∗Number of mice with clinical signs/total mice.

2.5. Histopathology. To perform histopathology, the liver tissue was fixed in 10% neutral-buffered formalin. Tissue samples were then embedded into paraffin and sectioned into 4 μm thick slices, followed by staining with hematoxylin and eosin (H&E) solution (Sigma-Aldrich, St. Louis, MO, USA). The stained sections were examined under a light microscope (Olympus Microscope System CKX53; Olympus, Tokyo, Japan).

2.6. Hematology. Blood samples from the experimental mice were collected into complete blood count bottles containing ethylenediaminetetraacetic acid (EDTA)-2K (Sewon Medical Co., Cheonan, Korea), and were analyzed for red blood cell (RBC) count, hemoglobin (HB) concentration, hematocrit (HCT), mean corpuscular volume (MCV), mean corpuscular hemoglobin (MCH), mean corpuscular hemoglobin concentration (MCHC), platelet (PLT), white blood cell (WBC) count, and differential leucocyte count (neutrophils, lymphocytes, monocytes, eosinophils, and basophils) using an ADVIA 2120i hematology analyzer (Siemens; Tarrytown, NY, USA).

2.7. Serum Biochemistry. For assessing biochemical parameters, blood samples from the experimental mice were centrifuged at 3,000 rpm for 10 min in a separation tube on the day of necropsy and analyzed using a TBA 120FR chemistry analyzer (Toshiba Co., Tokyo, Japan). The serum biochemical parameters measured were creatinine (CRE), glucose (GLU), glutamic oxaloacetic transaminase (GOT), glutamic pyruvic transaminase (GPT), blood urea nitrogen (BUN), and total bilirubin (TBIL).

2.8. Statistical Analyses. Body weight, hematology, serum biochemistry, and organ weight values are presented as mean ± standard deviation (SD). The statistical significance between the groups was analyzed using an analysis of variance (ANOVA), followed by Dunnett's multiple comparison test. We did not calculate the median lethal dose (LD_{50}) because no mortality was observed.

Table 3: Gross findings in male mice after 2 weeks of repeated oral administration of MO.

Group (mg/kg/day)	Gross finding	Frequency
0	No gross findings	5/5
50	No gross findings	5/5
150	No gross findings	5/5
450	No gross findings	5/5

3. Results

3.1. Clinical Signs and Change of Body Weight in Mice Treated with MO Extract. In the present study, we did not observe any mortality in mice administered the oral extract of MO during the 2-week study period (Table 1). In addition, as shown in Table 2, no MO treatment-related clinical signs were observed in mice during the study period. At the scheduled necropsy, no gross findings in mice were observed either. A time- and dose-dependent increase in the body weight of mice was observed (Figure 2(b)). There were no statistically significant changes in body weight between the 450 mg/kg/day group and the normal control group (0 mg/kg/day).

3.2. Gross Findings in Mice Treated with MO Extract. Necropsy was performed 2 weeks after the administration of the MO extract. We did not observe any abnormal finding in the internal organs including the lungs, liver, spleen, kidneys, and testis (Table 3).

3.3. Organ Weight and Histopathological Changes in Mice Treated with MO Extract. We next monitored changes in organ weight and histopathological changes in mice treated

Table 4: Organ weights in male mice after 2 weeks of repeated oral administration of MO.

Parameters (g)	Group (mg/kg/day)			
	0	50	150	450
Lung	0.137 ± 0.004	0.134 ± 0.018	0.128 ± 0.008	0.134 ± 0.021
Liver	1.266 ± 0.063	1.228 ± 0.101	1.276 ± 0.083	1.244 ± 0.140
Spleen	0.061 ± 0.017	0.057 ± 0.016	0.056 ± 0.017	0.050 ± 0.007
Kidney	0.321 ± 0.017	0.294 ± 0.024	0.296 ± 0.036	0.300 ± 0.021
Testis	0.178 ± 0.011	0.172 ± 0.019	0.170 ± 0.031	0.174 ± 0.009

Values are expressed as means ± SD of five mice at sacrifice.

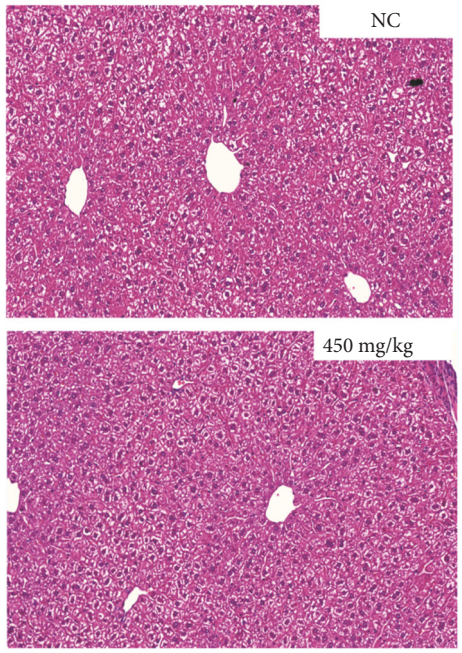

Figure 3: Histopathological examination of the liver in mice exposed to repeated MO extract doses of 0 and 450 mg/kg/day. Representative images (H&E stained) showing histological changes in the liver of vehicle and 450 mg/kg/day-treated mice samples.

with MO extract. Mice in the MO extract-treated groups showed no significant change in the absolute weight of the five principal organs, namely, the lungs, liver, spleen, kidneys, and testis compared with organs in the normal control group (Table 4). Similarly, histopathological examination of the liver revealed no abnormal findings at the highest dose of 450 mg/kg/day in the MO extract-treated group compared with the normal control group (Figure 3).

3.4. Hematology and Serum Biochemistry in Mice Treated with MO Extract. Table 5 shows the results of the hematological analyses. No significant differences were observed in the hematological parameters of the MO extract-treated mice compared to the normal control mice. As shown in Table 6, serum biochemical examinations showed reduced GLU levels in the group administered 50 mg/kg/day MO extract compared to the normal control group. We also detected significantly decreased GOT levels in mice administered MO extract at doses of 50 and 450 mg/kg/day compared to mice in the normal control group. Other parameters did not exhibit any significant differences between the MO extract-treated and normal control groups.

4. Discussion

Numerous traditional medicines are currently widely used worldwide to treat various ailments; however, they are sometimes associated with potential risks. Therefore, toxicological assessment of these medicines is essential to evaluate their safety, determine suitable doses, and evaluate their side-effects [8]. Moreover, with the increasing demand for insect-based drugs in traditional medicine and their associated toxicity, the safety and efficacy of drugs have become a major public health concern [9]. Toxic components can limit the pharmacological activity of drugs. Additionally, excessive or prolonged exposure to drugs could result in definite damage to organs. In the present study, we evaluated the safety of MO water extract using a standard toxicological study design to assess the potential oral dose toxicity. During the study period of 2 weeks, male C57BL/6 mice were orally administered once daily with doses of 0, 50, 150, or 450 mg/kg/day of MO extract after which several study parameters of mortality, clinical signs, changes in body weight, gross findings, organ weight, histopathological examinations, and hematology were assessed.

Changes in body weight have been previously reported to be linked to the adverse effects of drugs [10]. We observed a similar increase in body weight among MO extract-treated and control mice. In addition, mice treated with the MO extract at 50, 150, and 450 mg/kg/day did not show mortality and clinical signs throughout the study, similar to the control group. These findings indicate that oral administration of repeated doses of the MO extract did not exert any toxicity on the growth and function of mice.

It is well known that a change in the organ weight is a sensitive indicator of the potential toxicity of chemicals [11]. As described above, repeated oral dosing with the MO extract had no effect on the body weight gain in mice administered ≤ 450 mg/kg/day MO extract.

Similar to the body weight, we did not observe any change in the absolute weight of organs, such as the lungs, liver, spleen, kidneys, and testis in mice treated with MO extract. Moreover, no corresponding histopathological changes or accompanying biochemical alterations were detected. Therefore, we concluded that MO extract-mediated

Table 5: Hematological values in male mice after 2 weeks of repeated oral administration of MO.

Parameters	Group (mg/kg/day)			
	0	50	150	450
RBC ($\times 10^6/\mu g$)	8.480 ±1.182	7.400 ± 2.224	8.680 ± 2.366	9.620 ± 0.554
HB (g/dL)	14.600 ±1.140	10.200 ± 3.347	12.600 ± 3.782	14.400 ± 0.894
HCT (%)	42.100 ± 11.520	36.480 ± 12.156	42.640 ± 12.182	47.680 ± 2.310
MCV (fl)	49.420 ± 1.099	48.820 ± 2.922	48.940 ± 1.122	49.640 ± 1.016
MCH (pg)	14.800 ± 0.447	14.200 ± 0.837	14.400 ± 0.894	14.800 ± 0.447
MCHC (g/dL)	29.880 ± 0.879	28.200 ± 2.021	28.860 ± 1.252	29.620 ± 0.610
PLT ($\times 10^3/\mu g$)	729.400 ± 122.100	685.200 ± 249.905	661.000 ± 83.382	715.800 ± 65.370
WBC ($\times 10^3/\mu g$)	2.240 ± 1.314	2.720 ± 1.224	2.320 ± 1.274	3.160 ± 1.383
NEU (%)	15.320 ± 9.066	10.200 ± 1.495	17.360 ± 8.914	21.180 ± 15.790
LYM (%)	79.140 ± 11.305	84.960 ± 3.087	76.440 ± 9.095	74.360 ± 17.568
MON (%)	3.300 ± 0.846	3.280 ± 1.152	3.440 ± 1.410	2.960 ± 1.601
EOS (%)	1.640 ± 2.263	1.100 ± 1.177	1.860 ±1.633	1.040 ± 1.488
BAS (%)	0.620 ± 0.567	0.480 ± 0.634	0.900 ± 0.552	0.460 ± 0.650

RBC, red blood cells; HB, hemoglobin; HCT, hematocrit; MCV, mean corpuscular volume; MCH, mean corpuscular hemoglobin; MCHC, mean corpuscular hemoglobin concentration; PLT, platelet; WBC, white blood cell; NEU, neutrophil; LYM, lymphocyte; MON, monocyte; EOS, eosinophil; BAS, basophil.
Values are expressed as means ± SD of five mice at sacrifice.

Table 6: Serum biochemical values in male mice after 2 weeks of repeated oral administration of MO.

Parameters	Group (mg/kg/day)			
	0	50	150	450
CRE (mg/dL)	1.620 ± 0.228	1.320 ± 0.259	1.560 ± 0.451	1.600 ± 0.678
GLU (mg/dL)	172.000 ± 6.218	152.500 ± 12.793*	159.750 ± 29.113	161.250 ± 33.925
GOT (U/L)	85.000 ± 5.354	72.500 ± 8.515*	81.500 ± 15.000	72.750 ± 4.646*
GPT (U/L)	55.000 ± 9.566	53.800 ± 9.039	64.400 ± 37.226	52.000 ± 12.268
BUN (mg/dL)	25.675 ± 2.712	24.920 ± 2.543	24.240 ± 2.237	25.780 ± 2.160
TBIL (mg/dL)	0.725 ± 0.222	0.900 ± 0.082	1.050 ± 0.173	1.025 ± 0.126

CRE, creatinine; GLU, glucose; GOT, glutamic oxaloacetic transaminase; GPT, glutamic pyruvic transaminase; BUN, blood urea nitrogen; TBIL, total bilirubin.
Values are expressed as means ± SD of five mice at sacrifice.
*Significantly different from the normal control at $p < 0.05$.

changes in weight of these organs are toxicologically insignificant.

The hematopoietic system serves as one of the most important indicators for estimating the toxicity of drugs. Moreover, it is regarded as a critical index of the physiological and pathological status of humans and animals [12] because it reflects the status of bone marrow activity and intravascular effects such as hemolysis and anemia [13]. Therefore, in the present study we assessed the effect of MO extract on various hematological parameters and observed that at repeated doses of up to 450 mg/kg/day MO extract did not cause any hematological abnormalities in the tested mice.

Results of the present 2-week repeated oral dose toxicity study clearly revealed that administration of MO extract did not exert any adverse effect on male mice. Although the correct LD_{50} dose of MO extract remains unclear, the present study provided evidence that acute exposure to different doses of MO extract did not result in any significant toxic effects on male mice, suggesting that the oral LD_{50} of MO extract was greater than 450 mg/kg/day in male mice.

5. Conclusion

The extract of MO has traditionally been used as a medicine in several Asian countries, including Korea and China. However, its safety or toxicity has not been reported. In conclusion, a 14-day repeated oral dosing of MO extract to mice resulted in a significant alteration in clinical signs, body weight, and hematological, biochemical, and histopathological parameters at doses of ≤ 450 mg/kg/day. Although we could not confirm the toxic dose of MO extract, the present study is the first of its kind to confirm the toxicity of MO extract.

Data Availability

The data used to support the findings of this study are available from the corresponding author upon request.

Conflicts of Interest

The authors declare no conflicts of interest.

Acknowledgments

This work was supported by the Verification of Efficacy and Safety for Chung-bu medicinal Materials Described in the Dong Ui Bo Gam (K18411).

References

[1] L. Kouřimská and A. Adámková, "Nutritional and sensory quality of edible insects," *NFS Journal*, vol. 4, pp. 22–26, 2016.

[2] R. W. Pemberton, "Insects and other arthropods used as drugs in Korean traditional medicine," *Journal of Ethnopharmacology*, vol. 65, no. 3, pp. 207–216, 1999.

[3] J. T. Shin, M. A. Baker, and Y. W. Kim, "Edible insects uses in South Korean gastronomy: "Korean edible insect laboratory" case study," *Edible Insects in Sustainable Food Systems*, pp. 147–159, 2018.

[4] Y. W. Kim, *The 50 Ways to Cook Edible Insects*, Bumwoo Publication, Seoul, Republic of Korea, 2014.

[5] A. Im, W. Yang, Y. Park, S. Kim, and S. Chae, "Hepatoprotective effects of insect extracts in an animal model of nonalcoholic fatty liver disease," *Nutrients*, vol. 10, no. 6, p. 735, 2018.

[6] C. M. Kim, M. K. Shin, D. K. Ahn, and K. S. Lee, *Chinese Medicine Dictionary*, chapter 5, Jungdam, Seoul, Republic of Korea, 2006.

[7] Z. Tan, Y. Lei, B. Zhang, and L. Huang, "Comparison of pharmacological studies on ootheca Mantidis," *China Journal of Chinese Materia Medica*, vol. 22, no. 8, pp. 496–499, 1997.

[8] S. A. Jordan, D. G. Cunningham, and R. J. Marles, "Assessment of herbal medicinal products: challenges, and opportunities to increase the knowledge base for safety assessment," *Toxicology and Applied Pharmacology*, vol. 243, no. 2, pp. 198–216, 2010.

[9] S. Lee, K. S. Ahn, H. Y. Ryu et al., "Safety evaluation of cricket(Gryllus bimaculatus) extract in Sprague-Dawley rats," *International Journal of Industrial Entomology*, vol. 32, no. 1, pp. 12–25, 2016.

[10] J. T. Mukinda and P. F. K. Eagles, "Acute and sub-chronic oral toxicity profiles of the aqueous extract of *Polygala fruticosa* in female mice and rats," *Journal of Ethnopharmacology*, vol. 128, no. 1, pp. 236–240, 2010.

[11] J. C. Kim, D. H. Shin, S. H. Kim et al., "Subacute toxicity evaluation of a new camptothecin anticancer agent CKD-602 administered by intravenous injection to rats," *Regulatory Toxicology and Pharmacology*, vol. 40, no. 3, pp. 356–369, 2004.

[12] V. B. Liju, K. Jeena, and R. Kuttan, "Acute and Sub-chronic toxicity as well as mutagenic evaluation of essential oil from turmeric (Curcuma longa)," *Food and Chemical Toxicology*, vol. 53, pp. 52–61, 2013.

[13] G. L. Voigt and S. L. Swist, *Hematology Techniques and Concepts for Veterinary Technicians*, Wiley-Blackwell, Hoboken, NJ, USA, 2nd edition, 2011.

Hindawi
Evidence-Based Complementary and Alternative Medicine
Volume 2019, Article ID 4534167, 10 pages
https://doi.org/10.1155/2019/4534167

Research Article

Anticonvulsant Effects of Dingxian Pill in Pentylenetetrazol-Kindled Rats

Yudan Zhu,[1] **Shuzhang Zhang**,[2] **Mei Shen**,[1] **Zhiping Zhang**,[2] **Kan Xu**,[1] **Jiwei Cheng**,[1] **Yiqin Ge**,[1] **and Jie Tao**[1]

[1]*Central Laboratory, Department of Neurology and Neurosurgery, Putuo Hospital, Shanghai University of Traditional Chinese Medicine, Shanghai, China*
[2]*Laboratory of Neuropharmacology and Neurotoxicology, School of Life Science, Shanghai University, Shanghai, China*

Correspondence should be addressed to Jiwei Cheng; chengjiwei1@126.com, Yiqin Ge; gyq200083@163.com, and Jie Tao; jietao_putuo@foxmail.com

Yudan Zhu and Shuzhang Zhang contributed equally to this work.

Received 13 December 2018; Accepted 24 February 2019; Published 18 March 2019

Guest Editor: Gunhyuk Park

Dingxian pill has been used as an antiepilepsy agent in China from ancient to modern times, of which the concrete pharmacological characterization and the underlying molecular mechanism remain unclear. The present study was undertaken to investigate them by animal behavior, electroencephalogram (EEG), Morris water maze, immunohistochemistry, transcriptomics, and real-time PCR. In our results, the treatment of Dingxian pill dose-dependently inhibited PTZ-induced seizure-like behavior and reduced the seizure grades, LFP power spectral density, and brain wave of the epileptiform EEG component induced by PTZ. In Morris water maze tests, the learning and memory ability of kindled epileptic rats could be attenuated more efficiently by Dingxian pill. For the immediate early gene c-fos, the expression was reduced after Dingxian pill treatment, and the difference was significant between the treatment and the model group. Through the transcriptome analysis of the gene expression in hippocampus, Egr3, Nrg, Arc, and Ptgs2, closely related to epilepsy, had been proved to be downregulated by application of Dingxian pill. All of the results not only highlight the antiepileptic effects of Dingxian pill and its molecular mechanism, but also provide a modern validity theory for the clinical application of traditional Chinese medicine (TCM).

1. Introduction

Epilepsy, as one of the most common and treatable neurologic diseases, is invoked by the abnormal discharge of brain neurons and characterized as a progressive loss of neurological function [1]. So far, 9 millions of people have suffered epilepsy in China, which is about one-sixth of the world's population suffering from epilepsy, and the sufferers were grown with 300-400 thousands in every year [2, 3]. Moreover, sudden unexpected deaths in epilepsy (SUDEP) is an important factor of premature death [4]. On the one hand, the routine antiepileptic drugs focus on reducing the convulsive symptoms with side effects such as cognitive impairment or liver injury [5–8]. On the other hand, 30% of patients, without being improved the pathogenesis after treatment with conventional antiepileptic drugs, still develop into the intractable epilepsy [9–12]. Therefore, it is urgent to explore effective drugs and pharmacological mechanisms for the treatment of epilepsy.

Dingxian pill has been widely used in treating epilepsy, as a classic prescription for treating epilepsy in China, containing Gastrodia elata, Scorpion, Bombyx batryticatus, Tendrilleaf fritillary bulb, Ternate pinellia, Indian buead, Bile Arisaema, Acorus gramineus, Amber, Tangerine peel, Thin-leaf milkwort root, salvia miltiorrhiza, Dwarf lilyturf root tuber, Mercury blende, and bamboo juice. The application of Dingxian pill is extended to treat the temporal lobe epilepsy and pediatric epilepsy. Compared with the clinical efficacy of routine antiepileptic drugs in pediatric epilepsy, the total effective rate of Dingxian pill (87.5%) was higher than that of

sodium valproate group (75%, $P<0.05$) [13]. In foundational research, Dingxian pill had a significant effective effect for temporal lobe epilepsy by reducing the frequency of seizures in rats [14]. It not only prevents the seizure of rats, but also prolongs the incubation period of convulsions on penicillin, an antagonist to GABA receptors, induced epilepsy rats [14]. Meanwhile, the glutamate content decreased, GABA level increased, and the expression of c-fos was suppressed by Dingxian pill in the hippocampus of rats [15]. The results partly implied the anticonvulsant effects of Dingxian pill; however, the mechanism is still unclear.

So far, as the epilepsy has been a hot issue, the targets such as voltage-gated sodium channels and GABA receptors on the neuron have attracted more and more attention. Additionally, c-fos is one of immediate-early gene and has a strong connection between the voltage-gated sodium channels and GABA receptor [12, 16]. Thus more attention and study have paid attention to a suitable traditional herbal Chinese medicine of seizure, which could improve the therapeutic effect and reduce the side effects in digestive, nerves, and cognition function system [17]. From the Dingxian pill, Gastrodia elata, which was an herbal medicine, has been shown to have remarkable anticonvulsant effects on various rodent models of epilepsy in vivo [18], and its active ingredient Gastrodin (GAS) could decrease seizure severity and recovery time through inhibiting Nav1.6 sodium currents in a gerbil epilepsy model [19]. Scorpion could significantly reduce the incidence and average duration of convulsion in rats, and the sodium channels were inhibited by the bioactive extract BmK IT2 and BmK AS [20, 21]. Bombyx batryticatus has great treatment effects on the central nervous system disease, including antiepileptic, anticonvulsant, hypnotic effects, and so on. Although the latent period of isoniazid-induced or nikethamide-induced convulsion in mice could be prolonged by the beauvericin, the mechanisms of biological activities of Bombyx batryticatus should need to be further explored [22]. These studies of components also partly reminded the antiepileptic mechanism of Dingxian pill.

The previous studies of Dingxian pill are mainly aimed at the intervention effects and molecular mechanism of single herb or single agent rather than the prescription on epilepsy. In the present study, the behavior tests, EEG recording, and water maze are performed, and the effect of Dingxian pill on c-fos expression was also studied. Finally the possible molecular mechanism underlying the antiepileptic effects of Dingxian pill was illustrated by transcriptomic analysis.

2. Materials and Methods

2.1. Reagents. Dingxian pill was prepared in accordance with standards formulated from the Jiangsu Hospital of Traditional Chinese Medicine (Nanjing, Jiangsu Province, China). Pentrazol (PTZ) and pentobarbital sodium salt were purchased from Sigma Aldrich Co. (St. Louis, MO, USA), sodium valproate (VPA) from Sanofi-Aventis Co. (Paris, France), and anti-c-Fos from Novus Biologicals (NB110-75039, Colorado, USA). The SABC-POD kit, DAB coloring kit, and IgG-Biotin were obtained from Boster Company (Wuhan, China). The kits of RT-PCR and Trizol were purchased from Novizan Biotechnology Co. (Nanjing, China).

2.2. Animals. The number of 70 male Sprague-Dawley rats (body weight 200-220 g) was obtained from Shanghai Slac Laboratory Animal Co. Ltd. (Shanghai, China). They raised under controlled conditions at temperature (25±2°C) and 12h light-dark cycle with free access to food and water, for at least seven days before experiment. All experiments performed in animals were in accordance with the China legislation on the use and care of laboratory animals and approved by the Animal Care and Use Committee of Shanghai University of Traditional Chinese Medicine (ACSHU-2011-G115).

2.3. Establishment of Epilepsy Rat Model and Drug Treatment. Pentylenetetrazol (PTZ) water solution (35 mg/kg) was administered by intraperitoneal injection for 28 days to induce chronic epilepsy model. On the fifth day after operation, the PTZ solution (35 mg/kg) was injected into rats again, and within 1 hour following the injection, the rats started to develop symptoms of seizures. The seizure activities were rated according to the Racine Scale by observing behavioral postures (i.e., lordosis, straight tail, jumping/running, forelimb clonus, and/or rearing) [23]. Then animals that exhibited at least 2 recurrent seizures per day were selected for further experimentation [24]. At the end of the experiment, 49 rats were divided into 5 groups for further experimentation.

Following the PTZ injection (i.p.), the 5 groups of rats were treated with different drugs once a day for 28 days. In detail, the solutions of Dingxian pill were applied intragastrically to 3 groups (low, middle, and high) at a dose of 0.6 g/kg, 1.2 g/kg, and 2.4 g/kg, respectively. The remaining two groups were treated with VPA (0.2 g/kg) and the same volume of saline. During the treatment period, rats were injected with PTZ again in the 7th, 14th, 21st, and 28th day.

2.4. Electrophysiological Recordings of Rats. The rats were fixed in the stereotaxic instrument under anesthesia with pentobarbital in a dose of 30 mg/kg (i.p., 2.5%). When the rats were deeply anesthetized, making a 20 mm incision on the head using a scalpel, then find the bregma and lambda points on the skull by pulling the scalp away with forceps. The pacing electrodes were applied to the sites (AP: 4.0 mm, L: 2.2 mm; H: 2.5 mm) through consulting the Rat Brain in Stereotaxic Coordinates [25], and the rats were subjected to craniotomy with dentist's micro-drill. The dura was broken with a syringe needle, and the depth of the electrode should be inserted into 2.2±0.2 mm below the hippocampus CA1. After full recovery, connect the electrodes implanted on the skull of rats to the amplifier in its own cage. Connect the amplifier to an analogue-to-digital converter and attach the converter to a computer. After getting the baseline recording, inject the pup intraperitoneally with PTZ (35 mg/kg) to induce epileptic seizures. 1 hour after the PTZ injection observe and record the epileptic discharges.

2.5. Morris Water Maze Test. The detailed procedure of Morris water maze (MWM) test was conducted according to the described previously [26]. Forty-nine epilepsy rats were

randomly divided into 5 groups (n=9-10/group), namely, vehicle-treated group, VPA (0.2 g/kg)-treated group, low dose of Dingxian pill (0.6 g/kg)-treated group, middle dose of Dingxian pill (1.2 g/kg)-treated group, and high dose of Dingxian pill (2.4 g/kg)-treated group. Dingxian pill and VPA were administered by oral gavage for 4 weeks prior to the behavioral testing. Then in the testing, the escape latency and path length were recorded and analyzed.

2.6. Immunohistochemistry. All rats were anesthetized with PTZ (35 mg/kg) 2 h after injection and were perfused transcardially with 50 mL of saline followed by 200 mL of 4% paraformaldehyde. Brains were removed and 20 μm coronal frozen sections cut on a sliding knife microtome. The sections were collected in a cryoprotective solution. Immunohistochemical staining for c-fos was carried out via the avidin-biotin procedure. Briefly, the sections were first incubated for 30 min in 10% normal serum plus 5% BSA in PBS to block nonspecific binding and then were incubated overnight at 4°C with rabbit polyclonal c-fos antiserum (1:500 dilution). For control purposes, the sections were either incubated with antiserum that had been exposed to saturating levels of the c-fos peptide (preabsorption control) or incubated in the absence of the primary antibody. The sections were then incubated with an anti-rabbit biotinylated IgG for 45 min and subsequently reacted with SABC for 20 min. The peroxidase reaction was developed in a chromagen solution containing 100 mM nickel sulfate, 125 mM sodium acetate, 10 mM imidazole, 0.03% diaminobenzidine (DAB), and 0.01% hydrogen peroxide at pH 6.5. The sections were then mounted and photomicrographed [27].

2.7. Quantitative RT-PCR Analysis. Total RNA was prepared from rat brain hippocampus, and mRNA levels of Egr3, Nrg1, Arc, and cox-2 were measured using the SYBR Green PCR Master Mix Kit (Nanjing, China) on a 7500 FAST Real-Time PCR System (Applied Biosystems, Foster City, CA, USA) with the GADPH as an internal control.

2.8. Statistical Analysis. All data were analyzed using the Origin 8.5 (OriginLab, USA) and expressed as mean±SEM unless otherwise indicated. The escape latency and escape rate data in MWM test were analyzed using one-way analysis of variance (ANOVA) with repeated measures. The other behavioral data and the biomarkers changes were analyzed by one-way ANOVA followed by Tukey's post hoc test. For all statistical tests, the value of $P < 0.05$ was regarded as significant.

3. Results

3.1. Anticonvulsant Effects of Dingxian Pill on Seizure-Like Behavior Induced by PTZ. The stereotypical oral and masticatory movements, hypokinesia, head bobbing, and wet-dog shakes were developed, following the systemic administration of PTZ (35 mg/kg). And the initial behavior rapidly progressed through the kindling stages from the seventh day. To explore whether Dingxian pill could prevent against PTZ-induced chronic epilepsy, the latency of seizure among the groups was observed. As Figure 1 showed, the latency of high dose group was increased remarkably compared to the control rats in the 14th, 21st, and 28th day (Figures 1(b)–1(d), 368.47 ± 43.63 s versus 183.00 ± 26.87 s $P< 0.05$; 347.19 ± 51.94 s versus 173.20 ± 38.28 s $P< 0.05$; and 445.06 ± 52.33 s versus 189.70 ± 24.78 s $P< 0.001$) and the high dose group had no significant difference with VPA group (Figure 1(d) 445.06 ± 52.33 s versus 394.38 ± 53.67 s) in the 28th day. Besides, the incubation period of the middle dose group was significantly longer than that of the CTRL group at day 21 (Figure 1(c) 347.18 ± 51.94 s versus 173.20 ± 38.28 s, $P< 0.001$).

For the percentage of seizure stage, the Dingxian pill treatment groups showed a significant decrease than control group in seizure 4,5 from the 7th day, especial for the high group (13.33% versus 80%, 7th day; 20% versus 80%, 14th day; 13.3% versus 80%, 21st day and 6.67% versus 60%, 28th day, Figures 1(e)–1(h)).

3.2. Modulatory Effects of Dingxian Pill on the Electrographic Seizures Induced by PTZ. To explore whether Dingxian pill could affect the level of epileptiform EEG traces, the VPA and the high dose of Dingxian pill (2.4 g/kg) treatment groups were analyzed after PTZ treatment. As shown in Figure 2(a), the spectrums of control and high dose of Dingxian pill treatment groups were compared.

An increased seizure frequency was found in both groups, but the frequency of control group was increased compared to the high dose group significantly after PTZ. The comparison of the mean power spectral density among the CTRL, VPA, and Dingxian pill groups showed sharp decrease of spectral power around the CTRL group (Figure 2(b)).

While the LFP of the three groups was enhanced in the hippocampus following the PTZ induced, the amplitude of the local field potential in the high dose group and the VPA group was lower than that in the CTRL group (Figure 2(c)).

Based on deep study, which is shown in Figure 2(d), there was a general tendency that the activities of brain waves in the high dose of Dingxian pill and VPA groups were decreased, and the decrease of Dingxian pill reached statistical significance in the brain wave α, δ, θ (0.93 ± 0.17 versus 2.64 ± 0.38, $P< 0.001$; 1.25 ± 0.11 versus 1.98 ± 0.38, $P< 0.01$; 0.66 ± 0.06 versus 0.85 ± 0.13, $P< 0.05$, respectively), compared to the CTRL group.

3.3. Dingxian Pill Attenuated Cognitive Impairments of PTZ Induced-Epileptic Rats. The improvement of memory and cognition in the treatment groups was measured in PTZ-induced epilepsy rats by the Morris water maze (MWM) tasks. In the hidden platform-swimming trials, the mice of VPA and high dose of Dingxian pill-treated groups (except the low and middle dose) showed markedly improving memory as the path length (Figure 3(a)) and their escape latency (Figure 3(b), 21.13 ± 2.50 versus 33.31 ± 3.49, $P<0.01$; 19.06 ± 3.37 versus 33.31 ± 3.49, $P<0.01$) on the fifth testing day were effectively shortened compared to the control. Above all, both VPA and the high dose of Dingxian pill

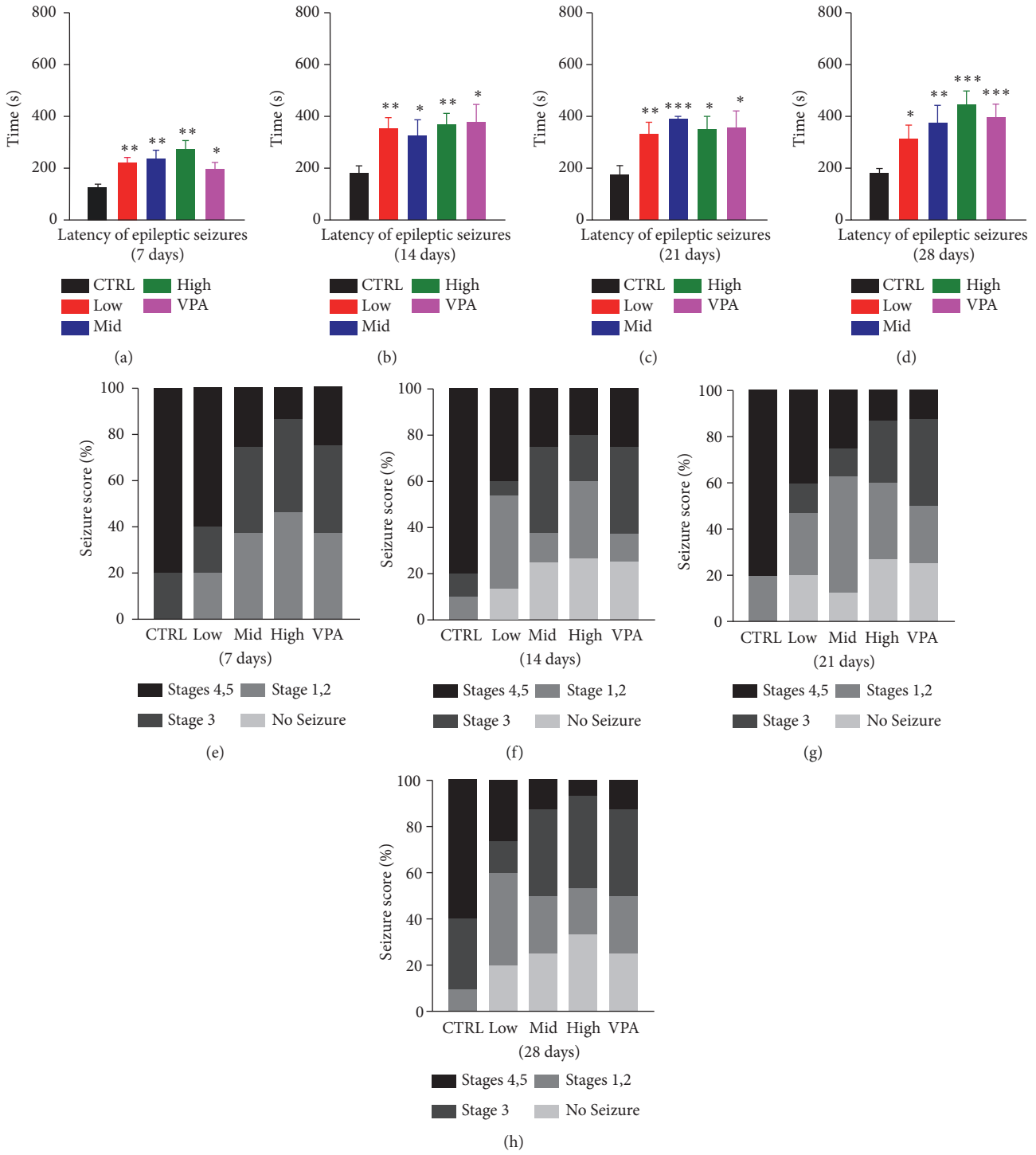

Figure 1: The anticonvulsant effects of Dingxian pill on seizure-like behaviour induced by PTZ: the latency of epileptic seizures ((a)–(d)) and the percentage of seizure stage ((e)–(h)).

administration significantly improved spatial learning and memory of cognitively impaired mice.

3.4. The Expression of c-Fos Was Decreased by Dingxian Pill in the Hippocampus of PTZ Induced-Epileptic Rats. To explore the effect of Dingxian pill on the expression of immediately early gene c-fos in PTZ kindling epilepsy rat brain, the protein expression was compared in the different treatment groups by immunohistochemistry assay, exhibited in Figure 4. The expression of c-fos positive cells in the high dose group ($P<0.01$) and VPA ($P<0.05$) group was significantly lower than that in the CTRL group and the low dose group. These results indicated that Dingxian pill significantly antagonizes the c-fos protein expression of rat hippocampus caused by

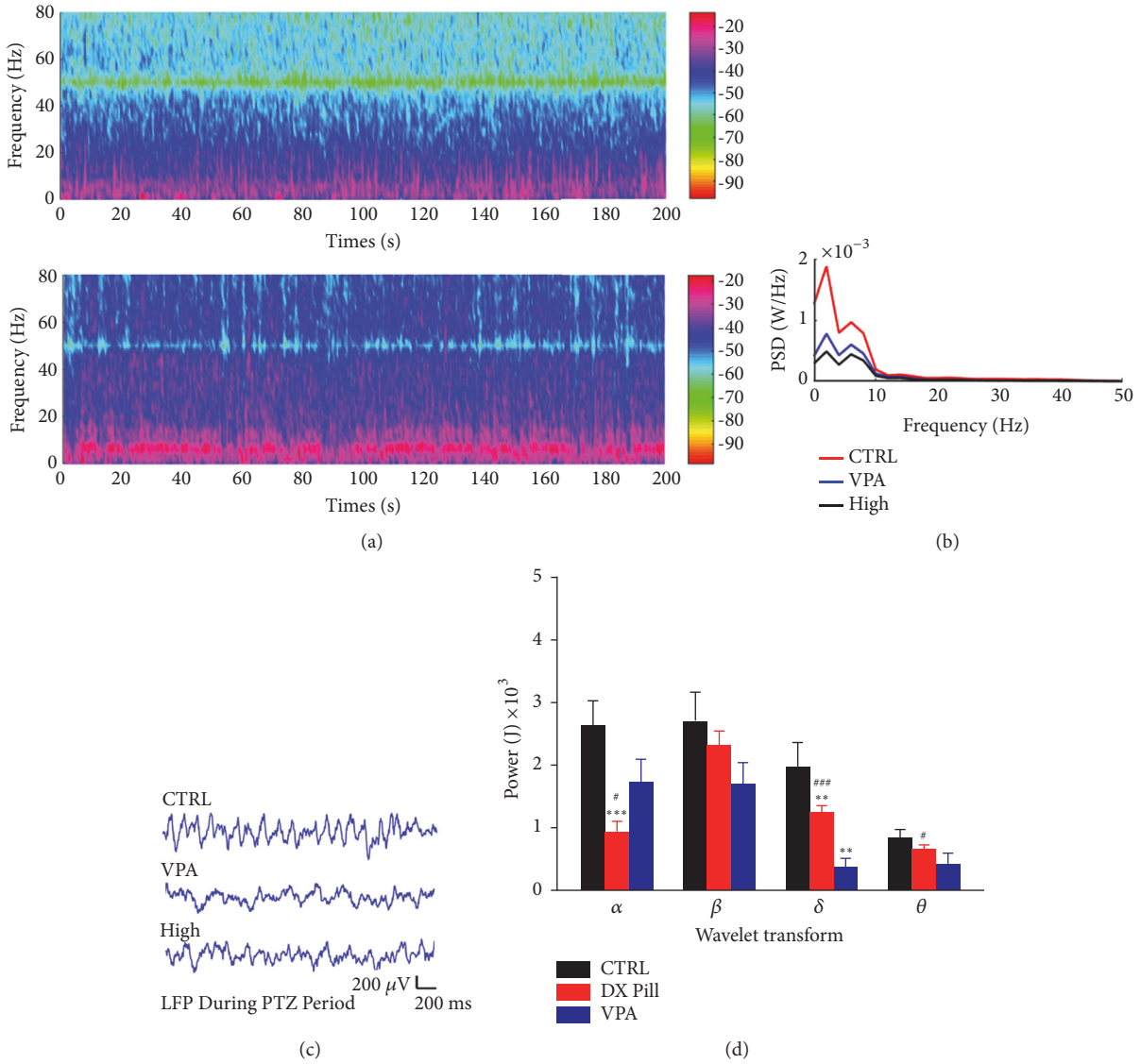

Figure 2: The effect of Dingxian pill on the electroencephalogram (EEG) in rats with chronic preeclampsia induced by PTZ: the EEG spectrum analysis of high dose group ((a) figure above) and control group ((a) figure below). The average power spectral densities (PSD) of all the frequencies among CTRL, high, and VPA group (b). The representative local field potential (LFP) of epilepsy rats recorded during PTZ period (c). The energy of each single waveform in rats during PTZ period among CTRL, Dingxian pill, and VPA group (d).

PTZ, which may be one of the mechanisms of Dingxian pill prevention and treatment of epilepsy.

3.5. The Transcriptomic Analysis of Dingxian Pill Treatment on PTZ Induced-Epileptic Model. Molecular mechanism of Dingxian pill intervention in chronic epilepsy had been explored by the transcript analysis (Figure 5). The results indicated that there are 57 differentially expressed genes in the intervention group and the control group (more than 2 times the expression level), some of which are closely related to epilepsy such as Egr3, Nrg1, Arc, and cox-2. Based on GO and pathway analysis, differentially expressed genes are mainly involved in the function of synaptic plasticity, receptor binding, redox and neurotransmitter secretion, and signaling pathway for MAPK-ERK, JAK-Stat, and GABA receptor synthesis. In addition, quantitative RT-PCR analysis showed that the mRNA level of Egr3 (0.66±0.05), Arc (0.74±0.06), and cox-2 (0.68±0.06) was obviously decreased compared with control group (1.00±0.09) ($P<0.01$, $P<0.05$, $P<0.05$, n=5, respectively), especially for Nrg1 (0.30±0.09, $P<0.01$, n=5).

4. Discussion

Epilepsy is a common neurodegenerative disease, and the voltage-gated sodium channels, GABA receptor, and c-fos are closely related. As a hot and difficult problem in modern time, the effective and few side-effective drugs are still to be discovered, especially for the temporal lobe epilepsy. Dingxian pill is used for treating epilepsy in China, but the mechanism is still unclear. Thus, the pharmacodynamics and

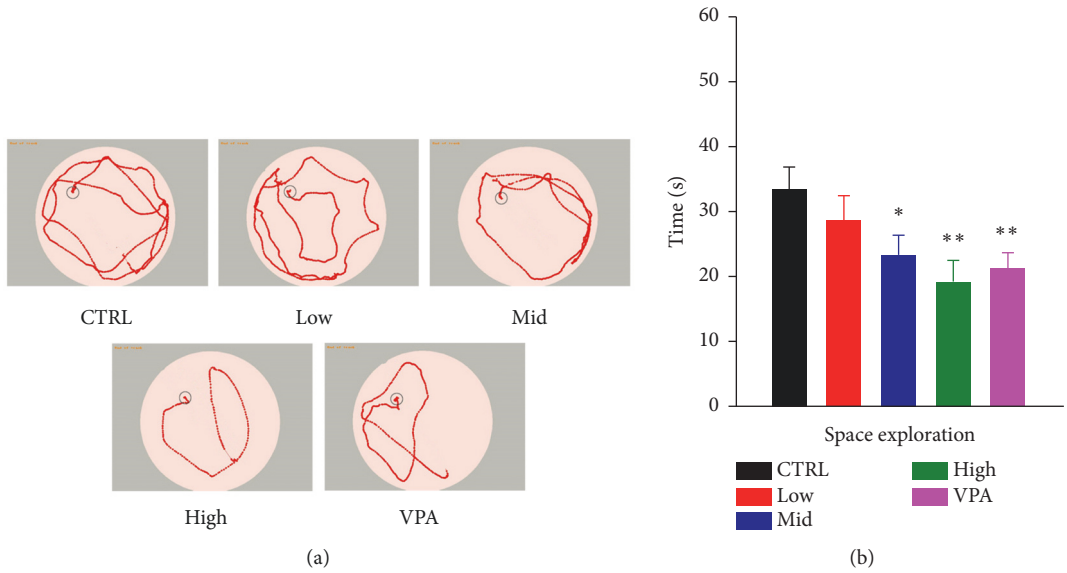

Figure 3: Effects of Dingxian pill on PTZ-induced memory-impaired rats: swimming tracks of rats in water tank (a) and escape latency of rats in hidden platform tests on the fifth testing day.

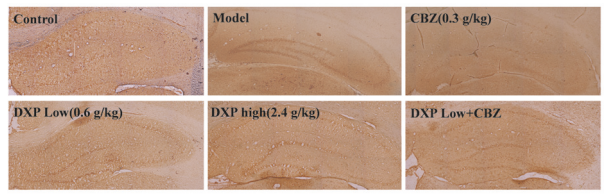

Figure 4: The expression of c-fos in the hippocampus cortex of epilepsy rat among control, model, VPA, DXP-low, DXP-middle, and DXP-high groups.

the mechanism of Dingxian pill were researched in present study.

The results showed that long-time Dingxian pill treatment could reduce the seizures frequency through inhibiting the abnormal discharge of hippocampal neurons and the expression of c-fos gene, which is closely related to epilepsy. It shows that c-fos is commonly present in the central nervous system and the expression level of c-fos is generally low, but the expression would be increased with epileptogenesis [27]. Gastrodia elata, which is one component of Dingxian pill, could antagonize the impairment of learning and memory on c-fos expression [28]. BmK IT2, a β-like neurotoxin containing 61 amino acid residues, was extracted from scorpion, a Chinese drug in Dingxian pill. Application of different doses of BmK IT2 (0.05, 0.1, and 0.5 mg) induced a dose-dependent suppression of the c-Fos expression in hippocampus [29]. Dingxian pill also could be improving the learning and memory on memory deficits in chronic epilepsy rats. In addition, the significant effect of Dingxian pill may be via mediating the Egr3-GABRA4, NRG1-ErbB4, MAPK-ERK-Arc, and cox-2-Pgp signal-pathways, which were associated with epilepsy. For the Egr3-GABRA4 pathway, Egr3 as a critical regulator of endogenous GABRA4, one of the inhibitory subunits underlying the $GABA_A$ receptor, during development, had a major role in developing neurons and in epileptogenesis [28, 29]. Even more interesting, the mRNA expression of GABRA1-4 had been compared in our study. The results showed that the mRNA level of GABRA1 after Dingxian pill treatment was elevated compared with PTZ group, but the mRNA level of GABRA4 was decreased and others had no change, which indicated that antiepileptic effects of Dingxian pill may be closely related to GABRA1 and GABRA4 (Supplementary Material, GABRA1, saline: 1.00±0.22, Dingxian pill: 1.97±0.29; GABRA4, saline: 1.00±0.17, Dingxian pill: 0.54±0.04, n=3, $P<0.05$, SFigure1). As for NRG1-ErbB4 pathway, downregulation of NRG1 expression could improve the activity of voltage-gated sodium channel and the excitability of ErbB4 positive intermediate neurons, then promoting the release of GABA, inhibiting the discharge of hippocampal pyramidal neurons, and interfering with the occurrence of epilepsy [30, 31]. The activity-regulated cytoskeletal associated protein (Arc), as a marker neuronal activation, was associated with the granule cells born after pilocarpine-induced SE [32], and the expression of Arc was reduced after therapeutic interventions [33]. In addition, the P-glycoprotein (Pgp) was overexpressed after seizure and the

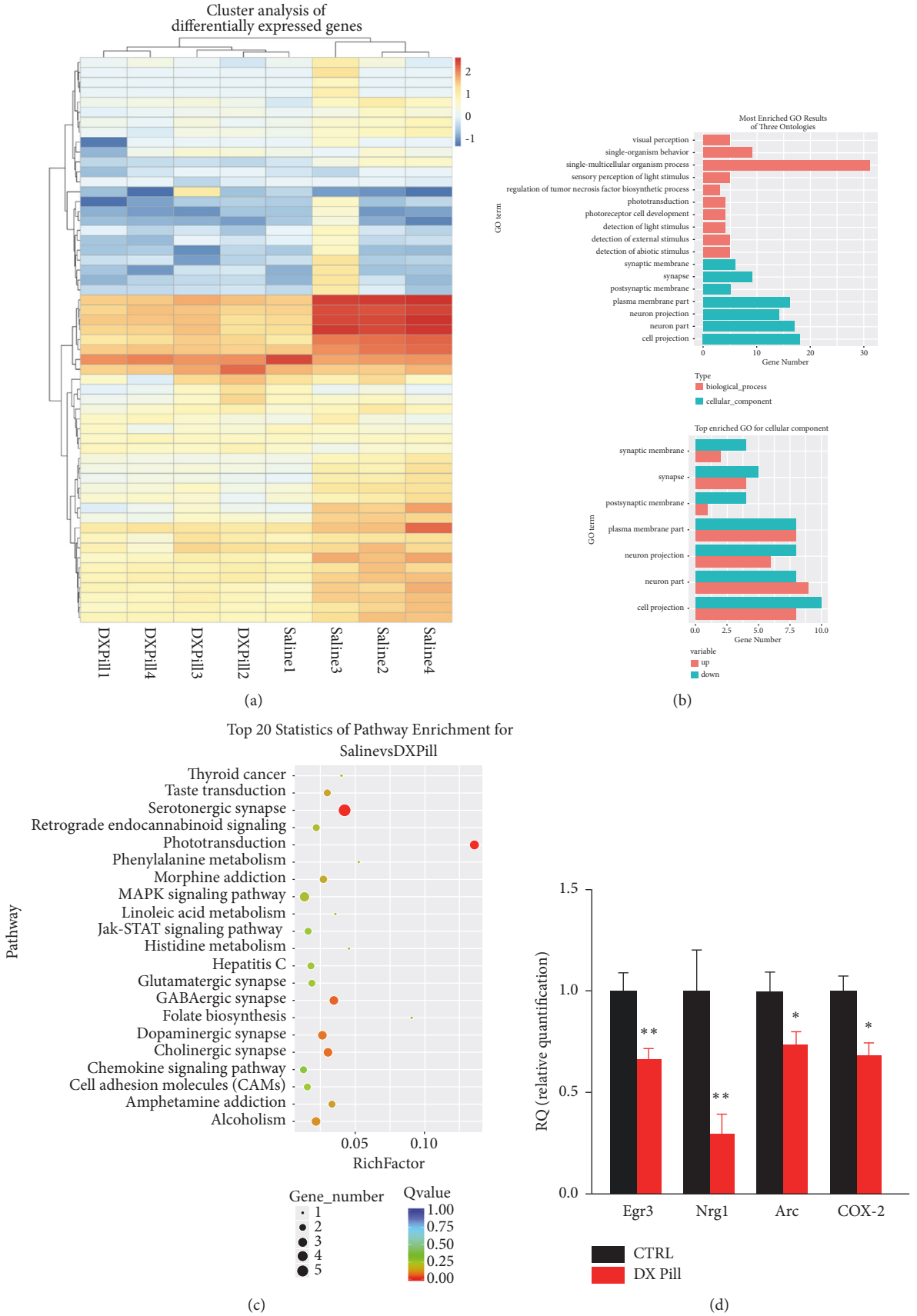

Figure 5: The transcriptome analysis of Dingxian pill-intervened rats: analysis of differentially expressed genes ((a), each column represents an experimental condition, each row represents a log2 ratio value of a gene or log10 (FPKM + 0.01), and different expression variants or expression levels are expressed in different colors.); the analysis of GO function of differentially expressed genes (b); KEGG pathway enrichment analysis of differential expression genes (c); and the comparison of differential gene expression between CTRL and DX pill group by real-time PCR analysis (d).

mechanism with glutamate could enhance the Pgp expression in the blood-brain barrier through NMDA receptor and cox-2 [34].

The temporal lobe epilepsy (TLE) as a research focus, the hippocampal sclerosis, is the most common neuropathologic finding, including neuron loss, glial proliferation, and synapse formation [26]. Although new antiepileptic drugs have been introduced into clinical practice, their effects remain poor [35, 36]. The pathogenesis of TLE is complex and still unclear, but the possible mechanisms of resistance were concluded, including drugs hard to reach the target, the targets changed, and the true target unknown. Thus exploring and developing new antiepileptic drugs are of great significance for further study.

So far, the treatment of TLE by Chinese traditional medicine has a better curative effect on inhibiting the frequency of epilepsy, improving curative effect, and reducing side effect of clinical treatment. Many studies have showed that the traditional Chinese medicine (TCM) has effective clinical effect on treating TLE. And it looks like patients would be safer on TCM than on other drugs for long periods of time. Thus TCM would be the best choice for the patients, when considering the fear of attacks, concerns about long-term medication.

The traditional Chinese medicine has a centuries-old tradition of use by epilepsy patients around the world. And herbal therapies are often used for general health maintenance or for chronic conditions like epilepsy in developing countries [37]. In addition, clinical experience suggests that patients may try some herbal therapies in order to reduce AED-related adverse effects or comorbid conditions [38]. Thus, many Chinese herbal prescriptions, Chinese herbs, and the monomer of treating epilepsy were compared by the modern molecular biotechnology. For the antiepileptic herb, Gastrodia elata blume (GE) is used to treat epilepsy in East Asia, which is one medicine of Dingxian pill. And gastrodin, a phenolic glucoside derived from GE, had been the major monomer for antiepilepsy [39]. It is indicated that herbal prescriptions, herbs, and monomer have been shown to have neuroprotective properties [40–42], efficacy in animal models of epilepsy [43–45] and hippocampal slice models [46], and effects on gene expression [47]. However, the effective basic principles of many herbal prescriptions have not been studied, because the ingredients are complicated. Through the "effective on the basis of chemical substances" study, the efficacy of Chinese medicine would be clarified.

5. Conclusion

Dingxian pills can relieve the seizures of chronic epilepsy rats injected by PTZ through inhibiting the abnormal discharge of hippocampal neurons in epileptic rats. The treatment of epilepsy pill can effectively improve the spatial learning and memory ability of epilepsy model. The Dingxian pills might interfere with epilepsy as well as cognitive dysfunction through Egr3-GABRA4 signal, NRG1-ErbB4 signal, and ERK-Arc pathway.

Data Availability

The data used to support the findings of this study are included within the article.

Ethical Approval

The protocols of animal experiments complied with the current ethical considerations of Shanghai University of Traditional Chinese Medicine's Animal Ethic Committee, which is in accordance with the National Research Council criteria. All animal experiments and procedures were reviewed and approved by the Institutional Animal Care and Use Committee (IACUC) of Shanghai University of Traditional Chinese Medicine and were performed in accordance with the relevant guidelines and regulations as well as approved by the guidelines on ethical standards for investigation of experimental pain in conscious animals.

Consent

All participants signed an informed consent that the data to this article can be processed anonymously for scientific purposes.

Conflicts of Interest

The authors have no conflicts of interest to declare.

Authors' Contributions

Yudan Zhu, Jie Tao, Yiqin Ge, and Jiwei Cheng conceived and designed the experiments. Yudan Zhu, Shuzhang Zhang, and Mei Shen performed the experiments. Jiwei Cheng, Shuzhang Zhang, Mei Shen, and Zhiping Zhang analyzed the data. Shuzhang Zhang, Mei Shen, Zhiping Zhang, and Yiqin Ge contributed reagents/materials/analysis tools. Yudan Zhu and Jie Tao wrote the paper. Yudan Zhu and Shuzhang Zhang have contributed equally to this work.

Acknowledgments

We thank Dr. Detao Wang and Associate Professor Peihao Yin for their guidance on the experiments and manuscript. This work was supported by National Science Foundation of China (Nos. 81603410 and 31771191), Innovation Fund of Putuo District Health System (No. 17-PT-10), Shanghai Municipal Commission of Health and Family Planning Fund (Nos. 20184Y0086, 2016JP007, and 2018JQ003), Project within Budget of Shanghai University of Traditional Chinese Medicine (No. 18TS086), and Research Project of Putuo Hospital, Shanghai University of Traditional Chinese Medicine (No. 2016208A).

Supplementary Materials

Supplementary Figure 1: effects of DX pill on the expression of GABAA receptor subunits in PTZ-induced seizure model

as detected using real-time PCR. Data are expressed as the mean±S.E.M., n=3, P>0.05, compared with the saline group. *(Supplementary Materials)*

References

[1] J. S. Duncan, J. W. Sander, S. M. Sisodiya, and M. C. Walker, "Adult epilepsy," *The Lancet*, vol. 367, no. 9516, pp. 1087–1100, 2006.

[2] T. L. Mac, D. Tran, F. Quet, P. Odermatt, P. Preux, and C. T. Tan, "Epidemiology, aetiology, and clinical management of epilepsy in Asia: a systematic review," *The Lancet Neurology*, vol. 6, no. 6, pp. 533–543, 2007.

[3] D. Ding, Z. Hong, W.-Z. Wang et al., "Assessing the disease burden due to epilepsy by disability adjusted life year in rural China," *Epilepsia*, vol. 47, no. 12, pp. 2032–2037, 2006.

[4] C. M. DeGiorgio, D. Markovic, R. Mazumder, and B. D. Moseley, "Ranking the leading risk factors for sudden unexpected death in epilepsy," *Frontiers in Neurology*, vol. 8, p. 473, 2017.

[5] R. Kumar, R. Arora, A. Agarwal, and Y. K. Gupta, "Protective effect of Terminalia chebula against seizures, seizure-induced cognitive impairment and oxidative stress in experimental models of seizures in rats," *Journal of Ethnopharmacology*, vol. 215, pp. 124–131, 2018.

[6] Y. Zhu, J. Feng, J. Ji et al., "Alteration of monoamine receptor activity and glucose metabolism in pediatric patients with anticonvulsant-induced cognitive impairment," *Journal of Nuclear Medicine*, vol. 58, no. 9, pp. 1490–1497, 2017.

[7] S. N. Ahmed and Z. A. Siddiqi, "Antiepileptic drugs and liver disease," *Seizure*, vol. 15, no. 3, pp. 156–164, 2006.

[8] J. S. Au and P. J. Pockros, "Drug-induced liver injury from antiepileptic drugs," *Clinics in Liver Disease*, vol. 17, no. 4, pp. 687–697, 2013.

[9] B. Schmeiser, J. Zentner, B. J. Steinhoff et al., "The role of presurgical EEG parameters and of reoperation for seizure outcome in temporal lobe epilepsy," *Seizure*, vol. 51, pp. 174–179, 2017.

[10] F. Salehi, M. Sharma, T. M. Peters, and A. R. Khan, "White matter tracts in patients with temporal lobe epilepsy: pre- and postoperative assessment," *Cureus*, vol. 9, article e1735, no. 10, 2017.

[11] M. Vrinda, A. Sasidharan, S. Aparna, B. N. Srikumar, B. M. Kutty, and B. S. Shankaranarayana Rao, "Enriched environment attenuates behavioral seizures and depression in chronic temporal lobe epilepsy," *Epilepsia*, vol. 58, no. 7, pp. 1148–1158, 2017.

[12] M. L. Bell, S. Rao, E. L. So et al., "Epilepsy surgery outcomes in temporal lobe epilepsy with a normal MRI," *Epilepsia*, vol. 50, no. 9, pp. 2053–2060, 2009.

[13] Y. Zhu, B. Wu, Y.-J. Feng, J. Tao, and Y.-H. Ji, "Lipid bilayer modification alters the gating properties and pharmacological sensitivity of voltage-gated sodium channel," *Sheng Li Xue Bao*, vol. 67, no. 3, pp. 271–282, 2015.

[14] Y. Zhu, S. Zhang, Y. Feng, Q. Xiao, J. Cheng, and J. Tao, "The Yin and Yang of BK Channels in Epilepsy," *CNS & Neurological Disorders - Drug Targets*, vol. 17, no. 4, pp. 272–279, 2018.

[15] J. Tao, Z. Zhou, B. Wu, J. Shi, X. Chen, and Y. Ji, "Recombinant expression and functional characterization of martentoxin: a selective inhibitor for BK channel (α + β4)," *Toxins*, vol. 6, no. 4, pp. 1419–1433, 2014.

[16] M. S. Martin, B. Tang, L. A. Papale, F. H. Yu, W. A. Catterall, and A. Escayg, "The voltage-gated sodium channel Scn8a is a genetic modifier of severe myoclonic epilepsy of infancy," *Human Molecular Genetics*, vol. 16, no. 23, pp. 2892–2899, 2007.

[17] B. Schmitz, "Effects of antiepileptic drugs on mood and behavior," *Epilepsia*, vol. 47, no. 2, pp. 28–33, 2006.

[18] H. Shao, Y. Yang, A.-P. Qi et al., "Gastrodin Reduces the Severity of Status Epilepticus in the Rat Pilocarpine Model of Temporal Lobe Epilepsy by Inhibiting Nav1.6 Sodium Currents," *Neurochemical Research*, vol. 42, no. 2, pp. 360–374, 2017.

[19] S.-J. An, S.-K. Park, I. K. Hwang et al., "Gastrodin decreases immunoreactivities of γ-aminobutyric acid shunt enzymes in the hippocampus of seizure-sensitive gerbils," *Journal of Neuroscience Research*, vol. 71, no. 4, pp. 534–543, 2003.

[20] R. Zhao, X.-Y. Zhang, J. Yang et al., "Anticonvulsant effect of BmK IT2, a sodium channel-specific neurotoxin, in rat models of epilepsy," *British Journal of Pharmacology*, vol. 154, no. 5, pp. 1116–1124, 2008.

[21] M.-M. Zhu, J. Tao, M. Tan, H.-T. Yang, and Y.-H. Ji, "U-shaped dose-dependent effects of BmK AS, a unique scorpion polypeptide toxin, on voltage-gated sodium channels," *British Journal of Pharmacology*, vol. 158, no. 8, pp. 1895–1903, 2009.

[22] L. Nybo, "CNS fatigue and prolonged exercise: effect of glucose supplementation," *Medicine & Science in Sports & Exercise*, vol. 35, no. 4, pp. 589–594, 2003.

[23] C. S. Paulose, F. Chathu, S. Reas Khan, and A. Krishnakumar, "Neuroprotective role of Bacopa monnieri extract in epilepsy and effect of glucose supplementation during hypoxia: glutamate receptor gene expression," *Neurochemical Research*, vol. 33, no. 9, pp. 1663–1671, 2008.

[24] A. S. Shashkov, M. Wang, E. M. Turdymuratov et al., "Structural and genetic relationships of closely related O-antigens of Cronobacter spp. and Escherichia coli: C. sakazakii G2594 (serotype O4)/E. coli O103 and C. malonaticus G3864 (serotype O1)/E. coli O29," *Carbohydrate Research*, vol. 404, pp. 124–131, 2015.

[25] P. A. Williams, P. Larimer, Y. Gao, and B. W. Strowbridge, "Semilunar granule cells: Glutamatergic neurons in the rat dentate gyrus with axon collaterals in the inner molecular layer," *The Journal of Neuroscience*, vol. 27, no. 50, pp. 13756–13761, 2007.

[26] H.-G. Wieser and Epilepsy ICoNo, "ILAE Commission Report. Mesial temporal lobe epilepsy with hippocampal sclerosis," *Epilepsia*, vol. 45, no. 6, pp. 695–714, 2004.

[27] G. Bing, E. A. Stone, Y. Zhang, and D. Filer, "Immunohistochemical studies of noradrenergic-induced expression of c-fos in the rat CNS," *Brain Research*, vol. 592, no. 1-2, pp. 57–62, 1992.

[28] D. S. Roberts, Y. Hu, I. V. Lund, A. R. Brooks-Kayal, and S. J. Russek, "Brain-derived neurotrophic factor (BDNF)-induced synthesis of early growth response factor 3 (Egr3) controls the levels of type A GABA receptor alpha 4 subunits in hippocampal neurons," *The Journal of Biological Chemistry*, vol. 281, no. 40, pp. 29431–29435, 2006.

[29] D. S. Roberts, Y. H. Raol, S. Bandyopadhyay et al., "Egr3 stimulation of GABRA4 promoter activity as a mechanism for seizure-induced up-regulation of GABA(A) receptor alpha4 subunit expression," *Proceedings of the National Academy of Sciences of the United States of America*, vol. 102, no. 33, pp. 11894–11899, 2005.

[30] J. M. Zhu, K. X. Li, S. X. Cao et al., "Increased NRG1-ErbB4 signaling in human symptomatic epilepsy," *Scientific Reports*, vol. 7, no. 1, p. 141, 2017.

[31] J. Tian, F. Geng, F. Gao et al., "Down-Regulation of Neuregulin1/ErbB4 Signaling in the Hippocampus Is Critical for

Learning and Memory," *Molecular Neurobiology*, vol. 54, no. 6, pp. 3976–3987, 2017.

[32] F. Gao, X. Song, D. Zhu et al., "Dendritic morphology, synaptic transmission, and activity of mature granule cells born following pilocarpine-induced status epilepticus in the rat," *Frontiers in Cellular Neuroscience*, vol. 9, p. 384, 2015.

[33] C. Mandel-Brehm, J. Salogiannis, S. C. Dhamne, A. Rotenberg, and M. E. Greenberg, "Seizure-like activity in a juvenile Angelman syndrome mouse model is attenuated by reducing Arc expression," *Proceedings of the National Acadamy of Sciences of the United States of America*, vol. 112, no. 16, pp. 5129–5134, 2015.

[34] H. Potschka, "Modulating P-glycoprotein regulation: future perspectives for pharmacoresistant epilepsies?" *Epilepsia*, vol. 51, no. 8, pp. 1333–1347, 2010.

[35] K. Sadowski, K. Kotulska-Jóźwiak, and S. Jóźwiak, "Role of mTOR inhibitors in epilepsy treatment," *Pharmacological Reports*, vol. 67, no. 3, pp. 636–646, 2015.

[36] D. L. Wahner-Roedler, P. L. Elkin, A. Vincent et al., "Use of complementary and alternative medical therapies by patients referred to a fibromyalgia treatment program at a Tertiary Care Center," *Mayo Clinic Proceedings*, vol. 80, no. 1, pp. 55–60, 2005.

[37] S. C. Schachter, "Botanicals and herbs: a traditional approach to treating epilepsy," *Neurotherapeutics*, vol. 6, no. 2, pp. 415–420, 2009.

[38] H.-J. Kim, K.-D. Moon, S.-Y. Oh, S.-P. Kim, and S.-R. Lee, "Ether fraction of methanol extracts of Gastrodia elata, a traditional medicinal herb, protects against kainic acid-induced neuronal damage in the mouse hippocampus," *Neuroscience Letters*, vol. 314, no. 1-2, pp. 65–68, 2001.

[39] J. Zhang, X. Chen, M. Kårbø et al., "Anticonvulsant effect of dipropofol by enhancing native GABA currents in cortical neurons in mice," *Journal of Neurophysiology*, vol. 120, no. 3, pp. 1404–1414, 2018.

[40] C.-L. Hsieh, N.-Y. Tang, S.-Y. Chiang, C.-T. Hsieh, and L. Jaung-Geng, "Anticonvulsive and free radical scavenging actions of two herbs, Uncaria rhynchophylla (MIQ) Jack and Gastrodia elata Bl., in kainic acid-treated rats," *Life Sciences*, vol. 65, no. 20, pp. 2071–2082, 1999.

[41] C.-L. Hsieh, C.-H. Chang, S.-Y. Chiang et al., "Anticonvulsive and free radical scavenging activities of vanillyl alcohol in ferric chloride-induced epileptic seizures in Sprague-Dawley rats," *Life Sciences*, vol. 67, no. 10, pp. 1185–1195, 2000.

[42] L.-C. Chiou, J.-Y. Ling, and C.-C. Chang, "Chinese herb constituent β-eudesmol alleviated the electroshock seizures in mice and electrographic seizures in rat hippocampal slices," *Neuroscience Letters*, vol. 231, no. 3, pp. 171–174, 1997.

[43] C.-L. Hsieh, M.-F. Chen, T.-C. Li et al., "Anticonvulsant effect of Uncaria rhynchophylla (Miq) Jack. in rats with kainic acid-induced epileptic seizure," *American Journal of Chinese Medicine*, vol. 27, no. 2, pp. 257–264, 1999.

[44] E. Minami, H. Shibata, Y. Nunoura, M. Nomoto, and T. Fukuda, "Efficacy of Shitei-To, a traditional chinese medicine formulation, against convulsions in mice," *American Journal of Chinese Medicine*, vol. 27, no. 1, pp. 107–115, 1999.

[45] A. Ameri, J. Gleitz, and T. Peters, "Bicuculline-induced epileptiform activity in rat hippocampal slices: Suppression by Aconitum alkaloids," *Planta Medica*, vol. 63, no. 3, pp. 228–232, 1997.

[46] E. Sugaya, N. Yuyama, K. Kajiwara et al., "Regulation of gene expression by herbal medicines–a new paradigm of gene therapy for multifocal abnormalities of genes," *Research Communications in Molecular Pathology and Pharmacology*, vol. 106, no. 3, pp. 171–180, 1999.

[47] E. Ernst, "Serious psychiatric and neurological adverse effects of herbal medicines—a systematic review," *Acta Psychiatrica Scandinavica*, vol. 108, no. 2, pp. 83–91, 2003.